UNIVERSITY OF CALIFORNIA, SAN DIEGO

Cell Cycle and DNA Damage Response Regulation by Spy1, and the Intersection of FGFR and NFkappaB Pathways

A dissertation submitted in partial satisfaction of the
requirements for the degree Doctor of Philosophy

in

Chemistry

by

Christopher William McAndrew

Committee in charge:

Professor Daniel J. Donoghue, Chair
Professor Steven Dowdy
Professor Partho Ghosh
Professor Judy Kim
Professor Susan Taylor

2010

The Dissertation of Christopher William McAndrew is approved, and it is acceptable in quality and form for publication on microfilm and electronically:

_____

_____

_____

_____

_____

_____

Chair

University of California, San Diego

2010

DEDICATION

This work is dedicated to my friends, family, and all the people who have helped and inspired me during my doctoral study.…

TABLE OF CONTENTS

LIST OF FIGURES

Chapter 1

Chapter 2

Chapter 3

Chapter 4

Chapter 5

Chapter 6

Chapter 7

Chapter 8

LIST OF TABLES

Chapter 2

Chapter 4

ACKNOWLEDGEMENTS

I would like to thank my parents, Brian and Kathryn McAndrew, and my brother, Michael McAndrew, for their motivation and support during my graduate studies.

I would also like to recognize my mentor Dan Donoghue for preparing me for a career in science and for his support, permitting me to perform experiments that animated me. I would also like to thank the current and past members of the Donoghue Group for being a major part of my graduate experience. Finally, I would like to acknowledge the NIH/NCI Training Grant in the Biochemistry of Growth Regulation and Oncogenesis.

Chapter 1, in full, is material published in The Wiley Encyclopedia of Chemical Biology, McAndrew, CW; Gastwirt, RF; and Donoghue, DJ (2007). The dissertation author was the primary author of this paper.

Chapter 2, in full, is material published in Cell Cycle, Gastwirt, RF; McAndrew, CW; and Donoghue, DJ (2007). The dissertation author was a primary author of this paper.

Chapter 3, in full, is material published in Cell Cycle, McAndrew, CW; Gastwirt, RF; Meyer, AN; Porter, LA; and Donoghue, DJ (2007). The dissertation author was the primary investigator and a primary author of this paper.

Chapter 4, in full, is material published in The Journal of Biological Chemistry, Gastwirt, RF; Slavin, DA; McAndrew, CW; and Donoghue, DJ (2006). The dissertation author was a co-author of this paper.

Chapter 5, in full, is material published in Cell Cycle, Gastwirt, RF; McAndrew, CW; and Donoghue, DJ (2008). The dissertation author was the primary investigator and a primary author of this paper

Chapter 6, in full, is material published in The Handbook of Cell Signaling, second edition, Drafahl, KA; McAndrew, CW; and Donoghue, DJ (2007).The dissertation author was a primary author of this paper.

Chapter 7, in full, is material submitted for publication in Cancer Research, Drafahl, KA.; McAndrew, CW; Meyer, AN; and Donoghue, DJ (2009). The dissertation author is a primary investigator and co-author of this paper.

Chapter 8, in full, is Chapter 8, in full, is material that is currently being prepared for submission. The dissertation author was a primary investigator of this work.

Appendix A, in full, is a reprint of material as is appears in Cancer Research, Meyer, AN; McAndrew, CW; and Donoghue, DJ (2008). The dissertation author is a co-author of this paper.

VITA

2004	Bachelor of Science, University of Delaware
2007	Master of Science, University of California, San Diego
2010	Doctor of Philosophy, University of California, San Diego

PUBLICATIONS

Yeung, D; Josse, D; Nicholsona, J; Khanal, A; McAndrew, CW; Bahnson, BJ; Lenza, DE; and Cerasolia, DM (2004). Structure/function analyses of human serum paraoxonase (HuPON1) mutants designed from a DFPase-like homology model. Biochim Biophys Acta.; 1702(1):67-77.

Gastwirt, RF; Slavin, DA; McAndrew, CW; and Donoghue, DJ (2006). Spy1 expression prevents normal cellular responses to DNA damage: Inhibition of apoptosis and checkpoint activation. J. Biol. Chem. 281(46).

McAndrew, CW; Gastwirt, RF; and Donoghue, DJ (2007). Regulation of the Cell Cycle. Wiley Encyclopedia of Chemical Biology (In Press)

McAndrew, CW; Gastwirt, RF; Meyer, AN; Porter, LA; and Donoghue, DJ (2007). Spy1 enhances phosphorylation and degradation of the cell cycle inhibitor p27. Cell Cycle 6(15).

Gastwirt, RF; McAndrew, CW; and Donoghue, DJ (2007). Speedy/RINGO Regulation of CDKs in Cell Cycle, Checkpoint Activation and Apoptosis. Cell Cycle 6(10).

Drafahl KA; McAndrew CW; and Donoghue, DJ (2008). Signaling from FGF Receptors in Development and Disease. Humana Press.

Meyer AN; McAndrew CW; and Donoghue, DJ (2008). Nordihydroguaiaretic acid inhibits an activated fibroblast growth factor receptor 3 mutant and blocks downstream signaling in multiple myeloma cells. Cancer Res.; 68(18):7362-70.

McAndrew CW; Gastwirt RF; and Donoghue, DJ (2009). The atypical CDK activator Spy1 regulates the intrinsic DNA damage response and is dependent upon p53 to inhibit apoptosis. Cell Cycle. 8(1).

FIELDS OF STUDY

Major Field: Chemistry and Biochemistry

Studies in the Biochemistry, Cellular, and Molecular Biology

Professor Daniel J. Donoghue

ABSTRACT OF THE DISSERTATION

Cell Cycle and DNA Damage Response Regulation by Spy1, and the Intersection of FGFR and NFkappaB Pathways

by

Christopher William McAndrew

Doctor of Philosophy in Chemistry

University of California, San Diego, 2010

Professor Daniel J. Donoghue, Chair

Understanding the activation and regulatory functions of cyclin dependent kinases and their inhibitors is of great importance to cancer biology. Experiments from our lab and others have identified the Speedy/RINGO family of proteins as important regulators of mammalian cell cycle control. I show that Spy1 activates CDKs and stimulates $p27^{Kip1}$ degradation, thereby relieving an important cell cycle progression restraint. Using *in vitro* purified proteins in defined reactions, I demonstrate that Spy1 can directly activate CDK2 to phosphorylate p27 on Thr187, thereby targeting it for degradation and promoting S-phase entry.

We also show that Spy1 is a component of the mammalian DNA damage response, preventing the DNA damage response and enhancing the survival of cells

treated with DNA damaging agents. We show that Spy1 expression suppresses apoptosis in a p53- and p21-dependent fashion, allows for UV irradiation resistant DNA synthesis (UVDS), and inhibits the S- and G_2/M- checkpoints through inhibition of checkpoint response proteins. This leads to DNA damage tolerance and prevention of repair cyclobutane pyrimidine dimers through nucleotide excision repair suppression. Knockdown of Spy1 activates intrinsic damage responses, indicating that Spy1 is required to promote tolerance of endogenous and exogenous damage. The novel modes of CDK regulation by Speedy/RINGO proteins may be important during cell cycle transitions, in the tolerance of normal intrinsic damage or in response to exogenous DNA damage.

Misregulation of FGFR signaling can lead to uncontrolled downstream signaling associated with many developmental syndromes and cancers. NFκB also regulates apoptosis and proliferation of many human cancers, and activation of inflammatory responses. Interestingly, our research identifies a novel link between FGFR signaling and the NFκB pathway. We show FGFR2 and FGFR4 interact with IKKβ, a critical component of NFκB signaling. We demonstrate tyrosine phosphorylation of IKKβ resulting from FGFR4 or FGFR2 expression, and show suppressed NFκB signaling upon FGFR activation, which is dependent upon FGFR kinase activity. This work provides a unique model of NFκB inactivation and implicates FGFR4 as a tumor suppressor in prostate cancer and indicates FGFR2 may play dual roles as a tumor promoter and a tumor suppressor in breast cancer cell lines.

Chapter 1:

Regulation of the Cell Cycle

Abstract

Normal regulation of the cell cycle ensures the passage of genetic material without mutations and aberrations. Proper completion of each phase is critical to the initiation of the following phase and the pathways controlling cell division occur in an ordered, sequential, and irreversible procession. The two major cell cycle events that are tightly regulated are DNA replication and cell division. Progression through each phase transition is regulated by extracellular signaling, transcription factors, cyclin-dependent kinases (CDKs), and checkpoints, which prevent uncontrolled cell division. Cyclin/CDK complexes are the primary factors responsible for the timely order of cell cycle progression, including entry into S phase, initiation of DNA replication, and mitotic entry. Each phase of the cell cycle and the different cyclin/CDK complexes, as well as other important factors regulating cell cycle progression and checkpoints, will be discussed.

Introduction

The cell cycle is the sequence of events by which growing cells duplicate and divide into two daughter cells. In mammalian cells and other eukaryotes, cell division represents a process of highly ordered and tightly regulated molecular events. The cell cycle is composed of five phases in mammals, including G_0, G_1, S, G_2, and M phases. Replication of DNA occurs during S phase and division in M phase. During the two gap phases, G_1 and G_2, cells produce RNA and proteins required for the subsequent S and M phases, respectively. Cells in a resting, quiescent state are in G_0 phase. Stimulation by external growth factors or mitogens triggers quiescent cells to reenter the cell cycle in G_1 by activating numerous signaling cascades, and leads to the sequential activation of cyclin dependent kinases (CDKs). Activation of CDKs requires interaction with a cyclin partner, T-loop phosphorylation at T160 (CDK2) or T161 (CDK1) catalyzed by CDK activating kinase (CAK), and dephosphorylation at T14 and Y15 by CDC25 dual phosphatases. The inhibitory phosphorylations at T14 and Y15 are catalyzed by the serine/threonine kinase Wee1 and threonine/tyrosine kinase Myt1 and cause misalignment of the glycine-rich loop (G-loop) and the ATP phosphate moiety. CDKs phosphorylate multiple substrates and the proper regulation of CDKs is necessary for orderly cell cycle phase transitions. A general representation of the key players and events during the cell cycle can be seen in Figure 1-1.

Numerous checkpoints also exist to ensure normal cell cycle progression and the transmission of an unaltered genome. These checkpoints are conserved signaling pathways that monitor cell growth conditions, cell cycle progression, structural and

functional DNA defects, and are critical for cell survival or death. Checkpoint responses induce and sustain a delay in cell cycle progression, and subsequently activate machinery to respond to changes in cell growth conditions, repair DNA and stall replication. When cellular damage cannot be repaired, these checkpoints can induce apoptosis, or programmed cell death. The mammalian checkpoints include the quiescent checkpoint, G_1/S checkpoint, replication checkpoint, G_2 checkpoint, mitotic checkpoint, and the DNA damage checkpoints. Improper checkpoint control promotes tumorigenesis through increased mutation rates, aneuploidy, and chromosome instability. The following sections will give an overview of the regulation of the various phases of the mammalian cell cycle, activation of specific checkpoints, and the molecules involved in the mechanisms that regulate these processes.

From Quiescence to the Point of No Return

G_0-G_1 Transition

Upon cell division, the daughter cell enters into G_0 phase where it becomes ready to divide again before entering into G_1. In most cases, the newly formed cell increases in size and mass for division to occur again, by enhancing ribosome biosynthesis (1). This is accomplished by phosphorylation of the S6 ribosomal subunit by S6 kinase (2). This kinase is regulated by members of the PI3K family, including TOR, PDK1, and PI3K, which are activated by insulin receptor signaling (3, 4). These family members phosphorylate the translational inhibitor 4E-BP1, leading to dissociation of the initiation factor eIEF4E, which promotes cyclin D and Myc translation (5). In the absence of growth factors, these kinases are inactive and unable to signal progression from quiescence to G_1. Acetylation and phosphorylation of the tumor suppressor p53 also appears to be involved in maintaining cellular quiescence (6, 7).

G_1 Phase

In the presence of growth factors during the G_0 and G_1 phases, ras and mitogen-activated protein kinase (MAPK) cascades are activated and subsequently regulate cell cycle progression (8). MAPK directly regulates cyclin D expression by controlling the activation protein-1 (AP-1) and ETS transcription factors, which transactivate the cyclin D promoter (9, 10). Consequently, the MAPK cascade activates cyclin D-dependent kinases (CDK4 and CDK6), and regulates cell

proliferation. Additionally, the MAPK cascade directly regulates the synthesis of the CIP/KIP family of CDK inhibitors (CKIs), specifically $p21^{CIP}$ and $p27^{KIP}$, which negatively regulate CDK activity and influence cyclin D/CDK4/6 complex formation in G_1 (11, 12).The growth factor-dependent synthesis of D-type cyclins occurs during the G_0/G_1 transition and peak in concentration in late G_1 phase (13). These proteins have a very short half-life and are rapidly degraded upon removal of mitogenic stimulation. The INK family of CKIs primarily inhibits cyclin D/CDK4/6 complexes. Only when the concentration of cyclin D exceeds that of the INK proteins can these cyclin D/CDK4/6 complexes overcome their inhibition (14, 15).

In early to mid G_1 phase, active cyclin D/CDK4/6 complexes phosphorylate the three Rb pocket proteins (Rb, p130, and p107), resulting in their partial repression (13). The phosphorylation status of these proteins controls E2F transcriptional activity and S phase entry by mediating passage through the restriction point in late G_1 (16-18). E2F proteins (E2F1-6) form heterodimers with a related family of DP proteins (DP1-3), and can act as both activators and repressors of transcriptional activity, depending on their interaction with Rb. In G_0 and early G_1, Rb is in an active, hypophosphorylated form. Active Rb represses the activity of the E2F transcription factor family by directly binding to the transactivation domain of E2F proteins and recruiting histone deacetylases, methyltransferases, and chromatin remodeling complexes to E2F-regulated promoters (19, 20). This results in the modification of histones, compaction of chromatin structure, and prevents promoter access by transcription machinery (20). Phosphorylation of Rb by cyclin D/CDK4/6 complexes

during G_1 releases histone deacetylase, thereby partially alleviating transcriptional repression (13, 19, 20). As a result, the E2F/DP transcription factors activate the transcription of cyclin E, and the many genes responsible for the G_1/S transition and DNA synthesis, including CDK2, cyclin A, cyclin E, RPA1, MAT1, PCNA, DHFR, c-Myc, DNA polymerase-α, $p220^{NPAT}$, and CDC25A (21).

G_1/S Transition

Cyclin E expression in mid to late G_1 results in the formation of cyclin E/CDK2 complexes, which are required for S phase entry and the initiation of DNA replication. Cyclin E/CDK2 also phosphorylates Rb, except on different residues than those catalyzed by cyclin D/CDK4/6 complexes (22). Cyclin E/CDK2 phosphorylation of Rb promotes the dissociation of E2F transcription factors from Rb, resulting in complete relief of transcriptional repression (23). Thus, Rb inactivation occurs through the sequential phosphorylation by CDK4/6 and CDK2. Further E2F and cyclin E/CDK2 activity increases through a positive feedback mechanism since cyclin E is one of the genes activated by E2F (24). Cyclin E/CDK2 activity further enhances this positive feedback by promoting the degradation of its own inhibitor, $p27^{KIP}$. These complexes have been shown to phosphorylate $p27^{KIP}$ at T187, which promotes its association with the Skp-Cullin-F-box^{SKP2} (SCF^{SKP2}) complex to target $p27^{KIP}$ for ubiquitination and proteasomal degradation (25). Cyclin D/CDK4/6 complexes have been hypothesized to sequester the bound CKI inhibitor $p27^{KIP}$ away from cyclin E/CDK2 complexes to facilitate their activation (26). However, recently

$p27^{KIP}$ was shown to be phosphorylated by Src-family tyrosine kinases at Y88, which reduces its steady-state binding to cyclin E/CDK2. This facilitates $p27^{KIP}$ phosphorylation at T187 by cyclin E/CDK2 to promote its degradation (27, 28). Thus, rather than cyclin D/CDK4/6 sequestration of $p27^{KIP}$, these tyrosine kinases may be responsible for activation of $p27^{KIP}$-bound cyclin E/CDK2 complexes at the G_1/S transition.

The *c-myc* proto-oncogene encodes another transcription factor involved in many processes, including E2F regulation (29). Its expression is induced by mitogenic stimulation, promotes S phase entry in quiescent cells, and increases total cell mass. Myc activates the transcription of cyclin E, CDC25A, and several other genes (30). The Myc-induced proliferation mechanism directly activates cyclin E/CDK2 activity through increased cyclin E levels and CDC25A activity, thereby removing T14 and Y15 inhibitory CDK2 phosphorylation catalyzed by Wee1/Myt1 (31). Additionally, this activity is enhanced indirectly through Myc by mediating the sequestration of $p27^{KIP}$ from cyclin E/CDK2 into cyclin D/CDK4/6 complexes, which in turn promotes the cyclin E/CDK2 catalyzed phosphorylation and degradation of $p27^{KIP}$ (32). Cul-1, a component of the SCF^{SKP2} complex, was shown to be a transcriptional target of Myc, which may explain the link between $p27^{KIP}$ degradation and Myc activation (33).

Cyclin E/CDK2 also phosphorylates $p220^{NPAT}$, a protein involved in the regulation of histone gene expression, a major event that occurs as cells begin to enter S phase (34). The phosphorylation of $p220^{NPAT}$ by cyclin E/CDK2 is required for histone gene expression activation at the onset of S phase (35). Once cells have passed

through the restriction point, they are committed to initiate DNA synthesis and complete mitosis. Cell cycle progression continues independently of the presence of growth factor stimulation after passage through the restriction point.

Regulation of DNA Synthesis and Mitotic Entry

S phase

At the G_1/S transition, the cell enters S phase where DNA synthesis occurs and each chromosome duplicates into two sister chromatids. Upon S phase entry, the initiation of replication occurs at sites on chromosomes termed origins of replication. Replication origins are found in two states within cells: a pre-replicative complex (pre-RC) that is present in G_1 before DNA replication initiation, and the other that exists from the onset of S phase until the end of M phase, or the post-replicative complex (post-RC) (36). At the onset of S phase, there is an increase in cyclin A expression and cyclin A/CDK2 activity (37, 38) and the protein kinase GSK-3β phosphorylates cyclin D and signals its relocalization to the cytoplasm, where it is degraded by the proteasome (39, 40). Cyclin A/E/CDK2 activity controls each round of DNA replication, and dictates the state of the replicative complexes. Low CDK activity permits the assembly of the pre-RC to form a licensed origin at the end of M phase, while the increase in CDK activity during the G_1/S transition triggers initiation of DNA replication and converts origins to the post-RC form (41). Reformation of the pre-RC is prevented by high CDK activity, which acts to inhibit re-replication events that would result in numerous copies of chromosomes.

The initiation of DNA replication requires both the assembly of the pre-RC complex at origins of replication, and activation of these complexes by CDKs and other kinases to initiate DNA synthesis (42-44). Numerous proteins are required for pre-RC formation and DNA replication initiation, and include the Origin Recognition Complex (ORC), cdc6/18, cdc45, cdt1, the GINS complex, and mini chromosome maintenance (MCM) proteins (43). ORC proteins (ORC1-6) bind directly to replication origins as a hexamer and facilitate the loading of other components of the pre-RC (45, 46). The cdc6/18 and cdt1 proteins play a central role in coordinating chromatin licensing. They bind directly to the ORC complex, independently of each other (47). Here, they cooperatively facilitate the loading of the MCM proteins (MCM2-7), which form a hexameric ring-complex that possess ATP-dependent helicase activity (48, 49). Cyclin E/CDK2 is recruited to replication origins through its interaction with cdc6, and regulates cdt1, cdc45 and MCM loading, thereby making chromatin replication competent. Upon binding of the MCM proteins, the affinity of both cdc6/18 and cdt1 for the ORC is reduced, and they dissociate (48, 49). Cyclin A/CDK2 then phosphorylates cdc6 to promote its export from the nucleus and cdt1 to target its ubiquitination by the SCF^{SKP2} complex (50, 51). In this way, after initiation and release of these factors from the ORC, cyclin A/CDK2 activity acts to prevent re-replication by inhibiting reformation of the pre-RC. On the other hand, cyclin E/CDK2 activity primarily acts to promote the initiation of DNA synthesis (52).

Dbf4 dependent kinase (DDK) contains the kinase subunit cdc7, and is also required for DNA replication initiation (53). DDK targets MCMs for phosphorylation,

thereby increasing the affinity of these proteins for cdc45, a factor required for the initiation and completion of DNA replication (49, 54, 55). The GINS complex, consisting of the four subunits Sld5, Psf1, Psf2, and Psf3, is required for the initiation and progression of eukaryotic DNA replication (56). This complex associates with Cdc45 and the MCM proteins to activate their helicase activity. Upon GINS and cdc45 binding to the MCM complex, the DNA is unwound, resulting in single stranded DNA (ssDNA) (49, 57). Replication protein A (RPA) is recruited to single stranded DNA, and is required for the subsequent binding and activation of DNA polymerase-α (58-60). The GINS complex also interacts with, and stimulates the polymerase activity of the DNA polymerase-α-primase complex (61).

G_2 Phase

Upon completion of DNA duplication, the cell enters the second restriction point of the cell cycle, or G_2 phase. Similar to what happens during G_1, in this second gap phase the cell halts in order to synthesize factors required for initiation and completion of mitosis, and check for any aberrations resulting from DNA synthesis (62, 63).

Cyclin B/CDK1 is the primary regulator of the G_2/M transition and its activity is required for entry into mitosis. It was termed the maturation-promoting factor (MPF) because it was originally shown to be essential for *Xenopus* oocytes maturation after hormonal stimulation, and subsequently found to be equivalent to a mitosis-promoting activity (64). CDK1 activity is primarily regulated by localization of cyclin

B, CDC25C activity, and $p21^{CIP}$ levels, which are controlled by checkpoint machinery (65). Cyclin B/CDK1 complexes remain inactive until their activity is required for mitosis entry in late G_2. Towards the end of S phase, cyclin B expression is increased. However, during the onset of G_2, cyclin B is retained in the cytoplasm by its cytoplasmic retention signal (CRS) and the CKI $p21^{CIP}$ inhibits CAK-mediated activation of cyclin/CDKs (66). Additionally, Wee1 and Myt1 phosphorylate T14 and Y15 on cyclin B/CDK1 in the cytoplasm to keep these complexes inactive, even when CDK1 is phosphorylated by CAK (67). The transcription factor p53 also mediates the inhibition of cyclin B/CDK1 activity by promoting p21 expression, and also downregulates expression of CDK1 (63, 68). Furthermore, cyclin A/CDK2 phosphorylates and inactivates members of the E2F transcription family in G_2 to suppress cell growth during this gap as well (69-71).

G_2/M Transition

During the G_2/M transition, the localization of cyclin B changes dramatically and regulates CDK1 activity (72). The CRS is phosphorylated by MAPK and polo-like kinase 1 (Plk1), which promotes its nuclear translocation (73, 74). Upon nuclear import, cyclin B is phosphorylated further to prevent association with CRM1, thus promoting its nuclear retention (75, 76). This relocalization occurs at the onset of mitosis towards the end of the G_2/M transition when the cell is ready to begin the mitotic process (77). Activation of cyclin B/CDK1 in late G_2 is achieved by preventing the access of cytoplasmic Wee1/Myt1 kinases to the complex and

promoting shuttling of the CDC25 phosphatases to the nucleus, where they dephosphorylate and activate CDK1 (78-80). Cyclin B/CDK1 complexes also phosphorylate CDC25A to promote its stability, and CDC25C to promote its activity (81). Both CDC25A and CDC25C further activate CDK1, resulting in a positive feedback loop that sustains cyclin B/CDK1 activity in the nucleus to signal mitotic entry (82, 83). ERK-MAP kinases also regulate cyclin B/CDK1 activity by phosphorylating CDC25C at T48 (84). ERK1/2 activation of CDC25C leads to removal of inhibitory phosphorylations of cyclin B/CDK1 complexes and is required for efficient mitotic induction. Thus, MAPKs are also involved in the positive feedback loop leading to cyclin B/CDK1 activation.

The increase in nuclear cyclin B/CDK1 activity promotes phosphorylation of nuclear substrates that are necessary for mitosis, such as nuclear envelope breakdown, spindle formation, chromatin condensation, and restructuring of the Golgi and endoplasmic reticulum (ER) (85, 86). Numerous cyclin B/CDK1 substrates have been defined, including nuclear lamins, nucleolar proteins, centrosomal proteins, components of the nuclear pore complex, and microtubule-associated proteins (87-89). Cyclin B/CDK1 complexes also phosphorylate MCM4 to block replication of DNA, the TFIIH subunit of RNA polymerase II to inhibit transcription, and the ribosomal S6 protein kinase to prevent translation during mitosis (90-92).

Regulation of Cell Division

The Centrosome

The centrosome is normally comprised of two centrioles and the pericentriolar material. It not only functions as a microtubule nucleation center, but also as an integrated regulator of cell cycle checkpoints. Recent data also indicates it is required for cell cycle progression (93). The centrosome duplication process begins in late G_1 and is primarily regulated by CDK2 activity (94). Cyclin A/E/CDK2 phosphorylates the Mps1p kinase and nucleophosmin, two centrosome associated proteins. CDK2 activity is required for Mps1p stability and Mps1p-dependent centrosome duplication (95). Cyclin E/CDK2 phosphorylates nucleophosmin at T199, releasing it from unduplicated centrosomes, a requirement for centrosome duplication (96). Completion of centrosome duplication and initiation of their separation occur in G_2 and are dependent on cyclinA/E/CDK2 activity. These processes are necessary for proper spindle formation and balanced chromosome separation during mitosis.

The Aurora kinase family members play a role in centrosome function, spindle assembly, and chromosome alignment, and are essential for mitosis. Specifically, Aurora –A activity is maximal during G_2/M and regulates mitotic spindle assembly, centrosome separation, and facilitates the G_2/M transition by phosphorylating CDC25B at the centrosome, an important event for cyclin B localization to the nucleus (97). Aurora-B activity is maximal from metaphase to the end of mitosis and regulates chromatin protein modification, chromatid separation, and cytokinesis (98). During mitosis, a complex process of degradation and phosphorylation tightly regulate Aurora kinase activity to ensure proper mitotic advancement. Aurora-A is activated mainly by autophosphorylation (99), Ajuba (100), TPX2 (101), and HEF1 (102), while INCENP

is thought to activate Aurora-B (103). Both Aurora-A and B are degraded rapidly at the end of mitosis.

M Phase

The mitotic phase is divided into five phases, including prophase, prometaphase, metaphase, anaphase, and telophase. During prophase, nucleoli disappear, chromatin condensation takes place, and the mitotic spindle is formed at centrosomes that contain centrioles. In prometaphase, fragmentation of the nuclear envelope occurs and mitotic spindles extend from the poles toward the center of the cell. At metaphase, centrioles pair at opposite poles and the chromosomes align in the cell center, along the metaphase plate. Microtubules then bind to the kinetochores located at the centromeres of each chromatid of the chromosomes. The transition from metaphase to anaphase is triggered by MPF inactivation through the degradation of cyclin B by the E3 ubiquitin ligase anaphase promoting complex (APC/C) (104). Cdc20 is required for activation of the ubiquitin ligase activity of APC/C, which promotes degradation of securin. Subsequently, a release mechanism activates the protease known as separase, which cleaves cohesion, thereby promoting sister chromatid separation and anaphase entry (105, 106). This induces the separation of chromatids in anaphase as microtubules from each pole pull them apart through their kinetochore. In late anaphase, as a result of cyclin-B/Cdk1 inactivation, the major ubiquitin ligase activity is switched from APC/C-Cdc20 to APC/C-Cdh1. The latter continues to regulate many proteins whose

degradation is required for cell cycle progression, including Cdc20 which also becomes one of its targets and a substrate of the Aurora kinases. (107-111).

In telophase, nuclei for each daughter cell form at the two poles and the mitotic spindle apparatus disappears. Furthermore, nuclear membranes, nuclear lamina, nuclear pores and nucleoli are reformed. The cell is now ready for cytokinesis, or physical division of the cytoplasm. The cytoplasm divides as actin/myosin filaments contract and pinch off the plasma membrane, resulting in two daughter cells that enter into G_0 or G_1 for another round of division. The main checkpoint that exists during M phase in mammalian cells is the spindle checkpoint, and is in place to ensure proper microtubule assembly, proper cell division and that each daughter cell receives one copy of DNA.

Spindle Checkpoint

The spindle checkpoint is activated when microtubules fail to attach to the kinetochores of each sister chromatid and/or when there is misalignment of chromosomes along the metaphase plate (112-114). This mechanism blocks entry into anaphase and ensures proper segregation of the chromatids to opposite spindle poles. Misregulation of this checkpoint results in aneuploid daughter cells after division (115, 116). Checkpoint proteins associated with kinetochores monitor microtubule-kinetochore attachment and tension, and regulate this checkpoint by preventing cdc20 binding to the APC/C (117-119).

The main spindle checkpoint proteins include Mad1, Mad2, BubR1, Bub1, Bub3, Mps1p, and CENP-E. These proteins act both independently and dependently of their interaction with kinetochores. Association of Mad2 with kinetochores and cdc20 requires the presence of Mad1 (120). At the kinetochore, Mad2 is converted to a form capable of binding and sequestering cdc20 away from the APC/C, resulting in its inhibition (121). Additionally, formation of the mitotic checkpoint complex BubR1/Bub3/Mad2/cdc20 (MCC) occurs independently of interaction with unattached kinetochores, and signals anaphase to wait by directly binding and inhibiting the APC/C (122, 123). An unattached kinetochore activates a kinase cascade involving the dual-specificity kinase Mps1p, and the serine/threonine kinases BubR1 and Bub1 that amplifies this wait signal (124, 125). Furthermore, BubR1 directly interacts with the kinesin-like protein CENP-E to regulate microtubule tension at kinetochores, which is also involved in regulation of the spindle checkpoint (126, 127). Thus, this checkpoint serves to inhibit the APC/C indirectly through cdc20 sequestration and directly through association with MCC, and regulates the tension at kinetochores required for anaphase entry (128).

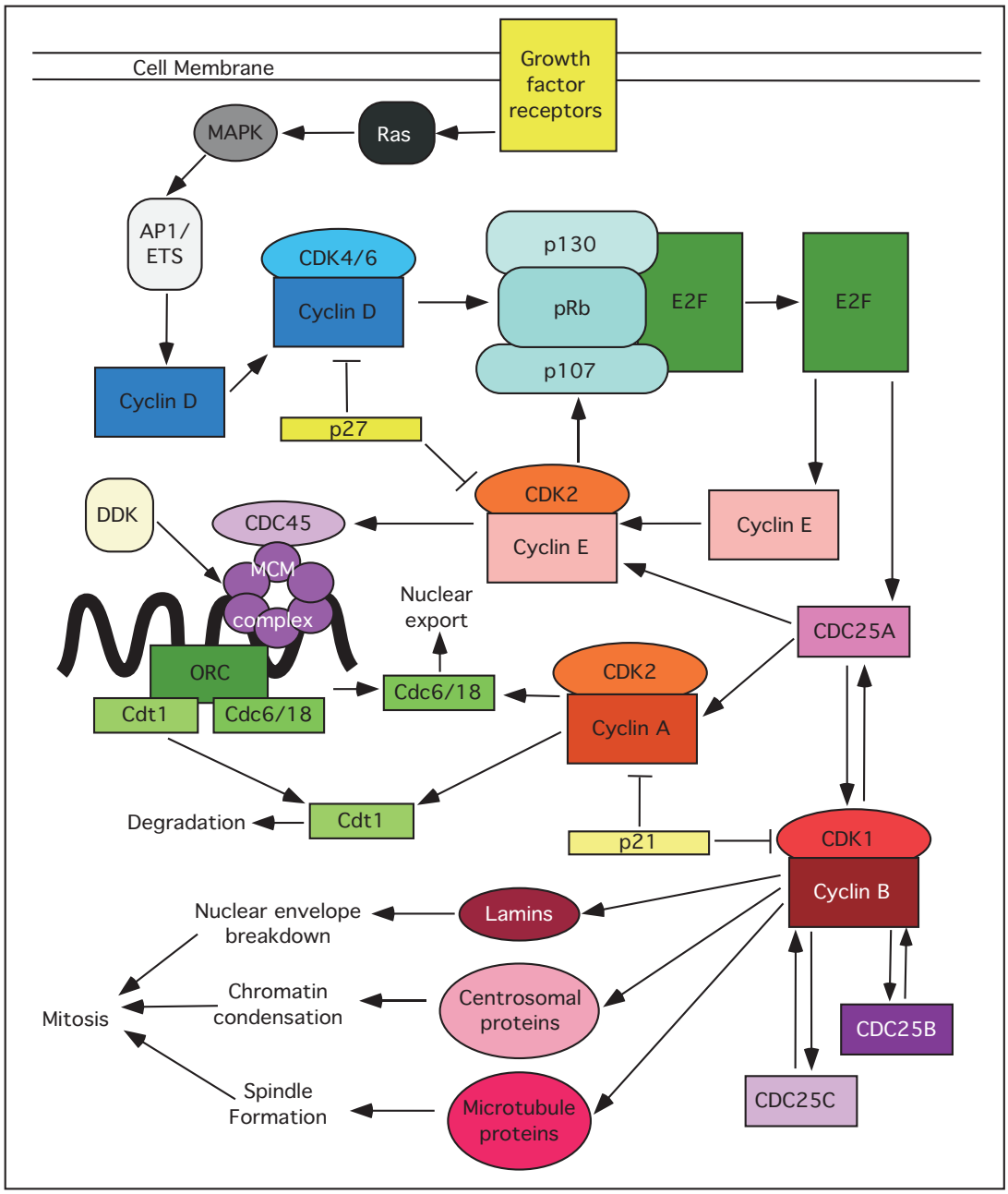

Figure 1-1. Regulation of the mammalian cell cycle by cyclin/CDKs.
Activation of growth factor receptors in G0 leads to activation of many signaling cascades leading to the expression of cyclin D. Progression into S phase is mediated by Rb and E2Fs leading to the initiation and progression of DNA synthesis through cyclin E/A/CDK2 activity. Upon completion of DNA replication cyclin B/CDK1 activity promotes phosphorylation of substrates required for entry into mitosis and eventual cytokinesis, producing two identical daughter cells.

DNA Damage Checkpoints

In addition to checkpoints that ensure normal cell cycle progression, there are numerous DNA damage checkpoints in mammalian cells. These exist to regulate the highly conserved mechanisms controlling DNA replication and mitosis to ensure mutations within the genome are not passed on to the daughter cells. Misregulation of these pathways is associated with genomic instability and cancer development. The key players involved in the DNA damage checkpoint cascade (Figure 1-2) include the DNA damage sensors ATM (Ataxia Telangiectasia Mutated), ATR (ATM and Rad3 Related), Rad1, Rad9, Hus1, and ATRIP, and the effectors Chk1/2 (Checkpoint Kinase 1/2), and CDC25.

G_1/S Phase Checkpoint

The primary DNA damage checkpoint is the G_1/S checkpoint, and acts to prevent the replication initiation of damaged DNA. During G_1 and even after passage through the restriction point (but prior to initiation of DNA synthesis), DNA damage sequentially activates two checkpoint-signaling pathways, and both function to inhibit CDK2 activity. The first pathway initiated is p53-independent and is very rapid and short lived (129). This pathway results in phosphorylation and degradation of CDC25A (130, 131). DNA damage leads to the activation of ATM and ATR, which phosphorylate and activate Chk1 and Chk2 (132, 133). CDC25A is phosphorylated by these kinases, and target its ubiquitination and proteasomal degradation (134). As a result, the inhibitory phosphorylations of CDK2 are increased, effectively diminishing

CDK2 activity. This lack of CDK2 activity ultimately inhibits cdc45 loading to pre-RCs, and the subsequent initiation of DNA replication, to halt the cell cycle and allow time for repair of the damaged DNA (133).

The second pathway activated in the presence of DNA damage prior to initiation of DNA synthesis acts in a p53-dependent manner. As stated above, the tumor suppressor p53, is a transcription factor, and acts primarily to increase expression of the CKI $p21^{CIP}$ during DNA damage. Like CDC25A, the activation of ATM/ATR promotes the phosphorylation of p53, which enhances the stability of p53 by preventing efficient interaction with the E3 ubiquitin ligase MDM2, a protein responsible for targeting p53 degradation (135). This leads to the transcription and accumulation of p21, thereby effectively silencing CDK2 activity to prevent cell cycle progression and allow for DNA repair (136). MDM2 is also a target of p53 transcription, which creates a negative feedback loop with p53 (137). After repair of damaged DNA has been completed, the checkpoint is turned off and progression into S phase resumes.

S Phase Checkpoints

Cells that have passed the G_1/S checkpoint are ready to begin S phase and DNA replication. The S phase checkpoints are a group of three mechanistically distinguishable checkpoints (138) of which two respond directly to DNA damage. One is independent of ongoing replication and is activated in response to DNA double-stranded breaks (DSBs) and is known as the intra-S Phase checkpoint. The second

checkpoint, the replication checkpoint, responds to replication fork stalling caused by the collision of replication machinery with DNA damage, the direct inhibition of polymerases, or depletion of dNTPs. Although these two checkpoints respond to different forms of stress, both prevent cell cycle advance, inhibit ongoing replication, prevent origin firing, and stabilize the replication fork so that repair and replication resumption can occur. The third type of S phase checkpoint is the S/M checkpoint. This checkpoint is currently not understood as well as the previous two, but is known to prevent entry into mitosis when replication is stalled or incomplete. It acts to preserve genomic stability by preventing premature chromatin condensation and breaks at common fragile sites.

The Replication Checkpoint

The replication checkpoint is activated when the replication machinery encounters DNA damage or when the replicative polymerase is inhibited and stalls (139, 140). This checkpoint stabilizes stalled replication forks and signals for DNA damage repair while preventing exit from S phase. Stalling causes uncoupling of the helicase from the polymerase, leading to DNA unwinding, without subsequent new strand polymerization. This leads to accumulation of ssDNA, a trigger for checkpoint activation (141-143). ssDNA is also believed to activate other checkpoints, including those initiated by DNA repair mechanisms such as nucleotide excision repair (144, 145) or recession of DSBs generated during homologous recombination (146, 147). The ssDNA is coated by RPA proteins (148, 149), which set up a scaffold for the

recruitment and localization of DNA damage sensors in S phase. ATR is central to the replication checkpoint and is recruited to RPA coated ssDNA through its interaction with its binding partner, ATRIP (150-152). In addition, other sensors of DNA damage including Rad17, an RFC-like clamp loader, and the 9-1-1 complex, a heterotrimeric clamp composed of Rad9, Rad1, and Hus1, are recruited to RPA coated ssDNA and serve to fully activate ATR and help recruit and activate downstream mediators of the checkpoint (153-155).

After ATR activation and recruitment/activation of other sensors, numerous proteins are recruited to the site of damage and act as mediators of the DNA damage signaling cascade. The majority of these mediators are involved in the activation of the effecter kinase Chk1 (156). One of these mediators, Claspin, is recruited to sites of damage, is phosphorylated by ATR, and subsequently recruits Chk1. Direct interaction between Claspin and Chk1 is required for phosphorylation and activation by ATR (157-160). Other mediators include BRCA1 and BRCA1 C-terminal motif (BRCT) containing proteins. These mediators form large multimeric complexes and are often visualized as nuclear foci by immunofluorescence microscopy (156, 161). MDC1 (Mediator of DNA damage-checkpoint protein 1) further recruits mediators of the checkpoint such as 53BP1 and NBS1 (162-164). These proteins function to maintain foci oligomerization and promote ATR mediated phosphorylation of its substrates which include all of these mediators and SMC1 (Structural maintenance of chromosomes 1). SMC1 is part of the cohesin complex and is required for sister chromatid cohesion in S phase (165, 166).

Finally, Chk1 is recruited to these nuclear foci containing the large scaffold of BRCT containing proteins and is activated in an ATR/Rad17/9-1-1/BRCA1/Claspin dependent fashion (157-159). Chk1 then facilitates the checkpoint by phosphorylating CDC25 family members (167) and p53 (see above for more detail on these events) leading to cell cycle arrest, DNA repair, and survival choices.

The Intra-S Phase Checkpoint

Unlike the replication checkpoint, the intra-S phase checkpoint does not require replication to be activated (138, 168). At the head of this checkpoint is the ATM protein kinase, a member of the PI3K family of protein kinases (including ATR and DNA-PK). ATM and the intra-S phase checkpoint are activated by the detection of DSBs, which can be achieved without direct interaction of the replication machinery with sites of damage. Another interesting difference between the replication checkpoint and the intra-S phase checkpoint is that activation of the latter does not alter the progression of active replication units, only inhibition of late origin firing (169). Thus, the intra-S phase checkpoint causes delays in, but not complete arrest of, S phase progression (138). While the sensors of DSBs are not definitively known, two protein complexes serve as excellent candidates due to their ability to enhance ATM activity. These complexes are the MRN (Mre11-Nbs1-Rad50) complex and the Rad17/9-1-1 complex (discussed above). The MRN complex has nuclease activity and localizes to DSBs independently of ATM. At sites of damage, it plays a role in activation of ATM, efficient phosphorylation of ATM substrates, and recession

of DSBs (170-172). While much of the checkpoint from here out involves the same mediators including 53BP1, BRCA1, MDC1, and SMC1, it has two more distinct features compared to the replication checkpoint.

The first involves the recession of DSBs, which activates a parallel ATR/ssDNA signaling cascade similar to that discussed above (146, 173, 174). The second involves the activation of Chk2. Unlike Chk1, which is only present in S and G_2 phases, Chk2 is present throughout the entire cell cycle (175, 176). Chk2 also differs from Chk1 in that it must dimerize to be fully active (177-179) and in response to DNA damage it becomes soluble in the nucleus and dissipates from damage sites as a mechanism to enhance signaling (180, 181). When phosphorylated by ATM, Chk2 plays similar roles as Chk1, specifically in the degradation of CDC25 family members and phosphorylation of p53.

While the replication and intra-S phase checkpoints have distinct mechanisms of activation and signaling, the final goal is the same: delay or inhibit S phase progression providing time and signaling events that lead to DNA repair, so that mutations are not transmitted to daughter cells in the ensuing mitotic division.

S/M Checkpoint

The S/M checkpoint can be activated by replication inhibition or when DNA replication is not completed (182-186). This checkpoint signals through the ATR/Chk1 pathways and prevents premature chromatin condensation (PCC) and entry into mitosis (183, 185, 187). Depletion of ATR in *Xenopus* egg extracts or Chk1 in

embryonic stem cells, results in premature entry into mitosis prior to completion of replication (183, 185). In addition, different regions of the genome replicate at different rates and common fragile sites are known to be late replicating regions. These common fragile sites are often left unreplicated upon mitotic entry (188-191). PCC causes breaks when fragile sites are not fully replicated (189). Therefore, mitotic delay is required to ensure the proper replication of the entire genome to prevent breaks that might occur due to PCC. Both ATR (187) and Chk1 (188) are involved in the stability of common fragile sites, indicating that the S/M checkpoint is required to maintain genomic stability by ensuring proper replication prior to mitotic entry.

G_2/M Phase Checkpoint

The G_2/M checkpoint acts to ensure that cells, which experience DNA damage in G_2 or contain unresolved damage from the previous G_1 or S phase, do not initiate mitosis. Much like the G_1 checkpoint and in some contrast to the S checkpoints, cell cycle arrest or delay resulting from the G_2 checkpoint involves a combination of acute/transient and delayed/sustained mechanisms. The acute/transient mechanisms involve the rapid post-translational modification of effector proteins, while the delayed/sustained mechanism involves the alteration of transcriptional programs (192).

Of all the molecules targeted in the G_2/M checkpoint, cyclin B/CDK1 seems to be the most important as its activity directly stimulates mitotic entry. DNA damage in the G_2 phase activates ATM/ATR pathways (as described above) resulting in

Chk1/Chk2-mediated inhibition of the Cdc25C phosphatase that would normally activate CDK1 and trigger transition through the G2/M boundary. In G_2, Cdc25B is also targeted for degradation by Chk1 and Chk2, via the mechanisms described above, and is the only known mechanism of cell cycle arrest that is shared across all the checkpoints. Cdc25 degradation is one of the key mechanisms of the acute/transient branch of the checkpoint.

The more delayed and prolonged mechanisms by which the checkpoint silences CDK1 activity is through the activation of the p53 pathway. Activation of p53 is achieved by phosphorylation by ATM/ATR or Chk1/Chk2 and results in nuclear localization, tetramerization, and stimulation of p53 transcriptional activity toward $p21^{CIP}$. In G_2, BRCA1 can stimulate p21 expression in a p53 independent fashion (193), and along with two other p53 targets, GADD45 and 14-3-3ε may cooperate to achieve maximal inhibition of CDK1 and prevent mitotic entry to allow for repair of DNA lesions (68).

The centrosome also regulates the G_2/M DNA damage response, and numerous checkpoint proteins are associated with the centrosome (194). Centrosome separation is regulated by the kinases Nek2 and Plk1 and this process is inhibited by DNA damage in an ATM-dependent manner. ATM activation leads to Plk1 and Nek2 inhibition resulting in de-regulation of the centrosome (195). By this mechanism, centrosome separation is inhibited and contributes to maintaining the G_2/M checkpoint (196). Plk1 is also known to phosphorylate and activate CDC25C (197). Thus, Plk1

inhibition also results in CDC25C inhibition, inactivation of cyclin B/CDK1, and a halt in cell cycle progression.

Normally, cell cycle progression resumes when DNA damage repair is completed, or apoptosis prevents genomic instability if the damage is excessive and beyond repair. However, data from *S. cerevisiae*, *Xenopus*, and recently human cells, suggests pathways to re-enter cell cycle progression exists even when unrepaired DNA damage is present. This process of "checkpoint adaptation" has been shown to allow mitotic entry in response to ionizing radiation (IR) in human cells, in a Plk1 dependent manner, and may promote carcinogenesis and genomic instability (198, 199). It has been speculated that activation of centrosomal cyclin B/CDK1 plays a central role in this process, and may occur through Plk1 mediated degradation of Wee1 and/or inhibition of Chk1 activity leading to stabilization of CDC25 (200). Although its function is not well understood, checkpoint adaptation has been proposed to move cells into a phase where they can die, allow progression into other phases where difficult DNA damage is able to be repaired, and even exist to allow natural evolution (201).

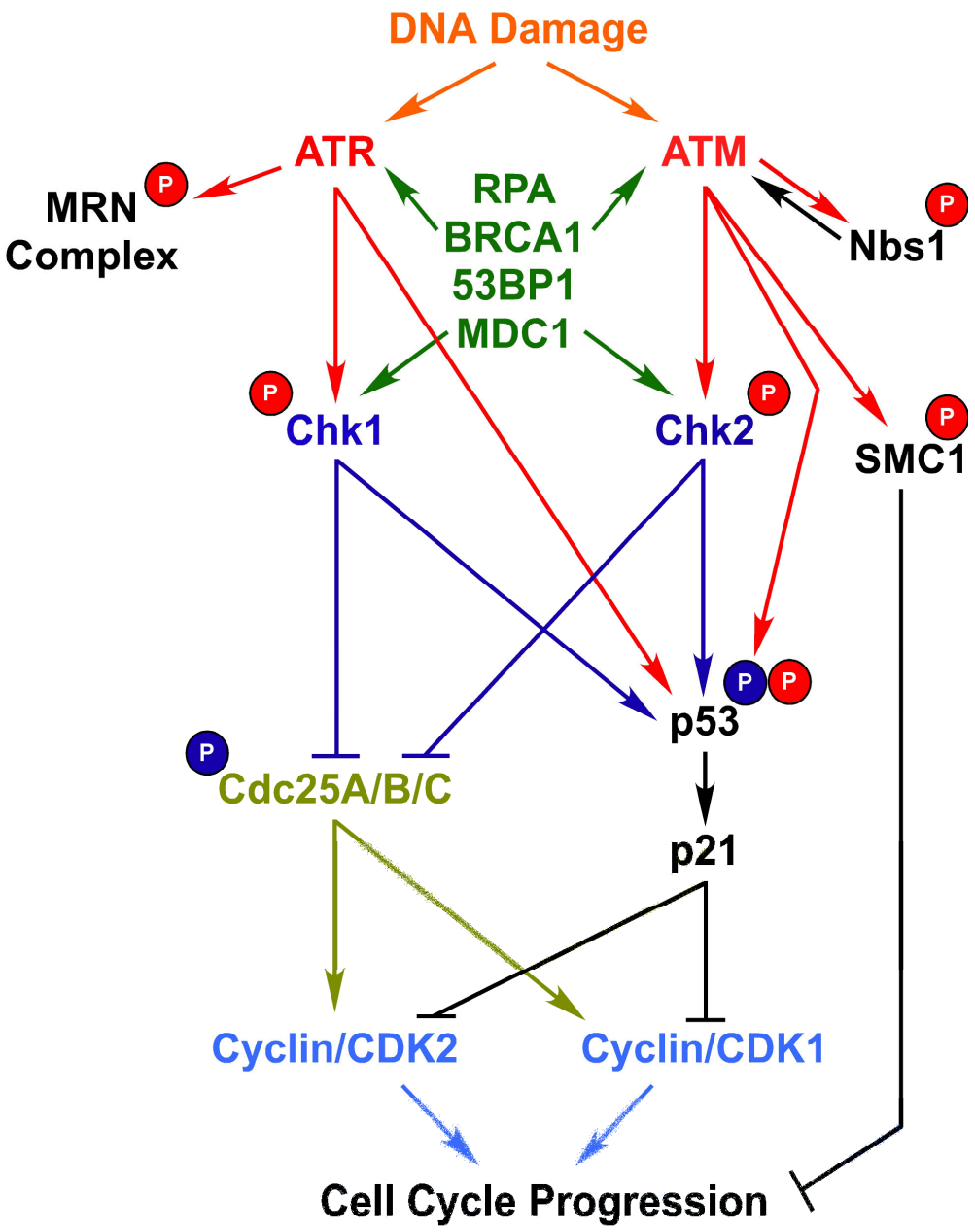

Figure 1-2. Brief model of DNA damage checkpoint signaling.
DNA damage elicits a conserved response headed by the ATM and ATR kinases. Phosphorylation cascades and localization of mediators to sites of damage, allows for signaling to the effector kinases Chk1 and Chk2. Chk1/2 elicit cell cycle arrest through phosphorylation-dependent degradation of the Cdc25 family of phosphatases. Parallel activation of p53 by both ATM/ATR and Chk1/Chk2 leads to upregulation of the CDK inhibitor p21, further enforcing cell cycle arrest. See text for in depth discussion of the checkpoint pathways.

Conclusions

The mammalian cell cycle is controlled by numerous factors involved in regulation of CDKs and checkpoint responses. Although many proteins involved in the pathways leading to activation or inactivation of these have been elucidated over the years, much remains to be explored. Although the majority of CDKs control the cell division cycle, regulation of the cell cycle is clearly more than progression from growth to DNA synthesis to division and transmission of genetic material. There is growing evidence for the role of CDKs in controlling the balance between senescence, cell growth, checkpoint activation, and apoptotic signaling. Clearly, the inability to properly respond to DNA damage and cellular stress through checkpoint activation and apoptosis has a role in oncogenic potential as well as therapeutic considerations. The identification of novel factors and signal cascades mediating the regulation of the cell cycle will ultimately lead to new drug targets in the fight against cancer and numerous other diseases.

Acknowledgements

Chapter 1, in full, is material published in The Wiley Encyclopedia of Chemical Biology, McAndrew, CW; Gastwirt, RF; and Donoghue, DJ (2007). The dissertation author was the primary author of this paper.

References

1. Geyer PK, Meyuhas O, Perry RP, Johnson LF. Regulation of ribosomal protein mRNA content and translation in growth-stimulated mouse fibroblasts. Mol Cell Biol 1982;2(6):685-93.

2. Dufner A, Thomas G. Ribosomal S6 kinase signaling and the control of translation. Exp Cell Res 1999;253(1):100-9.

3. Long X, Muller F, Avruch J. TOR action in mammalian cells and in Caenorhabditis elegans. Curr Top Microbiol Immunol 2004;279:115-38.

4. Um SH, D'Alessio D, Thomas G. Nutrient overload, insulin resistance, and ribosomal protein S6 kinase 1, S6K1. Cell Metab 2006;3(6):393-402.

5. Costa LJ. Aspects of mTOR biology and the use of mTOR inhibitors in non-Hodgkin's lymphoma. Cancer Treat Rev 2007;33(1):78-84.

6. Brooks CL, Gu W. Ubiquitination, phosphorylation and acetylation: the molecular basis for p53 regulation. Curr Opin Cell Biol 2003;15(2):164-71.

7. Knights CD, Catania J, Di Giovanni S, et al. Distinct p53 acetylation cassettes differentially influence gene-expression patterns and cell fate. J Cell Biol 2006;173(4):533-44.

8. Torii S, Yamamoto T, Tsuchiya Y, Nishida E. ERK MAP kinase in G cell cycle progression and cancer. Cancer Sci 2006;97(8):697-702.

9. Shaulian E, Karin M. AP-1 in cell proliferation and survival. Oncogene 2001;20(19):2390-400.

10. Shen Q, Uray IP, Li Y, et al. The AP-1 transcription factor regulates breast cancer cell growth via cyclins and E2F factors. Oncogene 2007.

11. Milde-Langosch K, Bamberger AM, Methner C, Rieck G, Loning T. Expression of cell cycle-regulatory proteins rb, p16/MTS1, p27/KIP1, p21/WAF1,

cyclin D1 and cyclin E in breast cancer: correlations with expression of activating protein-1 family members. Int J Cancer 2000;87(4):468-72.

12. Sherr CJ, Roberts JM. CDK inhibitors: positive and negative regulators of G1-phase progression. Genes Dev 1999;13(12):1501-12.

13. Coqueret O. Linking cyclins to transcriptional control. Gene 2002;299(1-2):35-55.

14. Ekholm SV, Reed SI. Regulation of G(1) cyclin-dependent kinases in the mammalian cell cycle. Curr Opin Cell Biol 2000;12(6):676-84.

15. Ohtani N, Yamakoshi K, Takahashi A, Hara E. The p16INK4a-RB pathway: molecular link between cellular senescence and tumor suppression. J Med Invest 2004;51(3-4):146-53.

16. Weinberg RA. The retinoblastoma protein and cell cycle control. Cell 1995;81(3):323-30.

17. Harbour JW, Dean DC. The Rb/E2F pathway: expanding roles and emerging paradigms. Genes Dev 2000;14(19):2393-409.

18. Sherr CJ. The Pezcoller lecture: cancer cell cycles revisited. Cancer Res 2000;60(14):3689-95.

19. Harbour JW, Dean DC. Chromatin remodeling and Rb activity. Curr Opin Cell Biol 2000;12(6):685-9.

20. Wang C, Fu M, Mani S, Wadler S, Senderowicz AM, Pestell RG. Histone acetylation and the cell-cycle in cancer. Front Biosci 2001;6:D610-29.

21. Muller H, Bracken AP, Vernell R, et al. E2Fs regulate the expression of genes involved in differentiation, development, proliferation, and apoptosis. Genes Dev 2001;15(3):267-85.

22. Lundberg AS, Weinberg RA. Functional inactivation of the retinoblastoma protein requires sequential modification by at least two distinct cyclin-cdk complexes. Mol Cell Biol 1998;18(2):753-61.

23. Dynlacht BD, Flores O, Lees JA, Harlow E. Differential regulation of E2F transactivation by cyclin/cdk2 complexes. Genes Dev 1994;8(15):1772-86.

24. Geng Y, Eaton EN, Picon M, et al. Regulation of cyclin E transcription by E2Fs and retinoblastoma protein. Oncogene 1996;12(6):1173-80.

25. Nakayama KI, Hatakeyama S, Nakayama K. Regulation of the cell cycle at the G1-S transition by proteolysis of cyclin E and p27Kip1. Biochem Biophys Res Commun 2001;282(4):853-60.

26. Soos TJ, Kiyokawa H, Yan JS, et al. Formation of p27-CDK complexes during the human mitotic cell cycle. Cell Growth Differ 1996;7(2):135-46.

27. Chu I, Sun J, Arnaout A, et al. p27 phosphorylation by Src regulates inhibition of cyclin E-Cdk2. Cell 2007;128(2):281-94.

28. Grimmler M, Wang Y, Mund T, et al. Cdk-inhibitory activity and stability of p27Kip1 are directly regulated by oncogenic tyrosine kinases. Cell 2007;128(2):269-80.

29. Obaya AJ, Mateyak MK, Sedivy JM. Mysterious liaisons: the relationship between c-Myc and the cell cycle. Oncogene 1999;18(19):2934-41.

30. Leone G, DeGregori J, Sears R, Jakoi L, Nevins JR. Myc and Ras collaborate in inducing accumulation of active cyclin E/Cdk2 and E2F. Nature 1997;387(6631):422-6.

31. Berns K, Hijmans EM, Bernards R. Repression of c-Myc responsive genes in cycling cells causes G1 arrest through reduction of cyclin E/CDK2 kinase activity. Oncogene 1997;15(11):1347-56.

32. Muller D, Bouchard C, Rudolph B, et al. Cdk2-dependent phosphorylation of p27 facilitates its Myc-induced release from cyclin E/cdk2 complexes. Oncogene 1997;15(21):2561-76.

33. O'Hagan RC, Ohh M, David G, et al. Myc-enhanced expression of Cul1 promotes ubiquitin-dependent proteolysis and cell cycle progression. Genes Dev 2000;14(17):2185-91.

34. Zhao J, Kennedy BK, Lawrence BD, et al. NPAT links cyclin E-Cdk2 to the regulation of replication-dependent histone gene transcription. Genes Dev 2000;14(18):2283-97.

35. Stein GS, van Wijnen AJ, Stein JL, et al. An architectural perspective of cell-cycle control at the G1/S phase cell-cycle transition. J Cell Physiol 2006;209(3):706-10.

36. Zannis-Hadjopoulos M, Sibani S, Price GB. Eucaryotic replication origin binding proteins. Front Biosci 2004;9:2133-43.

37. Desdouets C, Sobczak-Thepot J, Murphy M, Brechot C. Cyclin A: function and expression during cell proliferation. Prog Cell Cycle Res 1995;1:115-23.

38. Yam CH, Fung TK, Poon RY. Cyclin A in cell cycle control and cancer. Cell Mol Life Sci 2002;59(8):1317-26.

39. Benzeno S, Lu F, Guo M, et al. Identification of mutations that disrupt phosphorylation-dependent nuclear export of cyclin D1. Oncogene 2006;25(47):6291-303.

40. Diehl JA, Cheng M, Roussel MF, Sherr CJ. Glycogen synthase kinase-3beta regulates cyclin D1 proteolysis and subcellular localization. Genes Dev 1998;12(22):3499-511.

41. Diffley JF. Regulation of early events in chromosome replication. Curr Biol 2004;14(18):R778-86.

42. Stillman B. Cell cycle control of DNA replication. Science 1996;274(5293):1659-64.

43. Teer JK, Dutta A. Regulation of S phase. Results Probl Cell Differ 2006;42:31-63.

44. Ritzi M, Knippers R. Initiation of genome replication: assembly and disassembly of replication-competent chromatin. Gene 2000;245(1):13-20.

45. Da-Silva LF, Duncker BP. ORC function in late G1: maintaining the license for DNA replication. Cell Cycle 2007;6(2):128-30.

46. DePamphilis ML. The 'ORC cycle': a novel pathway for regulating eukaryotic DNA replication. Gene 2003;310:1-15.

47. Hua XH, Newport J. Identification of a preinitiation step in DNA replication that is independent of origin recognition complex and cdc6, but dependent on cdk2. J Cell Biol 1998;140(2):271-81.

48. Maiorano D, Lutzmann M, Mechali M. MCM proteins and DNA replication. Curr Opin Cell Biol 2006;18(2):130-6.

49. Lei M, Tye BK. Initiating DNA synthesis: from recruiting to activating the MCM complex. J Cell Sci 2001;114(Pt 8):1447-54.

50. Liu E, Li X, Yan F, Zhao Q, Wu X. Cyclin-dependent kinases phosphorylate human Cdt1 and induce its degradation. J Biol Chem 2004;279(17):17283-8.

51. Petersen BO, Lukas J, Sorensen CS, Bartek J, Helin K. Phosphorylation of mammalian CDC6 by cyclin A/CDK2 regulates its subcellular localization. Embo J 1999;18(2):396-410.

52. Woo RA, Poon RY. Cyclin-dependent kinases and S phase control in mammalian cells. Cell Cycle 2003;2(4):316-24.

53. Jiang W, McDonald D, Hope TJ, Hunter T. Mammalian Cdc7-Dbf4 protein kinase complex is essential for initiation of DNA replication. Embo J 1999;18(20):5703-13.

54. Masai H, Taniyama C, Ogino K, et al. Phosphorylation of MCM4 by Cdc7 kinase facilitates its interaction with Cdc45 on the chromatin. J Biol Chem 2006;281(51):39249-61.

55. Sheu YJ, Stillman B. Cdc7-Dbf4 phosphorylates MCM proteins via a docking site-mediated mechanism to promote S phase progression. Mol Cell 2006;24(1):101-13.

56. Chang YP, Wang G, Bermudez V, Hurwitz J, Chen XS. Crystal structure of the GINS complex and functional insights into its role in DNA replication. Proc Natl Acad Sci U S A 2007;104(31):12685-90.

57. Zou L, Stillman B. Formation of a preinitiation complex by S-phase cyclin CDK-dependent loading of Cdc45p onto chromatin. Science 1998;280(5363):593-6.

58. Sharova NP, Abramova EB. Initiation of DNA replication in eukaryotes is an intriguing cascade of protein interactions. Biochemistry (Mosc) 2002;67(11):1217-23.

59. Walter J, Newport J. Initiation of eukaryotic DNA replication: origin unwinding and sequential chromatin association of Cdc45, RPA, and DNA polymerase alpha. Mol Cell 2000;5(4):617-27.

60. Zou L, Stillman B. Assembly of a complex containing Cdc45p, replication protein A, and Mcm2p at replication origins controlled by S-phase cyclin-dependent kinases and Cdc7p-Dbf4p kinase. Mol Cell Biol 2000;20(9):3086-96.

61. De Falco M, Ferrari E, De Felice M, Rossi M, Hubscher U, Pisani FM. The human GINS complex binds to and specifically stimulates human DNA polymerase alpha-primase. EMBO Rep 2007;8(1):99-103.

62. Stark GR, Taylor WR. Analyzing the G2/M checkpoint. Methods Mol Biol 2004;280:51-82.

63. Stark GR, Taylor WR. Control of the G2/M transition. Mol Biotechnol 2006;32(3):227-48.

64. Pines J. Regulation of the G2 to M transition. Results Probl Cell Differ 1998;22:57-78.

65. Jackman MR, Pines JN. Cyclins and the G2/M transition. Cancer Surv 1997;29:47-73.

66. Aprelikova O, Xiong Y, Liu ET. Both p16 and p21 families of cyclin-dependent kinase (CDK) inhibitors block the phosphorylation of cyclin-dependent kinases by the CDK-activating kinase. J Biol Chem 1995;270(31):18195-7.

67. Fattaey A, Booher RN. Myt1: a Wee1-type kinase that phosphorylates Cdc2 on residue Thr14. Prog Cell Cycle Res 1997;3:233-40.

68. Taylor WR, Stark GR. Regulation of the G2/M transition by p53. Oncogene 2001;20(15):1803-15.

69. Dynlacht BD, Moberg K, Lees JA, Harlow E, Zhu L. Specific regulation of E2F family members by cyclin-dependent kinases. Mol Cell Biol 1997;17(7):3867-75.

70. Kitagawa M, Higashi H, Suzuki-Takahashi I, et al. Phosphorylation of E2F-1 by cyclin A-cdk2. Oncogene 1995;10(2):229-36.

71. Xu M, Sheppard KA, Peng CY, Yee AS, Piwnica-Worms H. Cyclin A/CDK2 binds directly to E2F-1 and inhibits the DNA-binding activity of E2F-1/DP-1 by phosphorylation. Mol Cell Biol 1994;14(12):8420-31.

72. Porter LA, Donoghue DJ. Cyclin B1 and CDK1: nuclear localization and upstream regulators. Prog Cell Cycle Res 2003;5:335-47.

73. Li J, Meyer AN, Donoghue DJ. Nuclear localization of cyclin B1 mediates its biological activity and is regulated by phosphorylation. Proc Natl Acad Sci U S A 1997;94(2):502-7.

74. Toyoshima-Morimoto F, Taniguchi E, Shinya N, Iwamatsu A, Nishida E. Polo-like kinase 1 phosphorylates cyclin B1 and targets it to the nucleus during prophase. Nature 2001;410(6825):215-20.

75. Hagting A, Karlsson C, Clute P, Jackman M, Pines J. MPF localization is controlled by nuclear export. Embo J 1998;17(14):4127-38.

76. Yang J, Bardes ES, Moore JD, Brennan J, Powers MA, Kornbluth S. Control of cyclin B1 localization through regulated binding of the nuclear export factor CRM1. Genes Dev 1998;12(14):2131-43.

77. Jackman M, Lindon C, Nigg EA, Pines J. Active cyclin B1-Cdk1 first appears on centrosomes in prophase. Nat Cell Biol 2003;5(2):143-8.

78. Kallstrom H, Lindqvist A, Pospisil V, Lundgren A, Rosenthal CK. Cdc25A localisation and shuttling: characterisation of sequences mediating nuclear export and import. Exp Cell Res 2005;303(1):89-100.

79. Takizawa CG, Morgan DO. Control of mitosis by changes in the subcellular location of cyclin-B1-Cdk1 and Cdc25C. Curr Opin Cell Biol 2000;12(6):658-65.

80. Uchida S, Ohtsubo M, Shimura M, et al. Nuclear export signal in CDC25B. Biochem Biophys Res Commun 2004;316(1):226-32.

81. Perdiguero E, Nebreda AR. Regulation of Cdc25C activity during the meiotic G2/M transition. Cell Cycle 2004;3(6):733-7.

82. Hoffmann I, Clarke PR, Marcote MJ, Karsenti E, Draetta G. Phosphorylation and activation of human cdc25-C by cdc2--cyclin B and its involvement in the self-amplification of MPF at mitosis. Embo J 1993;12(1):53-63.

83. Pomerening JR, Sontag ED, Ferrell JE, Jr. Building a cell cycle oscillator: hysteresis and bistability in the activation of Cdc2. Nat Cell Biol 2003;5(4):346-51.

84. Wang R, He G, Nelman-Gonzalez M, et al. Regulation of Cdc25C by ERK-MAP kinases during the G2/M transition. Cell 2007;128(6):1119-32.

85. Lowe M, Rabouille C, Nakamura N, et al. Cdc2 kinase directly phosphorylates the cis-Golgi matrix protein GM130 and is required for Golgi fragmentation in mitosis. Cell 1998;94(6):783-93.

86. Moore JD, Kirk JA, Hunt T. Unmasking the S-phase-promoting potential of cyclin B1. Science 2003;300(5621):987-90.

87. Nigg EA. The substrates of the cdc2 kinase. Semin Cell Biol 1991;2(4):261-70.

88. Peter M, Nakagawa J, Doree M, Labbe JC, Nigg EA. In vitro disassembly of the nuclear lamina and M phase-specific phosphorylation of lamins by cdc2 kinase. Cell 1990;61(4):591-602.

89. Sirri V, Hernandez-Verdun D, Roussel P. Cyclin-dependent kinases govern formation and maintenance of the nucleolus. J Cell Biol 2002;156(6):969-81.

90. Hendrickson M, Madine M, Dalton S, Gautier J. Phosphorylation of MCM4 by cdc2 protein kinase inhibits the activity of the minichromosome maintenance complex. Proc Natl Acad Sci U S A 1996;93(22):12223-8.

91. Long JJ, Leresche A, Kriwacki RW, Gottesfeld JM. Repression of TFIIH transcriptional activity and TFIIH-associated cdk7 kinase activity at mitosis. Mol Cell Biol 1998;18(3):1467-76.

92. Papst PJ, Sugiyama H, Nagasawa M, Lucas JJ, Maller JL, Terada N. Cdc2-cyclin B phosphorylates p70 S6 kinase on Ser411 at mitosis. J Biol Chem 1998;273(24):15077-84.

93. Fu J, Bian M, Jiang Q, Zhang C. Roles of Aurora kinases in mitosis and tumorigenesis. Mol Cancer Res 2007;5(1):1-10.

94. Winey M. Cell cycle: driving the centrosome cycle. Curr Biol 1999;9(12):R449-52.

95. Fisk HA, Mattison CP, Winey M. Human Mps1 protein kinase is required for centrosome duplication and normal mitotic progression. Proc Natl Acad Sci U S A 2003;100(25):14875-80.

96. Tokuyama Y, Horn HF, Kawamura K, Tarapore P, Fukasawa K. Specific phosphorylation of nucleophosmin on Thr(199) by cyclin-dependent kinase 2-cyclin E and its role in centrosome duplication. J Biol Chem 2001;276(24):21529-37.

97. Cazales M, Schmitt E, Montembault E, Dozier C, Prigent C, Ducommun B. CDC25B phosphorylation by Aurora-A occurs at the G2/M transition and is inhibited by DNA damage. Cell Cycle 2005;4(9):1233-8.

98. Katayama H, Brinkley WR, Sen S. The Aurora kinases: role in cell transformation and tumorigenesis. Cancer Metastasis Rev 2003;22(4):451-64.

99. Cheetham GM, Knegtel RM, Coll JT, et al. Crystal structure of aurora-2, an oncogenic serine/threonine kinase. J Biol Chem 2002;277(45):42419-22.

100. Hirota T, Kunitoku N, Sasayama T, et al. Aurora-A and an interacting activator, the LIM protein Ajuba, are required for mitotic commitment in human cells. Cell 2003;114(5):585-98.

101. Tsai MY, Wiese C, Cao K, et al. A Ran signalling pathway mediated by the mitotic kinase Aurora A in spindle assembly. Nat Cell Biol 2003;5(3):242-8.

102. Pugacheva EN, Golemis EA. The focal adhesion scaffolding protein HEF1 regulates activation of the Aurora-A and Nek2 kinases at the centrosome. Nat Cell Biol 2005;7(10):937-46.

103. Bolton MA, Lan W, Powers SE, McCleland ML, Kuang J, Stukenberg PT. Aurora B kinase exists in a complex with survivin and INCENP and its kinase activity is stimulated by survivin binding and phosphorylation. Mol Biol Cell 2002;13(9):3064-77.

104. Harper JW, Burton JL, Solomon MJ. The anaphase-promoting complex: it's not just for mitosis any more. Genes Dev 2002;16(17):2179-206.

105. Yu H. Regulation of APC-Cdc20 by the spindle checkpoint. Curr Opin Cell Biol 2002;14(6):706-14.

106. Waizenegger I, Gimenez-Abian JF, Wernic D, Peters JM. Regulation of human separase by securin binding and autocleavage. Curr Biol 2002;12(16):1368-78.

107. Baker DJ, Dawlaty MM, Galardy P, van Deursen JM. Mitotic regulation of the anaphase-promoting complex. Cell Mol Life Sci 2007;64(5):589-600.

108. Kramer ER, Scheuringer N, Podtelejnikov AV, Mann M, Peters JM. Mitotic regulation of the APC activator proteins CDC20 and CDH1. Mol Biol Cell 2000;11(5):1555-69.

109. Bembenek J, Yu H. Regulation of the anaphase-promoting complex by the dual specificity phosphatase human Cdc14a. J Biol Chem 2001;276(51):48237-42.

110. Prinz S, Hwang ES, Visintin R, Amon A. The regulation of Cdc20 proteolysis reveals a role for APC components Cdc23 and Cdc27 during S phase and early mitosis. Curr Biol 1998;8(13):750-60.

111. Reis A, Levasseur M, Chang HY, Elliott DJ, Jones KT. The CRY box: a second APCcdh1-dependent degron in mammalian cdc20. EMBO Rep 2006;7(10):1040-5.

112. Malmanche N, Maia A, Sunkel CE. The spindle assembly checkpoint: preventing chromosome mis-segregation during mitosis and meiosis. FEBS Lett 2006;580(12):2888-95.

113. May KM, Hardwick KG. The spindle checkpoint. J Cell Sci 2006;119(Pt 20):4139-42.

114. Musacchio A, Salmon ED. The spindle-assembly checkpoint in space and time. Nat Rev Mol Cell Biol 2007;8(5):379-93.

115. Bharadwaj R, Yu H. The spindle checkpoint, aneuploidy, and cancer. Oncogene 2004;23(11):2016-27.

116. Kops GJ, Weaver BA, Cleveland DW. On the road to cancer: aneuploidy and the mitotic checkpoint. Nat Rev Cancer 2005;5(10):773-85.

117. Chan GK, Liu ST, Yen TJ. Kinetochore structure and function. Trends Cell Biol 2005;15(11):589-98.

118. Pinsky BA, Biggins S. The spindle checkpoint: tension versus attachment. Trends Cell Biol 2005;15(9):486-93.

119. Vanoosthuyse V, Hardwick KG. Bub1 and the multilayered inhibition of Cdc20-APC/C in mitosis. Trends Cell Biol 2005;15(5):231-3.

120. Yu H. Structural activation of Mad2 in the mitotic spindle checkpoint: the two-state Mad2 model versus the Mad2 template model. J Cell Biol 2006;173(2):153-7.

121. Fang G, Yu H, Kirschner MW. The checkpoint protein MAD2 and the mitotic regulator CDC20 form a ternary complex with the anaphase-promoting complex to control anaphase initiation. Genes Dev 1998;12(12):1871-83.

122. Fang G. Checkpoint protein BubR1 acts synergistically with Mad2 to inhibit anaphase-promoting complex. Mol Biol Cell 2002;13(3):755-66.

123. Sudakin V, Chan GK, Yen TJ. Checkpoint inhibition of the APC/C in HeLa cells is mediated by a complex of BUBR1, BUB3, CDC20, and MAD2. J Cell Biol 2001;154(5):925-36.

124. Morrow CJ, Tighe A, Johnson VL, Scott MI, Ditchfield C, Taylor SS. Bub1 and aurora B cooperate to maintain BubR1-mediated inhibition of APC/CCdc20. J Cell Sci 2005;118(Pt 16):3639-52.

125. Yu H, Tang Z. Bub1 multitasking in mitosis. Cell Cycle 2005;4(2):262-5.

126. Chan GK, Jablonski SA, Sudakin V, Hittle JC, Yen TJ. Human BUBR1 is a mitotic checkpoint kinase that monitors CENP-E functions at kinetochores and binds the cyclosome/APC. J Cell Biol 1999;146(5):941-54.

127. Jablonski SA, Chan GK, Cooke CA, Earnshaw WC, Yen TJ. The hBUB1 and hBUBR1 kinases sequentially assemble onto kinetochores during prophase with hBUBR1 concentrating at the kinetochore plates in mitosis. Chromosoma 1998;107(6-7):386-96.

128. Zhou J, Yao J, Joshi HC. Attachment and tension in the spindle assembly checkpoint. J Cell Sci 2002;115(Pt 18):3547-55.

129. Rotman G, Shiloh Y. ATM: a mediator of multiple responses to genotoxic stress. Oncogene 1999;18(45):6135-44.

130. Falck J, Mailand N, Syljuasen RG, Bartek J, Lukas J. The ATM-Chk2-Cdc25A checkpoint pathway guards against radioresistant DNA synthesis. Nature 2001;410(6830):842-7.

131. Mailand N, Falck J, Lukas C, et al. Rapid destruction of human Cdc25A in response to DNA damage. Science 2000;288(5470):1425-9.

132. Niida H, Nakanishi M. DNA damage checkpoints in mammals. Mutagenesis 2006;21(1):3-9.

133. Sancar A, Lindsey-Boltz LA, Unsal-Kacmaz K, Linn S. Molecular mechanisms of mammalian DNA repair and the DNA damage checkpoints. Annu Rev Biochem 2004;73:39-85.

134. Busino L, Chiesa M, Draetta GF, Donzelli M. Cdc25A phosphatase: combinatorial phosphorylation, ubiquitylation and proteolysis. Oncogene 2004;23(11):2050-6.

135. Tibbetts RS, Brumbaugh KM, Williams JM, et al. A role for ATR in the DNA damage-induced phosphorylation of p53. Genes Dev 1999;13(2):152-7.

136. Nayak BK, Das GM. Stabilization of p53 and transactivation of its target genes in response to replication blockade. Oncogene 2002;21(47):7226-9.

137. Wu X, Bayle JH, Olson D, Levine AJ. The p53-mdm-2 autoregulatory feedback loop. Genes Dev 1993;7(7A):1126-32.

138. Bartek J, Lukas C, Lukas J. Checking on DNA damage in S phase. Nat Rev Mol Cell Biol 2004;5(10):792-804.

139. Feehan HF, Mancusi Ungaro A. The use of cocaine as a topical anesthetic in nasal surgery. A survey report. Plast Reconstr Surg 1976;57(1):62-5.

140. Andreassen PR, Ho GP, D'Andrea AD. DNA damage responses and their many interactions with the replication fork. Carcinogenesis 2006;27(5):883-92.

141. Byun TS, Pacek M, Yee MC, Walter JC, Cimprich KA. Functional uncoupling of MCM helicase and DNA polymerase activities activates the ATR-dependent checkpoint. Genes Dev 2005;19(9):1040-52.

142. Cortez D. Unwind and slow down: checkpoint activation by helicase and polymerase uncoupling. Genes Dev 2005;19(9):1007-12.

143. Costanzo V, Gautier J. Single-strand DNA gaps trigger an ATR- and Cdc7-dependent checkpoint. Cell Cycle 2003;2(1):17.

144. Bomgarden RD, Lupardus PJ, Soni DV, Yee MC, Ford JM, Cimprich KA. Opposing effects of the UV lesion repair protein XPA and UV bypass polymerase eta on ATR checkpoint signaling. Embo J 2006;25(11):2605-14.

145. Costa RM, Chigancas V, Galhardo Rda S, Carvalho H, Menck CF. The eukaryotic nucleotide excision repair pathway. Biochimie 2003;85(11):1083-99.

146. Garcia-Muse T, Boulton SJ. Distinct modes of ATR activation after replication stress and DNA double-strand breaks in Caenorhabditis elegans. Embo J 2005;24(24):4345-55.

147. Valerie K, Povirk LF. Regulation and mechanisms of mammalian double-strand break repair. Oncogene 2003;22(37):5792-812.

148. Zou L, Liu D, Elledge SJ. Replication protein A-mediated recruitment and activation of Rad17 complexes. Proc Natl Acad Sci U S A 2003;100(24):13827-32.

149. Lao Y, Gomes XV, Ren Y, Taylor JS, Wold MS. Replication protein A interactions with DNA. III. Molecular basis of recognition of damaged DNA. Biochemistry 2000;39(5):850-9.

150. Ball HL, Myers JS, Cortez D. ATRIP binding to replication protein A-single-stranded DNA promotes ATR-ATRIP localization but is dispensable for Chk1 phosphorylation. Mol Biol Cell 2005;16(5):2372-81.

151. Namiki Y, Zou L. ATRIP associates with replication protein A-coated ssDNA through multiple interactions. Proc Natl Acad Sci U S A 2006;103(3):580-5.

152. Zou L, Elledge SJ. Sensing DNA damage through ATRIP recognition of RPA-ssDNA complexes. Science 2003;300(5625):1542-8.

153. Parrilla-Castellar ER, Arlander SJ, Karnitz L. Dial 9-1-1 for DNA damage: the Rad9-Hus1-Rad1 (9-1-1) clamp complex. DNA Repair (Amst) 2004;3(8-9):1009-14.

154. Zou L, Cortez D, Elledge SJ. Regulation of ATR substrate selection by Rad17-dependent loading of Rad9 complexes onto chromatin. Genes Dev 2002;16(2):198-208.

155. Thelen MP, Venclovas C, Fidelis K. A sliding clamp model for the Rad1 family of cell cycle checkpoint proteins. Cell 1999;96(6):769-70.

156. Gottifredi V, Prives C. The S phase checkpoint: when the crowd meets at the fork. Semin Cell Dev Biol 2005;16(3):355-68.

157. Wang X, Zou L, Lu T, et al. Rad17 phosphorylation is required for claspin recruitment and Chk1 activation in response to replication stress. Mol Cell 2006;23(3):331-41.

158. Lin SY, Li K, Stewart GS, Elledge SJ. Human Claspin works with BRCA1 to both positively and negatively regulate cell proliferation. Proc Natl Acad Sci U S A 2004;101(17):6484-9.

159. Chini CC, Chen J. Human claspin is required for replication checkpoint control. J Biol Chem 2003;278(32):30057-62.

160. Lee J, Kumagai A, Dunphy WG. Claspin, a Chk1-regulatory protein, monitors DNA replication on chromatin independently of RPA, ATR, and Rad17. Mol Cell 2003;11(2):329-40.

161. Wang Y, Cortez D, Yazdi P, Neff N, Elledge SJ, Qin J. BASC, a super complex of BRCA1-associated proteins involved in the recognition and repair of aberrant DNA structures. Genes Dev 2000;14(8):927-39.

162. Goldberg M, Stucki M, Falck J, et al. MDC1 is required for the intra-S-phase DNA damage checkpoint. Nature 2003;421(6926):952-6.

163. Lou Z, Chini CC, Minter-Dykhouse K, Chen J. Mediator of DNA damage checkpoint protein 1 regulates BRCA1 localization and phosphorylation in DNA damage checkpoint control. J Biol Chem 2003;278(16):13599-602.

164. Stewart GS, Wang B, Bignell CR, Taylor AM, Elledge SJ. MDC1 is a mediator of the mammalian DNA damage checkpoint. Nature 2003;421(6926):961-6.

165. Kim ST, Xu B, Kastan MB. Involvement of the cohesin protein, Smc1, in Atm-dependent and independent responses to DNA damage. Genes Dev 2002;16(5):560-70.

166. Kitagawa R, Bakkenist CJ, McKinnon PJ, Kastan MB. Phosphorylation of SMC1 is a critical downstream event in the ATM-NBS1-BRCA1 pathway. Genes Dev 2004;18(12):1423-38.

167. Xiao Z, Chen Z, Gunasekera AH, et al. Chk1 mediates S and G2 arrests through Cdc25A degradation in response to DNA-damaging agents. J Biol Chem 2003;278(24):21767-73.

168. Falck J, Petrini JH, Williams BR, Lukas J, Bartek J. The DNA damage-dependent intra-S phase checkpoint is regulated by parallel pathways. Nat Genet 2002;30(3):290-4.

169. Merrick CJ, Jackson D, Diffley JF. Visualization of altered replication dynamics after DNA damage in human cells. J Biol Chem 2004;279(19):20067-75.

170. D'Amours D, Jackson SP. The Mre11 complex: at the crossroads of DNA repair and checkpoint signalling. Nat Rev Mol Cell Biol 2002;3(5):317-27.

171. Lee JH, Paull TT. Direct activation of the ATM protein kinase by the Mre11/Rad50/Nbs1 complex. Science 2004;304(5667):93-6.

172. Uziel T, Lerenthal Y, Moyal L, Andegeko Y, Mittelman L, Shiloh Y. Requirement of the MRN complex for ATM activation by DNA damage. Embo J 2003;22(20):5612-21.

173. Cuadrado M, Martinez-Pastor B, Murga M, et al. ATM regulates ATR chromatin loading in response to DNA double-strand breaks. J Exp Med 2006;203(2):297-303.

174. Jazayeri A, Falck J, Lukas C, et al. ATM- and cell cycle-dependent regulation of ATR in response to DNA double-strand breaks. Nat Cell Biol 2006;8(1):37-45.

175. Kaneko YS, Watanabe N, Morisaki H, et al. Cell-cycle-dependent and ATM-independent expression of human Chk1 kinase. Oncogene 1999;18(25):3673-81.

176. Lukas C, Bartkova J, Latella L, et al. DNA damage-activated kinase Chk2 is independent of proliferation or differentiation yet correlates with tissue biology. Cancer Res 2001;61(13):4990-3.

177. Ahn JY, Li X, Davis HL, Canman CE. Phosphorylation of threonine 68 promotes oligomerization and autophosphorylation of the Chk2 protein kinase via the forkhead-associated domain. J Biol Chem 2002;277(22):19389-95.

178. Oliver AW, Paul A, Boxall KJ, et al. Trans-activation of the DNA-damage signalling protein kinase Chk2 by T-loop exchange. Embo J 2006;25(13):3179-90.

179. Xu X, Tsvetkov LM, Stern DF. Chk2 activation and phosphorylation-dependent oligomerization. Mol Cell Biol 2002;22(12):4419-32.

180. Li J, Stern DF. DNA damage regulates Chk2 association with chromatin. J Biol Chem 2005;280(45):37948-56.

181. Lukas C, Falck J, Bartkova J, Bartek J, Lukas J. Distinct spatiotemporal dynamics of mammalian checkpoint regulators induced by DNA damage. Nat Cell Biol 2003;5(3):255-60.

182. Guo Z, Kumagai A, Wang SX, Dunphy WG. Requirement for Atr in phosphorylation of Chk1 and cell cycle regulation in response to DNA replication blocks and UV-damaged DNA in Xenopus egg extracts. Genes Dev 2000;14(21):2745-56.

183. Hekmat-Nejad M, You Z, Yee MC, Newport JW, Cimprich KA. Xenopus ATR is a replication-dependent chromatin-binding protein required for the DNA replication checkpoint. Curr Biol 2000;10(24):1565-73.

184. Nghiem P, Park PK, Kim Y, Vaziri C, Schreiber SL. ATR inhibition selectively sensitizes G1 checkpoint-deficient cells to lethal premature chromatin condensation. Proc Natl Acad Sci U S A 2001;98(16):9092-7.

185. Niida H, Tsuge S, Katsuno Y, Konishi A, Takeda N, Nakanishi M. Depletion of Chk1 leads to premature activation of Cdc2-cyclin B and mitotic catastrophe. J Biol Chem 2005;280(47):39246-52.

186. Petermann E, Caldecott KW. Evidence that the ATR/Chk1 pathway maintains normal replication fork progression during unperturbed S phase. Cell Cycle 2006;5(19):2203-9.

187. Casper AM, Nghiem P, Arlt MF, Glover TW. ATR regulates fragile site stability. Cell 2002;111(6):779-89.

188. Durkin SG, Arlt MF, Howlett NG, Glover TW. Depletion of CHK1, but not CHK2, induces chromosomal instability and breaks at common fragile sites. Oncogene 2006;25(32):4381-8.

189. El Achkar E, Gerbault-Seureau M, Muleris M, Dutrillaux B, Debatisse M. Premature condensation induces breaks at the interface of early and late replicating chromosome bands bearing common fragile sites. Proc Natl Acad Sci U S A 2005;102(50):18069-74.

190. Le Beau MM, Rassool FV, Neilly ME, et al. Replication of a common fragile site, FRA3B, occurs late in S phase and is delayed further upon induction: implications for the mechanism of fragile site induction. Hum Mol Genet 1998;7(4):755-61.

191. Wang L, Darling J, Zhang JS, Huang H, Liu W, Smith DI. Allele-specific late replication and fragility of the most active common fragile site, FRA3B. Hum Mol Genet 1999;8(3):431-7.

192. Lukas J, Lukas C, Bartek J. Mammalian cell cycle checkpoints: signalling pathways and their organization in space and time. DNA Repair (Amst) 2004;3(8-9):997-1007.

193. Nyberg KA, Michelson RJ, Putnam CW, Weinert TA. Toward maintaining the genome: DNA damage and replication checkpoints. Annu Rev Genet 2002;36:617-56.

194. Fletcher L, Muschel RJ. The centrosome and the DNA damage induced checkpoint. Cancer Lett 2006;243(1):1-8.

195. Smits VA, Klompmaker R, Arnaud L, Rijksen G, Nigg EA, Medema RH. Polo-like kinase-1 is a target of the DNA damage checkpoint. Nat Cell Biol 2000;2(9):672-6.

196. Lange BM. Integration of the centrosome in cell cycle control, stress response and signal transduction pathways. Curr Opin Cell Biol 2002;14(1):35-43.

197. Toyoshima-Morimoto F, Taniguchi E, Nishida E. Plk1 promotes nuclear translocation of human Cdc25C during prophase. EMBO Rep 2002;3(4):341-8.

198. Bartek J, Lukas J. DNA damage checkpoints: from initiation to recovery or adaptation. Curr Opin Cell Biol 2007;19(2):238-45.

199. Syljuasen RG, Jensen S, Bartek J, Lukas J. Adaptation to the ionizing radiation-induced G2 checkpoint occurs in human cells and depends on checkpoint kinase 1 and Polo-like kinase 1 kinases. Cancer Res 2006;66(21):10253-7.

200. van Vugt MA, Bras A, Medema RH. Polo-like kinase-1 controls recovery from a G2 DNA damage-induced arrest in mammalian cells. Mol Cell 2004;15(5):799-811.

201. Syljuasen RG. Checkpoint adaptation in human cells. Oncogene 2007;26(40):5833-9.

Chapter 2:

Speedy/RINGO Regulation of CDKs in Cell Cycle, Checkpoint Activation and Apoptosis

Introduction

Cell cycle transitions are controlled by cyclin-dependent kinases (CDKs) and their regulatory cyclin subunits. During the cell cycle, cyclins are tightly controlled by synthesis and degradation, which provides temporal control over CDK activation. Further control is achieved by post-translational modifications and protein-protein interactions. Inhibitory phosphorylation, catalyzed by Wee1/Myt1, and association of cyclin dependent kinase inhibitors (CKIs), negatively regulate CDK activity. Conversely, dephosphorylation catalyzed by CDC25 phosphatases and phosphorylation by CAK, positively regulates CDK activity in a cell cycle dependent manner. Cyclin B/CDK1, cyclin A/CDK1, cyclin E/CDK2 and cyclin D/CDK4/6 complexes have been shown to regulate the G2/M, S/G2, G1/S and G1 phases respectively.

Although the majority of CDK complexes control the cell division cycle, it is clear that regulation of the cell cycle is more than progression from growth to DNA synthesis and cell division for transmission of genetic material. There is growing evidence that CDKs control the balance between senescence, cell growth, checkpoint activation, and apoptotic signaling. Although the mechanisms of CDK regulation in these processes and the precise contribution of CDKs to these pathways have not been fully elucidated, definitive connections have been established. Considering numerous cyclin/CDK complexes are deregulated in multiple cancer cell types, further studies are needed to unravel novel mechanisms that contribute to abnormal cell cycle regulation and malignancy.

A new protein family termed Speedy/RINGO binds and activates Cdc2 (CDK1) and CDK2, yet have no homology to cyclins. This family of proteins is required for and enhances meiotic maturation in *Xenopus* oocytes, increases cell proliferation in mammalian cells, and promotes cell survival through prevention of apoptosis in cell lines challenged with DNA damaging agents. A human homologue in this family named Speedy A1 (Spy1) is expressed in a cell cycle dependent manner and a correlation between Spy1 overexpression and breast cancer was recently established (1). While members of this family are important for meiotic maturation (2-5), the novel roles of the Speedy/RINGO proteins in regulating the normal mammalian cell cycle and the DNA damage response will be the focal point of this review.

Speedy/RINGO Family Members

Xenopus Speedy (xSpy) was originally identified in a screen for genes that conferred resistance to a Rad1 deficient strain of *Schizosaccharomyces pombe* when challenged with UV or gamma irradiation (6). XRINGO was identified in an independent screen for genes involved in the G2/M transition in *Xenopus* oocytes. Expression of XRINGO in G2 arrested oocytes caused enhanced meiotic maturation compared to progesterone induction or Mos expression. Knock down of endogenous XRINGO caused a delay in oocyte maturation when induced with progesterone, indicating XRINGO is required for oocyte maturation (3). Similarly, a recent study using porcine Speedy A2 has shown accelerated meiotic maturation in porcine oocytes indicating this function may be conserved for the mammalian Speedy/RINGO proteins

as well (7). Although a potential Speedy/RINGO gene has been found in the most primitive branching clade of chordates (*Ciona intestinalis*), there has yet to be a homologue identified in invertebrates (8).

Spy1, the first human homologue identified, has 40% homology to its *Xenopus* counterpart (9). To date six mammalian homologues have been identified. See Table 1 for a full list of Speedy/RINGO family members, their identifying characteristics, expression patterns and CDK preference. All of the Speedy/RINGO proteins contain a central region termed the Speedy/RINGO box, which has 51-67% homology among the family members. Mutagenesis and deletion of conserved residues within the Speedy/RINGO box resulted in reduced CDK binding and GVBD, indicating its necessity for Speedy/RINGO function (8, 10). Analysis of CDK2 mutants indicates that Speedy/RINGO proteins bind similarly to cyclins, although involvement of specific residues within the PSTAIRE domain and activation loop differ (10).

The residues flanking the conserved core have also been implicated in the function of Speedy/RINGO proteins. C-terminal truncation mutants of Speedy/RINGO A2 can bind to but not activate CDK2, indicating this region may be necessary for CDK2 activation. It has also been proposed that the N-terminus may be involved in regulating expression of Speedy/RINGO (8). Considering the termini of Speedy/RINGO proteins have little homology and differ in length between family members, these regions may provide specificity for activation of different CDKs and alter their expression patterns.

XRINGO and Speedy/RINGO A2 activated CDK1 and CDK2 respectively, both *in vivo* and *in vitro*. Interestingly, the activation of CDK1 or CDK2 by Speedy/RINGO proteins was independent of the activating T-loop phosphorylation catalyzed by CAK (5, 8, 11). Furthermore, Speedy/RINGO A2 was found to be a poor substrate for CAK (11). This is in stark contrast to cyclin activated CDKs, which absolutely require T-loop phosphorylation for catalytic activity and are efficiently phosphorylated by CAK. Additionally, XRINGO/CDK1 was phosphorylated less efficiently by Myt1, when compared to cyclin B/CDK1 (5).

Table 2-1. Members of the Speedy/RINGO Family

Name	Alternate Name	Tissue Expression	Species	Length (AA)	CDK Preference	Accession #	Reference
X-RINGO	X-RINGO A, ls26	Oocyte	Xenopus laevis	299	Cdc2/ CDK2	Q9PU13	(3)
X-Spy1	X-RINGO B, ls27	Oocyte	Xenopus laevis	298	Cdc2/ CDK2	Q9YGL1	(3), (6)
Speedy/ RINGO A1	Spy A1, RINGO 3	Ubiquitous (high in testis)	Homo sapiens/ Mus musculus	286/ 283	CDK2	AAW30394, AAW32476	(9), (10)
Speedy/ RINGO A2	Spy A2	Ubiquitous (high in testis)	Homo sapiens/ Mus musculus/ Sus scrofa	313/ 310/ 311	Cdc2/ CDK2	Q5MJ70, Q5IBH7, BAE00070.1	(7), (8)
Speedy/ RINGO B	RINGO 4	Testis only	Mus musculus	268	Cdc2	Q5IBH6	(8), (10)
Speedy/ RINGO C	RINGO 2	Testis, liver, placenta, bone marrow, kidney, small intestine	Homo sapiens	293	Cdc2/ CDK2	Q5MJ68	(8), (10)
Speedy/ RINGO D	RINGO 5	?	Mus musculus	339	?	?	(8), (10)
Speedy/ RINGO E	RINGO 1	?	Homo sapiens	336	Cdc2/ CDK2/ CDK5	?	(10)

Human Spy1 Regulation of the Mammalian Mitotic Cell Cycle

In addition to the ability of XRINGO and porcine Speedy/RINGO A2 to accelerate meiotic maturation of oocytes, there is a growing body of evidence indicating that this family functions in the mitotic cell cycle. In mammalian cell culture, Spy1 expression enhances the rate of cell replication and division as demonstrated by 2-3 fold higher BrdU incorporation and increased mitochondrial activity measured using a MTT assay. Notably, flow cytometry profiles determined Spy1-expressing cells consistently exhibited a reduced G1 phase population compared to mock cells (9). Evidence indicating Spy1 expression enhances DNA synthesis is supported by a recent report showing that the inability to degrade XRINGO during the meiosis I-meiosis II transition induces unscheduled DNA replication (2). Using chemical inhibitors and catalytically inactive CDK mutants, the enhanced cell proliferation caused by Spy1 was found to be dependent on CDK2 activity. Knockdown of endogenous Spy1 using siRNA caused a decrease in CDK2 kinase activity and a higher percentage of cells to be in late G1/early S phase, where Spy1 mRNA is normally up-regulated (9). These effects of Spy1 knockdown on cell growth implicate Spy1 as an essential protein for cell proliferation. This parallels data from knock down experiments in oocytes where XRINGO was shown to be necessary for meiotic maturation.

In conjunction with phosphorylation and cyclin binding, CDK activity is regulated by binding of CKIs to cyclin/CDK complexes. The CKIs $p21^{cip}$ and $p27^{kip}$ bind to cyclin proteins through a conserved RXL motif and inhibit kinase activity by

inserting their C-termini into the ATP binding pocket of CDKs. $p21^{cip}$ was determined to be a poor inhibitor of XRINGO/CDK1 and XRINGO/CDK2 complexes *in vitro* and *in vivo* compared to cyclin B/CDK1 and cyclin A/CDK2, respectively (5). Using a two-hybrid screen, $p27^{kip}$ was identified as a binding partner for Spy1. This novel interaction was confirmed both *in vitro* and *in vivo*, and domain analysis indicated that Spy1 binds to the CDK binding region of p27 rather than the cyclin binding domain (12). Interestingly, the ability of the Speedy/RINGO proteins to bind p27 when expressed in *Xenopus* oocytes inversely correlated with their ability to bind CDK1, with XRINGO and Spy1 binding the most efficiently (10). In mammalian cells, Spy1 expression overcame a p27-induced cell cycle arrest, allowing for DNA synthesis and increased CDK2 kinase activity. Furthermore, in p27-null cell lines, Spy1-enhanced cell proliferation was found to be dependent on the presence of endogenous p27 (12). However, Spy1 still bound CDK2 in these cells, supporting other p27-independent functions.

Considering the data presented above, an exciting model by which Spy1 promotes cell proliferation may be achieved through enhanced p27 degradation at the G1/S transition. Phosphorylation by CDK2 down-regulates $p27^{Kip1}$ at the G1/S transition by inducing its proteasome-mediated degradation. Using synchronized HeLa cells, Spy1 expressing cells enter S phase significantly sooner than control cells. However, S phase is delayed after entry such that exit from S phase occurs at the same time in Spy-expressing and control cells (unpublished observations). The premature entry into S phase caused by Spy1 resulted in quicker elimination of p27 as well, and

also enhanced p27 T187 phosphorylation, an event required for p27 degradation through the SCF^{Skp2} complex in late G1 and throughout S phase.

Substrate Specificity of Speedy/RINGO/Cdk Complexes

Recently, Speedy/RINGO A2/CDK2 was shown to have low enzymatic activity toward conventional cyclin/CDK2 substrates with the consensus site (S/T)PX(K/R). Speedy/RINGO/CDK2 complexes show nearly 1000-fold less activity toward Histone H1 compared to that of cyclin A/CDK2 complexes, yet display broad substrate specificity with respect to the +3 position of the target sequence. Using GST-tagged pentapeptide substrates of the form KSPRX (where X is any amino acid), Speedy/RINGO A2/CDK2 tolerated all but three amino acid substitutions at the +3 position. The best substrates contained tyrosine, arginine, and tryptophan, but not lysine as for cyclin/CDK2 complexes, in this position. Furthermore, the CDC25 phosphatases, were found to be phosphorylated only 10-fold less (not 1000-fold less as with H1) by Speedy/RINGO A2/CDK2, compared to cyclin A/CDK2 (11). Phosphopeptide mapping revealed numerous non-canonical sites were phosphorylated by Speedy/RINGO A2/CDK2 and not by cyclin A/CDK2, accounting for this difference in total phosphorylation (11). Thus, Speedy/RINGO-activated CDK2 can phosphorylate non-canonical substrate sites, which are not targets of cyclin A/CDK2.

The results presented above raise the question of how Speedy/RINGO-activated CDKs achieve their substrate specificity. Like cyclins, which contain specific motifs to interact with their substrates, Speedy/RINGO proteins may have

their own unique substrate interaction motifs to target a separate set of substrates under variable conditions. These substrates may be involved in cellular processes such as the checkpoint response, apoptosis, or other instances when CDK activation is uniquely regulated. The role of Speedy/RINGO proteins in the checkpoint and apoptotic responses is discussed below.

Speedy/RINGO and the DNA Damage Response

Cyclin dependent kinases have long been known to play a role in cellular response to DNA damage, including checkpoint activation and apoptosis. The tight regulation of CDK activity by numerous mechanisms contributes to checkpoint propagation, DNA damage repair, and apoptosis. Checkpoint activation inhibits cell cycle progression, allowing for damage repair or activation of apoptosis. Multiple mechanisms exist to ensure that CDK activity is tightly controlled after DNA damage. These include Chk1/Chk2-mediated destruction of CDC25 phosphatases (13, 14) and p53-mediated CDK inhibition by induction of p21 (15, 16). While both mechanisms inhibit CDK activity in temporally and spatially distinct ways, positive CDK2 regulation also occurs simultaneously.

In response to DNA damage, Spy1 is upregulated, presumably to impart some CDK2 activity in the face of the inhibitory processes mentioned previously (17). A general view of the DNA damage response and how Speedy/RINGO modulates CDK activity during this response can be found in Figure 2-1. Specifically, as mentioned above, a Spy1/CDK2 complex can phosphorylate members of the CDC25 family (11)

and may participate in a positive feedback loop leading to continued activation of CDK2 as similarly reported for cyclin B/Cdc2 (18). Whether CDC25 phosphorylated by Spy1/CDK2 is active toward a cyclin/CDK2 complex or only a Spy1/CDK2 complex is unknown and its contribution to CDK2 activity in response to DNA damage still remains to be investigated. However, it does indicate that some CDK2 activity, whether solely mediated by Spy1/CDK2 or both Spy1 and cyclin bound complexes, may be required for normal checkpoint events.

Another unique aspect of Speedy/RINGO regulation of CDK2 relates to inhibition achieved by p21 and p27. Previously, it has been shown that Spy1/CDK complexes are not susceptible to inhibition by p21 (5). This lack of inhibitory potential would allow for a pool of active CDK2 during checkpoints when CDK activity is normally inhibited. In addition to this inhibitory bypass, Speedy/RINGO/CDK2 complexes have different substrate specificities than cyclin/CDK complexes, as mentioned earlier (11). Thus, active Spy1/CDK2 may selectively phosphorylate substrates unique to DNA damage responses while having little or no activity toward cyclin/CDK substrates that promote cell cycle advance, DNA synthesis, or cell division. Atypical Speedy/RINGO/CDK2 phosphorylation sites are present in many DNA damage and checkpoint proteins including CDC25, Chk1/2, Rad9, etc., and often flank consensus cyclin/CDK sites. How phosphorylation of these atypical sites functions in the checkpoint response may shed light on the precise role and regulation of CDK2.

Recently, CDK2 has been shown to be more than a passive target of checkpoint signaling, as well as a major propagator and regulator of this signaling. Several studies demonstrate that complete CDK2 inhibition does not occur during the DNA damage response, and that CDK2 activity positively and negatively regulates the DNA damage response. The results presented above fit well with this model and may help explain some of the differences seen in CDK activity during certain DNA damage response events. Specifically, total inhibition of CDK2 by small molecule inhibitors or by siRNA has been shown to activate checkpoint signaling (19-21), creating feedback to Chk1, leading to its down regulation, and further activating the checkpoint (21). This evidence shows CDK inhibition is essential to checkpoint activation and suggests full CDK2 activation would be detrimental to checkpoint activation.

Other studies investigating the regulation of CDK2 activity indicate that complete inhibition of CDK2 is not advantageous for a damaged cell. In fact, while CDK2 inhibition may enhance checkpoint signaling, it also impairs DNA damage repair, especially repair of double strand breaks (22). In support of this observation, it was shown that Spy1 may affect DNA repair processes through its activation of CDK2. In response to damage caused by the topoisomerase inhibitor camptothecin, Spy1 expression decreased the formation of comet tails in an alkaline comet assay, which detects damaged DNA (17). These results indicate that Spy1/CDK2 activation plays a role in DNA repair. Hence, global CDK activation, achieved by cyclins, or atypical CDK activation achieved by Speedy/RINGO family members may counteract or temper checkpoint responses while enhancing damage repair processes and cellular

fate decisions, such as apoptosis, which occur in parallel to checkpoint activation. Indeed this may be the case when CDK2 is hyperactivated by expression of Spy1 (23).

In response to DNA damage caused by ultraviolet irradiation, Chk1 is activated by phosphorylation, an event critical for checkpoint activation (24-27). Expression of Spy1 under inducible control in U2OS cells causes total suppression of Chk1 phosphorylation at both activating sites (23). In addition, CDK2 activation mediated by Spy1 expression inhibits phosphorylation of RPA and the histone variant H2A.X (23). These effects of Spy1 expression require interaction with CDK2. Cells expressing a Spy1 mutant that does not bind CDK2 show no difference in checkpoint signaling compared to mock cells (23). These results show Spy1 expression prevents Chk1, H2A.X, and RPA32 phosphorylation, may be attributable to defects in ATR activation/signaling. Previous reports establish connections between CDK2 activity and ATR activity, both in the normal cell cycle and in the response to DNA damage (21, 28, 29). These reports show the opposition of ATR/ATM and CDK2 activities and correlate well with the Spy1 mediated inhibition of common ATR targets.

The S-phase, or replication checkpoint, arrests DNA replication by inhibiting origin firing through CDK2 inhibition, preventing cells from progressing into G2 with DNA damage or incomplete DNA synthesis (30). Our recent work shows that Spy1 overexpression leads to a partial UV-resistant DNA synthesis phenotype (UVDS) and bypass of the S-phase checkpoint (23). The G2/M checkpoint prevents cells from entering mitosis by inhibiting Cdc2. This is accomplished through Chk1-dependent CDC25A degradation (13, 14, 31). When assayed for G2 checkpoint activation by

examining levels of phospho-histone H3, Spy1-expressing cells were refractory to cell cycle arrest (23). These results indicate Spy1 plays an important role in modulating checkpoints by direct CDK2 activation. Furthermore, the role of CDK2 in the checkpoint response clearly is not as simple as inhibition of it kinase activity. The contributions of Spy1/CDK2 activity compared to cyclin/CDK activity may be pivotal in checkpoint regulation.

During checkpoint activation, modulation of CDK activity by Speedy/RINGO family members has dramatic effects on the fate of cells challenged with DNA damage. While total CDK2 activity in response to DNA damage may only be slightly affected by Speedy/RINGO family members, it is clear that Spy1 and its homologues have profound effects on cellular responses. The evidence above has begun to elucidate the mechanisms by which tightly regulated CDK activation can be achieved without significantly altering total activity, as well as how this specific type of regulation contributes to cell cycle and checkpoint control.

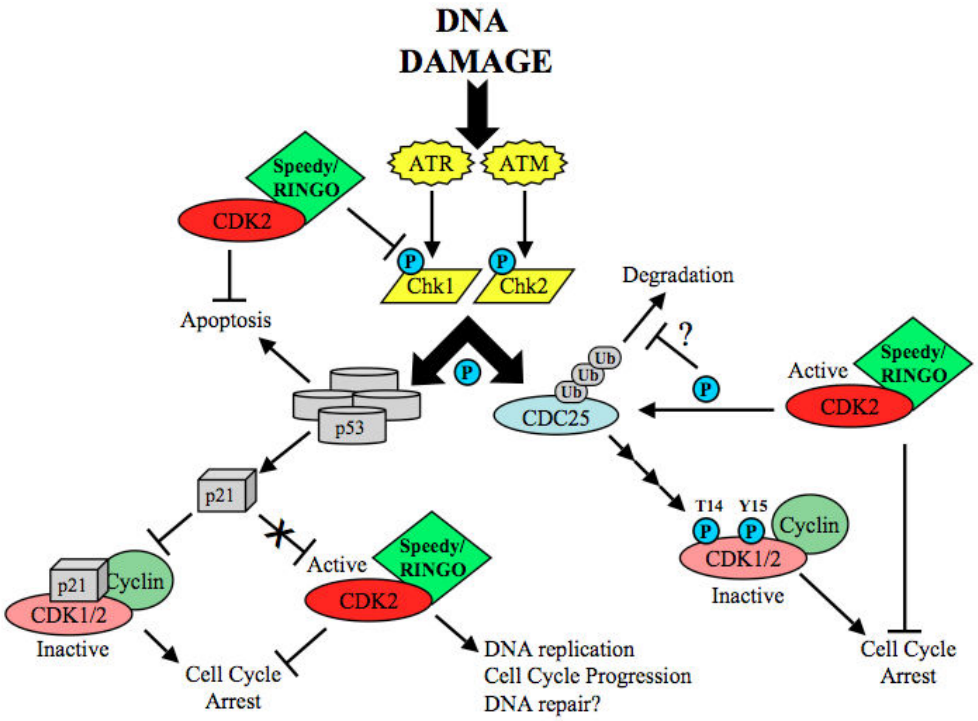

Figure 2-1. Role of Spy1/RINGO in the regulation of DNA damage responses. An overall perspective is presented on the role of Spy1/RINGO in regulating CDKs in response to DNA damage and thereby affecting cell cycle progression, apoptosis, or DNA repair/replication.

Speedy/RINGO and the Regulation of Apoptosis

The role of Spy1/CDK2 in regulating apoptosis further shows the complexity of CDK2 regulation. A recent study reveals that CDK2 must be inhibited to achieve apoptosis (13), while another report shows that CDK2 activity may be required for certain apoptotic events (32, 33). It is also known that caspases cleave p21 and p27, events that activate CDK2 and are required for apoptosis (34-38). Again, a paradigm is presented in which CDK2 must be active and inactive at the same time to regulate apoptosis. The following will describe current information on the role of Spy1 and its activation of CDK2 in the apoptotic response.

In a number of recent studies, the role of Spy1 in the DNA damage response and cell survival was examined. These reports have established Spy1 as a mediator of cell survival in response to cellular stresses. The first report looked at the effect of Spy1 overexpression in 293T cells treated with genotoxic agents. Compared to control cells, Spy1 expression decreased sensitivity to hydroxyurea, cis-platin, and camptothecin and increased cell survival (17). These results were obtained over a range of drug concentrations, and were primarily due to enhanced survival, not enhanced proliferation.

To expand on these results, the role of Spy1 in mediating apoptosis in response to UV irradiation was examined (23). In this study, the decrease in sensitivity to DNA damage conferred by Spy1 expression was re-affirmed in a Spy1-inducible U2OS cell line and subsequently shown to be a result of direct inhibition of apoptosis. Over a range of UV doses and an extended time course, Spy1-expressing cells had

significantly fewer markers of apoptosis, including DNA cleavage, AnnexinV staining of outer membrane leaflet phosphatidylserine, and caspase activation. Interestingly, these results were dependent on both CDK2 and p53. Camptothecin sensitivity in Spy1-expressing cells was returned to control levels when a dominant negative form of CDK2 was co-expressed. When a mutant of Spy1 that cannot bind CDK2 (point mutations within Speedy/RINGO box) was expressed, sensitivity to UV was no different than the matched control. These results clearly demonstrate and reconfirm that Spy1-mediated effects on the cell cycle and DNA damage response are dependent on interaction with CDK2. Furthermore, these results establish a role for non-cyclin-mediated CDK2 functions in apoptotic events. Again, a Spy1/CDK2 complex, which for the most part, is not susceptible to the common inhibitory mechanisms, may play a role in allowing for specific CDK2 activity, while the global levels of CDK2 kinase activity remain inhibited by the checkpoint response.

The significance of these results was further examined for long-term survival of cells that evade cell death. Clonogenic assays show that Spy1-expressing cells continue to grow and form colonies in response to camptothecin treatment, indicating subversion of growth control that may lead to genomic instability, which is significant for oncogenesis. A recent report found Spy1 to be one of the 50 most upregulated genes in a SAGE library derived from an invasive ductal carcinoma of the breast (1). Further examination of the NIH/NCI SAGE database revealed high levels of Spy1 expression in colon, pancreatic, and other forms of cancer (cgap.nci.nih.gov/SAGE).

As mentioned above, apoptotic inhibition conferred by Spy1 expression is p53-dependent. When Spy1 is expressed in p53 null cells irradiated with UV, the amount of apoptosis is equal to control cells (Unpublished work from our lab). This indicates that Spy/CDK2 complexes may interact with and inhibit p53 pathways. Further research is underway to elucidate molecular mechanisms that may link Spy1 with the functions of this important tumor suppressor.

Interestingly, the essential role of Spy1 and Spy1/CDK2 activity in regulating apoptosis was shown using siRNA-mediated knockdown of endogenous Spy1. When Spy1 is knocked down and cells are treated with either camptothecin (17) or UV radiation (unpublished work from our lab), the sensitivity of these cells is increased. In response to both DNA damaging agents, apoptosis is significantly increased when Spy1 is knocked down. However, treatment of cells with siSpy1 itself does not cause apoptosis. These data establish an essential role for Spy1 and Spy1/CDK2 activity in regulating apoptosis and sensitivity to DNA damaging agents. Further research needs to be done in order to determine the molecular mechanisms by which Spy1 and CDK2 exert effects over apoptosis. It is exciting to speculate that Spy1 expression and knockdown may be used diagnostically or therapeutically to enhance tumor sensitivity to chemotherapeutic drugs that work by damaging DNA.

Conclusions

The mechanisms of action conferred by the Speedy/RINGO family represent novel modes by which CDKs are regulated, and provide the possibility of multiple

CDK pools with different activation states, substrates, and functions. The information presented above clearly shows that Speedy/RINGO family members regulate CDKs in a fashion much different from conventional regulation by cyclins. CDK activation without requirement of phosphorylation events and in the face of inhibition allows for small pools to be active while still globally restricting CDK activity. This type of regulation may be important at cell cycle transitions where inhibition by p21, p27, and Wee1/Myt1 keep the majority of CDKs inactive; at times of cell cycle re-entry where the majority of CDK is inactive; during meiosis where atypical cell division occurs without an intervening S-phase; or in response to DNA damage where CDK inhibition is required to prevent cell cycle progression while some activity is required to catalyze DNA damage repair or make the decision to undergo apoptosis. It is clear that the Speedy/RINGO family plays roles in all of these processes and the exact mechanism by which they function will shed light on intricacies of CDK regulation of the cell cycle.

It has long been known that misregulation of CDKs and cyclins have been associated with oncogenesis. Furthermore, misregulation of CKIs such as p21 and p27, as well as inhibition of the tumor suppressor p53 and its pathways, has a strong correlation to cancer. Clearly, the inability to properly respond to DNA damage and cellular stress through checkpoint activation and apoptosis has a role in oncogenic potential as well as therapeutic considerations. It is therefore not surprising to find that Spy1 overexpression has been found in cancer tissues and cancer cell lines. The loss of control over a molecule like Spy1, which has such potent effects on CDK activation,

growth control, checkpoints and apoptosis, poses a threat to genomic stability, and may be oncogenic in nature. Lastly, it may prove invaluable to know the implications of Speedy/RINGO family members in the diagnosis and treatment of cancer. The outcome of common and experimental chemotherapeutic and anti-cancer drugs may be greatly influenced by the status of the Speedy/RINGO family members. Future research should define an important role for this novel family of cell cycle regulators in cell biology and cancer biology.

Acknowledgements

We thank Laura Castrejon for editorial assistance. This investigation was supported by NIH/NCI R01 CA090900, USAMRMC/CDMRP/DOD #W81XWH-06-1-0385, and a Ruth L. Kirschstein National Research Service Award - NIH/NCI T32 CA009523 (RG). Chapter 2, in full, is material published in Cell Cycle, Gastwirt, RF; McAndrew, CW; and Donoghue, DJ (2007). The dissertation author was a primary author of this paper.

References

1. Zucchi I, Mento E, Kuznetsov VA, et al. Gene expression profiles of epithelial cells microscopically isolated from a breast-invasive ductal carcinoma and a nodal metastasis. Proc Natl Acad Sci U S A 2004;101(52):18147-52.

2. Gutierrez GJ, Vogtlin A, Castro A, et al. Meiotic regulation of the CDK activator RINGO/Speedy by ubiquitin/proteasome-mediated processing and degradation. In review 2006;Gustavo Gutierrez: personal communication.

3. Ferby I, Blazquez M, Palmer A, Eritja R, Nebreda AR. A novel p34(cdc2)-binding and activating protein that is necessary and sufficient to trigger G(2)/M progression in Xenopus oocytes. Genes Dev 1999;13(16):2177-89.

4. Terret ME, Ferby I, Nebreda AR, Verlhac MH. RINGO efficiently triggers meiosis resumption in mouse oocytes and induces cell cycle arrest in embryos. Biol Cell 2001;93(1-2):89-97.

5. Karaiskou A, Perez LH, Ferby I, Ozon R, Jessus C, Nebreda AR. Differential regulation of Cdc2 and Cdk2 by RINGO and cyclins. J Biol Chem 2001;276(38):36028-34.

6. Lenormand JL, Dellinger RW, Knudsen KE, Subramani S, Donoghue DJ. Speedy: a novel cell cycle regulator of the G2/M transition. Embo J 1999;18(7):1869-77.

7. Kume S, Endo T, Nishimura Y, Kano K, Naito K. Porcine SPDYA2 (RINGO A2) stimulates CDC2 activity and accelerates meiotic maturation of porcine oocytes. Biol Reprod 2007;76(3):440-7.

8. Cheng A, Xiong W, Ferrell JE, Jr., Solomon MJ. Identification and Comparative Analysis of Multiple Mammalian Speedy/Ringo Proteins. Cell Cycle 2005;4(1):155-65.

9. Porter LA, Dellinger RW, Tynan JA, et al. Human Speedy: a novel cell cycle regulator that enhances proliferation through activation of Cdk2. J Cell Biol 2002;157(3):357-66.

10. Dinarina A, Perez LH, Davila A, Schwab M, Hunt T, Nebreda AR. Characterization of a new family of cyclin-dependent kinase activators. Biochem J 2004;386:349-55.

11. Cheng A, Gerry S, Kaldis P, Solomon MJ. Biochemical characterization of Cdk2-Speedy/Ringo A2. BMC Biochem 2005;6:19.

12. Porter LA, Kong-Beltran M, Donoghue DJ. Spy1 interacts with p27Kip1 to allow G1/S progression. Mol Biol Cell 2003;14(9):3664-74.

13. Xiao Z, Chen Z, Gunasekera AH, et al. Chk1 mediates S and G2 arrests through Cdc25A degradation in response to DNA-damaging agents. J Biol Chem 2003;278(24):21767-73.

14. Jin J, Shirogane T, Xu L, et al. SCFbeta-TRCP links Chk1 signaling to degradation of the Cdc25A protein phosphatase. Genes Dev 2003;17(24):3062-74.

15. Niculescu AB, 3rd, Chen X, Smeets M, Hengst L, Prives C, Reed SI. Effects of p21(Cip1/Waf1) at both the G1/S and the G2/M cell cycle transitions: pRb is a critical determinant in blocking DNA replication and in preventing endoreduplication. Mol Cell Biol 1998;18(1):629-43.

16. Ogryzko VV, Wong P, Howard BH. WAF1 retards S-phase progression primarily by inhibition of cyclin-dependent kinases. Mol Cell Biol 1997;17(8):4877-82.

17. Barnes EA, Porter LA, Lenormand JL, Dellinger RW, Donoghue DJ. Human Spy1 promotes survival of mammalian cells following DNA damage. Cancer Res 2003;63(13):3701-7.

18. Solomon MJ, Glotzer M, Lee TH, Philippe M, Kirschner MW. Cyclin activation of p34cdc2. Cell 1990;63(5):1013-24.

19. Savio M, Cerri M, Cazzalini O, et al. Replication-dependent DNA damage response triggered by roscovitine induces an uncoupling of DNA replication proteins. Cell Cycle 2006;5(18):2153-9.

20. Zhu Y, Alvarez C, Doll R, et al. Intra-S-phase checkpoint activation by direct CDK2 inhibition. Mol Cell Biol 2004;24(14):6268-77.

21. Maude SL, Enders GH. Cdk inhibition in human cells compromises chk1 function and activates a DNA damage response. Cancer Res 2005;65(3):780-6.

22. Deans AJ, Khanna KK, McNees CJ, Mercurio C, Heierhorst J, McArthur GA. Cyclin-Dependent Kinase 2 Functions in Normal DNA Repair and Is a Therapeutic Target in BRCA1-Deficient Cancers. Cancer Res 2006;66(16):8219-26.

23. Gastwirt RF, Slavin DA, McAndrew CW, Donoghue DJ. Spy1 expression prevents normal cellular responses to DNA damage: inhibition of apoptosis and checkpoint activation. J Biol Chem 2006;281(46):35425-35.

24. Zhao H, Piwnica-Worms H. ATR-mediated checkpoint pathways regulate phosphorylation and activation of human Chk1. Mol Cell Biol 2001;21(13):4129-39.

25. Liu Q, Guntuku S, Cui XS, et al. Chk1 is an essential kinase that is regulated by Atr and required for the G(2)/M DNA damage checkpoint. Genes Dev 2000;14(12):1448-59.

26. Guo Z, Kumagai A, Wang SX, Dunphy WG. Requirement for Atr in phosphorylation of Chk1 and cell cycle regulation in response to DNA replication blocks and UV-damaged DNA in Xenopus egg extracts. Genes Dev 2000;14(21):2745-56.

27. Kumagai A, Kim SM, Dunphy WG. Claspin and the activated form of ATR-ATRIP collaborate in the activation of Chk1. J Biol Chem 2004;279(48):49599-608.

28. Shechter D, Costanzo V, Gautier J. ATR and ATM regulate the timing of DNA replication origin firing. Nat Cell Biol 2004;6(7):648-55.

29. Shechter D, Gautier J. ATM and ATR Check in on Origins: A Dynamic Model for Origin Selection and Activation. Cell Cycle 2005;4(2).

30. Bartek J, Lukas C, Lukas J. Checking on DNA damage in S phase. Nat Rev Mol Cell Biol 2004;5(10):792-804.

31. Shimuta K, Nakajo N, Uto K, Hayano Y, Okazaki K, Sagata N. Chk1 is activated transiently and targets Cdc25A for degradation at the Xenopus midblastula transition. Embo J 2002;21(14):3694-703.

32. Golsteyn RM. Cdk1 and Cdk2 complexes (cyclin dependent kinases) in apoptosis: a role beyond the cell cycle. Cancer Lett 2005;217(2):129-38.

33. Kim SG, Kim SN, Jong HS, et al. Caspase-mediated Cdk2 activation is a critical step to execute transforming growth factor-beta1-induced apoptosis in human gastric cancer cells. Oncogene 2001;20(10):1254-65.

34. Zhang Y, Fujita N, Tsuruo T. Caspase-mediated cleavage of p21Waf1/Cip1 converts cancer cells from growth arrest to undergoing apoptosis. Oncogene 1999;18(5):1131-8.

35. Levkau B, Koyama H, Raines EW, et al. Cleavage of p21Cip1/Waf1 and p27Kip1 mediates apoptosis in endothelial cells through activation of Cdk2: role of a caspase cascade. Mol Cell 1998;1(4):553-63.

36. Gervais JL, Seth P, Zhang H. Cleavage of CDK inhibitor p21(Cip1/Waf1) by caspases is an early event during DNA damage-induced apoptosis. J Biol Chem 1998;273(30):19207-12.

37. Polyak K, Waldman T, He TC, Kinzler KW, Vogelstein B. Genetic determinants of p53-induced apoptosis and growth arrest. Genes Dev 1996;10(15):1945-52.

38. Gorospe M, Cirielli C, Wang X, Seth P, Capogrossi MC, Holbrook NJ. p21(Waf1/Cip1) protects against p53-mediated apoptosis of human melanoma cells. Oncogene 1997;14(8):929-35.

Chapter 3:

Spy1 Enhances Phosphorylation and Degradation of the Cell Cycle Inhibitor p27

Abstract

The cyclin dependent kinase inhibitor (CKI) $p27^{Kip1}$ binds to cyclin E/CDK2 complexes and prevents premature S-phase entry. During late G_1 and throughout S-phase, p27 phosphorylation at T187 leads to its subsequent degradation, which relieves CDK2 inhibition to promote cell cycle progression. However, critical events that trigger CDK2 complexes to phosphorylate p27 remain unclear. Utilizing recombinant proteins, we demonstrate that human Speedy (Spy1) activates CDK2 to phosphorylate p27 at T187 *in vitro*. Addition of Spy1 or Spy1/CDK2 to a preformed, inhibited cyclin E/CDK2/p27 complex also promoted this phosphorylation. Furthermore, Spy1 protected cyclin E/CDK2 from p27 inhibition toward histone H1, *in vitro*. Inducible Spy1 expression in U2OS cells reduced levels of endogenous p27 and exogenous $p27^{WT}$, but not a $p27^{T187A}$ mutant. Additionally, Spy1 expression in synchronized HeLa cells enhanced T187 phosphorylation and degradation of endogenous p27 in late G_1 and throughout S-phase. Our studies provide evidence that Spy1 expression enhances CDK2-dependent p27 degradation during late G_1 and throughout S-phase.

Introduction

Temporal control over activity of cyclin dependent kinases (CDKs) is critical for orderly cell cycle progression and is deregulated in numerous cancer types (1-4). Their activity is controlled by interaction with cyclin proteins, phosphorylation, dephosphorylation, and association with CDK inhibitors (CKIs) (5-8). Members of the Speedy/RINGO family are novel activators of CDKs although they have no homology to cyclin proteins (9-14). Unlike cyclins, Speedy/RINGO proteins activate CDKs independent of activating T-loop phosphorylation and are less susceptible to $p21^{cip}$ inhibition (11, 15). Spy1 was the first human homologue identified and was shown to enhance CDK2-dependent cell growth and activity, promote DNA replication, and is essential for efficient S-phase entry in mammalian cells (14). *Xenopus* Speedy/RINGO is required for the G_2/M transition during oocyte maturation and its expression also promotes DNA synthesis (9, 14, 16-18). Interestingly, Spy1 expression promotes cell survival in response to DNA damage and prevents UV-induced apoptosis and checkpoint activation (19, 20).

Cyclin E/CDK2 activation is necessary for DNA replication and particularly important for the G_1/S transition (21-23). Interestingly, Spy1 mRNA is also expressed during this phase in a variety of human tissues and cell lines (14). Protein levels of the CKI $p27^{kip1}$ are normally high during the G_0 and G_1 phases of the cell cycle and are primarily responsible for inhibiting cyclin E/CDK2 to prevent premature S-phase entry (3, 24-28). Free cyclin E/CDK2 was shown to phosphorylate p27 at T187 when bound to an inhibited, trimeric cyclin E/CDK2 complex (29, 30). CDK2-mediated

phosphorylation of p27 at T187 targets it to SCF^{Skp2} complex for ubiquitin-dependent degradation during late G_1/S phase (29, 31-42). Subsequently, cyclin E/CDK2 becomes active which facilitates progression through S-phase (21, 22, 31, 32). The T187-dependent p27 degradation pathway was shown to be operational during S-phase rather than G_1, and is dependent on CDK2 activity (43). This pathway was proposed to permit efficient S-phase progression by maintaining p27 below inhibitory levels.

Using a two-hybrid screen, p27 was identified as a binding partner for Spy1. This novel interaction was confirmed both *in vitro* and *in vivo* and Spy1 was shown to co-localize with p27 in the nucleus (17). Furthermore, Spy1 was shown to bind the CDK binding region of p27 rather than the cyclin binding domain. Interestingly, using p27-null cell lines, Spy1-enhanced cell growth was shown to be partially dependent on endogenous p27 (17). In this study, we have shown the Spy1/CDK2 complex phosphorylates p27 at T187 *in vitro*. Spy1 also promoted p27 phosphorylation on an inhibited cyclin E/CDK2 complex and partially protected cyclin E/CDK2 from p27 inhibition toward histone H1. Moreover, Spy1 expression reduced p27 protein levels and enhanced T187 phosphorylation *in vivo*. Additionally, synchronized cells expressing Spy1 degraded p27 more rapidly upon S-phase entry and maintained lower p27 levels throughout S-phase compared to mock cells. We propose possible mechanisms by which Spy1 promotes CDK2-dependent p27 degradation and cell cycle progression.

Materials and Methods

Plasmid Construction

The pGEX6P vector was used for production of bacterially expressed glutathione S-transferase (GST) fusion proteins. pGEX6P-myc-Spy1 was generated by a three part ligation with the EcoRI- NotI (pGEX6P) and BamHI- NotI (myc-Spy1) fragments and an in frame linker with EcoRI and BamHI overhangs (14). The myc-tag was deleted from pGEX6P-myc-Spy1 using EcoRI and ClaI sites and ligating in oligos (D2931/D2932) with EcoRI and ClaI overhangs to create pGEX6P-Spy1. All mutants were created using QuikChange Site-Directed Mutagenesis (Stratagene). Spy1 deletion mutants were created by introducing XbaI sites to generate an in frame stop codon within the pCS3-myc-Spy1 vector. ClaI and XbaI sites were used to subclone the mutants into the pGEX6P-Spy1 vector. The pMAL-c2e vector (a gift from Gustavo Gutierrez, Burnham Institute, La Jolla, CA) was used to construct all maltose-binding protein (MBP) fusion proteins. EcoRI and XbaI sites were used to sub-clone Spy1 and the truncation mutants from the respective GST-tagged constructs.

The pGEX6P-$p27^{WT}$ expression vector and a vector containing the $p27^{T187A}$ mutant was obtained from Dr. Kei-ichi Nakayama (Department of Molecular and Cellular Biology, Medical Institute of Bioregulation, Kyushu University, Japan) (44). The T187A mutant was subcloned into the pGEX6P-$p27^{WT}$ vector with SacII and XhoI sites.

pGEX6P-hCDK2 was constructed by introducing an upstream EcoRI site in a hCDK2-RcCMV vector (45), obtained from Dr. Ed Harlow (Massachusetts General

Hospital Cancer Center) then subcloned into the pGEX6P vector using EcoRI and XbaI sites. The $CDK2^{T160A}$ and $CDK2^{D145N}$ mutants were made in the pGEX6P-$CDK2^{WT}$ vector using primers D2933/D2934 and D2935/D2936. All DNA was sequenced by the UCSD Medical Center, Moores Cancer Center DNA Sequencing Shared Resource. The pGEX3X-cyclin E vector was a gift from Alex Almasan, Cleveland Clinic Foundation.

Protein Purification

Recombinant proteins were expressed in E. coli BL21 pLys(DE3) Rosetta cells (a gift from Patricia Jennings, UCSD). GST-fusion proteins were purified by affinity chromatography using glutathione-agarose resin (Sigma). Briefly, a single transformed colony was grown in 10mL LB containing ampicillin and chloramphenicol at 37^{o}C overnight. This culture was then diluted 1:100 into 1L fresh media until the OD_{600} was ~0.8. IPTG (0.1 mM) was then added and the culture was incubated for 16-18 hrs at 25^{o}C. Collected cells were lysed by sonification in 1X phosphate buffered saline (PBS) containing 1 mM DTT and protease inhibitors and insoluble material was removed via centrifugation. The supernatant was mixed with 1 ml of 50% glutathione-agarose resin (Sigma) at 4^{o}C 1h, washed with PBS, and bound proteins were eluted with 15 mM glutathione. Where indicated, the GST tag was removed from recombinant proteins using PreScission Protease (GE Healthcare) according to the manufacturers on column cleavage protocol. MBP-fusion proteins were purified by affinity chromatography using amylose resin (New England BioLabs) as described (9).

Eluted fractions were combined and dialyzed overnight at 4^{o}C to remove excess glutathione or maltose. When further purification was necessary, dialyzed proteins were concentrated with Centricon concentrators (Millipore), injected onto a Superdex 75 10/300 gel filtration column (GE Healthcare) and eluted fractions containing purified proteins were kept at -80^{o}C. Active, recombinant cyclin E/CDK2 from Sf21 insect cells was purchased from Upstate.

Western Blotting

Proteins were detected by immunoblotting with the indicated antisera followed by anti-mouse or anti-rabbit Ig-HRP conjugated secondary antibodies (GE Healthcare) and exposure to Enhanced ChemiLuminescence (ECL) (GE Healthcare). Primary mouse α-c-Myc (9E10) (sc-40), mouse α-p27 (F-8) (sc-1641), mouse α-Cdk2 (D-12) (sc-6248), mouse α-cyclin E (HE12) (sc-247), rabbit α-β-tubulin (H-235) (sc-9104), and rabbit α-p-p27 (Thr 187)-R (sc-16324-R) antibodies were purchased from Santa Cruz, Inc. Affinity purified rabbit antisera to Spy1 have been previously described (14). When necessary, membranes were stripped at 85°C for 1 h with stripping buffer (100 mM 2-mercaptoethanol, 2% SDS, 62.5 mM Tris-HCl pH 6.8) then blocked and reprobed.

In Vitro Kinase Assays

For kinase assays, purified proteins were incubated in Kinase Buffer (KB) (50 mM Tris-HCl pH 7.5, 1 mM DTT, 10 mM $MgCl_2$, 150 μM ATP) at 30^{o}C for the

indicated times. For radioactive assays, 1 μCi of [γ-^{32}P]-ATP (Perkin Elmer) and 1.4 μg histone H1 (Roche Applied Science) was used per reaction. Reactions were terminated by addition of 2X sample buffer. Proteins were resolved by 12.5% SDS-PAGE and analyzed by autoradiography or transferred to Immobilon-P (Millipore) for immunoblotting.

Protein Binding Assays

For binding of the Spy1 truncation mutants to CDK2 and p27, 5 μg of the indicated MBP-Spy1 fusion proteins were immobilized on 15 μl of amylose beads in 700 μl of binding buffer (BB) (50 mM Tris-HCl pH 7.5, 150 mM NaCl, 1 mM DTT, 1 mM EDTA, and 0.5% NP-40) at 4^{o}C for 1 h. After washing three times with BB, the amylase beads were incubated with equal molar ratios of CDK2 and/or p27 in 700 μl of BB. The beads were then washed four times with BB and bound proteins were eluted with 1x sample buffer, separated by 12.5% SDS-PAGE, and analyzed by immunoblotting.

For binding of p27^{WT} and p27^{T187A} to MBP-Spy1/CDK2, 5μg of MBP-Spy1 was incubated with an equal molar ratio of CDK2 in KB at 30^{o}C for 20 min. A two fold molar excess of p27^{WT} or p27^{T187A} was then added to the reactions and incubated 30 min further. 15 μl of amylose beads were then added to each reaction and incubated in 700 μl of BB at 4^{o}C for 1 h. After washing, bound proteins were eluted with sample buffer and resolved by SDS-PAGE.

Cell Culture

Myc-Spy1^{WT} and myc-Spy1$^{S/R\ box}$ inducible human osteosarcoma (U2OS) cell lines were cultured in DME supplemented with 0.1% penicillin-streptomycin, 10% FBS, 1.5 mM L-glutamine (Invitrogen), 0.48 mg/ml G418 and 0.5 mg/ml Zeocin (Invitrogen) and maintained at 37^{o}C in 5% CO_2 (19). Where indicated, U20S cells were transfected with 4μg of p27^{WT} or p27^{T187A} using FuGENE according to the manufacturer's protocol (Roche Applied Science). U2OS cell lines were induced for Spy1 expression with 1.25 nM ponasterone A (Invitrogen). Cells were starved in 0.02% FBS for 72 h prior to release into media containing serum and ponasterone A where indicated. MG132 (Sigma) was used at a final concentration of 1 μM.

HeLa cells were cultured in DME supplemented with 0.1% penicillin-streptomycin, 10% FBS, and maintained at 37^{o}C in 5% CO_2. Synchronization of HeLa cells in G_2/M was performed using a thymidine/nocodazole block as previously described (46). HeLa cells were transfected with 6 μg of pCS3-myc-Spy1 or empty vector using FuGENE. 4 h later, 2 mM thymidine was added to all plates and incubated 18 h further. Fresh media without thymidine was then added to the cells and incubated for 3 h. 100 nM nocodazole was then added to the plates and incubated 12 h further. Cells were harvested at the indicated time points, and split for lysis and immunoblot analysis or fixed for FACS analysis as previously described (19).

All cells were lysed in RIPA buffer (50 mM Tris-HCl pH 8.0, 150 mM NaCl, 1% NP-40, 0.5% deoxycholate, 0.1% SDS, 1 mM NaF and 1 mM Na_3VO_4) containing protease inhibitors (1 mM PMSF, and 10 μg/mL each of aprotinin and leupeptin),

clarified by centrifugation and protein concentrations were determined by DC protein assay (Bio-Rad). Equal amounts of lysate were resolved by 12.5% SDS-PAGE and transferred to Immobilon-P (Millipore).

Results

Spy1 activates CDK2 to phosphorylate p27 on T187 in vitro

In vitro kinase assays were performed to determine if a Spy1/CDK2 complex could phosphorylate p27. Recombinant Spy1 and CDK2 were incubated in the presence of 150μM ATP to allow for complex formation. $p27^{WT}$ was then added to the dimeric complex in the presence of [γ-^{32}P]-ATP and incubated 20 min further. Addition of $p27^{WT}$ to a Spy1/CDK2 complex, but not CDK2 alone, led to robust phosphorylation of p27 at T187 (Fig 3-1A). The $p27^{T187A}$ mutant exhibited background phosphorylation levels compared to wild type when examined by labeling with [γ-^{32}P]-ATP (Fig 3-1B). Immunoblotting with a phospho-T187 specific p27 antibody showed phosphorylation of $p27^{WT}$, but not $p27^{T187A}$, which increased over a 30-minute time course and with higher Spy1 concentrations (Fig 3-1C and D). These results demonstrate that Spy1/CDK2 phosphorylates p27 at T187 *in vitro*, and implicate a role for Spy1 in p27 regulation.

Spy1 requires T160 of CDK2 to phosphorylate p27 efficiently

Previously, members of the Speedy/Ringo family were shown to activate CDKs in the absence of T160 phosphorylation toward histone H1.(15, 47) To examine the catalytic contribution of this threonine residue, we assayed the ability of Spy1 to activate $CDK2^{WT}$ and $CDK2^{T160A}$ toward p27. Increasing concentrations of Spy1 were preincubated with $CDK2^{WT}$, $CDK2^{T160A}$, or $CDK2^{D145N}$ (kinase-dead) prior to p27 addition. Spy1/$CDK2^{WT}$ increased phosphorylation of p27 at T187, while

Spy1/CDK2^{T160A} phosphorylated p27 much less efficiently, and Spy1/CDK2^{D145N} exhibited no activity towards p27 (Fig 3-1 E and F). Thus, Spy1 activation of CDK2 with an alanine substitution at residue 160 clearly has negative catalytic effects. Considering recombinant CDK2 prepared from *E. coli* does not contain phosphorylated T160, this threonine residue itself, and not necessarily its phosphorylation may be important for efficient p27 phosphorylation catalyzed by Spy1/CDK2.

Characterization of the Spy1/p27 interaction

Recently, the C-terminus of Spy1 was shown to be required for activation of CDK2 toward histone H1 (11). Using purified recombinant C-terminal Spy truncation mutants (Fig 3-2A) and *in vitro* kinase assays, we show the C-terminus is also necessary for activation of CDK2 to phosphorylate p27. Addition of full length Spy1 to CDK2 catalyzed robust T187 phosphorylation while addition of the C-terminal truncation mutants Spy1$^{\Delta 215}$, Spy1$^{\Delta 160}$, or Spy1$^{\Delta 64}$ produced significantly decreased levels of T187 phosphorylation (Fig 3-2B).

To determine the region of Spy1 required for interaction with p27, binding of CDK2 and/or p27 to Spy1 truncation mutants was examined. MBP-Spy1 or the truncation mutants were bound to amylose beads prior to addition of CDK2, p27, or both CDK2 and p27, followed by incubation and elution. In the absence of CDK2, p27 displayed weak binding to full length Spy1 and no binding to Spy1$^{\Delta 215}$ or Spy1$^{\Delta 160}$ (Fig 3-2C). When Spy1 was assayed for binding to p27 in the presence of CDK2, the

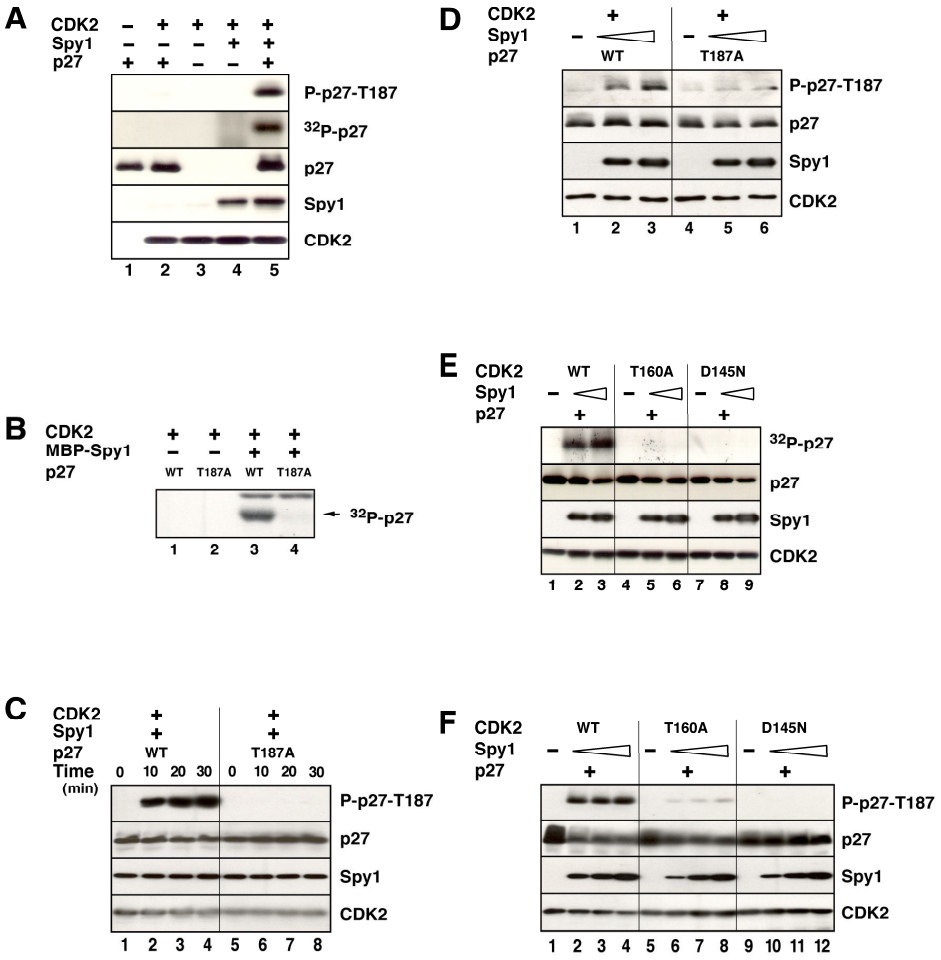

Figure 3-1. Spy1 activates CDK2 to phosphorylate p27 *in vitro*.
A, GST-CDK2 (0.5 µg) and GST-Spy1 (0.5 µg) were incubated in kinase buffer (KB) for 20 min. Samples were then split in half and a two-fold molar excess of p27 or p27 and [γ-^{32}P]-ATP was added to the reactions and incubated for 20 min. p27 phosphorylation was visualized by autoradiography or probing the p-p27 (Thr 187)-R antibody. Total levels of p27, Spy1 and CDK2 were detected by immunoblotting. *B,* CDK2 and MBP-Spy1 were incubated as in *A*. p27^{WT} or p27^{T187A} were then added in the presence of [γ-^{32}P]-ATP and incubated 20 min. ^{32}P-labeled proteins were visualized by autoradiography. *C*, GST-CDK2 was incubated with MBP-Spy1 as in *A*. After addition of p27^{WT} or p27^{T187A}, reactions were terminated at the indicated time points. *D*, GST-Spy1 (0.5 µg or 1 µg) and GST-CDK2 were incubated as in *A*. p27^{WT} or p27^{T187A} were added to the reactions and incubated for 20 min. *E*, Increasing amounts of MBP-Spy1 were incubated with GST-CDK2^{WT}, GST-CDK2^{T160A}, or GST-CDK2^{D145N} for 20 min. p27^{WT} was then added to each reaction and incubated for an additional 20 min. p27 phosphorylation was visualized by immunoblotting. *F*, Reactions were performed as in *E* in the presence of [γ-^{32}P]-ATP.

results demonstrate that p27 associates with a Spy1/CDK2 complex more robustly than Spy1 alone. The C-terminus of Spy1, as defined by the Δ215 endpoint, is not required for binding CDK2 or p27 in the presence of CDK2, but does promote activation of CDK2 to stimulate p27 phosphorylation.

Furthermore, the phosphorylation of p27 did not promote its dissociation from Spy1/CDK2. When $p27^{WT}$ or $p27^{T187A}$ were subjected to kinase reactions in the presence of MBP-Spy1/CDK2, and analyzed for binding to the complex, both the wild type and T187A mutants bound equally (Fig 3-2D). Indeed, these results resemble previous work demonstrating phosphorylation of p27 at T187, and does not promote dissociation or relieve inhibition of the cyclin E/CDK2complex (30).

Spy1 enhances cyclin E/CDK2 phosphorylation of p27

We hypothesized that Spy1 may also promote inhibited cyclin E/CDK2 to phosphorylate p27. To examine this phosphorylation event *in vitro*, Spy1 was added to a preformed cyclin E/CDK2/p27 complex. In the absence of Spy1, p27 was not efficiently phosphorylated. However, addition of Spy1 caused enhanced p27 phosphorylation at T187 over time (Fig 3-3A). Interestingly, although Spy1 addition to the inhibited complex promoted p27 phosphorylation, it did not relieve cyclin E/CDK2 inhibition toward histone H1, even when in 10-fold molar excess (Fig 3-3B). These results are consistent with prior observations that T187-phosphorylated p27 remains bound to and inhibits cyclin E/CDK2 (30, 32). This supports previous reports which proposed p27 degradation, and not the phosphorylation event, is required for increased and maximal CDK2 activity.

Spy1 can prevent p27 inhibition of cyclin E/CDK2 toward histone H1

We next examined whether Spy1 could protect active cyclin E/CDK2 complexes from inhibition by free p27, as might occur from *de novo* synthesis of p27 as cells progress through S-phase (3, 48-50). Incubation of Spy1 with cyclin E/CDK2, prior to p27 addition, partially protected cyclin E/CDK2 complexes from inhibition as seen by radio-labeled phosphate incorporation on histone H1 (Fig 3-3B and C). Consistent with the results above, the extent of p27 phosphorylation at T187 was again dependent on the Spy1 concentration preincubated with cyclin E/CDK2 (data not shown). These results indicate Spy1 can protect free cyclin E/CDK2 from p27 inhibition *in vitro*.

Previous work has shown free cyclin E/CDK2 is able to phosphorylate p27 bound to an inhibited cyclin E/CDK2 complex *in vitro* (30). We hypothesized that Spy1/CDK2 complexes could similarly phosphorylate p27 when bound to cyclin E/CDK2. To examine this, cyclin E, $CDK2^{D145N}$, and p27 were incubated for 20 min prior to the addition of preformed Spy1/$CDK2^{WT}$. $CDK2^{D145N}$ was used to eliminate any p27 phosphorylation catalyzed by cyclin E/CDK2. Addition of preformed Spy1/$CDK2^{WT}$, but not $CDK2^{WT}$ alone, catalyzed p27 phosphorylation at T187 (Fig 3-3D). Thus, a Spy1/CDK2 complex can phosphorylate p27 bound to cyclin E/CDK2 *in vitro*. Considering cyclin E/CDK2 complexes are inhibited before the G_1/S transition, Spy1 expression could activate a pool of free CDK2 and may be responsible for promoting phosphorylation of p27 bound to cyclin E/CDK2 to promote its degradation.

Spy1 expression enhances T187 phosphorylation and reduces p27 protein levels *in vivo*

To facilitate cell cycle progression, an increase in T187-dependent p27 proteolysis occurs in late G_1 and throughout S-phase, where phosphorylation of p27 by CDK2 induces its ubiquitination and eventual degradation by the 26S proteasome (31, 32, 51). To examine the effects of Spy1 expression on phosphorylation and p27 levels, myc-Spy1 inducible U2OS cells ($Spy1^{WT}$:U2OS) were induced for Spy1 expression for 24 hours, lysed, and proteins were resolved by SDS-PAGE (19). Lysates from mock-induced cells exhibited higher levels of endogenous p27 compared to Spy1-expressing cells using p27 specific antiserum. Accordingly, elevated immunoreactivity of T187 phosphorylation was observed in lysates from Spy1 induced cells (Fig 3-4A). To address the possibility that p27 was degraded by a T187-independent pathway, $p27^{WT}$ and $p27^{T187A}$ were transfected into $Spy1^{WT}$:U2OS cells prior to induction of Spy1 expression. Immunoblot analysis showed a reduction in total levels of $p27^{WT}$, but not $p27^{T187A}$. As with endogenous p27, exogenous $p27^{WT}$ displayed enhanced T187 phosphorylation with Spy1 expression, however, the T187A mutant displayed no immunoreactivity with the phospho-specific antibody (Fig 3-4B). These results indicate Spy1 expression promotes T187-dependent p27 degradation *in vivo*.

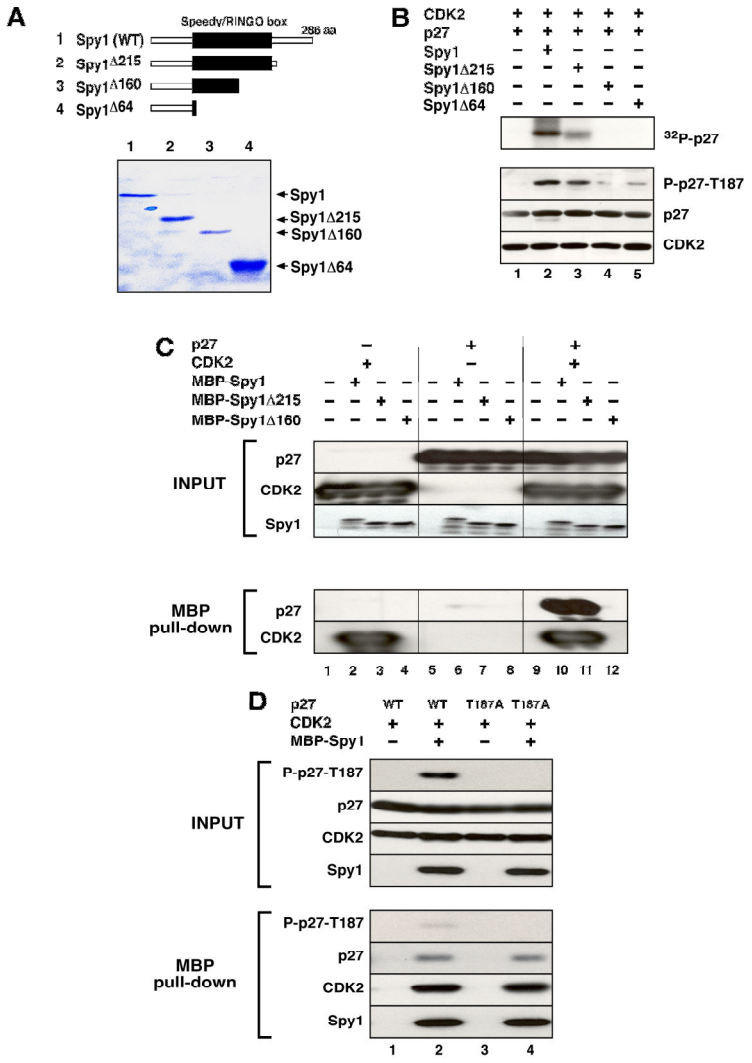

Figure 3-2. The interaction between p27 and Spy1 is enhanced by CDK2 and p27 phosphorylation does not cause dissociation from Spy1/CDK2.
A, A Coomassie stain of the purified GST-Spy1 proteins and a diagram illustrating the regions deleted are shown. *B*, Equal molar concentrations of the indicated GST-Spy1 fusion proteins were incubated with CDK2 in KB containing 1 μCi [γ-^{32}P]-ATP prior to addition of p27 to the reactions. Reactions were incubated for 20 min and p27 phosphorylation was analyzed by ^{32}P incorporation and immunoblot. *C*, 5 μg of the indicated MBP-Spy1 fusion proteins were immobilized on amylose resin in Binding Buffer (BB), washed, then incubated with p27^{WT} and/or CDK2. The beads were washed and bound proteins were analyzed by immunoblotting with the indicated antibodies. *D*, 5 μg of MBP-Spy1 was incubated with CDK2 in KB. p27^{WT} or p27^{T187A} was added to the indicated reaction and incubated 20 min. Amylose resin in BB was added to the reactions, incubated at 4^{o}C for 1 h, washed, and bound proteins were eluted with sample buffer and analyzed as in *C*.

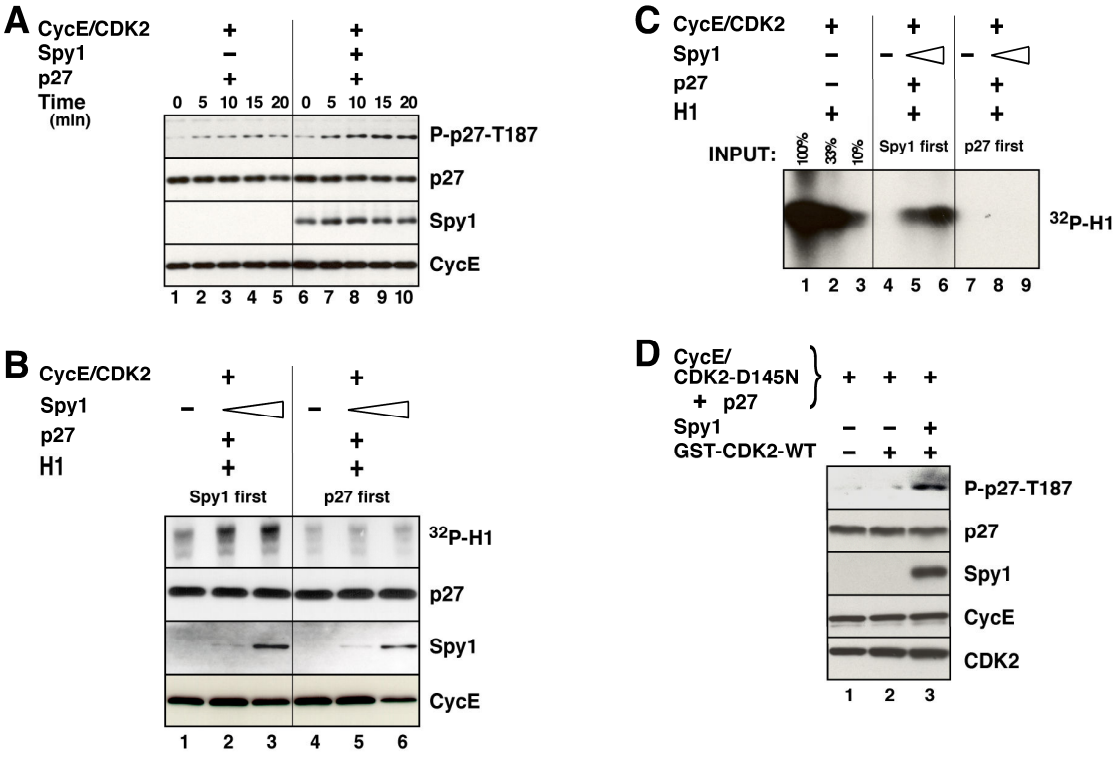

Figure 3-3. Spy1 increases the phosphorylation of p27 at T187 upon addition to a preinhibited complex of cyclin E/CDK2/p27.
A, Cyclin E/CDK2 was incubated with p27 to inhibit the complex. Recombinant myc-Spy1 was then added and the phosphorylation of p27 at T187 was analyzed over time. B, p27 or GST-Spy1 was incubated with cyclin E/CDK2 for 20 min. GST-Spy1 or p27 was then added to the indicated samples. Histone H1 and 1μCi of [γ-32P]-ATP were added after the second incubation and reactions were terminated after 20 min. An autoradiogram of phospho-histone H1 and immunoblots of p27, Spy1, and cyclin E are shown. C, Reactions were carried out as in B and histone H1 phosphorylation was analyzed by autoradiography. A control for uninhibited cyclin E/CDK2 is shown. D, GST-cyclin E, GST-CDK2D145N and p27 were incubated for 20 min prior to the addition of preformed Spy1/CDK2WT. Reactions were then incubated 20 min further and phosphorylation of p27 was analyzed by immunoblot.

Spy1-mediated p27 degradation is dependent on CDK2 and proteasomal activity

Previous research has shown p27 degradation proceeds through a proteasome-dependent mechanism (39, 41, 42). We set out to determine if the Spy1-enhanced reduction of p27 protein was proteasome-dependent. Upon Spy1 expression in induced Spy1^{WT}:U2OS cells released from starvation, p27 decreased to nearly undetectable levels after 12 h, while remaining constant in uninduced samples (Fig 3-4C). Spy1 expression clearly led to increased p27 phosphorylation at T187 as shown by phospho-specific immunoblotting, which became quite dramatic in MG132 treated cells (Fig 3-4C). These results indicate that expression of Spy1 in U2OS cells induces the degradation of p27 in a proteasome-dependent manner.

As stated above, the T187-dependent degradation of p27 in late G_1 and S-phase requires CDK2 activity. To demonstrate that Spy1-induced p27 degradation was CDK2-dependent, we used an inducible U2OS cell line that expresses a Spy1 mutant (Spy1$^{S/R\ box}$:U2OS) incapable of binding CDK2(19). Spy1$^{S/R\ box}$:U2OS cells were first starved to raise endogenous p27 levels, then released and induced. Cells were then harvested and lysed at the indicated time points. Total p27 and phospho-T187 levels were similar in mock and Spy1$^{S/R\ box}$-induced cells (Fig 3-4D). These results show Spy1-mediated p27 degradation is dependent on its ability to bind and activate CDK2.

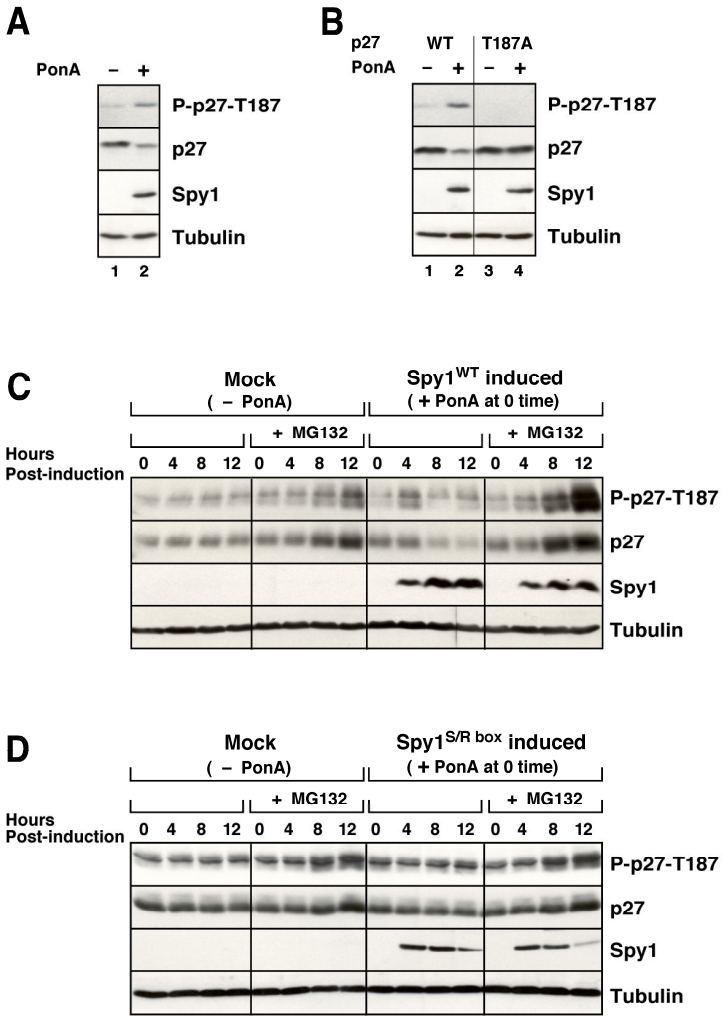

Figure 3-4. Spy1 expression enhances T187 phosphorylation, reduces p27 protein levels, and is dependent on CDK2 and the proteasome.
A, Spy1^{WT}:U2OS cells were induced with ethanol or ponasterone A for 24 h. Lysates were resolved by SDS-PAGE, transferred to membrane, and probed with anti-Myc (9E10) antiserum to detect myc-tagged Spy1 expression, anti-p27 (F-8) to show total p27 protein levels, and anti-p-p27 (T187)-R (sc-16324-R). ß-tubulin is shown as a loading control. *B*, Spy1^{WT}:U2OS cells were transfected with p27^{WT} or p27^{T187A} for 24 h. Cells were then induced for myc-Spy1 expression for 24 h, harvested, lysed, and analyzed as in *A*. *C*, Spy1^{WT}:U2OS cells were starved for 72 h in 0.02% FBS. Cells were then released with serum and induced with Ponasterone A. Where indicated, MG132 (1 µM) was added to the medium 4 h after induction. Cells were harvested and lysed at the indicated time points after induction and analyzed as in *A*. *D*, Spy1$^{S/R\ box}$:U2OS cells were treated as in *C*. Cells were then harvested, lysed, and analyzed as in *A*.

Spy1 expression promotes and maintains a reduced level of p27 during S-phase entry and progression

Previous research demonstrates that T187-dependent p27 degradation occurs during late G_1 and throughout S-phase (43). These results and the data mentioned above led us to assess the role of Spy1 in p27 degradation during this stage of the cell cycle. HeLa cells transfected with myc-Spy1 were synchronized in G_2/M using a thymidine/nocodazole block, as previously described, resulting in over 95% G_2/M cells upon release from nocodazole (46). At the onset of S-phase entry, Spy1-expressing cells exhibited a more rapid decrease in p27 levels compared to mock cells (Fig 3-5A). Furthermore, immunoblot analysis of lysates from Spy1 expressing cells in S-phase revealed reduced p27 levels compared to mock cells. Interestingly, T187 phosphorylation was detected throughout the entire cell cycle in cells expressing Spy1, but only during S-phase in control cells (Fig 3-5A). These results indicate that Spy1 expression causes enhanced turnover of p27 in late G_1 and throughout S-phase.

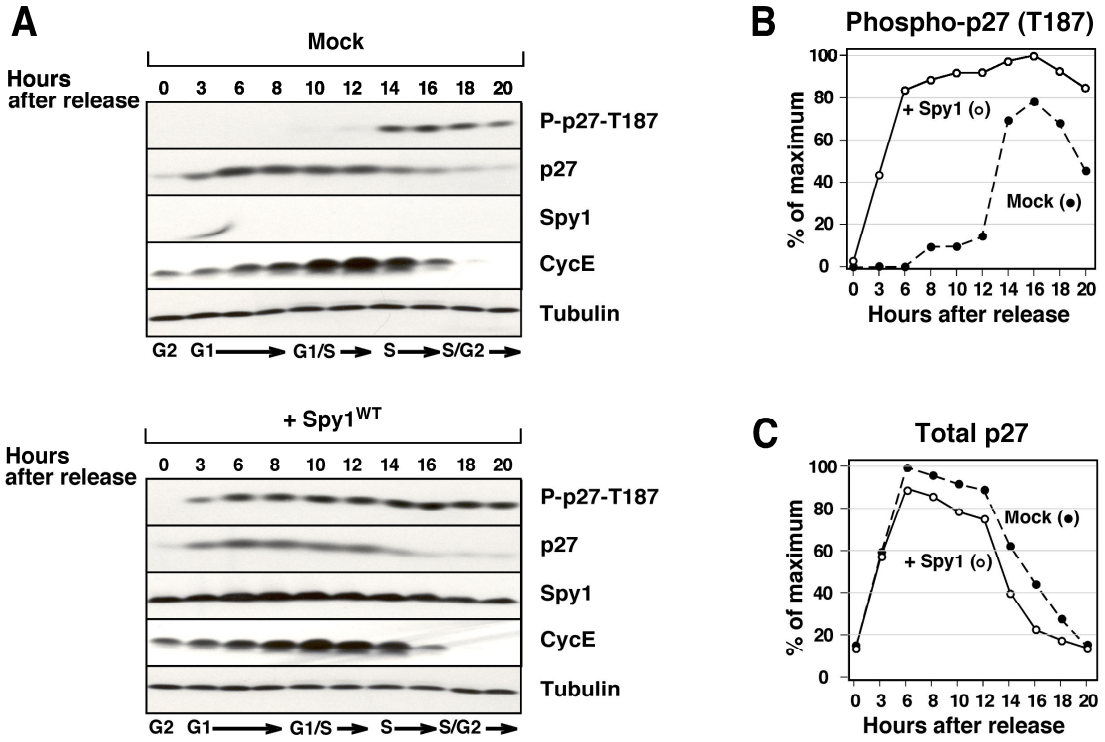

Figure 3-5. Spy1 promotes rapid loss of p27 in G_1/S and maintains lower p27 protein levels throughout S-phase.

A, HeLa cells were transfected with mock or myc-Spy1 DNA using FuGENE. Cells were then synchronized by thymidine-nocodazole block as described in Materials and Methods. After release from the nocodazole block, cells were harvested at the indicated time points. Half of the cells were fixed in 95% ethanol and stained with propidium iodide. The cell-cycle profile was analyzed by flow cytometry. Lysates were prepared from the remaining cells, resolved by SDS-PAGE, transferred to membrane, and probed with the indicated antibodies. One representative of five separate experiments is shown. *B*, Graph representing total phospho-p27 (T187) levels in mock (○) and Spy1 (●) cells from *A* over the time course shown. *C*, Graph representing total p27 levels in mock (○) and Spy1 (●) cells from *A*.

Discussion

Our lab and others previously demonstrated that Spy1 and Speedy/RINGO family members interact with p27 *in vivo*, and that Spy1 expression overcomes a p27-induced cell cycle arrest to allow for DNA synthesis and CDK2 activity (11, 17). To begin to identify the mechanisms by which Spy1 exerts its effects, we employed two complementary approaches: *in vitro* kinase reactions and interaction studies utilizing purified, recombinant proteins; and analysis of human cell lines expressing Spy1. In this report we demonstrate that Spy1 activates CDK2 to phosphorylate p27, and that Spy1 expression enhances p27 degradation upon entry into and throughout S-phase.

We found that Spy1 activates CDK2 to phosphorylate p27 at T187 both *in vitro* and *in vivo*. Additionally, Spy1 enhanced the phosphorylation of p27 when incubated with a preformed cyclin E/CDK2/p27 complex. Interestingly, cyclin E/CDK2 remained inhibited toward histone H1 in this assay, but incubation of Spy1 with cyclin E/CDK2 prior to p27 addition caused reduced inhibition. Furthermore, we demonstrate that a Spy1/CDK2 complex can phosphorylate p27 bound to a cyclin E/CDK2 complex as previously shown with cyclin E/CDK2 (30). Thus, in addition to activating free CDK2 to phosphorylate p27, Spy1 has effects on cyclin E/CDK2 activity with respect to p27 phosphorylation and inhibition. Spy1 expression in cells reduced p27 protein levels, which was dependent on CDK2 and proteasome activity. Moreover, synchronized HeLa cells expressing Spy1 eliminated p27 more rapidly upon S-phase entry and maintained lower p27 protein levels throughout S-phase compared to control cells.

It is well established that p27 degradation in late G_1 and during S-phase progression proceeds through T187 phosphorylation and is dependent on CDK2 activity. Although cyclin E/CDK2 is thought to promote this phosphorylation event, the results presented here suggest that formation of Spy1/CDK2 complexes at the G_1/S transition could contribute to the phosphorylation of p27 that is bound to an inhibited cyclin E/CDK2 complex. Considering Spy1 expression led to abundant p27 phosphorylation at T187 before S-phase entry, we believe Spy1 may prime p27 for rapid degradation upon entry into S-phase to facilitate the initiation of DNA replication and cell division. Additionally, Spy1 expression may simply enhance cyclin E/CDK2 activity toward p27 as we demonstrate *in vitro*. These activities would allow cells to tightly regulate their entry into S-phase and promote efficient progression toward cell division.

In addition to the rapid degradation of p27 upon S-phase entry, p27 protein levels are kept significantly reduced throughout S-phase by sustained T187 phosphorylation-mediated degradation. This pathway allows for cells to proceed with normal DNA replication and cell division by maintaining active cyclin/CDK2 complexes. To mediate this pathway, Spy1/CDK2 complexes could titrate p27 levels away from cyclin E/CDK2, thus preventing or relieving p27 inhibition and modulating the rate of replication. Aside from promoting p27 phosphorylation, Spy1 may also drive S-phase progression by protecting cyclin E/CDK2 complexes from p27-mediated inhibition as we demonstrate *in vitro*. By this mechanism, expression of

Spy1 could circumvent an increase in p27 protein levels that would otherwise inhibit cyclin E/CDK2 and slow cell cycle progression.

While p27 degradation in early G_1 is believed to be independent of T187 phosphorylation, p27 degradation at the G_1/S transition and throughout S-phase is regulated in most part by a T187-dependent pathway. This is proposed to maintain protein levels below concentrations that would completely halt DNA synthesis and cell cycle progression, but allow for cells to slow their progress when challenged with DNA damage or genomic stress by inhibiting this degradation pathway. Although Spy1 clearly has roles in normal cell cycle regulation, Spy1 could also provide the means to tightly regulate the balance between p27-mediated CDK2 inhibition and p27 degradation DNA damage induced checkpoint activation.

Although the importance of p27 in the checkpoint response is only beginning to be elucidated (52-55), it is clear that regulation of CDK2 activity is important for proper cell cycle progression and checkpoint regulation (56-61). Research from our lab has shown that Spy1 expression during S-phase may indeed play a role in activating CDK complexes in the face of inhibitory mechanisms. In a recent study, Spy1 expression was shown to cause bypass of an S-phase checkpoint, specifically allowing for UV irradiation resistant DNA synthesis (19). The effects of Spy1 expression on checkpoint responses may be related to its roles as an activator of CDK2 and trigger for p27 degradation, leading us to propose a likely model to explain the cellular effects caused by Spy1 expression. In this model, normal expression of Spy1 at the G_1/S transition and during S-phase provides cells with a means to rapidly

decrease and maintain p27 at low levels, allowing for cell growth unless faced with cellular stress (14). In the face of DNA damage and other cellular stresses, negative regulation of this degradation pathway, possibly by reducing Spy1/CDK2 activity, would provide a means to halt DNA replication, slow cell growth, and allow for DNA repair before division. Furthermore, there is evidence for a p21-dependent increase in p27 associated with cyclin E/CDK2 complexes in response to DNA damage, which prevents destabilizing phosphorylation of p27 (52). Thus, expression of Spy1 upon resolution of the DNA damage response may allow for activation of CDK2 complexes by enhancing p27 degradation.

At present, one unanswered question concerns the role of endogenous Spy1 in normal and/or cancer cells. Based on the results presented here demonstrating the effects of overexpressed Spy1, the ablation of endogenous Spy1 by knockdown techniques might be expected to delay T187 phosphorylation and degradation of p27 in late G_1 and throughout S-phase. In addition, based on previously published work showing that Spy1 overexpression promotes cell survival in response to DNA damage and prevents UV-induced apoptosis and checkpoint activation (19, 20), we might expect that Spy1 knockdown would enhance apoptosis and checkpoint activation in response to DNA damage. Although currently in progress, these experiments are complicated by the relatively low level of endogenous Spy1 expression together with the importance of analyzing effects at different times using synchronized populations of cells. Therefore, the inclusion of Spy1 knockdown experiments is beyond the scope of the results reported here.

In summary, we propose that the concurrent abilities of Spy1 to activate CDK2, to attenuate p27-mediated inhibition of cyclin E/CDK2, and to directly trigger CDK2-mediated phosphorylation and degradation of p27, may account for the observed S-phase checkpoint bypass in response to UV irradiation (19). It is likely that misregulation of Spy1 expression will lead to abundant CDK2 activity and low p27 levels, preventing damaged cells from slowing their growth and activating the proper checkpoint response. It is well known that p27 and CDK2 are misregulated in various cancers (62-65). Furthermore, Spy1 was recently shown to be one of the 50 genes most up-regulated in a human mammary epithelium library derived from an invasive ductal carcinoma (66). We believe the ability of Spy1 to prevent checkpoint activation and promote p27 phosphorylation and degradation may be correlative, thereby illuminating the connection between Spy1 overexpression and cancer development.

Acknowledgements

We thank Monica Kong-Beltran, Susanna Mac, and Shora Mobin for stimulating ideas and/or technical assistance; Laura Castrejon for editorial assistance; and support from a Ruth L. Kirchstein National Research Service Award - NIH/NCI #T32 CA009523 (RG) is acknowledged. Chapter 3, in full, is material published in Cell Cycle, McAndrew, CW; Gastwirt, RF; Meyer, AN; Porter, LA; and Donoghue, DJ (2007). The dissertation author was the primary investigator and primary author of this paper.

References

1. Santamaria D, Ortega S. Cyclins and CDKS in development and cancer: lessons from genetically modified mice. Front Biosci 2006;11:1164-88.

2. Morgan DO. Principles of CDK regulation. Nature 1995;374(6518):131-4.

3. Sherr CJ, Roberts JM. CDK inhibitors: positive and negative regulators of G1-phase progression. Genes Dev 1999;13(12):1501-12.

4. Hunter T, Pines J. Cyclins and cancer. II: Cyclin D and CDK inhibitors come of age. Cell 1994;79(4):573-82.

5. Sebastian B, Kakizuka A, Hunter T. Cdc25M2 activation of cyclin-dependent kinases by dephosphorylation of threonine-14 and tyrosine-15. Proc Natl Acad Sci U S A 1993;90(8):3521-4.

6. Poon RY, Yamashita K, Adamczewski JP, Hunt T, Shuttleworth J. The cdc2-related protein p40MO15 is the catalytic subunit of a protein kinase that can activate p33cdk2 and p34cdc2. Embo J 1993;12(8):3123-32.

7. Brown NR, Noble ME, Endicott JA, Johnson LN. The structural basis for specificity of substrate and recruitment peptides for cyclin-dependent kinases. Nat Cell Biol 1999;1(7):438-43.

8. Holmes JK, Solomon MJ. The role of Thr160 phosphorylation of Cdk2 in substrate recognition. Eur J Biochem 2001;268(17):4647-52.

9. Ferby I, Blazquez M, Palmer A, Eritja R, Nebreda AR. A novel p34(cdc2)-binding and activating protein that is necessary and sufficient to trigger G(2)/M progression in Xenopus oocytes. Genes Dev 1999;13(16):2177-89.

10. Dinarina A, Perez LH, Davila A, Schwab M, Hunt T, Nebreda AR. Characterization of a new family of cyclin-dependent kinase activators. Biochem J 2004;386:349-55.

11. Cheng A, Xiong W, Ferrell JE, Jr., Solomon MJ. Identification and Comparative Analysis of Multiple Mammalian Speedy/Ringo Proteins. Cell Cycle 2005;4(1):155-65.

12. Nebreda AR. CDK activation by non-cyclin proteins. Curr Opin Cell Biol 2006;18(2):192-8.

13. Lenormand JL, Dellinger RW, Knudsen KE, Subramani S, Donoghue DJ. Speedy: a novel cell cycle regulator of the G2/M transition. Embo J 1999;18(7):1869-77.

14. Porter LA, Dellinger RW, Tynan JA, et al. Human Speedy: a novel cell cycle regulator that enhances proliferation through activation of Cdk2. J Cell Biol 2002;157(3):357-66.

15. Karaiskou A, Perez LH, Ferby I, Ozon R, Jessus C, Nebreda AR. Differential regulation of Cdc2 and Cdk2 by RINGO and cyclins. J Biol Chem 2001;276(38):36028-34.

16. Gutierrez GJ, Vogtlin A, Castro A, et al. Meiotic regulation of the CDK activator RINGO/Speedy by ubiquitin-proteasome-mediated processing and degradation. Nat Cell Biol 2006;8(10):1084-94.

17. Porter LA, Kong-Beltran M, Donoghue DJ. Spy1 interacts with p27Kip1 to allow G1/S progression. Mol Biol Cell 2003;14(9):3664-74.

18. Terret ME, Ferby I, Nebreda AR, Verlhac MH. RINGO efficiently triggers meiosis resumption in mouse oocytes and induces cell cycle arrest in embryos. Biol Cell 2001;93(1-2):89-97.

19. Gastwirt RF, Slavin DA, McAndrew CW, Donoghue DJ. Spy1 expression prevents normal cellular responses to DNA damage: inhibition of apoptosis and checkpoint activation. J Biol Chem 2006;281(46):35425-35.

20. Barnes EA, Porter LA, Lenormand JL, Dellinger RW, Donoghue DJ. Human Spy1 promotes survival of mammalian cells following DNA damage. Cancer Res 2003;63(13):3701-7.

21. Reed SI. Control of the G1/S transition. Cancer Surv 1997;29:7-23.

22. Connell-Crowley L, Elledge SJ, Harper JW. G1 cyclin-dependent kinases are sufficient to initiate DNA synthesis in quiescent human fibroblasts. Curr Biol 1998;8(1):65-8.

23. Woo RA, Poon RY. Cyclin-dependent kinases and S phase control in mammalian cells. Cell Cycle 2003;2(4):316-24.

24. Toyoshima H, Hunter T. p27, a novel inhibitor of G1 cyclin-Cdk protein kinase activity, is related to p21. Cell 1994;78(1):67-74.

25. Hengst L, Dulic V, Slingerland JM, Lees E, Reed SI. A cell cycle-regulated inhibitor of cyclin-dependent kinases. Proc Natl Acad Sci U S A 1994;91(12):5291-5.

26. Polyak K, Kato JY, Solomon MJ, et al. p27Kip1, a cyclin-Cdk inhibitor, links transforming growth factor-beta and contact inhibition to cell cycle arrest. Genes Dev 1994;8(1):9-22.

27. Slingerland JM, Hengst L, Pan CH, Alexander D, Stampfer MR, Reed SI. A novel inhibitor of cyclin-Cdk activity detected in transforming growth factor beta-arrested epithelial cells. Mol Cell Biol 1994;14(6):3683-94.

28. Coats S, Flanagan WM, Nourse J, Roberts JM. Requirement of p27Kip1 for restriction point control of the fibroblast cell cycle. Science 1996;272(5263):877-80.

29. Sheaff RJ, Groudine M, Gordon M, Roberts JM, Clurman BE. Cyclin E-CDK2 is a regulator of p27Kip1. Genes Dev 1997;11(11):1464-78.

30. Xu X, Nakano T, Wick S, Dubay M, Brizuela L. Mechanism of Cdk2/Cyclin E inhibition by p27 and p27 phosphorylation. Biochemistry 1999;38(27):8713-22.

31. Vlach J, Hennecke S, Amati B. Phosphorylation-dependent degradation of the cyclin-dependent kinase inhibitor p27. Embo J 1997;16(17):5334-44.

32. Montagnoli A, Fiore F, Eytan E, et al. Ubiquitination of p27 is regulated by Cdk-dependent phosphorylation and trimeric complex formation. Genes Dev 1999;13(9):1181-9.

33. Hao B, Zheng N, Schulman BA, et al. Structural basis of the Cks1-dependent recognition of p27(Kip1) by the SCF(Skp2) ubiquitin ligase. Mol Cell 2005;20(1):9-19.

34. Ungermannova D, Gao Y, Liu X. Ubiquitination of p27Kip1 requires physical interaction with cyclin E and probable phosphate recognition by SKP2. J Biol Chem 2005;280(34):30301-9.

35. Kossatz U, Dietrich N, Zender L, Buer J, Manns MP, Malek NP. Skp2-dependent degradation of p27kip1 is essential for cell cycle progression. Genes Dev 2004;18(21):2602-7.

36. Pagano M. Control of DNA synthesis and mitosis by the Skp2-p27-Cdk1/2 axis. Mol Cell 2004;14(4):414-6.

37. Nakayama K, Nagahama H, Minamishima YA, et al. Skp2-mediated degradation of p27 regulates progression into mitosis. Dev Cell 2004;6(5):661-72.

38. Nakayama K, Nagahama H, Minamishima YA, et al. Targeted disruption of Skp2 results in accumulation of cyclin E and p27(Kip1), polyploidy and centrosome overduplication. Embo J 2000;19(9):2069-81.

39. Carrano AC, Eytan E, Hershko A, Pagano M. SKP2 is required for ubiquitin-mediated degradation of the CDK inhibitor p27. Nat Cell Biol 1999;1(4):193-9.

40. Amati B, Vlach J. Kip1 meets SKP2: new links in cell-cycle control. Nat Cell Biol 1999;1(4):E91-3.

41. Sutterluty H, Chatelain E, Marti A, et al. p45SKP2 promotes p27Kip1 degradation and induces S phase in quiescent cells. Nat Cell Biol 1999;1(4):207-14.

42. Tsvetkov LM, Yeh KH, Lee SJ, Sun H, Zhang H. p27(Kip1) ubiquitination and degradation is regulated by the SCF(Skp2) complex through phosphorylated Thr187 in p27. Curr Biol 1999;9(12):661-4.

43. Malek NP, Sundberg H, McGrew S, et al. A mouse knock-in model exposes sequential proteolytic pathways that regulate p27Kip1 in G1 and S phase. Nature 2001;413(6853):323-7.

44. Ishida N, Kitagawa M, Hatakeyama S, Nakayama K. Phosphorylation at serine 10, a major phosphorylation site of p27(Kip1), increases its protein stability. J Biol Chem 2000;275(33):25146-54.

45. van den Heuvel S, Harlow E. Distinct roles for cyclin-dependent kinases in cell cycle control. Science 1993;262(5142):2050-4.

46. Christensen J, Cloos P, Toftegaard U, et al. Characterization of E2F8, a novel E2F-like cell-cycle regulated repressor of E2F-activated transcription. Nucleic Acids Res 2005;33(17):5458-70.

47. Cheng A, Gerry S, Kaldis P, Solomon MJ. Biochemical characterization of Cdk2-Speedy/Ringo A2. BMC Biochem 2005;6:19.

48. Obaya AJ, Kotenko I, Cole MD, Sedivy JM. The proto-oncogene c-myc acts through the cyclin-dependent kinase (Cdk) inhibitor p27(Kip1) to facilitate the activation of Cdk4/6 and early G(1) phase progression. J Biol Chem 2002;277(34):31263-9.

49. Poon RY, Toyoshima H, Hunter T. Redistribution of the CDK inhibitor p27 between different cyclin. CDK complexes in the mouse fibroblast cell cycle and in cells arrested with lovastatin or ultraviolet irradiation. Mol Biol Cell 1995;6(9):1197-213.

50. Soos TJ, Kiyokawa H, Yan JS, et al. Formation of p27-CDK complexes during the human mitotic cell cycle. Cell Growth Differ 1996;7(2):135-46.

51. Pagano M, Tam SW, Theodoras AM, et al. Role of the ubiquitin-proteasome pathway in regulating abundance of the cyclin-dependent kinase inhibitor p27. Science 1995;269(5224):682-5.

52. He G, Kuang J, Huang Z, et al. Upregulation of p27 and its inhibition of CDK2/cyclin E activity following DNA damage by a novel platinum agent are dependent on the expression of p21. Br J Cancer 2006;95(11):1514-24.

53. Petrocelli T, Slingerland J. UVB induced cell cycle checkpoints in an early stage human melanoma line, WM35. Oncogene 2000;19(39):4480-90.

54. Zhou H, Kato A, Yasuda H, et al. The induction of cell cycle regulatory and DNA repair proteins in cisplatin-induced acute renal failure. Toxicol Appl Pharmacol 2004;200(2):111-20.

55. Balasubramanian S, Kim KH, Ahmad N, Mukhtar H. Activation of telomerase and its association with G1-phase of the cell cycle during UVB-induced skin tumorigenesis in SKH-1 hairless mouse. Oncogene 1999;18(6):1297-302.

56. Shechter D, Costanzo V, Gautier J. ATR and ATM regulate the timing of DNA replication origin firing. Nat Cell Biol 2004;6(7):648-55.

57. Zhu Y, Alvarez C, Doll R, et al. Intra-S-phase checkpoint activation by direct CDK2 inhibition. Mol Cell Biol 2004;24(14):6268-77.

58. Savio M, Cerri M, Cazzalini O, et al. Replication-dependent DNA damage response triggered by roscovitine induces an uncoupling of DNA replication proteins. Cell Cycle 2006;5(18):2153-9.

59. Shechter D, Gautier J. ATM and ATR Check in on Origins: A Dynamic Model for Origin Selection and Activation. Cell Cycle 2005;4(2).

60. Maude SL, Enders GH. Cdk inhibition in human cells compromises chk1 function and activates a DNA damage response. Cancer Res 2005;65(3):780-6.

61. Deans AJ, Khanna KK, McNees CJ, Mercurio C, Heierhorst J, McArthur GA. Cyclin-Dependent Kinase 2 Functions in Normal DNA Repair and Is a Therapeutic Target in BRCA1-Deficient Cancers. Cancer Res 2006;66(16):8219-26.

62. Sherr CJ. Cancer cell cycles. Science 1996;274(5293):1672-7.

63. Catzavelos C, Bhattacharya N, Ung YC, et al. Decreased levels of the cell-cycle inhibitor p27Kip1 protein: prognostic implications in primary breast cancer. Nat Med 1997;3(2):227-30.

64. Loda M, Cukor B, Tam SW, et al. Increased proteasome-dependent degradation of the cyclin-dependent kinase inhibitor p27 in aggressive colorectal carcinomas. Nat Med 1997;3(2):231-4.

65. Porter PL, Malone KE, Heagerty PJ, et al. Expression of cell-cycle regulators p27Kip1 and cyclin E, alone and in combination, correlate with survival in young breast cancer patients. Nat Med 1997;3(2):222-5.

66. Zucchi I, Mento E, Kuznetsov VA, et al. Gene expression profiles of epithelial cells microscopically isolated from a breast-invasive ductal carcinoma and a nodal metastasis. Proc Natl Acad Sci U S A 2004;101(52):18147-52.

Chapter 4:

Spy1 Expression Prevents Normal Cellular Responses to DNA Damage: Inhibition of Apoptosis and Checkpoint Activation

Abstract

Spy1 is the originally identified member of the Speedy/Ringo family of vertebrate cell cycle regulators, which can control cell proliferation and survival through the atypical activation of CDKs. Here we report a role for Spy1 in apoptosis and checkpoint activation in response to Ultraviolet (UV) irradiation. Using an inducible system allowing for regulated expression of Spy1, we show that Spy1 expression prevents activation of caspase-3 and suppresses apoptosis in response to UV irradiation. Spy1 expression also allows for UV irradiation resistant DNA synthesis (UVDS) and permits cells to progress into mitosis as demonstrated by phosphorylation on Histone H3, indicating that Spy1 expression can inhibit the S-phase/replication and G2/M checkpoints. We demonstrate that Spy1 expression inhibits phosphorylation of Chk1, RPA, and histone H2A.X, which may directly contribute to the decrease in apoptosis and checkpoint bypass. Furthermore, mutation of the conserved Speedy/Ringo Box, known to mediate interaction with CDK2, abrogates the ability of Spy1 to inhibit apoptosis and the phosphorylation of Chk1 and RPA. The data presented indicate that Spy1 expression allows cells to evade checkpoints and apoptosis, and suggests that Spy1 regulation of CDK2 is important for the response to DNA damage.

Introduction

Xenopus Speedy (X-Spy1) was originally identified by its ability to confer resistance to UV irradiation in a Rad1-deficient strain of S. *pombe* (1), and was found to bind to and activate CDK2 (1). Human Spy1 was subsequently shown to enhance cellular proliferation through the direct activation of CDK2. Moreover, RNAi knockdown of Spy1 prevented cellular proliferation by inhibiting efficient S-phase entry (2). In addition, Spy1 was shown to enhance mammalian cell survival in response to a number of genotoxic agents, including hydroxyurea, cisplatin and camptothecin (3). This survival effect of Spy1 was depressed when a CDK2 dominant negative was expressed (3), indicating that the ability of Spy1 to activate CDK2 may be required for Spy1-associated cell survival.

A Spy1 homolog, Ringo, also identified in *Xenopus* (4), was shown to activate both CDK2 and cdc2 independent of their respective cyclins (5). Recently, Spy1 and Ringo have been placed in a larger family of vertebrate proteins, designated the Speedy/Ringo family. The members of the Speedy/Ringo family share high sequence homology within a central region known as the Speedy/Ringo Box (S/R Box), which has been shown to mediate interaction with and activation of CDK2 (6, 7). Spy1 and its homologs can activate CDK2 in the absence of known mechanisms of activation (7). In fact, Spy1 has been shown to facilitate phosphorylation of cdc25 by CDK2 in an event that both stabilizes cdc25 and further activates CDK2 (8). Spy1 can also activate CDK2 in the absence of the T160 activating phosphorylation (8). This phosphorylation event is mediated by the CDK Activating Kinase (CAK), which is

known to be regulated by p53 in response to DNA damage (9). Finally, Spy1 and its homologs can prevent CDK inhibition by CDKIs such as p21 and p27 (5, 10).

Cancer arises when a cell evades normal proliferative controls, often by mutations in genes that control cell growth and division (11). Various checkpoints exist to ensure that cells replicate without genetic errors and repair damaged DNA, to avoid both the uncoupling of replication from cell cycle control as well as to avoid the transmission of genetic mutations (12-14). Recent evidence demonstrates that DNA damage responses are activated in early premalignant tissue but not in normal tissue (15). Checkpoints are often the targets for oncogenic mutation, thereby uncoupling proliferation from apoptosis while enhancing proliferation itself during transformation and tumorigenesis (11, 16, 17). In addition to evasion of checkpoints, cancer cells must also inactivate the apoptotic pathways (18). Apoptotic mechanisms exist to protect cells against the loss of checkpoints, irreparable DNA damage and sustained oncogenic stimuli.

Significantly, a correlation between Spy1 and breast cancer was recently published (19). This study examined the altered regulation of genes in nodal metastatic and invasive ductal breast carcinomas, identifying Spy1 as one of the fifty most up-regulated genes (19). These data suggest that deregulation of Spy1 expression plays a key role in oncogenesis.

In this study, we have investigated the role of Spy1 expression in apoptosis and checkpoint activation to begin to understand the molecular mechanisms by which Spy1 may contribute to oncogenesis as reported for breast cancer (19). In this study,

we show that Spy1 expression enhances cell survival in response to UV irradiation by preventing the activation of caspases and apoptosis in a U2OS osteosarcoma cell line. Interestingly, Spy1 expression suppresses the activation of both an S-phase/replication checkpoint, as well as a G2/M checkpoint. In addition, Spy1 expression prevents the activation of checkpoint proteins such as Chk1 and the histone variant H2A.X in response to UV irradiation, and prevents other ATR mediated signaling events such as the phosphorylation of RPA32 on its N-terminus. Furthermore, mutations within the Speedy/Ringo (S/R) Box of Spy1, known to mediate the interaction with and activation of CDK2 (6, 7), prevent these effects of Spy1. Expression of this mutant does not suppress the phosphorylation of Chk1 or RPA32 in response to UV-induced DNA damage, indicating a specific role for Spy1 and Spy1-associated CDK2 activity in the regulation of the DNA damage response. The expression of Spy1 thus facilitates the evasion of checkpoints and apoptotic pathways that are activated in response to DNA damage.

Experimental Procedures

Cell lines, creation of inducible cell lines, and UV irradiation conditions

U2OS, human osteosarcoma cells, with wild type p53, (American Type Culture Collection, Manassas, VA), and all derivatives, were maintained in DME (GIBCO), supplemented with 0.1% penicillin-streptomycin (Sigma, St. Louis, MO), 10% fetal bovine serum, and 1.5mM L-glutamine (Invitrogen, Carlsbad, CA). Cells were incubated at 37°C in 5% CO_2.

Inducible U2OS cell lines were created using the Ecdysone System (Invitrogen) (20) as follows: U2OS cells were transfected with pVgRXR regulatory vector and selected for 14 days with Zeocin. Subsequently, myc-Spy1 and the myc-$Spy^{S/RBox}$ mutant were cloned into the BamH1 and Xba1 sites of the pIND vector and transfected into pVgRXR expressing U2OS cells. Cells were selected with G418 and Zeocin (Invitrogen) for 14 days, colonies were isolated, and then tested for expression of myc-Spy1 or the myc-$Spy1^{S/RBox}$ mutant induced by Ponasterone A (20). Induction conditions were determined to be maximal with 1.25nM Ponasterone A (subsequently referred to as induction media). Cell culture conditions were as above with the inclusion of 0.48mg/ml G418 and 0.5mg/ml Zeocin.

For UV irradiation, media was aspirated and plates were washed twice with PBS. After removing as much PBS as possible, the cells were irradiated with 50 J/m^2 UVC (254nm) using a Stratalinker1800 (Stratagene, La Jolla, CA). Induction media was then added back and plates were returned to the incubator until processed. Where

indicated, the human pRcCMV-CDK2 expression plasmid was transfected into cells with FuGENE (Roche, Indianapolis, IN) according to manufacturer's protocol.

Creation of Spy1 S/R Box mutant

To create the S/R Box mutation of Spy1, BglII and MluI sites were cloned into wild type pIND-myc-Spy1, flanking the acidic region of the S/R Box at residues 458 and 525 respectively, using Quick Change (Stratagene), using the following primers: for BglII (GGGCTAAATTTACTATAAGTGAGCATACCAGATCTAATTTCTTTA TTGCTCTGTATCTG); for MluI (GAAACCAAGTACGCGTTTTTTCCATGGG CTTTAGGG). The region flanking the mutation sites was then excised using BglII and MluI. A short oligonucleotide containing the mutations E134, 135, 137, 138, 139→Q and D136→N was then ligated into these sites:(GATCTAATTTCTTTATTG CTCTGTATCTGGCTAATACAGTTCAACAAAATCAACAACAAACCAAGTA).

Antibodies

Anti-caspase-3 (FL) rabbit antibody (#9662), anti-cleaved caspase-3 Alexa Fluor 488 conjugated rabbit antibody (#9669), anti-phospho Chk1 (Ser345) rabbit antibody (#2341), anti-phospho Chk1 (Ser345)(133D3) rabbit monoclonal antibody (#2348), anti-phospho Chk1 (Ser317) rabbit antibody (#2344), and anti-phospho Histone H3 (Ser10) Alexa Fluor 488 conjugated rabbit antibody (#9708) were purchased from Cell Signaling Technology (Beverly, MA). Anti-myc (9E10) (sc-40) mouse antibody, anti-Chk1 (G4) (sc-8408) mouse antibody, anti-CDK2 (D12) (sc-

6248) mouse antibody, anti-RPA32 (C16) (sc-14692) goat antibody, anti-CDK2 (M2) (sc-163) rabbit antibody, and anti-β-tubulin (H235) (sc9104) rabbit antibody were purchased from Santa Cruz Biotechnology (Santa Cruz, CA). Anti-phospho Histone H2A.X (Ser139; γH2AX) clone JBW301 mouse antibody was purchased from Upstate (Lake Placid, NY). Anti-phospho RPA32 (Ser4, Ser8) (BL647) (A300-245A) was purchased from Bethyl Laboratories, Inc (Montgomery, Texas).

Detection of apoptosis

To determine apoptosis in response to UV, $5x10^5$ pIND:U2OS and Spy1:U2OS cells were seeded on 10cm plates, induced for 24 h and then irradiated with UV. Cells were allowed to recover in induction media until the indicated time points. Floating and adherent cells were collected by centrifugation, washed twice with PBS and fixed in 95% ethanol at 4°C overnight. After fixation, cells were washed twice with 1%BSA/PBS and resuspended in 1ml PBS. Cells were then stained with a propidium iodide solution (0.25mg/ml propidium iodide, 0.01% Triton-X100, 100µg/ml RNase A in PBS) and analyzed for Sub-G1 DNA content by flow cytometry using a FACScalibur (BD Biosciences, Franklin Lakes, NJ).

To detect apoptosis by Annexin V binding to the outer cell membrane, $5x10^5$ cells were seeded on 10cm plates and induced for 24 h. Cells were then irradiated with UV and incubated for 24 h in induction media. Floating and adherent cells were collected, washed twice with PBS, and resuspended in Annexin V binding buffer (BD Biosciences). $1x10^5$ cells were stained with Annexin V-FITC and 7-amino-

actinomycin D (7-AAD; to detect necrotic cells) as per manufacturer's instructions (BD Biosciences). Cells were analyzed for apoptosis by flow cytometry.

Western blotting

Cells were lysed in 0.1% NP-40 lysis buffer (20mM Tris, pH 8.0, 150mM NaCl, 0.1% NP-40, 1mM Na_3VO_4, 1mM NaF, 1mM PMSF, 10μg/ml aprotinin), clarified by centrifugation, and protein concentrations were determined by Bradford Assay (Bio-Rad). Equal amounts of protein for each sample were resolved by SDS-PAGE (10% SDS-PAGE except for caspase-3 experiment at 17.5%) and transferred to nitrocellulose. Proteins were detected by immunoblotting with the indicated antisera followed by secondary antibodies (anti-mouse Ig-HRP conjugate [GE Healthcare, Piscataway, NJ] or anti-rabbit Ig-HRP conjugate [GE Healthcare]), followed by Enhanced ChemiLuminescence (ECL) (GE Healthcare).

Detection of cleaved caspase-3 by intracellular staining and flow cytometry

To detect cleaved caspase-3 in response to UV irradiation, pIND:U2OS and Spy1:U2OS cells were induced for 24 h with Ponasterone A and then irradiated with UV. Cells were allowed to recover in induction media and at the indicated time points post irradiation, floating and adherent cells were collected, washed 2x with PBS, and fixed in 2% formaldehyde for 10 min at 37°C. Cells were put on ice for one min and then permeabilized with methanol so that the final concentration of methanol is 90%. Cells were kept in methanol at -20°C until all time points were collected. Cell were

then washed with 0.5%BSA/PBS by centrifugation and stained with anti-cleaved caspase-3 Alexa Fluor 488 conjugated rabbit antibody (Cell Signaling Technology). Cells were analyzed by flow cytometry for the presence of cleaved caspase-3.

UV irradiation resistant DNA synthesis assay (UVDS)

The UVDS assay was performed as previously described (21). Briefly, pIND:U2OS and Spy1:U2OS cells were induced for 24 h followed by incubation in induction media containing 20nCi/ml [^{14}C]thymidine (Applied Biosystems, Chicago, IL) for a subsequent 24 h. The media was then replaced with fresh normal induction media and incubated for another 24 h. Cells were then irradiated with UV and incubated in normal induction media for 0, 30, 60, or 120 min followed by a 15 min incubation with 5μCi/ml [^{3}H]thymidine (Applied Biosystems). Cells were harvested, washed twice in PBS and fixed in 70% methanol. Cells were transferred to Whatman filters and rinsed sequentially with 70% methanol then 90% methanol. Filters were allowed to dry and radioactivity was assayed by liquid scintillation counting. The ratio of ^{3}H cpm to ^{14}C cpm, corrected for channel crossover, was a measure of DNA synthesis.

G2/M Checkpoint assay

A G2/M checkpoint assay was performed similar to previous descriptions (22). Briefly, pIND:U2OS and Spy1:U2OS cells were induced for 24 h, irradiated with UV, and allowed to recover in induction media. At the indicated time points, cells were

harvested by trypsinization/centrifugation and stained with phospho-histone H3 Alexa fluor 488 conjugated antibody (Cell Signaling Technology) according to manufacturer's protocol. The percentage of phospho-histone H3 positive cells was determined by flow cytometry.

Immunofluorescence microscopy

Cells were seeded onto glass coverslips and induced for 24 h followed by irradiation with UV. 2 h post UV irradiation, coverslips were fixed with 4% formaldehyde for 10 min at room temperature and permeabilized with 0.1% Triton X-100 for 5 min at room temperature. Cells were then stained with either mouse anti-phospho-Histone H2A.X (Ser139) at 1:2500 or rabbit anti-phospho-Chk1 (S317) at 1:1000. After extensive washing, cells were counterstained with anti-mouse IgG (fab specific)-FITC conjugated antisera (Sigma) at 1:500 or goat anti-rabbit-Alexa Flour(488) conjugated antisera (Molecular Probes) at 1:5000, respectively. Hoechst dye 33342 (1μg/ml) was used to detect nuclei. For γH2AX: images were acquired using a Nikon Microphot-FXA microscope equipped with a Hamamatsu C5810 camera; For phospho-Chk1: images were acquired using an Applied Precision Delta Vision Deconvolution Microscope System (Nikon TE-200 Microscope) at the Digital Imaging Core UCSD Cancer Center.

Isolation of chromatin

To isolate chromatin-bound RPA, cells were removed from plates and pre-extracted with a chromatin isolation buffer (23) containing 20mM Hepes (pH7.4), 0.5% Triton X-100, 50mM NaCl, 3mM $MgCl_2$, 300mM sucrose, and protease/phosphatase inhibitors on ice for 5 min. Insoluble material was collected by centrifugation, sheared with a 23 gauge needle and treated with DNase (0.1 U/ml) to extract chromatin-bound proteins.

Results

Construction of Spy1 inducible and control cells in the U2OS osteosarcoma cell line

To investigate the role of Spy1 in apoptosis and checkpoint activation, we created U2OS osteosarcoma cell lines allowing inducible expression of Spy1 using the ecdysone-inducible system (Figure 4-1A). In brief, this expression system uses the steroid hormone Ponasterone A, an analog of ecdysone, to activate expression of the inserted gene via a heterodimeric nuclear receptor. The gene of interest is cloned into the vector pIND and transfected into cells stably expressing pVgRXR. The pVgRXR vector encodes the heterodimer of the ecdysone receptor (VgEcR) and the retinoid X receptor (RXR) that binds a hybrid ecdysone response element (E/GRE) in the presence of Ponasterone A (20).

Figure 4-1B presents an analysis of the U2OS-derived cell lines used in this study. The control cell line, designated pIND:U2OS, contains an empty expression vector, and does not express protein in response to Ponasterone A induction. A matched cell line, designated Spy1:U2OS, exhibits inducible expression of myc-Spy1 in response to Ponasterone A. Previously, our work and that of others has demonstrated that Spy1 is a potent regulator of CDK2 (and cdc2), activating the kinase through direct binding of the two proteins. The domain of Spy1 required for this interaction and subsequent activation of CDK2, is a central region containing an acidic stretch, known as the Speedy/Ringo (S/R) Box (6, 7). To examine whether Spy1

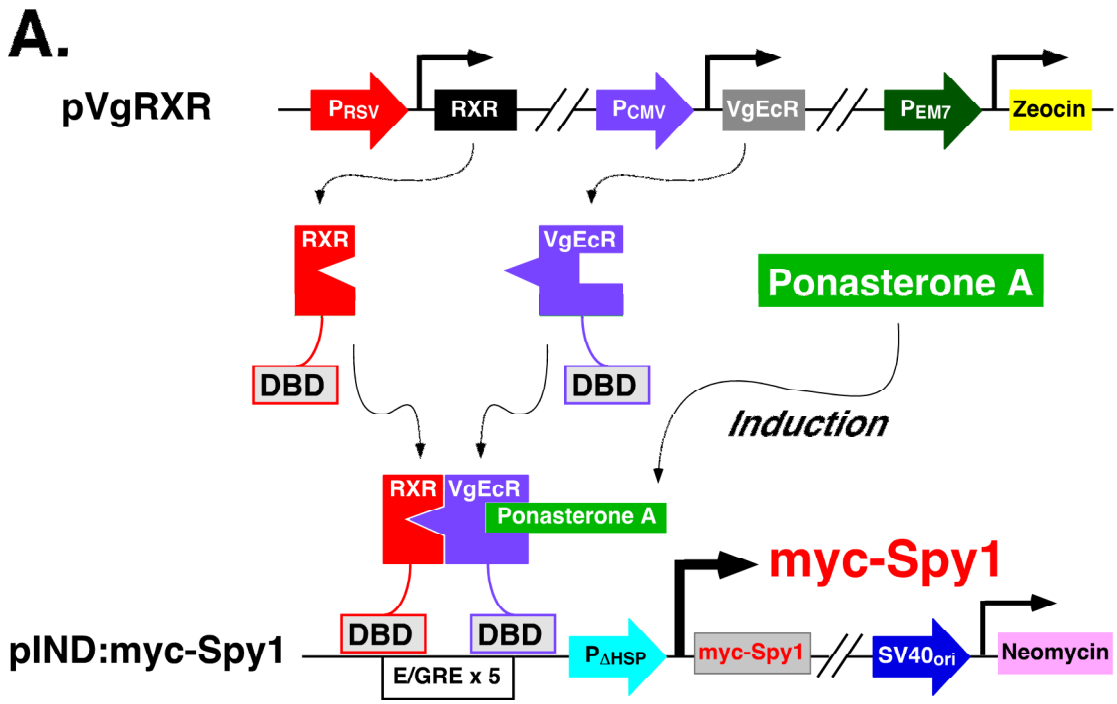

Figure 4-1. Spy1 and Spy1$^{S/RBox}$ inducible U2OS cells created with the Ecdysone system.

A) The Ecdysone system consists of the pVgRXR vector which encodes the heterodimer of the ecdysone receptor (VgEcR) and the retinoid X receptor (RXR) that binds a hybrid ecdysone response element (E/GRE) in the presence of Ponasterone A (PonA) and the pIND vector into which the gene of interest is cloned. U2OS cells were stably transfected with pVgRXR and either empty pIND vector (pIND:U2OS), pIND-Spy1 (Spy1:U2OS), or pIND-Spy1$^{S/RBox}$ (Spy1$^{S/RBox}$:U2OS).

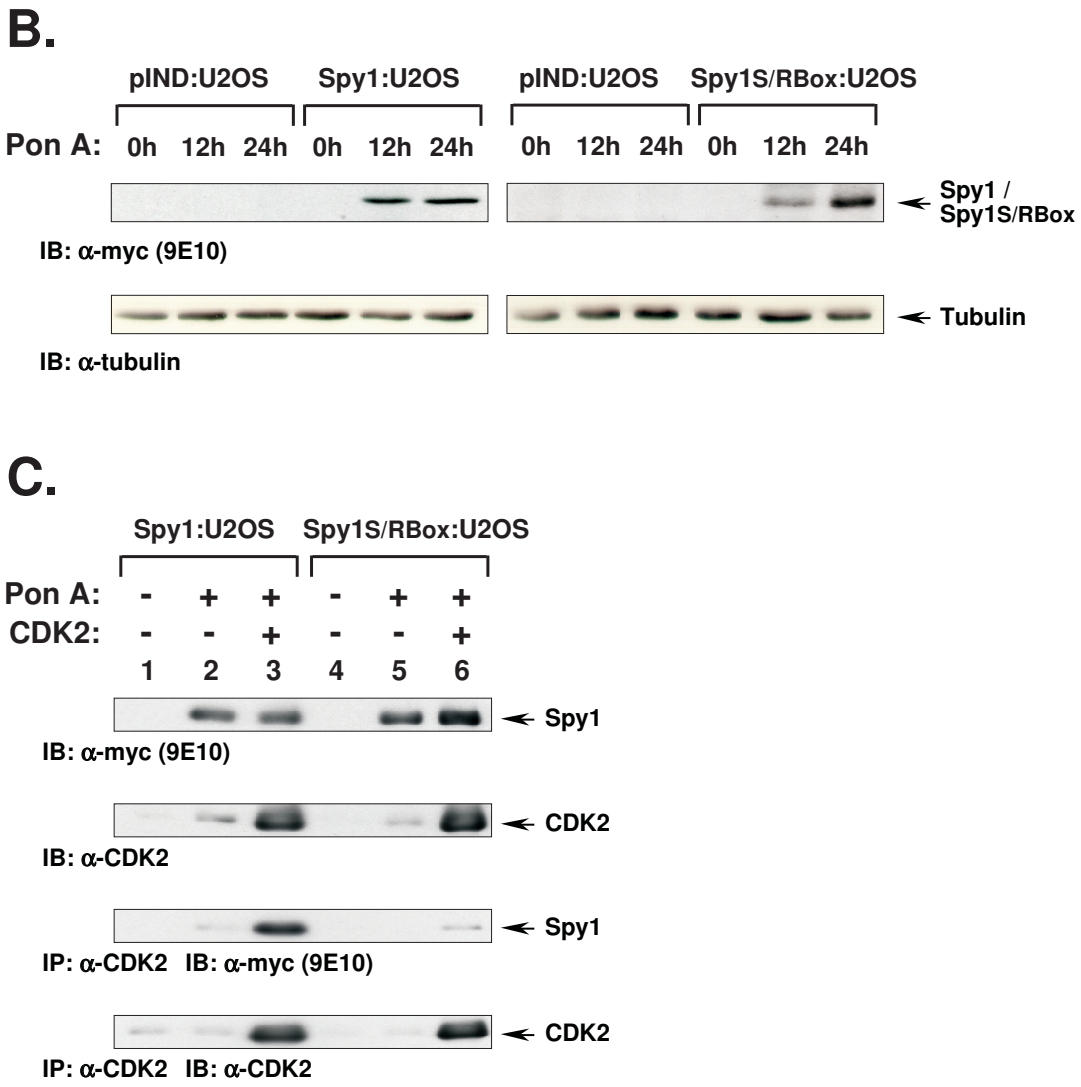

Figure 4-1. Spy1 and Spy1$^{S/RBox}$ inducible U2OS cells created with the Ecdysone system, continued.
B) U2OS inducible cells were induced with Ponasterone A for 12 or 24 h. Mock induced samples were prepared after 24 h. Lysates were resolved by SDS-PAGE, transferred to membrane and probed with anti-myc (9E10) antisera to detect myc-tagged Spy1 expression and tubulin as a loading control. C) Spy1:U2OS or Spy1$^{S/RBox}$:U2OS inducible cells were induced with Ponasterone A and either mock or CDK2 transfected for 24 h, after which cell lysates were resolved by SDS-PAGE, transferred to membrane and probed with anti-myc (9E10) antisera to detect myc-tagged Spy1 expression and also probed for CDK2 expression. Cell lysates were subsequently immunoprecipitated with CDK2 antisera, resolved by SDS-PAGE, transferred to membrane and probed with anti-myc (9E10) antisera to detect Spy1 protein binding to CDK2, and with CDK2 antisera to detect total CDK2.

requires CDK2 binding to mediate responses to UV irradiation, we created a construct based on mutations previously shown to prevent CDK2 binding and activation (6, 7), mutating the five glutamate residues and the one aspartate residue within the Speedy/Ringo Box to glutamine and asparagine, respectively (Spy1$^{S/RBox}$). We also constructed a matched cell line, Spy1$^{S/RBox}$:U2OS, allowing inducible expression of myc-Spy1$^{S/RBox}$ in response to Ponasterone A. Following induction with Ponasterone A, the inducible expression of myc-Spy1$^{S/RBox}$ was detected by immunoblotting of cell lysates with the myc (9E10) antibody (Figure 4-1B). To confirm the inability of the Spy1$^{S/RBox}$ mutant protein to bind CDK2 efficiently (7), in Figure 3-1C we compared CDK2 immunoprecipitates prepared from induced Spy1:U2OS cells and from induced Spy1$^{S/RBox}$:U2OS cells. Due to low levels of endogenous CDK2 expression (2rd panel, lanes 1 and 3), CDK2 was overexpressed by transfection in this experiment. Under these conditions, binding of myc-Spy1 to CDK2 was readily detected, whereas binding of the mutant myc-Spy1$^{S/RBox}$ protein to CDK2 was barely detectable (3rd panel, lanes 2 and 4).

Spy1 prevents apoptosis in U2OS cells, and requires interaction with CDK2 through the Speedy/Ringo Box

To examine the effect of Spy1 expression on UV-induced apoptosis, control pIND and Spy1:U2OS-inducible cell lines were irradiated with 50 J/m^2 UVC after being induced for 24 h. At the indicated time points after UV irradiation, cells were collected, and apoptosis was determined by staining for DNA content using propidium

iodide. The percentage of cells containing Sub-G1 DNA was determined and identified as apoptotic by flow cytometry. As seen in Figure 3-2A, Spy1 expression drastically decreases apoptosis in U2OS cells at 12, 24, 48, and 72 h after UV irradiation by approximately 13%, 20%, 55% and 50%, respectively. In the experiment presented, pIND:U2OS cells served as the negative control in comparison with Spy1:U2OS cells, both treated with Ponasterone A. As an additional negative control, Spy1:U2OS cells were examined in the absence of Ponasterone A, and exhibited UV-induced apoptosis similar to pIND:U2OS cells (Figure 4-2D). For the remainder of the paper, pIND:U2OS cells are used as the negative control, while Spy1:U2OS cells without induction were omitted.

To further confirm that Spy1 prevents apoptosis, an Annexin V binding assay was used. In response to apoptotic stimuli, cells lose the asymmetry of the cell membrane as indicated by flipping of phosphatidylserine (PS) from the inner membrane leaflet to the outer leaflet (24-27). Annexin V is a protein that specifically binds PS. Staining with an Annexin V-FITC conjugate allows for the detection of apoptotic cells by flow cytometry. After 24 h of induction, pIND:U2OS and Spy1:U2OS cells were irradiated with 50 J/m^2 UVC and allowed to recover for 24 h. Spy1-expressing cells have only small amounts of Annexin V positive staining (~7.5%) in response to UV, compared to control cells (~60%), further demonstrating that Spy1 expression is able to prevent apoptosis (Figure 4-2B).

When challenged with UV irradiation, $Spy1^{S/RBox}$ expressing cells underwent apoptosis to a similar extent as the control cells (20-25% at 24 h post UV and ~60% at

48 h), while the Spy1-expressing cells did not (less than 20% at either time point) (Figure 4-2C), indicating that Spy1 must interact with and activate CDK2 in order to suppress apoptosis. This suggests that non-cyclin mediated CDK2 activity may play an important role in the regulation of apoptosis in response to DNA damage.

Spy1 expression prevents the activation of the effector caspase, caspase-3

Caspases belong to a family of cysteine proteases that serve as major regulators of apoptosis (28). Initiator caspases, such as caspases 8, 9, 10 and 12, are activated by proapoptotic signals. Once activated, these caspases cleave and activate downstream effector caspases (including 3, 6 and 7) which, in turn, cleave cytoskeletal and nuclear proteins, such as poly(ADP-ribose) polymerase (PARP), α-fodrin, DNA fragmentation factor (DFF) and lamin A.

To confirm that Spy1 expression blocks apoptosis through the conventional caspase pathways, the cleavage of caspase-3 was examined. As seen by immunoblotting with caspase-3 antibody, cleaved fragments of caspase-3 appear in pIND:U2OS cells as early as 12 h post UV, and continue to increase over time (Figure 4-3A). In contrast, Spy1-expressing U2OS cells do not accumulate cleaved caspase-3 (Figure 4-3A) at any time post UV irradiation, indicating that the apoptotic program is not activated in response to UV when Spy1 is expressed.

To further confirm the suppression of apoptosis and inhibition of caspase-3 activation by Spy1 expression, we used intracellular immunostaining to detect active, cleaved caspase-3 by flow cytometry. As seen in Figure 4-3B, control pIND:U2OS

cells accumulated significant amounts of the cleaved form of caspase-3 at 12, 24 and 48 h after UV irradiation, indicated by shifts of the blue peaks, while Spy1:U2OS cells did not accumulate a significant amount of cleaved caspase-3. These results confirm that Spy1 prevents apoptosis by interfering with the activation of apoptotic pathways.

Spy1 prevents the activation of both the S-phase checkpoint and the G2/M checkpoint

Checkpoint activation integrates the signals that regulate DNA damage responses, including DNA damage repair, cell cycle arrest, cell senescence and apoptosis (12-14, 29, 30). To determine the role of Spy1 in S-phase checkpoints, pIND:U2OS and Spy1:U2OS cells were induced for 24 h and assayed for UV irradiation resistant DNA synthesis (UVDS) (21). The UVDS assay provides an indication of whether an S-phase or replication checkpoint is activated. As seen in Figure 4-4A, control pIND:U2OS cells activate the checkpoint response when challenged with UV irradiation, showing almost a 50% decrease in DNA synthesis within 15 min post irradiation. In these cells, the checkpoint persists through 135 min as demonstrated by continuous inhibition of DNA synthesis (31% of control DNA synthesis post irradiation). In contrast, Spy1:U2OS cells do not efficiently activate the S-phase checkpoint as demonstrated by only small amounts of DNA synthesis inhibition. At 15 min, Spy1-expressing cells still have 76% of control DNA synthesis post UV irradiation and 62% of control at the final time point of 135 min. These data indicate that Spy1 expression in U2OS cells confers a partial UVDS phenotype and

that the S-phase checkpoint is not efficiently activated. These results also show that Spy1 expression allows for replication in the presence of DNA damage.

The G2/M checkpoint is activated to prevent cells with damaged DNA or incomplete DNA replication from undergoing mitosis. Cells that fail to activate an S-phase checkpoint should prevent movement into mitosis by activating the G2/M checkpoint (31-33). To examine the effects of Spy1 expression on the G2/M checkpoint, pIND:U2OS and Spy1:U2OS cells were induced for 24 h, challenged with UV, and labeled with phospho-histone H3 antibody as a marker of M-phase entry (22, 34, 35). As shown in Figure 4-4B and C, a G2 arrest was observed in pIND:U2OS control cells as early as 2 h post irradiation (~30 fold decrease in phospho-histone H3 in UV-irradiated cells compared to unirradiated cells), and the G2/M checkpoints continued through 6 h, resulting in virtually no cells with detectable phospho-histone H3. In contrast, Spy1:U2OS cells showed no decrease in phospho-histone H3 staining compared to unirradiated cells at either time point. At 2 h and 6 h post UV irradiation, there was no detectable difference between the number of phospho-histone H3 positive UV-irradiated Spy1:U2OS cells as compared to unirradiated cells, suggesting that the cells continue to enter mitosis. Taken together, the data presented in Figure 4-4 indicate that Spy1 expression prevents activation of checkpoints, allowing both replication and cell division to continue even as cells accumulate DNA damage.

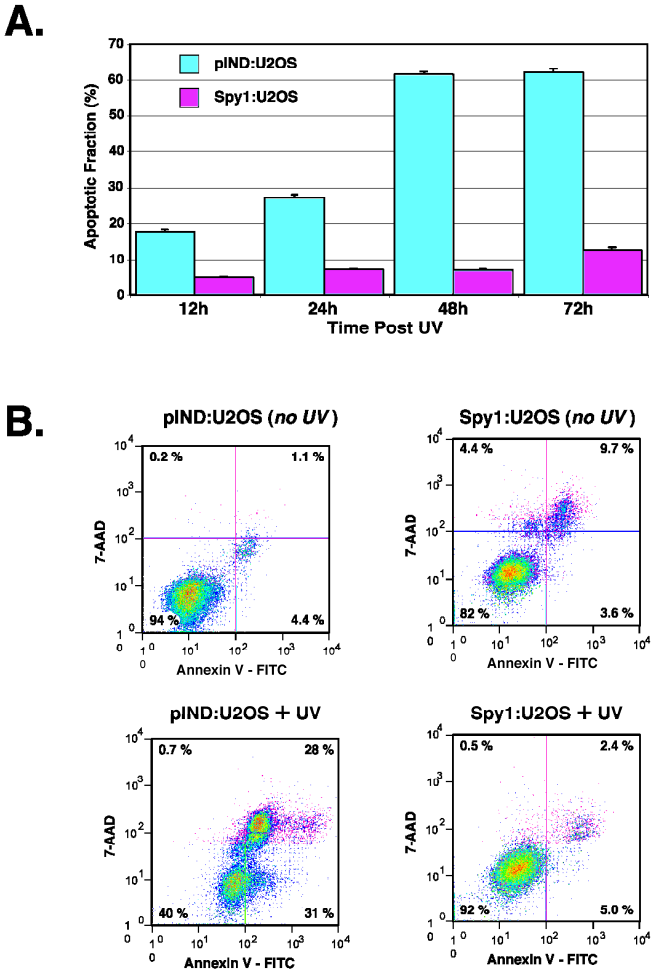

Figure 4-2. Spy1 prevents apoptosis in U2OS cells and requires the CDK2 interacting, Speedy/Ringo Box domain.
A) pIND:U2OS and Spy1:U2OS cells were induced with Ponasterone A for 24 h, irradiated with UV and harvested at 12, 24, 48 and 72 h post irradiation. Cells were fixed with ethanol, stained with propidium iodide and analyzed for DNA content. Apoptotic cells were identified by the presence of Sub-G1 DNA content. The percentage of apoptotic cells was calculated from at least three separate experiments and is presented as the mean +/- standard deviation normalized to unirradiated samples. B) pIND:U2OS and Spy1:U2OS cells were induced for 24 h and then irradiated with 50 J/m^2 UV. 24 h after irradiation cells were harvested, fixed and stained with Annexin V-FITC conjugate to detect apoptotic cells. Quadrants to the right of bar indicate Annexin V positive cells indicative of apoptosis. Cells in upper quadrants have begun to lose membrane integrity. The results from one representative experiment are shown.

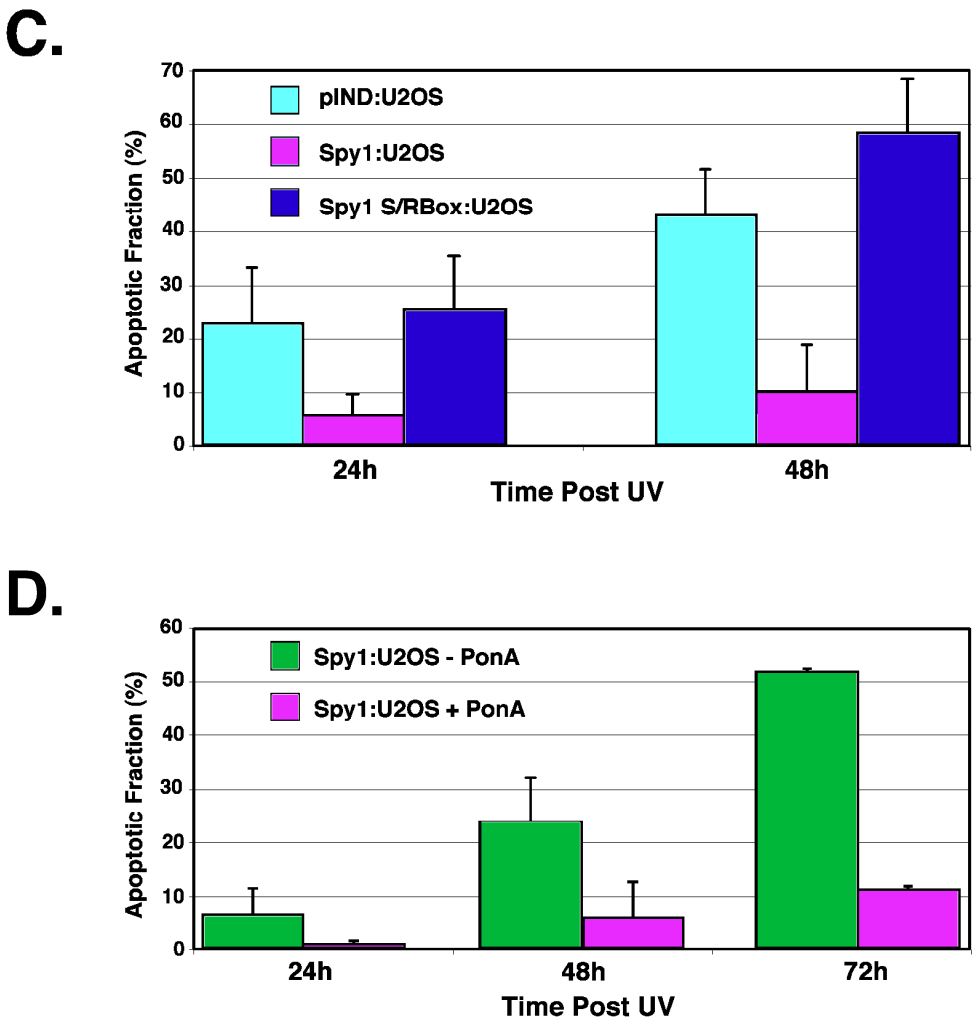

Figure 4-2. Spy1 prevents apoptosis in U2OS cells and requires the CDK2 interacting, Speedy/Ringo Box domain, continued.
C) pIND:U2OS, Spy1:U2OS, and Spy1$^{S/RBox}$:U2OS were induced for 24 h, irradiated with UV and analyzed for apoptosis as in (A). D) As an additional negative control, Spy1:U2OS cells in the absence or presence of Ponasterone A (24 h treatment) were irradiated with UV and harvested at 24, 48 and 72 h post irradiation and analyzed as in (A).

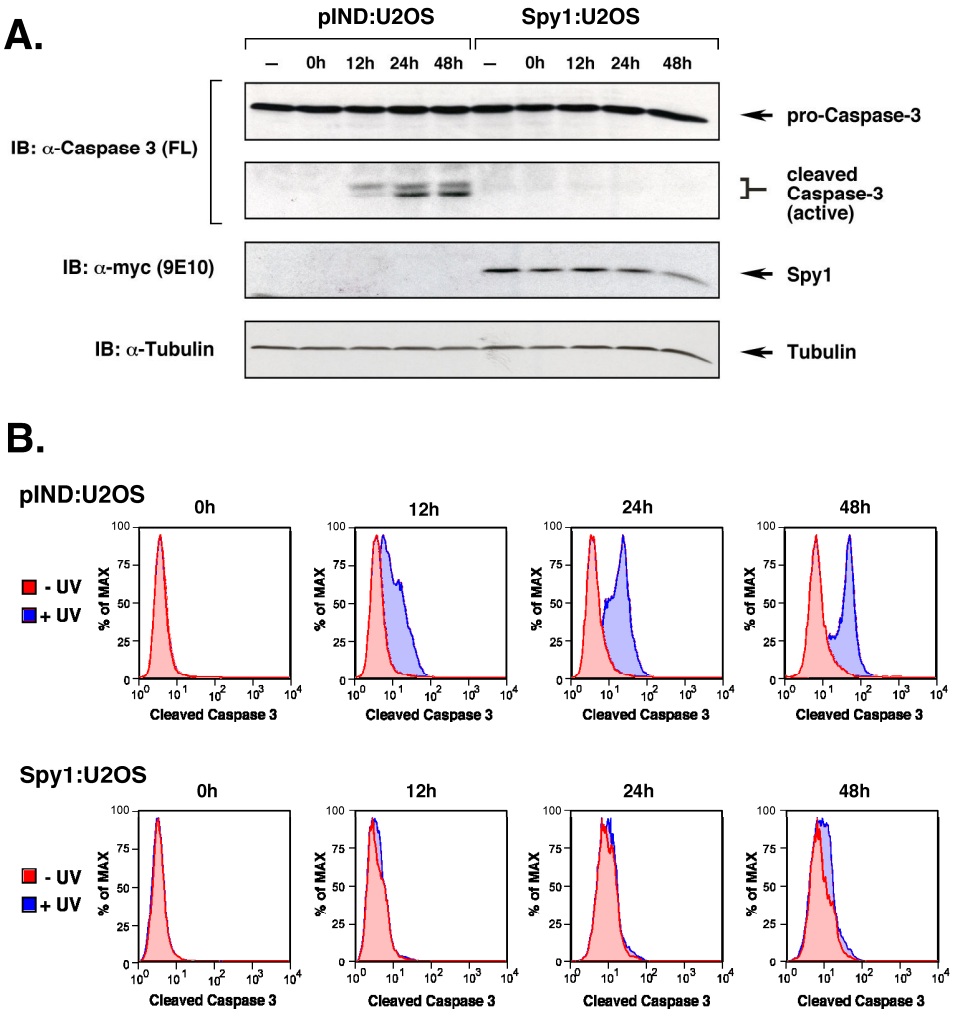

Figure 4-3. Spy1 expression prevents the cleavage associated activation of caspase-3.

A) pIND:U2OS and Spy1:U2OS cells were induced for 24 h and then irradiated with 50 J/m^2 UV. At the indicated times after irradiation, cell lysates were resolved by SDS-PAGE and immunoblotted with antisera against caspase-3 to detect both the full length and cleaved (active) fragments. The cleaved caspase-3 panel is a longer exposure of the blot in the upper panel (caspase-3 full length). B) pIND:U2OS and Spy1:U2OS cells were induced for 24 h, and then irradiated with 50 J/m^2 UV. At the indicated times, cells were harvested and fixed. Subsequently, cells were permeabilized and stained with antisera against the cleaved form of caspase-3 conjugated to Alexa Fluor 488. Flow cytometry was used to determine cells with active caspase-3. Results are representative of three independent experiments. Red peaks represent non-irradiated cells and blue peaks represent irradiated cells.

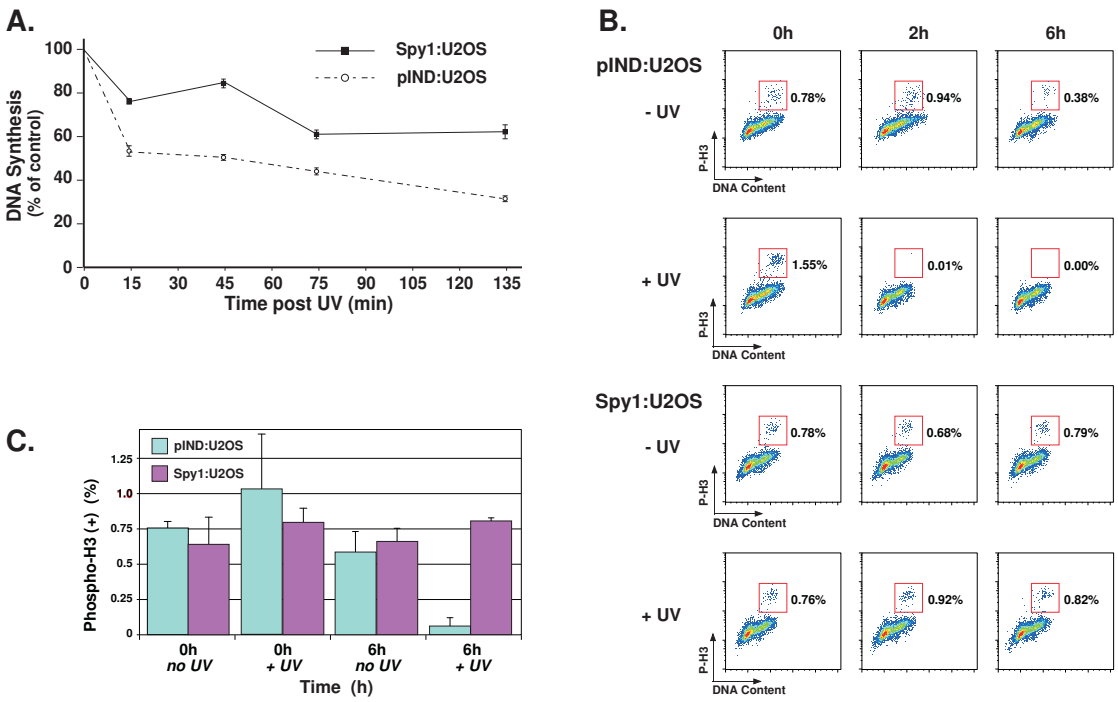

Figure 4-4. Spy1 expression prevents activation of the S-phase and G2/M Checkpoints.

A) UV irradiation induced S-phase checkpoint. pIND:U2OS and Spy1:U2OS cells were induced for 24 h and DNA synthesis was assessed 15, 35, 75 and 135 min after UV irradiation and shown as a percent of the control +/- standard deviation

B) UV irradiation induced G2/M checkpoint. pIND:U2OS and Spy1:U2OS cells were induced for 24 h and then irradiated with 50 J/m^2 UV. At 0, 2 and 6 h post irradiation, cells were harvested, fixed, permeabilized, and stained with phospho-histone H3-Alexa Fluor conjugated antibody and analyzed by flow cytometry. Data are representative of one of three independent experiments shown in (C).

C) Percentage of cells positive for phospho-histone H3 at 0 and 6 h post UV irradiation as determined by flow cytometry. Data from three independent experiments including that from (B) are shown +/- standard deviation.

Spy1 suppresses checkpoint signaling

Spy1 expression prevents maximal phosphorylation of H2A.X in response to UV irradiation.

To examine whether the anti-apoptotic effects and checkpoint bypass observed in Spy1-expressing cells resulted from impaired checkpoint signaling, we examined the phosphorylation and localization of the histone variant H2A.X. In response to DNA damage, histone H2A.X becomes phosphorylated (γH2A.X) and localizes to discrete foci at sites of DNA damage. The ability of ATR to phosphorylate H2A.X in response to UV-induced DNA damage is required for proper localization of repair machinery, and phosphorylation of H2A.X is a reliable indicator of whether DNA damage response pathways are activated in response to damage stimuli (36-38). γH2A.X is believed to play a role in the recruitment of repair factors to sites of DNA damage (38). When pIND:U2OS control cells were examined by immunofluorescence microscopy, the induction of foci formation of γH2A.X was readily apparent (Figure 4-5, compare panel A with panel C). In contrast, Spy1-expressing U2OS cells (Spy1:U2OS) showed very little phosphorylation or foci formation of γH2A.X, compared to control cells (Figure 4-5, panel G). Although a small increase in γH2A.X foci formation was observed in response to UV in the Spy1:U2OS cells, as compared to unirradiated control cells, the number of cells with foci compared to UV-irradiated pIND:U2OS cells was very low (Table 4-1). These results demonstrate that Spy1 expression interferes with the signaling of DNA damage to proteins such as histone

H2A.X, suggesting that Spy1 interferes not only with the activation of checkpoints and apoptosis, but also the signaling that leads to DNA repair in response to UV.

Spy1 expression prevents the phosphorylation of Chk1 and RPA32 N-terminus

To determine whether Spy1 expression prevents the phosphorylation of other ATR substrates, the activation of Chk1 by phosphorylation was examined. When Spy1-expressing cells were challenged with UV, phosphorylation of Chk1 at the activating site, Ser345, was inhibited compared to control cells (Figure 4-6A). As early as 30 min after UV irradiation, pIND:U2OS cells accumulated Ser345-phosphorylated Chk1, which persisted through 6 h post UV irradiation (Figure 4-6A). In marked contrast, Spy1:U2OS cells failed to accumulate phosphorylated Chk1 at any time point. These results clearly demonstrate that Spy1 expression interferes with the signaling of DNA damage to the checkpoint kinase Chk1. These results were confirmed by examining cells for Chk1 phosphorylation using immunofluorescence microscopy. In control pIND:U2OS cells, UV irradiation resulted in the formation of intranuclear phospho-Chk1 foci, while Spy1:U2OS cells did not show phosphorylation of Chk1 nor the formation of foci (Figure 4-6B), consistent with the data on γH2A.X foci formation.

Another ATR specific signaling event in response to DNA damage induced by UV irradiation is the phosphorylation of the 32kD subunit of RPA on its N-terminus (39, 40). Phosphorylation on Ser4 and Ser8 of RPA32 occurs after the coating of ssDNA by RPA and activation of ATR, and may play a role in defining distinct

regions of DNA for damage signaling and repair (41, 42). While hyperphosphorylation of RPA32 is associated with checkpoint activation, hypophosphorylation is associated with replication and replicative processivity (42, 43). Therefore, the phosphorylation of RPA32 by ATR may play a dual role in which distinct sites of repair are established while replication arrest is also promoted, which is an event required for the maximal activation of ATR and checkpoints in response to UV irradiation.

To further investigate the DNA damage signaling response, and to evaluate both ATR activity as well as replication status in response to UV irradiation, we examined phosphorylation of chromatin-bound RPA32 on Ser4 and Ser8. In response to UV irradiation, both control and Spy1-expressing cells had similar amounts of RPA32 bound to chromatin, indicating the presence of ssDNA, but the phosphorylation status of RPA32 was significantly different. In control cells, 3 h post irradiation, RPA32 was phosphorylated extensively on Ser4 and Ser8 (Figure 4-6C), and this modification persisted through 24 h. In marked contrast, Spy1:U2OS cells accumulated low amounts of phosphorylated RPA32. These results demonstrate that UV-induced DNA damage signaling is depressed by Spy1 expression. The hypophosphorylation of RPA32 further suggests that ATR is not fully activated in Spy1-expressing cells, consistent with the UVDS assay described above, demonstrating that DNA synthesis is not arrested in response to UV irradiation in Spy1-expressing cells (Figure 4-4A).

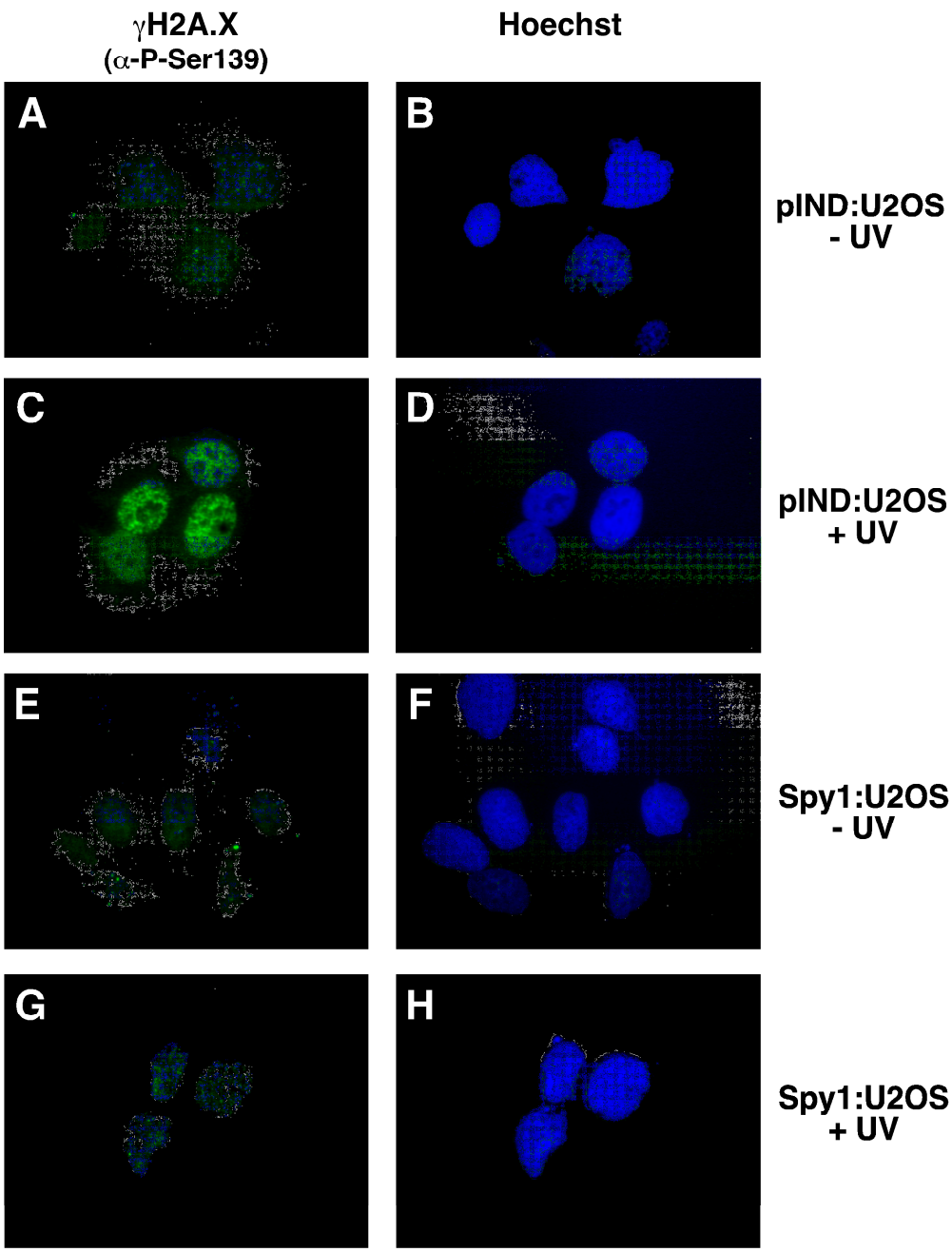

Figure 4-5. Spy1 expression impairs the phosphorylation of histone H2A.X.
A, C, E, G pIND:U2OS and Spy1:U2OS cells on coverslips were induced for 24 h and irradiated with 50 J/m^2 UV. 2 h later, coverslips were fixed and stained with antisera against phosphorylated histone H2A.X. Cells were counterstained with FITC-conjugated secondary antibody. 100 cells were examined per sample in three independent experiments. Representative cells are shown.
B, D, F, H Cells were stained with Hoechst to detect the nucleus.

Table 4-1. Effects of Spy1 Expression on γH2A.X Foci Formation in Response to UV Irradiation

	pIND:U2OS		Spy1:U2OS	
	no UV	+ UV	*no* UV	+ UV
% Cells with γH2A.X foci	**15.3**	**87.0**	**10.3**	**19.0**
Std. Dev.	**3.5**	**4.0**	**2.1**	**2.6**

Averages are representative of 3 separate experiments in which 100 cells per sample were counted.

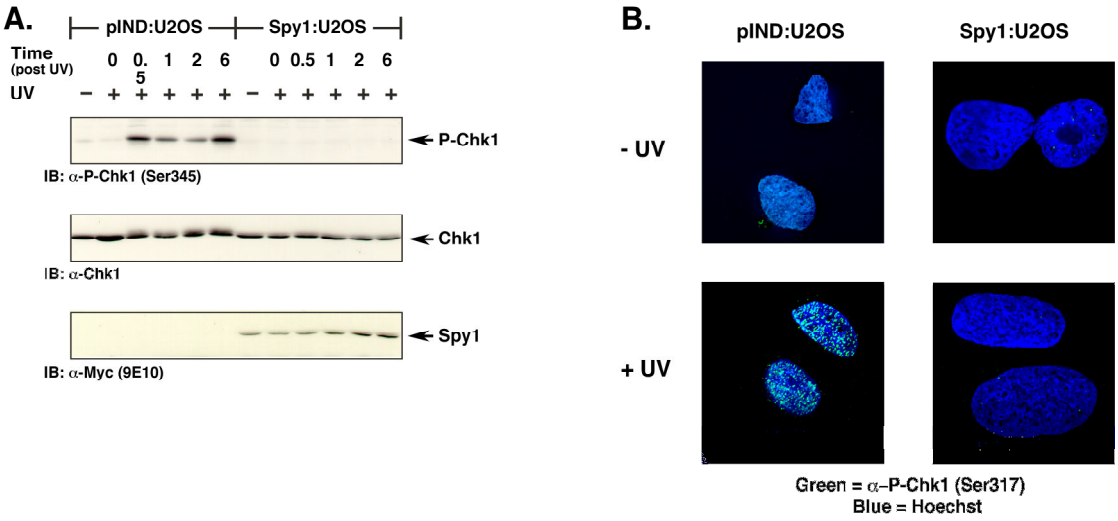

Figure 4-6. Spy1 expression prevents the activation of Chk1 and RPA.
A) pIND:U2OS and Spy1:U2OS cells were induced for 24 h and irradiated with 50 J/m^2. At 0, 0.5, 1, 2 and 6 h after UV irradiation, cell lysates were prepared, resolved by SDS-PAGE and transferred to membrane. The membrane was then blotted with phospho-Chk1 (Ser345) rabbit polyclonal antisera followed by chemiluminescence detection. The membrane was subsequently stripped and reprobed with total Chk1 antisera, followed by myc (9E10) antisera to detect myc-Spy1. B) Immunofluorescent detection of phospho-Chk1 intranuclear foci. pIND:U2OS and Spy1:U2OS cells were seeded onto coverslips, induced for 24 h, and irradiated with 50 J/m^2. 6 h after irradiation, coverslips were pulled and processed for phospho-Chk1 (Ser317) foci (Green – Alexa fluor 488). Cells were visualized with a Deltavision microscope and deconvolved.

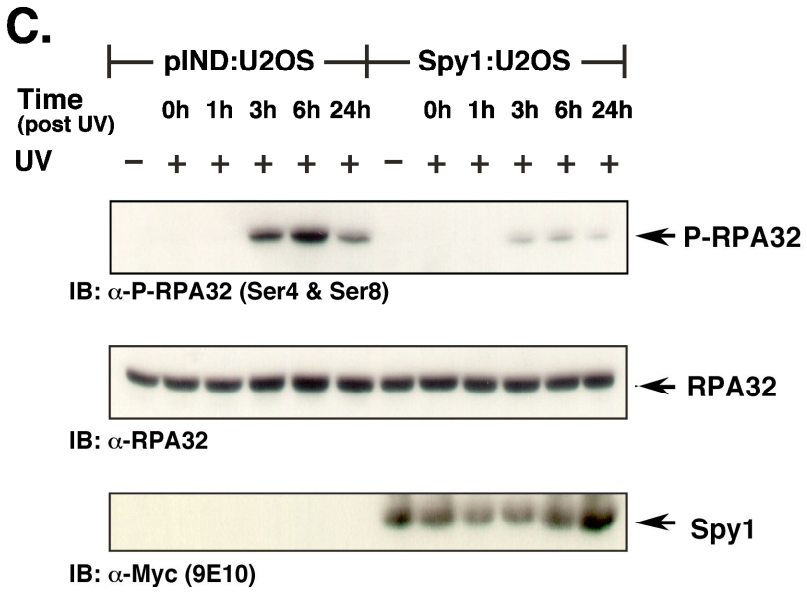

Figure 4-6. Spy1 expression prevents the activation of Chk1 and RPA, continued. C) pIND:U2OS and Spy1:U2OS cells were induced for 24 h and irradiated with 50 J/m^2. At the indicated time points, cells were harvested and pre-extracted to isolate chromatin-bound proteins. Extracts were resolved by SDS-PAGE and transferred to membrane. The membrane was then blotted with phospho-RPA32 (Ser4/Ser8) antisera followed by detection. The membrane was subsequently stripped and reprobed with RPA32 antisera to determine total levels. myc-Spy1 expression was detected by immunoblotting associated lysates with myc (9E10) antisera.

Inhibition of Chk1 and RPA32 phosphorylation by Spy1 requires its interaction and activation of CDK2.

To determine whether interaction with and activation of CDK2 by Spy1 is required for the inhibition of Chk1 phosphorylation in response to UV irradiation, we again used the S/R Box mutant of Spy1, which does not bind or activate CDK2. Unlike expression of wild type Spy1, expression of this mutant does not result in suppression of UV irradiation damage-induced phosphorylation of Chk1 (Figure 4-7A). Cells expressing the S/R Box mutant accumulate phosphorylated Chk1 (at Ser345) at comparable levels and kinetics when compared to the control pIND:U2OS cells (Figure 4-7A). These data indicate that Spy1 is required to bind and activate CDK2 for inhibition of Chk1 phosphorylation in response to UV-induced DNA damage, and therefore Spy1-mediated CDK2 activity plays a role in checkpoint regulation, modulating the dynamics of Chk1 and other checkpoint protein activation.

To determine whether the interaction and activation of CDK2 is also required to suppress phosphorylation of RPA32, we again used the S/R Box mutant of Spy1, and found that expression of this mutant had similar effects as those seen for Chk1 (Figure 4-7B). In response to UV irradiation, Spy1 S/R Box mutant expression does not have inhibitory effects on the phosphorylation of RPA32 compared to wild type Spy1. In fact, RPA32 phosphorylation in response to UV was increased over control when the mutant is expressed, indicating that the Spy1/CDK2 interaction plays a significant role in the regulation of RPA32 phosphorylation. This implies that Spy1-associated CDK2 activity may act to regulate the balance between replication

processivity, arrest and checkpoint activation, consistent with the previously described data demonstrating that Spy1 association with CDK2 functions in the regulation of apoptosis and checkpoint activation.

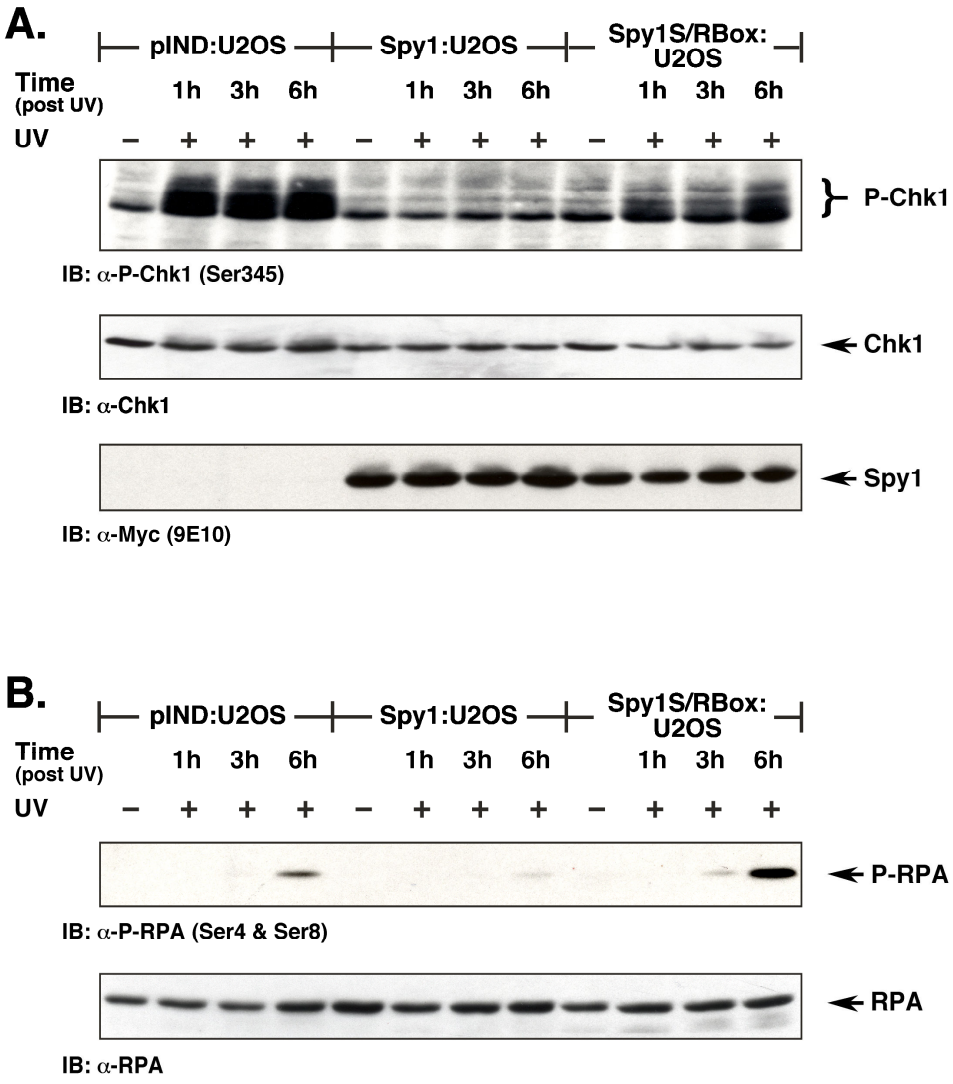

Figure 4-7. Binding of Spy1 to CDK2 is required for checkpoint inhibition.
A) pIND:U2OS, Spy1:U2OS, and Spy1$^{S/RBox}$:U2OS were induced for 24 h, irradiated with UV and harvested at the indicated time points. Half of the cells were lysed for use in immunoblotting, and half were used as in (B). Extracts were resolved by SDS-PAGE and transferred to membrane. The membrane was then blotted with a rabbit monoclonal antibody to phospho-Chk1 (Ser 345). The membrane was subsequently stripped and reprobed with total Chk1 antisera, followed by myc (9E10) antisera to detect myc-Spy1. B) Half of the cells from A were pre-extracted with chromatin buffer for 5 min on ice to isolate chromatin-bound proteins. Extracts were analyzed for phosphorylation on RPA32 using a phospho-RPA32 (Ser4/Ser8) antisera followed by chemiluminescence detection. The membrane was subsequently stripped and reprobed with RPA32 antisera to determine total levels. The myc (9E10) blot from (A) serves as the control for myc-Spy1 and myc-Spy1$^{S/RBox}$ for this experiment.

Discussion

We report here a role for Spy1 expression in checkpoint activation and apoptosis. We thus begin to describe the molecular mechanisms by which Spy1 exerts survival effects originally observed in our earlier report (3). We now show that Spy1 expression in U2OS cells decreases apoptosis in response to UV irradiation, and that Spy1 expression allows for the bypass of both the S-phase/replication checkpoint and the G2/M checkpoint. Furthermore, checkpoint signaling is inhibited by Spy1 expression, demonstrated by impairment of H2A.X phosphorylation, inhibition of Chk1 activation by phosphorylation, and inhibition of RPA32 phosphorylation. Lastly, we demonstrate that these effects are mediated through CDK2, as a Spy1 mutant deficient in CDK2 activation fails to inhibit the DNA damage response.

Inhibition of checkpoint signaling to Chk1, RPA, and H2A.X

When replication stress is detected, ATR becomes active and begins a signaling cascade that leads to the further activation of checkpoints and/or apoptosis. One substrate of ATR is the checkpoint kinase, Chk1, which mediates activation of checkpoints (32, 33, 44, 45). Histone H2A.X is also phosphorylated within minutes of UV irradiation, and localizes to sites of DNA damage (36). In this report, we show that Spy1-expressing cells do not accumulate activated Chk1. In addition, we found that histone H2A.X phosphorylation is impaired in Spy1-expressing cells. These results indicate impaired checkpoint responses, and demonstrate that the cellular programs that ensure genomic fidelity fail to be activated when Spy1 is overexpressed.

Another event during the response to UV-induced DNA damage is the phosphorylation of the N-terminus of RPA32 by ATR. This phosphorylation is believed to establish distinct domains for checkpoint signaling and DNA damage repair, while preventing the progression of replication (41, 42). In addition, hyperphosphorylation of the N-terminus of RPA32 promotes DNA repair, while hypophosphorylation is associated with DNA replication (42, 43). In the results presented here, we found that Spy1 expression prevented the accumulation of phosphorylated RPA32, consistent with the inability of Spy1-expressing cells to signal DNA damage and indicating that ATR is not activated at sites of damage. This may be attributable to the inability of cells to arrest DNA replication, prevent replication re-initiation, or prevent late origin firing.

In support of the replication arrest defects, we found that Spy1-expressing cells continue to synthesize DNA after UV irradiation, a phenomenon known as radio-resistant DNA synthesis (22). This result clearly demonstrates that DNA replication is not inhibited when Spy1 is expressed. We hypothesize that enhanced DNA repair would not account for the results we have observed, and suggest other mechanisms by which Spy1 could prevent activation of DNA damage signaling events mediated by ATR. First, through CDK2 hyperactivation, Spy1 could cause rapid re-initiation of stalled replication forks leading to virtually undisturbed DNA polymerase activity and replication. Second, Spy1 expression could promote bypass polymerization during which error prone polymerases synthesize DNA through UV-induced lesions, bypassing a fork-stalling event. Lastly, through its atypical activation of CDKs, Spy1

expression could effectively remove the targets of checkpoints, setting up feedback loops that result in checkpoint inactivation.

Checkpoint bypass in Spy1-expressing cells

The S-phase checkpoint, or replication checkpoint, arrests DNA replication by inhibiting the firing of late origins through inhibition of CDK2, thereby preventing cells from progressing into G2 with DNA damage or incomplete replication (30). Previous work has demonstrated that inhibition or depletion of many of the DNA damage response proteins, including ATM (46), ATR (47), Chk1 (48), and disruption of the checkpoint regulated cdc25A-CDK2 pathway (49), leads to a Radio-resistant DNA Synthesis (RDS) or UVDS phenotype. We assayed the activation of this checkpoint using a UV-resistant DNA Synthesis (UVDS) assay (21), and found that Spy1-expressing cells show a partial UVDS phenotype.

The G2/M checkpoint prevents cells from entering mitosis by inhibiting cdc2. This is accomplished through Chk1-dependent degradation of cdc25A (31, 50, 51). When assayed for G2 checkpoint activation, Spy1-expressing cells were refractory to cell cycle arrest. This may be explained by the fact that Chk1 is not activated in Spy1-expressing cells.

These results indicate that Spy1 plays an inhibitory role in checkpoint activation, achieved by direct inhibition of one of the checkpoint response pathways. One explanation for checkpoint bypass would be the hyperactivation of CDKs by Spy1, given that Spy1 and its homologs can activate CDKs in the absence of known

mechanisms of activation (7, 8). In fact, Spy1 would be able to overcome checkpoint inhibitory mechanisms that depend upon CDK2.

We show here that Spy1 expression prevents Chk1 phosphorylation, as well as H2A.X and RPA32 phosphorylation, which are most likely attributable to defects in ATR signaling. ATR activation in response to DNA damage requires DNA replication, or inhibition thereof, (52, 53), indicating that ATR activation is confined to the S-phase of the cell cycle. Spy1 may interfere with the ability of a cell to recognize disturbances in DNA replication in S-phase that normally lead to ATR activation. CDK2 has been shown to regulate the initiation of DNA synthesis, replication resumption after arrest, and the expression of many S-phase regulators (54-56). Thus, the hyperactivation of CDK2 by Spy1 may lead to S-phase disturbances that prevent activation of an ATR-dependent checkpoint.

Inhibition of Apoptosis by Spy1

We have observed (Figure 3-2) that inducible Spy1 expression protects cells from apoptosis in response to UV damage, and that the apoptotic machinery is not activated when Spy1 is expressed (Figure 3-3), reflected in the inhibition of caspase-3 activation. Apoptosis is activated in response to DNA damage by complex pathways involving checkpoint signaling. This inhibition of apoptosis may be attributed to the fact that Spy1-expressing cells fail to sense the accumulation of DNA damage that would normally impair replication, as described earlier, and therefore fail to activate appropriate responses such as programmed cell death.

In summary, we show that Spy1 expression prevents activation of apoptotic machinery and, importantly, prevents activation of both the S-phase/replication checkpoint and the G2/M checkpoint. Spy1 expression suppresses signaling to mediators of the checkpoint response, which are specific for apoptosis (caspase-3), checkpoint activation/DNA repair (γH2A.X and RPA), or which are common to both pathways (Chk1). Furthermore, we show that the interaction of Spy1 with CDK2 is required for these effects, suggesting that Spy1 association with CDKs may play a prominent role in abnormal cell cycle events such as the DNA damage response, checkpoint signaling, and apoptosis. The evasion of checkpoints and apoptosis are both traits selected by cancer cells. These findings are relevant to the role of Spy1 overexpression reported in invasive breast carcinomas (19).

Aknowledgements

We thank Jeff Esko and Omai Garner for assistance with flow cytometry; Geoff Wahl for critical discussion; Jim Feramisco and Kersi Pestonjamasp for assistance with deconvolution microscopy, and Mark Wade for valuable advice. This Investigation was supported by a Ruth L. Kirschstein National Research Service Award - NIH/NCI T32 CA009523 (RG). Chapter 4, in full, is material published in The Journal of Biological Chemistry, Gastwirt, RF; Slavin, DA; McAndrew, CW; and Donoghue, DJ (2006). The dissertation author was a co-author of this paper.

References

1. Lenormand JL, Dellinger RW, Knudsen KE, Subramani S, Donoghue DJ. Speedy: a novel cell cycle regulator of the G2/M transition. Embo J 1999;18(7):1869-77.

2. Porter LA, Dellinger RW, Tynan JA, et al. Human Speedy: a novel cell cycle regulator that enhances proliferation through activation of Cdk2. J Cell Biol 2002;157(3):357-66.

3. Barnes EA, Porter LA, Lenormand JL, Dellinger RW, Donoghue DJ. Human Spy1 promotes survival of mammalian cells following DNA damage. Cancer Res 2003;63(13):3701-7.

4. Ferby I, Blazquez M, Palmer A, Eritja R, Nebreda AR. A novel p34(cdc2)-binding and activating protein that is necessary and sufficient to trigger G(2)/M progression in Xenopus oocytes. Genes Dev 1999;13(16):2177-89.

5. Karaiskou A, Perez LH, Ferby I, Ozon R, Jessus C, Nebreda AR. Differential regulation of Cdc2 and Cdk2 by RINGO and cyclins. J Biol Chem 2001;276(38):36028-34.

6. Dinarina A, Perez LH, Davila A, Schwab M, Hunt T, Nebreda AR. Characterization of a new family of cyclin-dependent kinase activators. Biochem J 2004;386:349-55.

7. Cheng A, Xiong W, Ferrell JE, Jr., Solomon MJ. Identification and Comparative Analysis of Multiple Mammalian Speedy/Ringo Proteins. Cell Cycle 2005;4(1):155-65.

8. Cheng A, Gerry S, Kaldis P, Solomon MJ. Biochemical characterization of Cdk2-Speedy/Ringo A2. BMC Biochem 2005;6:19.

9. Schneider E, Montenarh M, Wagner P. Regulation of CAK kinase activity by p53. Oncogene 1998;17(21):2733-41.

10. Porter LA, Kong-Beltran M, Donoghue DJ. Spy1 interacts with p27Kip1 to allow G1/S progression. Mol Biol Cell 2003;14(9):3664-74.

11. Evan GI, Vousden KH. Proliferation, cell cycle and apoptosis in cancer. Nature 2001;411(6835):342-8.

12. Abraham RT. Cell cycle checkpoint signaling through the ATM and ATR kinases. Genes Dev 2001;15(17):2177-96.

13. Shiloh Y. ATM and related protein kinases: safeguarding genome integrity. Nat Rev Cancer 2003;3(3):155-68.

14. Zhou BB, Elledge SJ. The DNA damage response: putting checkpoints in perspective. Nature 2000;408(6811):433-9.

15. Bartkova J, Horejsi Z, Koed K, et al. DNA damage response as a candidate anti-cancer barrier in early human tumorigenesis. Nature 2005;434(7035):864-70.

16. Lowe SW, Cepero E, Evan G. Intrinsic tumour suppression. Nature 2004;432(7015):307-15.

17. Fridman JS, Lowe SW. Control of apoptosis by p53. Oncogene 2003;22(56):9030-40.

18. Brown JM, Attardi LD. The role of apoptosis in cancer development and treatment response. Nat Rev Cancer 2005;5(3):231-7.

19. Zucchi I, Mento E, Kuznetsov VA, et al. Gene expression profiles of epithelial cells microscopically isolated from a breast-invasive ductal carcinoma and a nodal metastasis. Proc Natl Acad Sci U S A 2004;101(52):18147-52.

20. No D, Yao TP, Evans RM. Ecdysone-inducible gene expression in mammalian cells and transgenic mice. Proc Natl Acad Sci U S A 1996;93(8):3346-51.

21. Tsao CC, Geisen C, Abraham RT. Interaction between human MCM7 and Rad17 proteins is required for replication checkpoint signaling. Embo J 2004;23(23):4660-9.

22. Lin SY, Li K, Stewart GS, Elledge SJ. Human Claspin works with BRCA1 to both positively and negatively regulate cell proliferation. Proc Natl Acad Sci U S A 2004;101(17):6484-9.

23. Syljuasen RG, Sorensen CS, Hansen LT, et al. Inhibition of human Chk1 causes increased initiation of DNA replication, phosphorylation of ATR targets, and DNA breakage. Mol Cell Biol 2005;25(9):3553-62.

24. Flores ER, Tsai KY, Crowley D, et al. p63 and p73 are required for p53-dependent apoptosis in response to DNA damage. Nature 2002;416(6880):560-4.

25. Martin SJ, Reutelingsperger CP, McGahon AJ, et al. Early redistribution of plasma membrane phosphatidylserine is a general feature of apoptosis regardless of the initiating stimulus: inhibition by overexpression of Bcl-2 and Abl. J Exp Med 1995;182(5):1545-56.

26. van Engeland M, Nieland LJ, Ramaekers FC, Schutte B, Reutelingsperger CP. Annexin V-affinity assay: a review on an apoptosis detection system based on phosphatidylserine exposure. Cytometry 1998;31(1):1-9.

27. Vermes I, Haanen C, Steffens-Nakken H, Reutelingsperger C. A novel assay for apoptosis. Flow cytometric detection of phosphatidylserine expression on early apoptotic cells using fluorescein labelled Annexin V. J Immunol Methods 1995;184(1):39-51.

28. Liu X, Kim CN, Yang J, Jemmerson R, Wang X. Induction of apoptotic program in cell-free extracts: requirement for dATP and cytochrome c. Cell 1996;86(1):147-57.

29. Bartek J, Lukas J. Pathways governing G1/S transition and their response to DNA damage. FEBS Lett 2001;490(3):117-22.

30. Bartek J, Lukas C, Lukas J. Checking on DNA damage in S phase. Nat Rev Mol Cell Biol 2004;5(10):792-804.

31. Xiao Z, Chen Z, Gunasekera AH, et al. Chk1 mediates S and G2 arrests through Cdc25A degradation in response to DNA-damaging agents. J Biol Chem 2003;278(24):21767-73.

32. Zhao H, Piwnica-Worms H. ATR-mediated checkpoint pathways regulate phosphorylation and activation of human Chk1. Mol Cell Biol 2001;21(13):4129-39.

33. Liu Q, Guntuku S, Cui XS, et al. Chk1 is an essential kinase that is regulated by Atr and required for the G(2)/M DNA damage checkpoint. Genes Dev 2000;14(12):1448-59.

34. Xu B, Kim S, Kastan MB. Involvement of Brca1 in S-phase and G(2)-phase checkpoints after ionizing irradiation. Mol Cell Biol 2001;21(10):3445-50.

35. Taylor WR. FACS-based detection of phosphorylated histone H3 for the quantitation of mitotic cells. Methods Mol Biol 2004;281:293-9.

36. Ward IM, Chen J. Histone H2AX is phosphorylated in an ATR-dependent manner in response to replicational stress. J Biol Chem 2001;276(51):47759-62.

37. Rogakou EP, Pilch DR, Orr AH, Ivanova VS, Bonner WM. DNA double-stranded breaks induce histone H2AX phosphorylation on serine 139. J Biol Chem 1998;273(10):5858-68.

38. Paull TT, Rogakou EP, Yamazaki V, Kirchgessner CU, Gellert M, Bonner WM. A critical role for histone H2AX in recruitment of repair factors to nuclear foci after DNA damage. Curr Biol 2000;10(15):886-95.

39. Carty MP, Zernik-Kobak M, McGrath S, Dixon K. UV light-induced DNA synthesis arrest in HeLa cells is associated with changes in phosphorylation of human single-stranded DNA-binding protein. Embo J 1994;13(9):2114-23.

40. Liu JS, Kuo SR, Melendy T. Phosphorylation of replication protein A by S-phase checkpoint kinases. DNA Repair (Amst) 2006;5(3):369-80.

41. Iftode C, Daniely Y, Borowiec JA. Replication protein A (RPA): the eukaryotic SSB. Crit Rev Biochem Mol Biol 1999;34(3):141-80.

42. Vassin VM, Wold MS, Borowiec JA. Replication protein A (RPA) phosphorylation prevents RPA association with replication centers. Mol Cell Biol 2004;24(5):1930-43.

43. Binz SK, Sheehan AM, Wold MS. Replication protein A phosphorylation and the cellular response to DNA damage. DNA Repair (Amst) 2004;3(8-9):1015-24.

44. Guo Z, Kumagai A, Wang SX, Dunphy WG. Requirement for Atr in phosphorylation of Chk1 and cell cycle regulation in response to DNA replication blocks and UV-damaged DNA in Xenopus egg extracts. Genes Dev 2000;14(21):2745-56.

45. Kumagai A, Kim SM, Dunphy WG. Claspin and the activated form of ATR-ATRIP collaborate in the activation of Chk1. J Biol Chem 2004;279(48):49599-608.

46. Morgan SE, Lovly C, Pandita TK, Shiloh Y, Kastan MB. Fragments of ATM which have dominant-negative or complementing activity. Mol Cell Biol 1997;17(4):2020-9.

47. Garg R, Callens S, Lim DS, Canman CE, Kastan MB, Xu B. Chromatin association of rad17 is required for an ataxia telangiectasia and rad-related kinase-mediated S-phase checkpoint in response to low-dose ultraviolet radiation. Mol Cancer Res 2004;2(6):362-9.

48. Wang JL, Wang X, Wang H, Iliakis G, Wang Y. CHK1-regulated S-phase checkpoint response reduces camptothecin cytotoxicity. Cell Cycle 2002;1(4):267-72.

49. Falck J, Mailand N, Syljuasen RG, Bartek J, Lukas J. The ATM-Chk2-Cdc25A checkpoint pathway guards against radioresistant DNA synthesis. Nature 2001;410(6830):842-7.

50. Shimuta K, Nakajo N, Uto K, Hayano Y, Okazaki K, Sagata N. Chk1 is activated transiently and targets Cdc25A for degradation at the Xenopus midblastula transition. Embo J 2002;21(14):3694-703.

51. Jin J, Shirogane T, Xu L, et al. SCFbeta-TRCP links Chk1 signaling to degradation of the Cdc25A protein phosphatase. Genes Dev 2003;17(24):3062-74.

52. Lupardus PJ, Byun T, Yee MC, Hekmat-Nejad M, Cimprich KA. A requirement for replication in activation of the ATR-dependent DNA damage checkpoint. Genes Dev 2002;16(18):2327-32.

53. Ward IM, Minn K, Chen J. UV-induced ataxia-telangiectasia-mutated and Rad3-related (ATR) activation requires replication stress. J Biol Chem 2004;279(11):9677-80.

54. Alexandrow MG, Hamlin JL. Chromatin decondensation in S-phase involves recruitment of Cdk2 by Cdc45 and histone H1 phosphorylation. J Cell Biol 2005;168(6):875-86.

55. Zhu Y. A model for CDK2 in maintaining genomic stability. Cell Cycle 2004;3(11):1358-62.

56. Ye X, Wei Y, Nalepa G, Harper JW. The cyclin E/Cdk2 substrate p220(NPAT) is required for S-phase entry, histone gene expression, and Cajal body maintenance in human somatic cells. Mol Cell Biol 2003;23(23):8586-600.

Chapter 5:

The Atypical CDK Activator Spy1 Regulates the Intrinsic DNA Damage Response and is Dependent upon p53 to Inhibit Apoptosis

Abstract

The intrinsic damage response is activated by DNA damage that arises during the cell division process. The ability of the cell to repair this damage during proliferation is important for normal cell growth and, when disrupted, may lead to increased mutatagenesis and tumorigenesis. The atypical CDK activator, Spy1, was previously shown to promote cell survival, prevent apoptosis, and inhibit checkpoint activation in response to DNA damage. Prior studies have shown that Spy1 is up-regulated in breast carcinomas and accelerates mammary tumorigenesis *in vivo*. In this report, first, we demonstrate that the ability of Spy1 to inhibit apoptosis and bypass UV-induced checkpoint activation is dependent on the presence of the gene regulatory protein p53 and the CKI p21. Second, we demonstrate that Spy1 expression has the following effects: prevents repair of cyclobutane pyrimidine dimers through bypass of nucleotide excision repair; increases the cellular mutation frequency; and reduces the formation of cyclin E induced γH2A.X foci. Lastly, we show that knockdown of endogenous Spy1 leads to γH2A.X foci formation, Chk1 phosphorylation, and proliferation defects, demonstrating a functional role for Spy1 in the intrinsic DNA damage response. These results also demonstrate that Spy1 fulfills a novel regulatory role in the intrinsic DNA damage response and maintains the balance between checkpoint activation, apoptosis, repair, and cell cycle progression in response to exogenous or intrinsic damage. Furthermore, the overexpression of Spy1 as a contributing factor in cancer progression will most likely be confined to p53-positive cells.

Introduction

In response to DNA damage and replication stress, cells activate a checkpoint response to induce cell cycle arrest, providing time to repair and maintain the genome [1]. Normally, when cells encounter unrepairable DNA damage they are eliminated from the proliferating population by inducing senescence or apoptosis. p53 is a pivotal sensor of genotoxic and nongenotoxic stresses which is involved in the activation of numerous signaling pathways, including DNA damage induced cell cycle checkpoints, cellular proliferation, and radiation sensitivity [2]. In addition to a variety of genotoxic agents, overexpression of numerous oncogenes including c-*myc*, *mos*, *cyclin E*, *CDC25A*, and *E2F1*, activates the DNA damage response and leads to cell death or senescence [3-9]. Recent work suggests a fundamental role for the DNA damage response as a barrier to early tumorigenesis [3]. In addition to controlling cell cycle progression, cyclin dependent kinases (CDKs) regulate the balance between senescence, growth, apoptosis, and checkpoint signaling. Misregulation of CDKs and other proteins involved in the DNA damage response is associated with cancer predisposition and tumor progression [10].

Unlike cyclins, members of the Speedy/RINGO family bind and activate CDKs independently of the activating T-loop phosphorylation catalyzed by CAK [11-14]. *Xenopus*-Spy1 (X-Spy1) was first shown to be required for and to induce oocyte maturation [15]. Subsequently, human Speedy A1 (Spy1) was found to be expressed in a variety of human tissues, and its overexpression enhances G_1-S phase progression, $p27^{kip}$ degradation, and cellular proliferation by activating CDK2 [16-19]. Spy1 also

enhances mammalian cell survival in response to a number of genotoxic agents, including UV irradiation where it prevents caspase activation and apoptosis [20, 21]. Spy1 expression prevents the activation of both S-phase/replication and G_2/M checkpoints in UV-challenged cells, as well as the activation of the checkpoint proteins Chk1, RPA, and H2A.X, which are dependent on the interaction of Spy1 with CDK2 [21].

Recent serial analysis of gene expression and microarray results have implicated Spy1 overexpression in breast cancer, and notably, s*py1* was one of the fifty most up-regulated genes in nodal metastatic and invasive ductal breast carcinomas [22]. Recently, Spy1 expression was shown to be tightly regulated during development of the mammary gland, and ectopic Spy1 expression leads to abnormal gland morphology. Using a mouse model, Spy1 overexpression was shown to accelerate mammary tumorigenesis *in vivo* [23]. The promotion of tumorigenesis may be attributed to the capacity of Spy1 to override DNA damage responses when overexpressed [20, 21].

Here, we demonstrate that the anti-apoptotic effects of Spy1 in cells exposed to UV irradiation are dependent on the presence of functional p53 indicating Spy1 may promote tumorigenesis in the small subset of cancers containing unaltered p53. We also evaluate the effect of Spy1 expression on the repair of UV induced lesions. Spy1 expression prevents the repair of cyclobutane pyrimidine dimers (CPDs), possibly through bypass of nucleotide excision repair, as shown in a single cell alkaline comet assay. Furthermore, Spy1 expression leads to an increased mutation frequency, and reduces γH2A.X foci formation during the DNA damage response induced by cyclin E

overexpression. Moreover, we evaluate the effect of Spy1 knockdown on the DNA damage response, and for the first time demonstrate a functional role of endogenous human Spy1. We show that Spy1 knockdown by siRNA leads to γH2A.X foci formation, increased Chk1 phosphorylation, and activation of an intrinsic DNA damage response. Furthermore, knockdown of Spy1 also causes proliferation defects in U2OS cells, indicating Spy1 plays a critical role in the intrinsic DNA damage response.

Materials and Methods

Spy1 shRNA Constructs and Cell Growth Assay

Oligonucleotides containing the siRNA target sequences were synthesized, annealed, and ligated into the pSuperior.puro vector (Oligoengine, Seattle, WA) pre-cut with *BglII* and *HindIII*. This vector was sequenced and assayed for efficient Spy1 knockdown. For growth assays, cells were plated at $3.75x10^5$ per 10 cm dish in the absence or presence of 5 μg/ml doxycycline. Cell counts were taken using the Trypan Blue exclusion method. Media was refreshed every three days.

Generation and Maintenance of cell lines

U2OS cells were obtained from American Type Culture Collection. Tet-repressor starter lines were generated by transfecting cells with the pcDNA6/TR plasmid (Invitrogen, Carlsbad, CA) followed by 5 μg/ml Blasticidin selection. Tet-repressor expressing U2OS cells were subsequently transfected with pSuperior.puro-siSpy1 and selected with 5 μg/ml Blasticidin and 1 μg/ml puromycin. Colonies were screened for Spy1 knockdown after treatment with 1 μg/ml tetracycline or doxycycline. Optimal Spy1 knockdown was achieved with doxycycline treatment for 48 h. Cells were maintained in DMEM supplemented with 0.1% penicillin-streptomycin, 10% Tet-free fetal bovine serum, 5 μg/ml Blasticidin, and 1 μg/ml puromycin and incubated at 37°C in 5% CO_2. Saos2 cells (a kind gift from Geoff Wahl, Salk Institute, La Jolla, CA) and myc-Spy1:U2OS cells were cultured in DMEM supplemented with 0.1% penicillin-streptomycin, 10% FBS, 1.5 mM

L-glutamine (Invitrogen), 0.48 mg/ml G418 and 0.5 mg/ml Zeocin (Invitrogen) and maintained at 37°C in 5% CO_{2}..

Inducible Saos2 cell lines were created using the Ecdysone System (Invitrogen). Briefly, myc-Spy1 was cloned into the BamH1 and Xba1 sites of the pIND vector and subsequently cotransfected with pVgRXR into Saos2 cells. Cells were selected with G418 and Zeocin (Invitrogen) for 14 days, colonies were isolated, and then tested for Ponasterone A (PonA) induced expression of myc-Spy1. The pIND:Saos2 and Spy1:Saos2 inducible cells were subsequently maintained as above with 0.48mg/ml G418 and 0.5mg/ml Zeocin. HCT116 $p53^{wt}$, HCT116 $p21^{wt}$, HCT116 $p53^{-/-}$, and HCT116 $p21^{-/-}$ cells (a kind gift from B. Vogelstein, Johns Hopkins School of Medicine, Baltimore, MD) were maintained in McCoy's 5A media (GIBCO), supplemented with 0.1% penicillin-streptomycin (Sigma-Aldrich), and 10% fetal bovine serum. Cells were incubated at 37°C in 5% CO_2.

For UV irradiation of cells, media was aspirated, plates were washed twice with PBS, and cells were irradiated with 10 or 50 J/m^2 UVC (254 nm) using a Stratalinker1800 (Stratagene; La Jolla, CA). For nocodazole/ aphidicholin synchronization, cells were treated with 100 nM nocodazole for 12 h, washed, and released into medium containing 2 μg/mL aphidicholin for 12 h. The cells were then washed, released into fresh media, and harvested and lysed at the time points indicated.

Detection of apoptosis

To determine apopotosis in response to UV by detection of Sub-G_1 DNA content, $5x10^5$ HCT116 $p53^{wt}$, HCT116 $p21^{wt}$, HCT116 $p53^{-/-}$, or HCT116 $p21^{-/-}$ cells were seeded on 10 cm plates, transfected with myc-Spy1 DNA (5μg) using Fugene 6 (Roche, Indianapolis, IN), and then irradiated with UV 24 h later. Cells were allowed to recover until the indicated time points. Floating and adherent cells were collected, washed twice with PBS by centrifugation, and fixed in 95% ethanol at 4°C overnight. Cells were then stained with a propidium iodide solution (0.25mg/ml propidium iodide, 0.01% Triton-X100, 100μg/ml RNase A in PBS) and analyzed for Sub-G1 DNA content by flow cytometry using a FACScalibur (Becton-Dickinson).

To detect apoptosis by Annexin V binding to the outer cell membrane, $5x10^5$ Saos2 cells were seeded on 10cm plates and induced for 24 h. Cells were then irradiated with UV and incubated for 24 h in induction media. Floating and adherent cells were collected and washed twice with PBS and resuspended in Annexin V binding buffer (BD Pharmingen). $1x10^5$ cells were stained with Annexin V-FITC and 7-amino-actinomycin D (7-AAD; to detect necrotic cells) as per manufacturer's instructions (BD Pharmingen). Cells were analyzed for apoptosis by flow cytometry.

Immuno-Southern Dot Blot Assay

5μg of genomic DNA isolated from cells using the Qiagen Genomic DNA purification kit (Qiagen, Valencia, CA) from each sample was dot blotted onto nitrocellulose and baked at 80°C under vacuum conditions for 2 h. The membrane was probed with mouse α-CPD sera (Sigma) followed by an anti-mouse-Ig-HRP

secondary antibody (GE Healthcare). Detection was achieved using an Enhanced ChemiLuminescence (ECL) kit (GE Healthcare).

Single Cell Alkaline Comet Assay

The alkaline comet assay used to detect nucleotide excision repair induced DNA strand breaks was performed as previously described with minor modifications [29]. Myc-Spy1:U2OS cells treated with UV were suspended in 0.65% low melting agarose, applied onto frosted glass microscope slides pre-coated with 1.4% normal melting agarose, and immersed in ice-cold lysis buffer (1% N-lauroylsarcosine, 2.5 M NaCl, 100 mM EDTA, 10 mM Tris-HCl, 1% Triton X-100, pH 10) for 1 h at 4°C in the dark. Slides were rinsed once with 1 M Tris-HCl, pH 7.5 then immersed in alkaline buffer (1 mM EDTA, 300 nM NaOH, pH > 13) at room temperature for 30 min in the dark to unwind the DNA. Electrophoresis was performed at 25V at a constant 300 mA for 25 min. Slides were then washed in Neutralization Buffer (0.4 M Tris-HCl, pH 7.5), fixed with ice cold methanol for 3 min, dried overnight, then flooded with a 1 μg/ml DAPI solution. Comet tails were visualized and photographed using a Nikon Microphot-FXA microscope equipped with a Hamamatsu C5810 camera at 60x magnification and processed in Adobe Photoshop. One hundred nuclei were examined per sample.

Immunofluorescence Microscopy

siSpy1:U2OS or myc-Spy1:U2OS cells were seeded onto coverslips and induced for siRNA expression with 5μg/ml doxycycline for 48 h or transfected with 6μg of pCDNA3-cyclin E-GFP using FuGene6 (Roche, Indianapolis, IN) after induction of myc-Spy1 expression for 24 h, respectively. γH2A.X and phospho-Chk1-S317 staining in siSpy1:U2OS cells were performed as previously described [21]. Cells expressing cyclin E-GFP (gift from Stephen Dowdy, UCSD) were visualized directly. For γH2AX staining (Fig. 5) cells were stained with mouse antiphosphohistone H2A.X (05-636) (Upstate), and counterstained with goat anti-mouse Texas Red-X (T6390) (Molecular Probes). Hoechst dye 33342 (1 μg/ml) was used to visualize nuclei.

Western Blotting

Cells were lysed in NP-40 lysis buffer (20 mM Tris-HCl, pH 8.0, 150 mM NaCl, 0.1% Nonidet P-40, 1 mM Na_3VO_4, 1 mM NaF, 1mM phenylmethylsulfonyl fluoride, 10 μg/ml aprotinin), clarified by centrifugation, and protein concentrations were determined by Bradford Assay (Bio-Rad). Equal amounts of total protein were resolved by SDS-PAGE, transferred to Immobilon-P (Millipore), and proteins were detected by immunoblotting with α-Myc (9E10) (sc-40), α-cyclin E (HE12) (sc-247), or α-β-tubulin (H-235) (sc-9104), and α-Chk1 (G4) (sc-8408) purchased from Santa Cruz Biotechnology (Santa Cruz, CA), and α-phospho Chk1 (Ser345)(133D3) purchased from Cell Signaling Technology (Beverly, MA), followed by secondary anti-mouse or anti-rabbit Ig-horseradish peroxidase conjugate (GE Healthcare) followed by ECL (GE Healthcare).

Mutagenesis Assay

Control or UV-irradiated pR2 (8μg) and unirradiated p205-KMT11 (4μg) plasmids were cotransfected into myc-Spy1:U2OS cells using FuGene6. Cells were incubated for three days to allow overexpression of the SV40 T-antigen carried by the p205-KMT11 and replication of the pR2 plasmid. Cells were collected and extrachromosomal plasmid DNA was recovered by a small-scale alkaline lysis procedure [31]. The DNA preparations were treated with *Dpn*I to degrade any unreplicated plasmid. DH5αMCR *Escherichia coli* were transformed with the recovered pR2 plasmid and plated on selective LB agar medium containing kanamycin (30 mg/ml), 0.8% 5-bromo-4-chloro-3-indolyl-β-D-galactoside (X-Gal), 100 mM isopropyl β-D-thiogalactoside (IPTG). Colonies were screened for β-galactosidase activity and white or light blue colonies indicating an inactivated *lacZ*' gene were isolated. White colonies were individually restreaked on selective medium in order to verify lack of β-galactosidase activity.

Results

Requirement for p53 and p21

We have previously shown that in U2OS cells, which contain wild type p53, inducible expression of Spy1 inhibits apoptosis [21]. The well studied involvement of p53 in DNA damage and repair pathways [24] led us to examine the role of p53 in Spy1 regulation of the DNA damage response. Using the Saos2 cell line, which is null for p53, we first examined whether Spy1 modulates the apoptotic response by utilizing a myc-Spy1:Saos2 inducible cell line (Fig. 5-1A). In contrast to the $p53^{WT}$ U2OS cells, Spy1 does not prevent apoptosis in Saos2 cells in response to UV, as measured by an Annexin V binding assay. 24 hours after irradiation with UV, and induction with Ponasterone A, pIND:Saos2 cells and myc-Spy1:Saos2 cells have comparable amounts of Annexin V positive cells, 37% and 35%, respectively (Fig. 5-1B). These results suggest that Spy1 is able to prevent apoptosis in response to UV only in the presence of functional p53.

In the absence of a normal isogenic cell line for Saos2, we chose to confirm that Spy1-mediated inhibition of apoptosis is p53 dependent using isogenic HCT116 colon carcinoma cell lines engineered to be p53 and p21 null by homologous recombination [25]. Here, cells were transfected with myc-Spy1 and irradiated with 50 J/m^2 UV. 48 hours after irradiation, cells were harvested, fixed, stained with propidium iodide, and analyzed by flow cytometry to determine cells containing Sub-G_1 DNA content as a marker of apoptosis. We found that UV-irradiated HCT116 $p53^{+/+}$ and HCT116 $p21^{+/+}$ cells transfected with Spy1 did not accumulate significant

levels of Sub-G_1 DNA content compared to irradiated mock transfected cells, indicating inhibition of apoptosis. Similarly to the Saos2 cells, HCT116 $p53^{-/-}$ and HCT116 $p21^{-/-}$ cells showed no suppression of apoptosis when myc-Spy1 was overexpressed (Fig. 5-1C). These results indicate that the inhibition of apoptosis by Spy1 expression is dependent on p53. The results presented in Fig. 1C also indicate a role for p21 in mediating the effects of Spy1 in DNA repair pathways, possibly as a transcriptional target of p53, although this was not further examined.

Previous work has shown that Spy1 expression in $p53^{wt}$ U2OS cells inhibits the phosphorylation and activation of Chk1 in response to UV-irradiation [21]. Next, we examined whether inhibition of Chk1 phosphorylation by Spy1 is also dependent on p53 using the HCT116 $p53^{+/+}$ or HCT116 $p53^{-/-}$ cell lines. Cells were transfected with myc-Spy1 and irradiated with UV. In agreement with previous observations in U2OS cells, expression of Spy1 in HCT116 $p53^{+/+}$ cells inhibits phosphorylation of Chk1 in response to UV-irradiation. Expression of Spy1 in HCT116 $p53^{-/-}$ cells is unable to inhibit phosphorylation of Chk1, again indicating that the Spy1-mediated effects in response to DNA damage require the presence of p53 (Fig 5-1D).

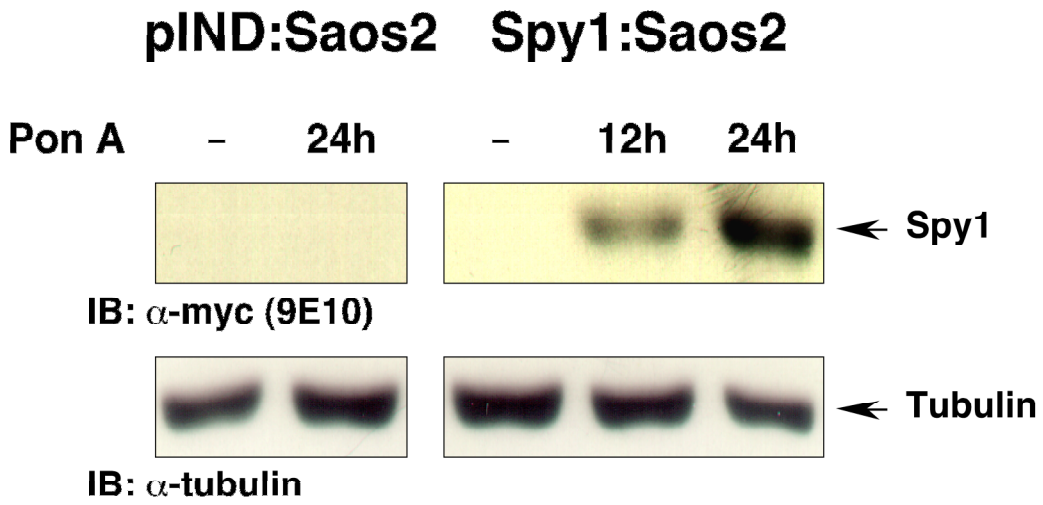

Figure 5-1. The anti-apoptotic effects of Spy1 in response to UV-irradiation are dependent on p53.
(A) Saos2 inducible cells were induced with 2.5µl PonA/ml of media for 12 or 24 hours. Mock induced samples (pIND:Saos2 cells) were prepared after 24 hours. Lysates were resolved by SDS-PAGE, transferred to membrane and probed to detect myc tagged Spy1 expression and tubulin as a loading control.

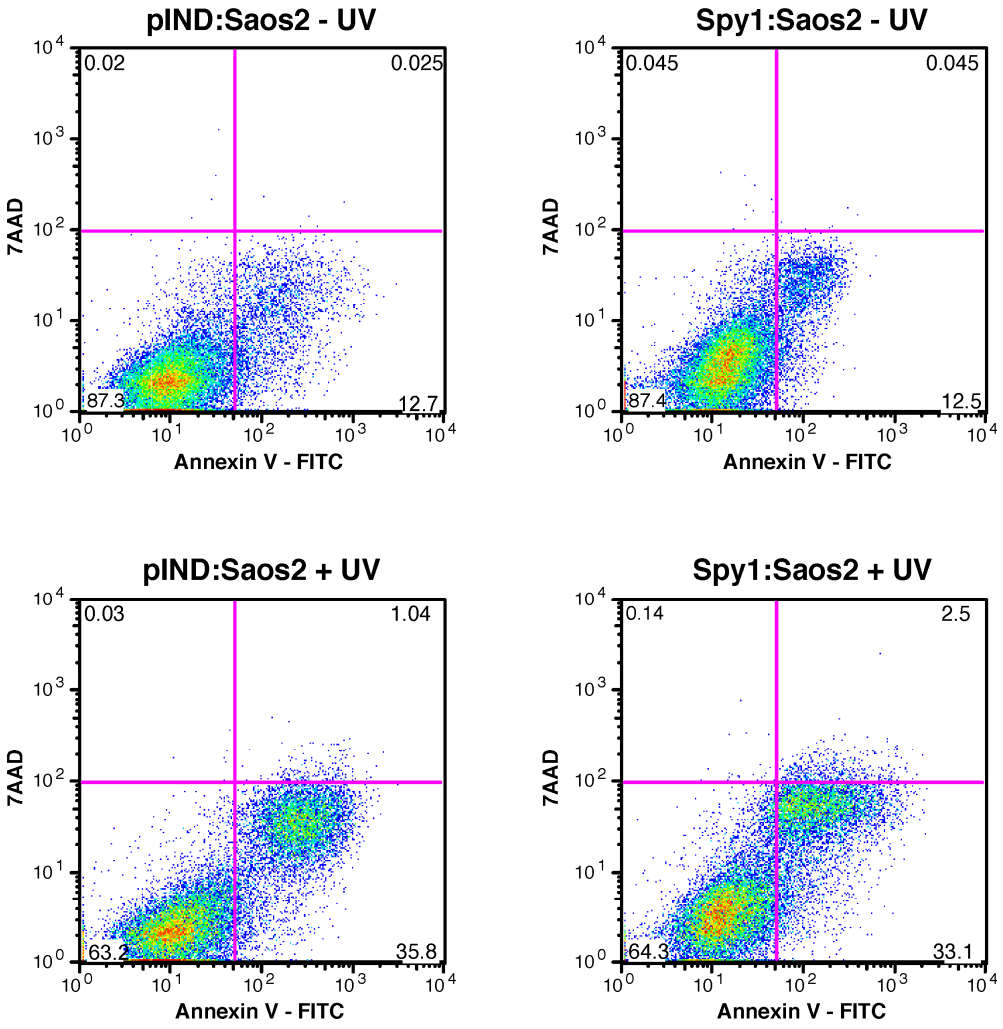

Figure 5-1. The anti-apoptotic effects of Spy1 in response to UV-irradiation are dependent on p53, continued.
(B) pIND:Saos2 and Spy1:Saos2 cells were induced for 24 hours and irradiated with 50 J/m^2 UV. After a 24 hour incubation, cells were analyzed for apoptosis using an Annexin V binding assay. Results from one representative experiment are shown.

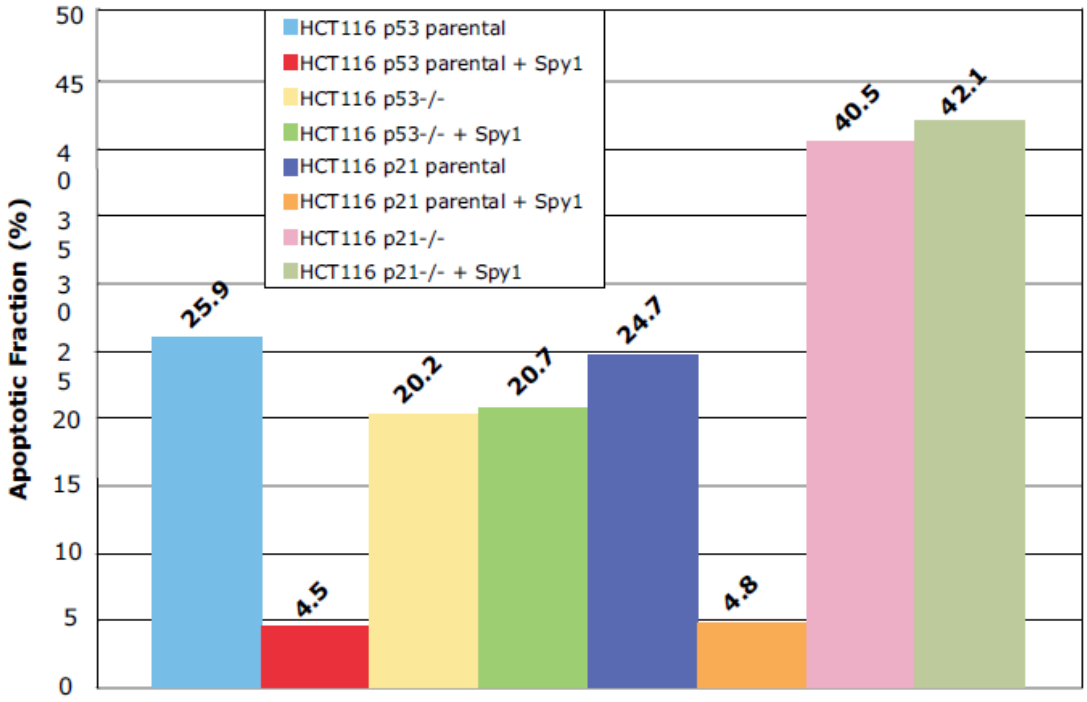

Figure 5-1. The anti-apoptotic effects of Spy1 in response to UV-irradiation are dependent on p53, continued.
(C) HCT116 cells were transfected with myc-Spy1 or mock. 24 hours later, cells were irradiated with 50 J/m^2 UV. Cells were allowed to recover for 48 hours and were then collected, fixed, stained with propidium iodide, and the percentage of cells exhibiting Sub-G_1 DNA content as a measurement of apoptosis were detected using FACS.

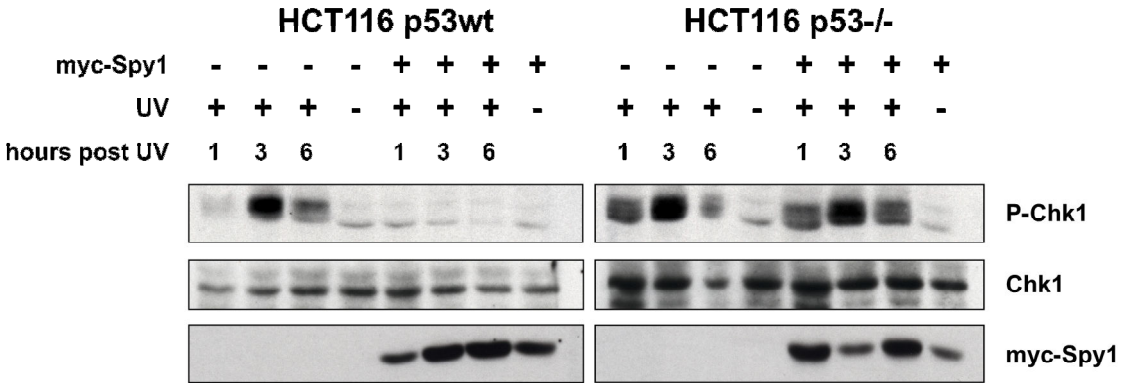

Figure 5-1. The anti-apoptotic effects of Spy1 in response to UV-irradiation are dependent on p53, continued.
(D) HCT116 $p53^{+/+}$ and $p53^{-/-}$ were transfected with myc-Spy1 or with mock. 24 hours later, cells were irradiated with 50 J/m^2 UV. Cells were collected at 1, 3, and 6 hours post irradiation and assayed for phosphorylation of Chk1 at Ser 345 by Western Blot. The membrane was sequentially stripped and reprobed for total Chk1 and myc-Spy1.

Spy1 and repair of DNA damage

UV irradiation causes the formation of cyclobutane pyrimidine dimers (CPDs), which block replication and transcription, eliciting activation of the DNA damage response [26]. Although we previously demonstrated that Spy1 expression prevents a UV-induced checkpoint response [21], the contribution of Spy1 to these effects remained unclear. We hypothesized that these effects may be attributable to an enhancement in repair of UV induced DNA damage. We therefore examined the effect of Spy1 expression on the removal of UV-induced CPDs using an immuno-southern dot blot assay [27]. Spy1:U2OS cells were induced for Spy1 expression or mock induced, irradiated with 10 J/m^2 UV or left untreated, and collected at 0 and 24 hours. Genomic DNA was isolated, dot-blotted onto nitrocellulose, and probed with α-CPD sera. After 24 hours, no CPDs remained in control cells, indicating the UV-induced damage was efficiently removed (Fig. 5-2A, left panel). In contrast, Spy1-expressing cells unexpectedly retained high CPD levels, demonstrating Spy1 expression prevents efficient CPD removal. Counter-staining with ethidium bromide demonstrates the presence of DNA in each sample (Fig. 5-2A, right panel). The difference in the CPD removal rates was then examined over a 24 hour time course in nocodazole/aphidicholin synchronized cells. Control cells removed CPDs at a higher rate than Spy1-expressing cells upon release from aphidicholin (Fig. 5-2B). These results indicate that Spy1 expression decreases the rate of CPD removal in UV-damaged cells.

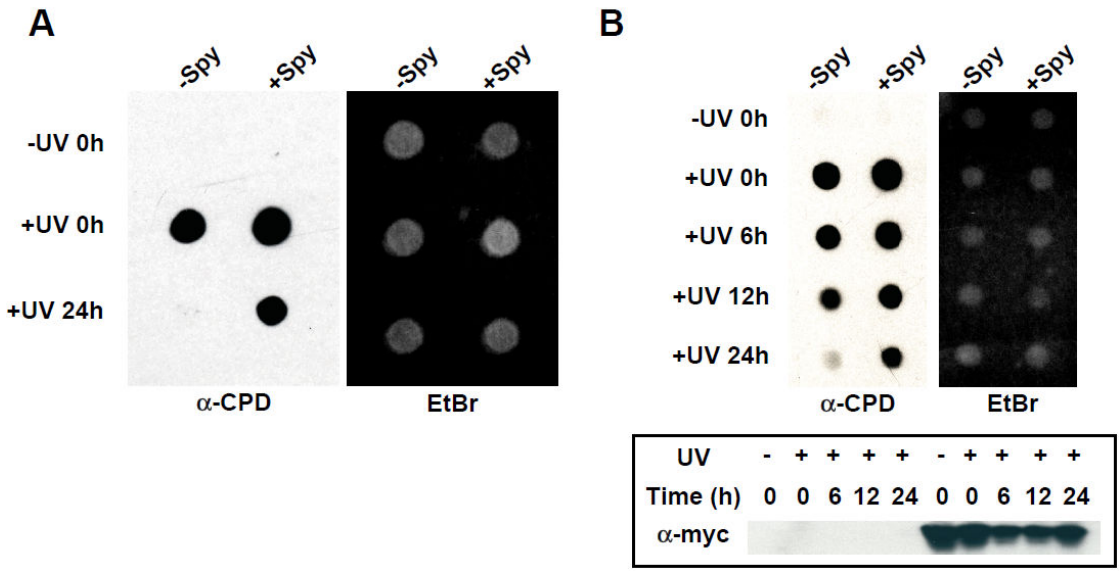

Figure 5-2. Spy1 prevents the efficient repair of CPDs.
(A) Spy1:U2OS cells were mock induced or induced with Ponasterone A for Spy1 expression and irradiated with 10 J/m^2 UV or left untreated. At 0 or 24 h after irradiation, total genomic DNA was isolated and dot-blotted onto nitrocellulose, probed with an α-cyclobutane pyrimidine dimer (CPD) antibody (left panel), and subsequently exposed to ethidium bromide (right panel). (B, upper panel) Spy1:U2OS cells were synchronized by a nocodazole block and released into serum containing aphidicholin for 12 h. The cells were then washed, irradiated with 10 J/m^2 UV, and released from aphidicholin and total genomic DNA was isolated, dot-blotted, and probed as in (A). (B, lower panel) Lanes 1-5 were mock induced and 6-10 were induced for Spy1 expression. Equal amounts of lysates were separated by SDS-PAGE, transferred to Immobilon-P, and probed for myc-Spy1 expression.

CPDs are removed from DNA by the nucleotide excision repair (NER) process [28]. To determine if Spy1 expression directly affects CPD repair mechanisms, we utilized an alkaline comet assay to evaluate NER. This assay allows for the detection of DNA strand breaks, which in the case of UV damage, occurs when NER enzymes cleave and excise bases from the DNA strand [29]. Thus, the presence of comet tails indicates NER is active [30]. Approximately 75% of control cells irradiated with UV were positive for comet tails, while only 18% of Spy1-expressing cells exhibited comet tails (Fig. 5-3A and 5-3B). Furthermore, control cells displayed longer comet tail lengths compared to the few comet tails present in Spy1-expressing cells on average (data not shown). These results indicate that Spy1 expression prevents efficient NER and may account for the extended presence of CPDs, suggesting Spy1 may regulate the NER machinery or proteins that directly regulate NER signaling or processes.

We next used a SV-40 shuttle vector system [31] to determine whether prevention of NER and CPD removal due to Spy1 expression increases the mutation frequency in cells. We chose to use this system over others, such as the HPRT assay [32], because it allows for screening changes in mutation frequency in any cell type, which enabled us to utilize our established myc-Spy1:U2OS cell line to perform the assay. Briefly, a UV-irradiated shuttle vector (pR2) was transfected into mock or Spy1-induced myc-Spy1:U2OS cells, and plasmid DNA (pR2) was isolated 72 hours later, transformed into *recA*$^{-}$ *E. coli*, and plated on selective medium to examine the mutation frequency in the *lac*Z' gene, as previously described [31]. We found that Spy1

expression led to about a two-fold increase in the mutation frequency compared to mock-induced cells at all UV doses tested (1000, 2000, and 5000 J/m^2) (Fig. 5-3C). As a control, the mutation frequency of the unirradiated plasmid (0 J/m^2) was zero in both cell types.

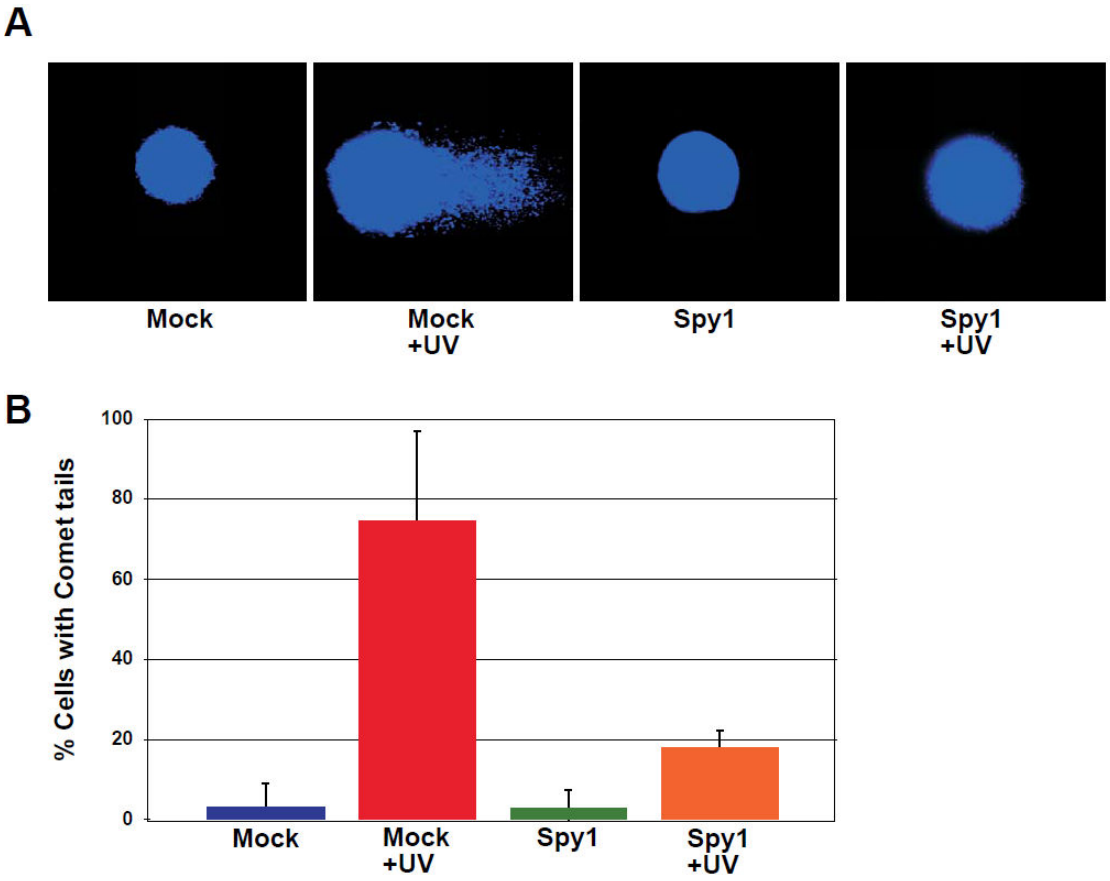

Figure 5-3. Spy1 inhibits comet tail formation and promotes shuttle vector mutation frequency in response to UV irradiation.
(A) Spy1:U2OS cells mock induced or induced for Spy1 expression were irradiated with 10 J/m^2 UV and analyzed for DNA strand breaks 3h after treatment. Alkaline comets were visualized by DAPI staining. (B) Quantization of comet tails in control or Spy1 expressing cells was performed by counting 100 nuclei from three independent experiments. The average number of cells positive for comets is shown +/- std. dev.

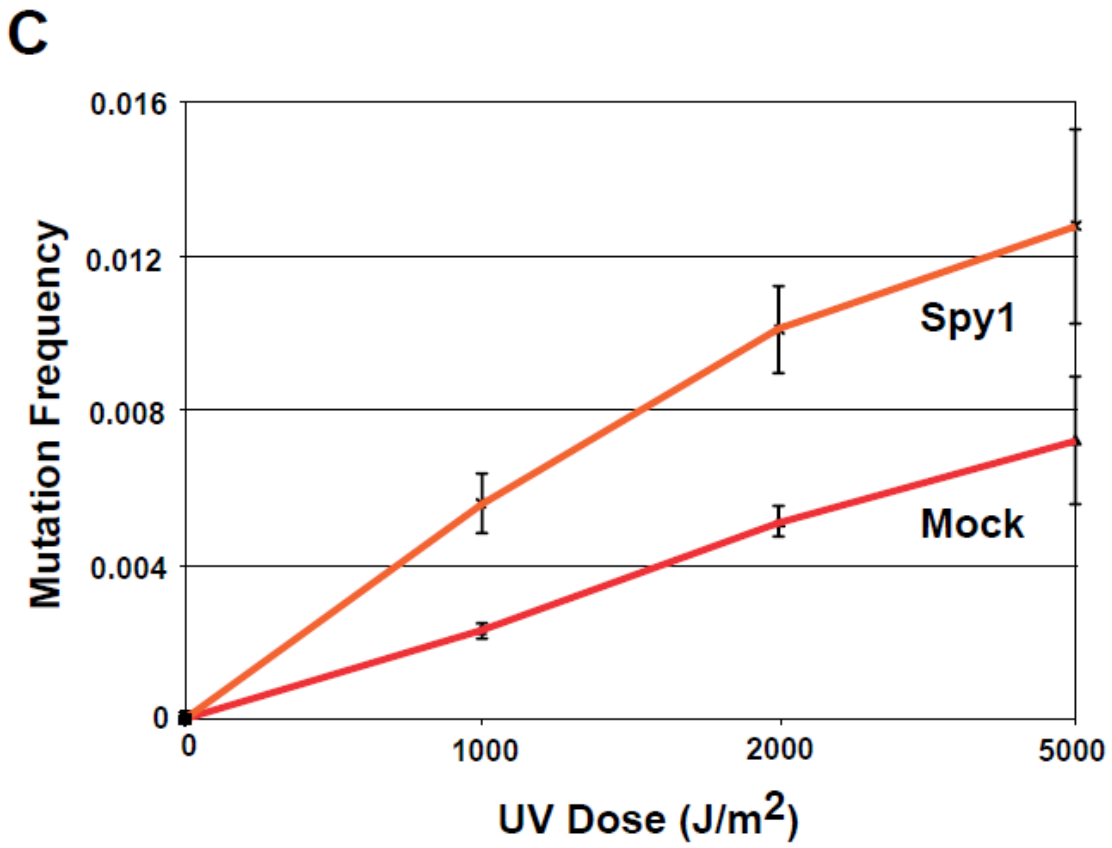

Figure 5-3. Spy1 inhibits comet tail formation and promotes shuttle vector mutation frequency in response to UV irradiation, continued.
(C) Shuttle vector mutation frequency was determined using Spy1:U2OS cells which were mock induced or induced with Ponasterone A, then transfected with the p205-KMT11 vector and the pR2 vector that was left unirradiated or irradiated with the UV dose indicated. Low M_w DNA was purified by a modified alkaline lysis method, and treated with DpnI. DH5αMCR *E. coli* were transformed with the DNA and plated onto agar plates containing kanamycin, IPTG, and X-gal for blue/white screening. Total and white colonies were counted. White colonies were restreaked on selective medium to confirm their color. The average ratio of white/total colonies at each UV dose from three independent experiments is shown +/- std. dev.

Spy1 and the intrinsic DNA damage response

Next, we examined the effects of knocking down endogenous Spy1 on the DNA damage response. Five different sites for siRNA targeting in Spy1 were identified using software at http://www.dharmacon.com/sidesign/ and the requisite oligos were ligated into the pSuperior.puro vector to allow inducible expression of short hairpin RNA (shRNA). Spy1 knockdown was initially tested transiently using HEK-293T cells cotransfected with pCS3-myc-Spy1 and the pSuperor.siSpy1 plasmids against various Spy1 target sequences. Cell lysates were examined 48 hours after transfection by immunoblotting with mAB 9E10 to determine whether transient expression of myc-Spy1 was diminished. Target #0311 yielded the best knockdown, target #0005 yielded partial knockdown, and the 3'UTR target #0112 exhibited no knockdown (data not shown). The U2OS human osteosarcoma cell line was chosen to make tetracycline inducible knockdown cell lines with target #0311 because we have already extensively characterized checkpoint responses in U2OS cells overexpressing Spy1 [21]. Clone 6 exhibited the best inducible knockdown of endogenous Spy1 mRNA, as examined by RT-PCR (Fig. 5-4A)**.** Clone 6 (further referred to as siSpy1:U2OS cells) was chosen for clonal expansion and used in subsequent experiments.

siSpy1:U2OS cells were then either mock induced or induced with doxycycline to knockdown endogenous Spy1, and assayed for activation of the damage response by examining γH2A.X foci formation. In undamaged cells, we found that knockdown of Spy1 led to ~20% increase in the number of γH2A.X and phospho-Chk1 foci positive cells compared to control cells, indicating that Spy1 knockdown

leads to an intrinsic DNA damage response (Fig. 5-4B, 5-4C). Knockdown of Spy1 in cells exposed to UV led to ~25% increase in γH2A.X foci positive cells compared to control cells (Fig. 5-4B, 5-4C). As a control, U2OS cells treated with doxycycline exhibited no γH2A.X foci, demonstrating that doxycycline alone does not cause formation of γH2A.X foci (data not shown). These results suggest that Spy1 functions to balance the signaling that occurs from stresses during cell growth.

Spy1 expression activates CDKs, promoting enhanced cell cycle progression and suppresses the DNA damage response, suggesting that Spy1 plays a role in modulating the balance between the damage response and replication. We hypothesized that knockdown of Spy1 by siRNA would also lead to proliferation defects due to an imbalance between checkpoint (anti-proliferative) signaling and replication (proliferative) signaling. siSpy1:U2OS cell proliferation was also monitored in the absence or presence of doxycycline for 5 days. The resultant growth curves of three independent experiments demonstrated that in the presence of doxycycline, there was a modest, yet significant, proliferation defect caused by Spy1 knockdown (Fig. 5-4D). This indicates that Spy1 plays an essential role in maintaining efficient proliferation, possibly attributable to its ability to balance replication and checkpoint signaling.

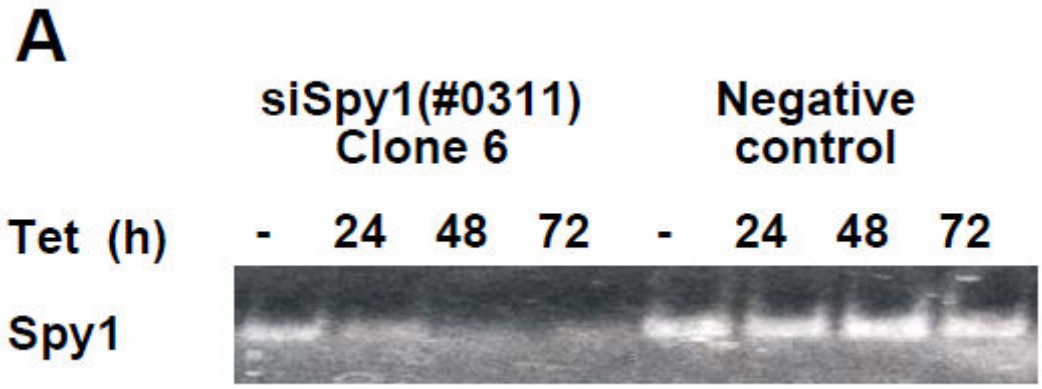

Figure 5-4. Spy1 knockdown induces an intrinsic damage response.
(A) Tetracycline was added for 0, 24, 48, or 72 h to clone 6 of siSpy1(#0311):U2OS, in comparison with a negative control. Clone 6 exhibits knockdown of endogenous Spy1 mRNA in U2OS cells assayed by RT-PCR.

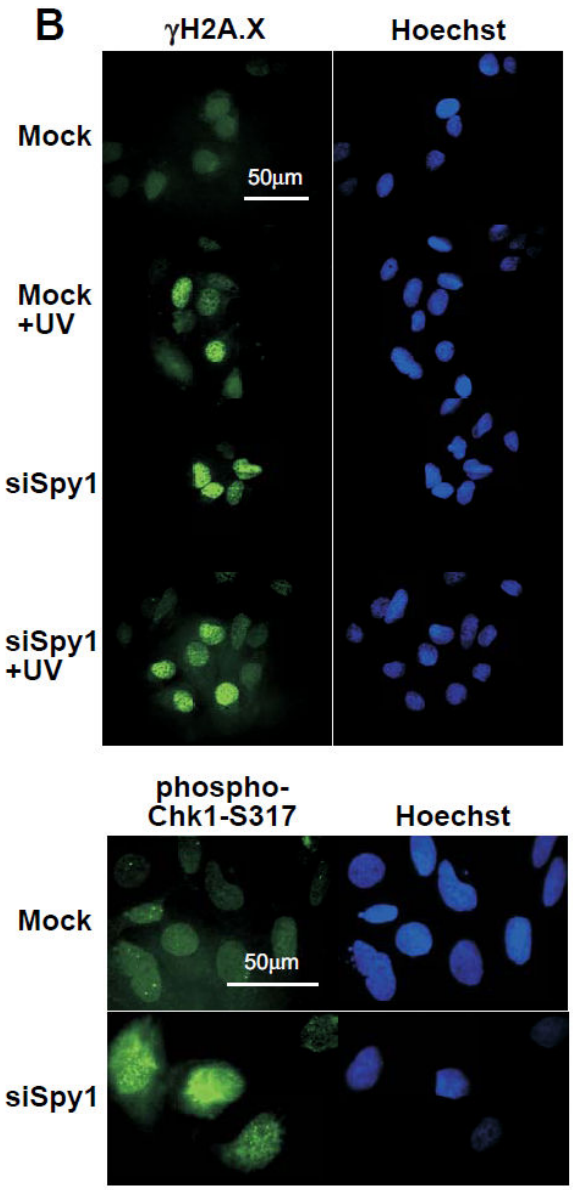

Figure 5-4. Spy1 knockdown induces an intrinsic damage response, continued. (B) siSpy1 U2OS cells were seeded on coverslips and either mock induced or induced for siSpy1 expression for 48h. Cells were then irradiated with UV and allowed to recover for 3 h. Coverslips were then stained for the formation of γH2A.X or phospho-Chk1 foci and counterstained with Hoechst to detect nuclei

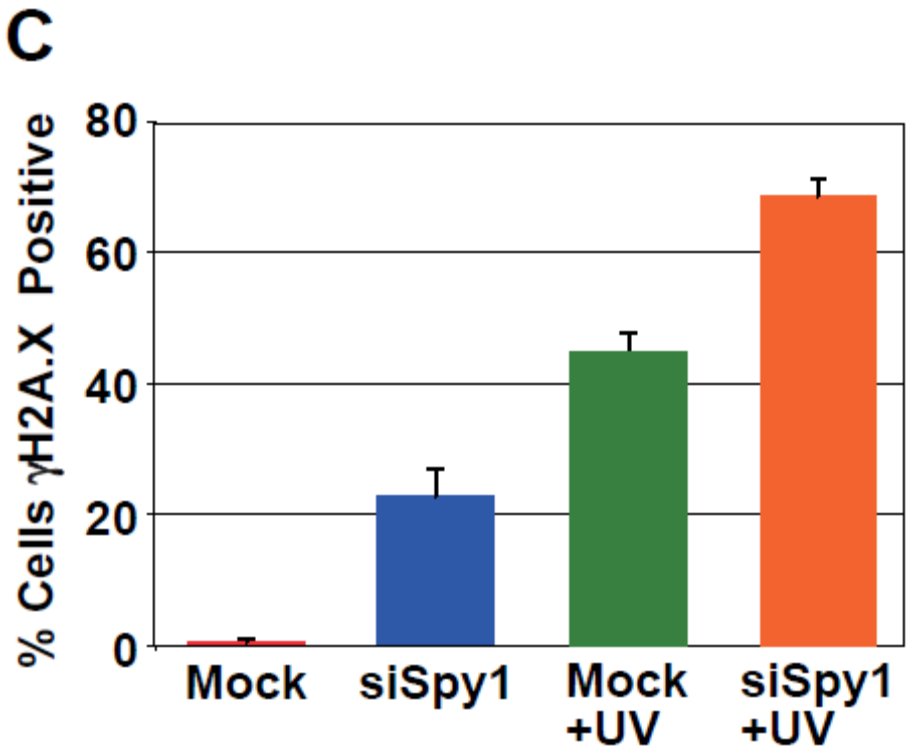

Figure 5-4. Spy1 knockdown induces an intrinsic damage response, continued. (C) 100 cells from (B) were counted and the average number of cells with γH2A.X foci from three independent experiments is shown +/- std. dev.

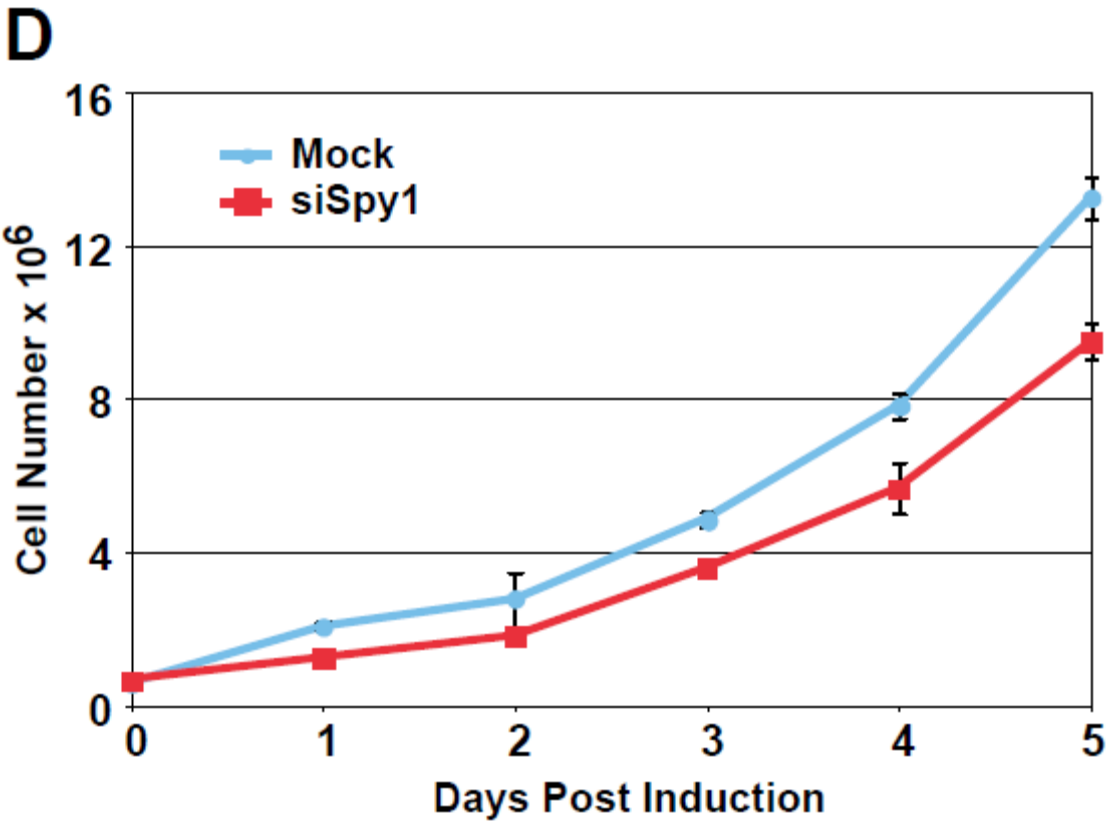

Figure 5-4. Spy1 knockdown induces an intrinsic damage response, continued. (D) siSpy1:U2OS cells were grown in the presence or absence of doxycycline. Cells were trypsinized and collected by centrifugation every 24 h and counted by Trypan Blue exclusion. The average number of cells per time point from three independent experiments is shown +/- std. dev.

Replication forks normally copy DNA without pausing, however, when damage is encountered, these forks may stall or even collapse, causing replication stress and activation of a DNA damage checkpoint. Bartkova et al. have previously shown that inducible overexpression of cyclin E in U2OS cells causes replication stress, which induces a DNA damage response as monitored by an increase in γH2A.X foci and strand breaks. In these experiments, cells entered senescence as a mechanism to guard against tumor progression caused by the *cyclin E* oncogene, in addition to the other oncogenes examined in these reports [3, 4]. To determine whether Spy1 could bypass the DNA damage response induced by cyclin E overexpression similarly to genotoxic agents and UV irradiation, cyclin E-GFP was transfected into myc-Spy1:U2OS cells induced for Spy1 expression or treated with vehicle as a control. In accordance with previous reports [3, 4], over 95% of the cells positive for cyclin E-GFP exhibited a dramatic increase in γH2A.X foci (Fig. 5-5A). The expression level of cyclin E was unaffected by overexpression of myc-Spy1 (Fig. 5-5B) and interestingly, the number of γH2A.X foci in Spy1-induced cells positive for cyclin E-GFP was decreased by over half (Fig. 5-5C). These results indicate that Spy1 may bypass the DNA damage response induced by cyclin E overexpression.

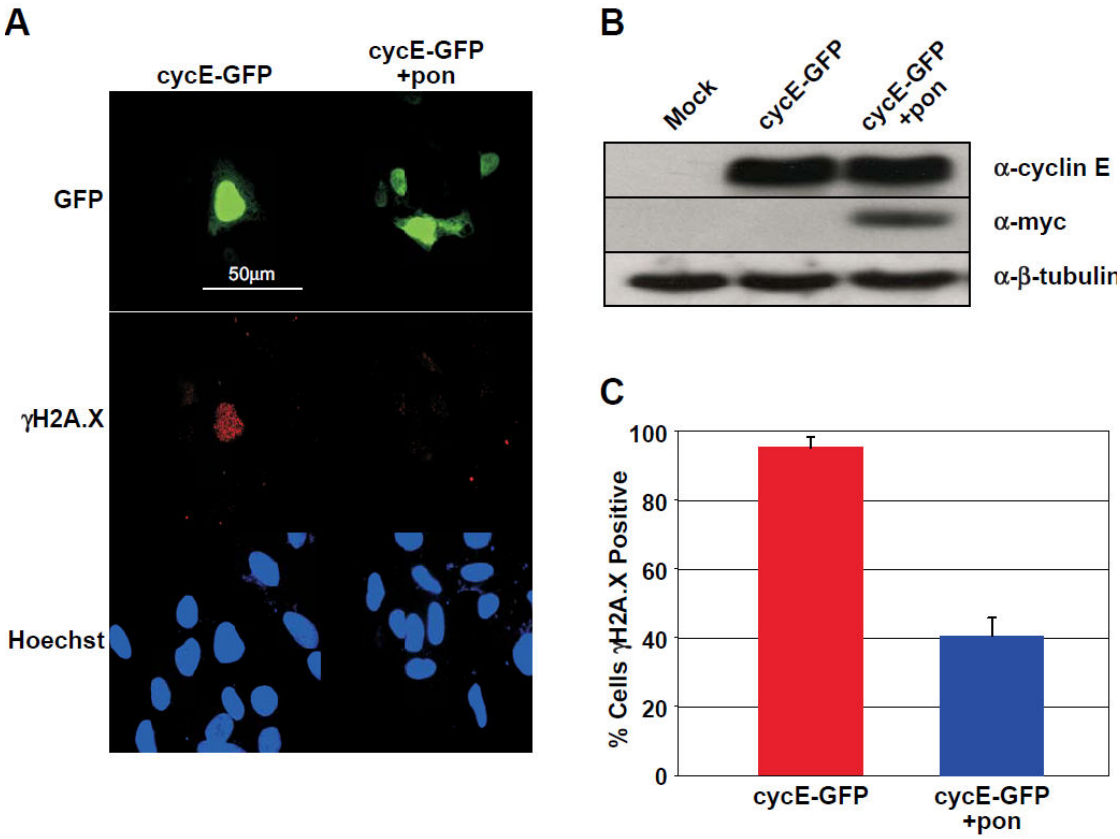

Figure 5-5. Spy1 expression partially prevents a cyclin E induced DNA damage response.

(A) Myc-Spy1:U2OS cells were seeded onto coverslips and induced with vehicle or Ponasterone A. Cyclin E-GFP was then transfected into the cells and grown for 72 h. Coverslips were stained for the formation of γH2A.X foci. Cells expressing cyclin E-GFP were visualized directly. (B) Equal amounts of lysates from one representative experiment from (A) were separated by SDS-PAGE, transferred to Immobilon-P, and probed with the indicated antibodies. (C) 50 cells expressing cyclin E-GFP from A were counted for each sample and the average number of cells with γH2A.X foci from three independent experiments is shown +/- std. dev.

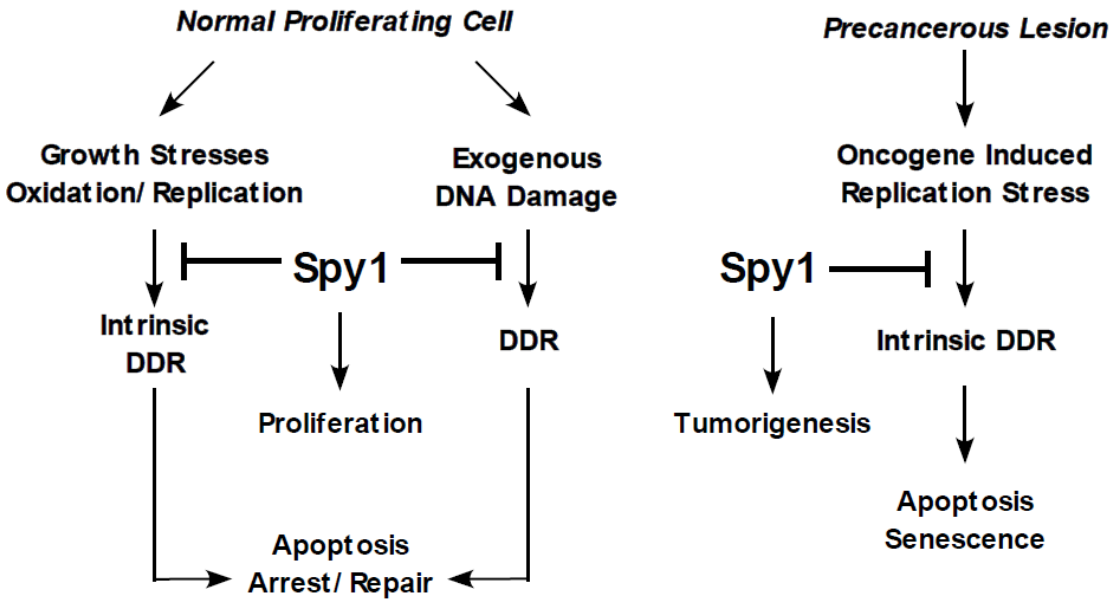

Figure 5-6. Model of Spy1 effects on the DNA damage response.
When a normal proliferating cell encounters DNA damage from intrinsic processes or exogenous sources, Spy1 expression bypasses checkpoint activation and leads to continued proliferation and mutagenesis. In precancerous lesions, misregulation of Spy1 may lead to tumorigenesis through bypass of apoptotic and senescence processes that cells use as a tumorigenic barrier.

Discussion

Using p53-null Saos2 cells and the isogenic HCT116 $p53^{+/+}$ and $p53^{-/-}$ cell lines, we demonstrate here that the ability of Spy1 to prevent checkpoint activation and apoptosis in response to UV damage is dependent on the presence of p53 (Fig. 5-1). The results presented here also suggest that endogenous Spy1 regulates the intrinsic DNA damage pathway by suppressing the checkpoint/apoptotic response to stresses and damage inherent to cell growth and proliferation. Using the previously characterized myc-Spy1:U2OS cell line [21], we demonstrate that Spy1 expression prevents the nucleotide excision repair of UV-induced CPDs, and increases the mutation frequency of UV damaged shuttle DNA (Fig. 5-2 and 5-3). Furthermore, for the first time, utilizing an inducible siSpy U2OS cell line, we also demonstrate that knockdown of Spy1 leads to activation of the DNA damage response as indicated by an increase in γH2A.X foci formation and Chk1 phosphorylation, and proliferation defects as monitored through cell growth assays (Fig. 5-4 and 5-5).

The p53 tumor suppressor pathway is impaired in many human cancers [33]. Our evidence suggests that overexpression of Spy1 in the large subset of cancers in which p53 is mutated may not promote their progression to tumorigenesis. Instead, Spy1 overexpression in the smaller subset of cancers which maintain intact, wild type p53 may lead to bypass of their apoptotic pathways, thus contributing to their survival and proliferative properties [23]. The results presented here, showing that Spy1-mediated abrogation of damage-induced Chk1 phosphorylation is dependent upon the presence of p53, indicates that Spy1 functions upstream of the key regulatory protein p53.

Although poorly understood, the intrinsic DNA damage pathway is of great biological importance. Over the last decade, increasing evidence points to this signaling pathway as having a pivotal role in tumorigenesis. Increased proliferation and replication induced by oncogene expression leads to intrinsic DNA damage signaling. Inactivation of the damage response by overexpression of proteins that oppose this response, or mutation of proteins that activate this response, including p53, c-myc, mos, cyclin E, CDC25A, and E2F1, are often selected for in cancer cells and appear to be a necessary step in oncogenic transformation [3-6].

Specialized activators of CDKs are required for many cellular processes to establish a balance between what is considered normal and deleterious (but necessary) to the cell. The results presented in this report indicate that the atypical CDK activator Spy1 regulates the intrinsic DNA damage pathway by controlling the balance between checkpoint activation, apoptosis, repair, and cell cycle progression. Spy1 overexpression may tip this balance toward continued cell proliferation, whether a cell experiences stresses from exogenous sources, intrinsic processes, or oncogenic stimulation (Figure 5-6). In support of this hypothesis, Spy1 expression suppresses the response to DNA damage by inhibiting both S-phase and G_2-phase checkpoints, allowing cells to continue to proliferate even when damage of mutational consequence is present [20, 21]. This may account for the reports of Spy1 overexpression in human invasive ductal carcinomas and the ability of Spy1 to cause mammary tumorigenesis in a mouse model [22, 23]. The selection for overexpression of Spy1 in cancer may reflect this ability to suppress the intrinsic damage response that occurs from oncogenic

stress. Conversely, Spy1 knockdown activates a DNA damage response, further demonstrating the novelty and relevance of Spy1 in regulating cell proliferation. Taken as a whole, the results presented here establish Spy1 as an important mediator of the DNA damage response, which is emerging as a crucial cellular mechanism for the regulation of cell growth and oncogenesis.

Acknowledgements

We thank Steve Dowdy for providing the cyclin E-GFP plasmid, Jeff Esko for use of the FACS equipment, Kristy Drafahl and April Meyer for help with the manuscript, Laura Castrejon for her editorial assistance, and Anne Stary and Alain Sarasin for providing the plasmids pR2 and p205-KMT11. This work was supported by an award from the Achievement Rewards for College Scientists (ARCS) Foundation to Chris McAndrew, and by a Ruth L. Kirschstein National Research Service Award (NIH/NCI T32 CA009523) to Randy Gastwirt. Chapter 5, in full, is material published in Cell Cycle, McAndrew, CW; Gastwirt, RF; and Donoghue, DJ (2008). The dissertation author was the primary investigator and a primary author of this paper.

References

1. Bartek J, Lukas J. DNA damage checkpoints: from initiation to recovery or adaptation. Curr Opin Cell Biol 2007; 19:238-45.

2. Attardi LD. The role of p53-mediated apoptosis as a crucial anti-tumor response to genomic instability: lessons from mouse models. Mutat Res 2005; 569:145-57.

3. Bartkova J, Horejsi Z, Koed K, Kramer A, Tort F, Zieger K, Guldberg P, Sehested M, Nesland JM, Lukas C, Orntoft T, Lukas J, Bartek J. DNA damage response as a candidate anti-cancer barrier in early human tumorigenesis. Nature 2005; 434:864-70.

4. Bartkova J, Rezaei N, Liontos M, Karakaidos P, Kletsas D, Issaeva N, Vassiliou LV, Kolettas E, Niforou K, Zoumpourlis VC, Takaoka M, Nakagawa H, Tort F, Fugger K, Johansson F, Sehested M, Andersen CL, Dyrskjot L, Orntoft T, Lukas J, Kittas C, Helleday T, Halazonetis TD, Bartek J, Gorgoulis VG. Oncogene-induced senescence is part of the tumorigenesis barrier imposed by DNA damage checkpoints. Nature 2006; 444:633-7.

5. Bartek J, Bartkova J, Lukas J. DNA damage signalling guards against activated oncogenes and tumour progression. Oncogene 2007; 26:7773-9.

6. Halazonetis TD, Gorgoulis VG, Bartek J. An oncogene-induced DNA damage model for cancer development. Science 2008; 319:1352-5.

7. Di Micco R, Fumagalli M, Cicalese A, Piccinin S, Gasparini P, Luise C, Schurra C, Garre M, Nuciforo PG, Bensimon A, Maestro R, Pelicci PG, d'Adda di Fagagna F. Oncogene-induced senescence is a DNA damage response triggered by DNA hyper-replication. Nature 2006; 444:638-42.

8. Courtois-Cox S, Jones SL, Cichowski K. Many roads lead to oncogene-induced senescence. Oncogene 2008.

9. Yaswen P, Campisi J. Oncogene-induced senescence pathways weave an intricate tapestry. Cell 2007; 128:233-4.

10. Santamaria D, Ortega S. Cyclins and CDKS in development and cancer: lessons from genetically modified mice. Front Biosci 2006; 11:1164-88.

11. Nebreda AR. CDK activation by non-cyclin proteins. Curr Opin Cell Biol 2006; 18:192-8.

12. Dinarina A, Perez LH, Davila A, Schwab M, Hunt T, Nebreda AR. Characterization of a new family of cyclin-dependent kinase activators. Biochem J 2004; 386:349-55.

13. Karaiskou A, Perez LH, Ferby I, Ozon R, Jessus C, Nebreda AR. Differential regulation of Cdc2 and Cdk2 by RINGO and cyclins. J Biol Chem 2001; 276:36028-34.

14. Cheng A, Xiong W, Ferrell JE, Jr., Solomon MJ. Identification and Comparative Analysis of Multiple Mammalian Speedy/Ringo Proteins. Cell Cycle 2005; 4:155-65.

15. Lenormand JL, Dellinger RW, Knudsen KE, Subramani S, Donoghue DJ. Speedy: a novel cell cycle regulator of the G2/M transition. Embo J 1999; 18:1869-77.

16. McAndrew CW, Gastwirt RF, Meyer AN, Porter LA, Donoghue DJ. Spy1 enhances phosphorylation and degradation of the cell cycle inhibitor p27. Cell Cycle 2007; 6:1937-45.

17. Porter LA, Kong-Beltran M, Donoghue DJ. Spy1 interacts with p27Kip1 to allow G1/S progression. Mol Biol Cell 2003; 14:3664-74.

18. Porter LA, Dellinger RW, Tynan JA, Barnes EA, Kong M, Lenormand JL, Donoghue DJ. Human Speedy: a novel cell cycle regulator that enhances proliferation through activation of Cdk2. J Cell Biol 2002; 157:357-66.

19. Gastwirt RF, McAndrew CW, Donoghue DJ. Speedy/RINGO regulation of CDKs in cell cycle, checkpoint activation and apoptosis. Cell Cycle 2007; 6:1188-93.

20. Barnes EA, Porter LA, Lenormand JL, Dellinger RW, Donoghue DJ. Human Spy1 promotes survival of mammalian cells following DNA damage. Cancer Res 2003; 63:3701-7.

21. Gastwirt RF, Slavin DA, McAndrew CW, Donoghue DJ. Spy1 expression prevents normal cellular responses to DNA damage: inhibition of apoptosis and checkpoint activation. J Biol Chem 2006; 281:35425-35.

22. Zucchi I, Mento E, Kuznetsov VA, Scotti M, Valsecchi V, Simionati B, Vicinanza E, Valle G, Pilotti S, Reinbold R, Vezzoni P, Albertini A, Dulbecco R. Gene expression profiles of epithelial cells microscopically isolated from a breast-invasive ductal carcinoma and a nodal metastasis. Proc Natl Acad Sci U S A 2004; 101:18147-52.

23. Golipour A, Myers D, Seagroves T, Murphy D, Evan GI, Donoghue DJ, Moorehead RA, Porter LA. The Spy1/RINGO family represents a novel mechanism regulating mammary growth and tumorigenesis. Cancer Res 2008; 68:In Press.

24. Livneh Z. Keeping mammalian mutation load in check: regulation of the activity of error-prone DNA polymerases by p53 and p21. Cell Cycle 2006; 5:1918-22.

25. Bunz F, Dutriaux A, Lengauer C, Waldman T, Zhou S, Brown JP, Sedivy JM, Kinzler KW, Vogelstein B. Requirement for p53 and p21 to sustain G2 arrest after DNA damage. Science 1998; 282:1497-501.

26. Brueckner F, Hennecke U, Carell T, Cramer P. CPD damage recognition by transcribing RNA polymerase II. Science 2007; 315:859-62.

27. Schwarz A, Stander S, Berneburg M, Bohm M, Kulms D, van Steeg H, Grosse-Heitmeyer K, Krutmann J, Schwarz T. Interleukin-12 suppresses ultraviolet radiation-induced apoptosis by inducing DNA repair. Nat Cell Biol 2002; 4:26-31.

28. de Laat WL, Jaspers NG, Hoeijmakers JH. Molecular mechanism of nucleotide excision repair. Genes Dev 1999; 13:768-85.

29. Wei Z, Lifen J, Jiliang H, Jianlin L, Baohong W, Hongping D. Detecting DNA repair capacity of peripheral lymphocytes from cancer patients with UVC challenge test and bleomycin challenge test. Mutagenesis 2005; 20:271-7.

30. Zheng W, He JL, Jin LF, Lou JL, Wang BH. Assessment of human DNA repair (NER) capacity with DNA repair rate (DRR) by comet assay. Biomed Environ Sci 2005; 18:117-23.

31. Stary A, Sarasin A. Simian virus 40 (SV40) large T antigen-dependent amplification of an Epstein-Barr virus-SV40 hybrid shuttle vector integrated into the human HeLa cell genome. J Gen Virol 1992; 73 (Pt 7):1679-85.

32. Wahl GM, Hughes SH, Capecchi MR. Immunological characterization of hypoxanthine-guanine phosphoribosyl transferase mutants of mouse L cells: evidence for mutations at different loci in the HGPRT gene. J Cell Physiol 1975; 85:307-20.

33. Vogelstein B, Lane D, Levine AJ. Surfing the p53 network. Nature 2000; 408:307-10.

Chapter 6:

Signaling from Fibroblast Growth Factor Receptors in Development and Disease

Abstract

FGFRs play an important role in cell growth, development, differentiation, and migration and are expressed in a multitude of tissues, indicating their importance in development. The large family of FGFs, as well as the various splice forms of the receptors, allows for specific activation of a variety of intracellular pathways depending on the type of receptor or ligand expressed. Misregulation of FGFR signaling, or overexpression of the receptors, can lead to uncontrolled downstream signaling associated with a range of developmental syndromes and diseases. Much is still unknown about the diverse nature of FGFR signaling, and expanding our understanding of this family of receptors will aid in the development of treatments for the many diseases and cancers linked to misregulation of FGFR signaling.

Introduction

Fibroblast growth factor receptors (FGFRs) constitute a family of four (FGFR1-4) (1-3) structurally related, cell surface receptor tyrosine kinases (RTKs), with 55-72% homology (4). FGFRs are involved in a variety of biological processes including cell growth, migration, differentiation, survival, and apoptosis and are essential for embryonic and neural development, skeletal and organ formation, and adult tissue homoeostasis (5, 6). Alternative splicing of *Fgfr* transcripts generates up to 15 isoforms, which transmit the signals of at least 22 fibroblast growth factors (FGF1-22) (7). Each receptor is comprised of an extracellular ligand binding domain consisting of three immunoglobulin (Ig)-like domains, an acidic box between IgI and IgII (4), a transmembrane domain, and a split intracellular tyrosine kinase domain composed of an ATP binding site and catalytic site. FGFR activation is achieved upon ligand binding (8, 9), resulting in receptor dimerization and transautophosphorylation of multiple conserved intracellular tyrosine residues (10), which stimulate the receptor's intrinsic kinase activity and recruit downstream adaptor and signaling proteins (11-13). Heparan sulfate proteoglycans (HSPGs) facilitate ligand binding and are obligate cofactors for FGFR activation by FGFs (14-17). The three main signaling pathways associated with FGFR activation include the Ras/MAPK, PI3-Kinase, and PLCg pathways. All but one of the mutations known for the *Fgfr* genes are gain-of-function mutations, and activation of these receptors is associated with many developmental and skeletal disorders (18, 19). Additionally, FGFR and FGF

overexpression has been observed in many tumor samples, and mutations are also likely to be involved in carcinogenesis.

FGFR Expression and Role during Development

During embryonic development, FGFR signaling is essential for organ growth and patterning of the embryo. All FGFRs are widely expressed in distinct spatial patterns during development and in adult tissues (20-24). FGFR1 expression is found mainly in the mesenchyme in the central nervous system and limbs, and targeted inactivation of *Fgfr1* in mice severely impairs growth and results in recessive embryonic lethality (25). During early neurogenesis, FGFR1 expression is upregulated in the ventricular zone of the neural tube and mesenchyme of developing limbs (26, 27), and at later stages is expressed in spinal cord motor neurons and maturing neurons in the brain (26, 28). Although required for correct axial organization and embryonic cell proliferation, FGFR1 is not directly required for mesoderm formation (25, 29). FGFR1 was also shown to play a role in neurulation, as chimeric mouse embryos, created by injection of FGFR1 deficient (R1-/-) embryonic stem (ES) cells into wild type blastocytes, showed limb bud and tail distortion, partial neural tube duplication, and spina bifida (30). FGFR2 is highly expressed in epithelial lineages during early gastrulation, and in both epithelial and mesenchymal cells during later development and organogenesis (26, 27). Like *Fgfr1*, targeted disruption of *Fgfr2* results in an embryonic lethal phenotype (31). Its expression is essential for limb outgrowth, mammalian lung branching morphogenesis (32), and keratinocyte differentiation (33). FGFR3 expression primarily occurs in the central nervous system and bone rudiments, specifically the developing brain, spinal cord, cochlea, and hypertrophic zone of the growth plate (32). Targeted disruption of *Fgfr3* in mice is not embryonic lethal, but

leads to severe skeletal and inner ear defects, and mouse models indicate FGFR3 negatively regulates bone growth and development (34, 35). FGFR3 also cooperates with FGFR4 to mediate liver functions and lung development. FGFR4 expression occurs in the definitive endoderm, somatic myotome, and the ventricular zone of developing dorsal root ganglia and spinal cord (36-38). Although, *Fgfr4* null mice appear normal, they exhibit elevated liver bile acids, enhanced cholesterol biosynthesis, and depleted gall bladders (39).

Signaling Pathways Mediated by FGFRs

Activation of FGFRs can result in a variety of outcomes by initiating various intracellular signaling pathways. In many cases, the pathways activated depend on the cell type or stage of differentiation, leading to specific activation of downstream targets (40). Specificity is also achieved through the binding of different FGFs of which many have unique and cell-specific roles. Splice variants of FGFRs also contribute to diverse cell signaling (40). Despite the varied outcomes of FGFR signaling, several key pathways are commonly activated in most cell types. FGFR activation results in tyrosine autophosphorylation, and these phosphorylated tyrosines serve as high-affinity binding sites for proteins containing Src-homology 2 (SH2) domains or phosphotyrosine binding (PTB) domains (41). These intracellular proteins then transduce the activation signal from the receptor through signaling cascades which eventually lead to changes in gene transcription and a biological response (42, 43).

The membrane-associated docking protein FGF receptor substrate 2 (FRS2) binds to the FGFR juxtamembrane domain (JM) through its PTB domain and is phosphorylated by the receptor (44). This leads to recruitment of a variety of adaptor proteins, including growth factor receptor bound protein 2 (Grb2), which then binds the guanine nucleotide exchange factor son of sevenless (Sos) (45). Recruitment of this complex to the plasma membrane activates the G-protein Ras, which stimulates the mitogen-activated protein kinase (MAPK) pathway (45). MAPK pathway activation results in a variety of outcomes depending on cell type or state, including DNA synthesis, proliferation, and/or differentiation. The adaptor molecule Shc is also phosphorylated by FGFR, leading to Grb2 recruitment and activation of the Ras/MAPK pathway (46).

FRS2 activation also signals through the PI3-Kinase pathway. The SH2 domain of Grb2 binds to a phosphorylated tyrosine residue on FRS2 while the C-terminal SH3 domain of Grb2 forms a complex with the proline-rich region of Grb2 associated binding protein 1 (Gab1) (47). Gab1 recruitment in close proximity to the receptor results in its tyrosine phosphorylation. Recruitment of PI3-Kinase and activation of AKT follows, leading to cell survival (48). FGFR binding and phosphorylation of FRS2 is essential for Gab1 recruitment and eventual activation of the PI3-Kinase cascade (47) indicating FGFR activation of FRS2 plays a prominent role in promoting cell survival. The N-terminal SH2 domain of SH2 tyrosine phosphatase 2 (Shp2) interacts with a phosphotyrosine on FRS2 and leads to phosphorylation of Shp2 itself. Phosphorylated Shp2 interacts with the Grb2/Sos

complex and forms a ternary complex with FRS2 (49). Shb also interacts with Shp2, and potentiates its FGF-mediated phosphorylation and FRS2 interaction. Interaction of phosphorylated Shp2 with FRS2 is essential for MAPK activation, indicating an important role for the adaptor Shb (50). FRS2 has also been shown to associate with Src, a non-receptor tyrosine kinase, which phosphorylates cortactin to affect cell migration (51, 52).

Autophosphorylation of Tyr766 in the carboxy-terminal tail of FGFR1 creates a specific binding site for the SH2 domain of PLCg (48). Activation of PLCg by tyrosine phosphorylation results in hydrolysis of phosphatidylinositol, generating diacylglycerol (DAG) and Ins(1,4,5)P3 (IP3) (53). Generation of these second messengers results in Ca^{+2} release and activation of PKC (53). Shb also interact with FGFR1 through Y766, although it does not seem to compete for binding with PLCg (50).

Other adaptor molecules link FGFR activation to various biological activities. Crk interacts with Tyr463 on FGFR1 and results in cellular proliferation in certain cell types (54, 55). The adaptor protein Nck also binds to phosphorylated FGFR, facilitating the interaction between Pak and Rac, and may link FGFR signaling to the actin cytoskeleton (56). Activated FGFR1, 3, and 4 also promote Stat1 and Stat3 activation (57) and FGFR3 can activate STAT5 through the adaptor protein SH2-B (58). Many of the interactions and signaling pathways activated by FGFRs described above are shown in Figure 6-1.

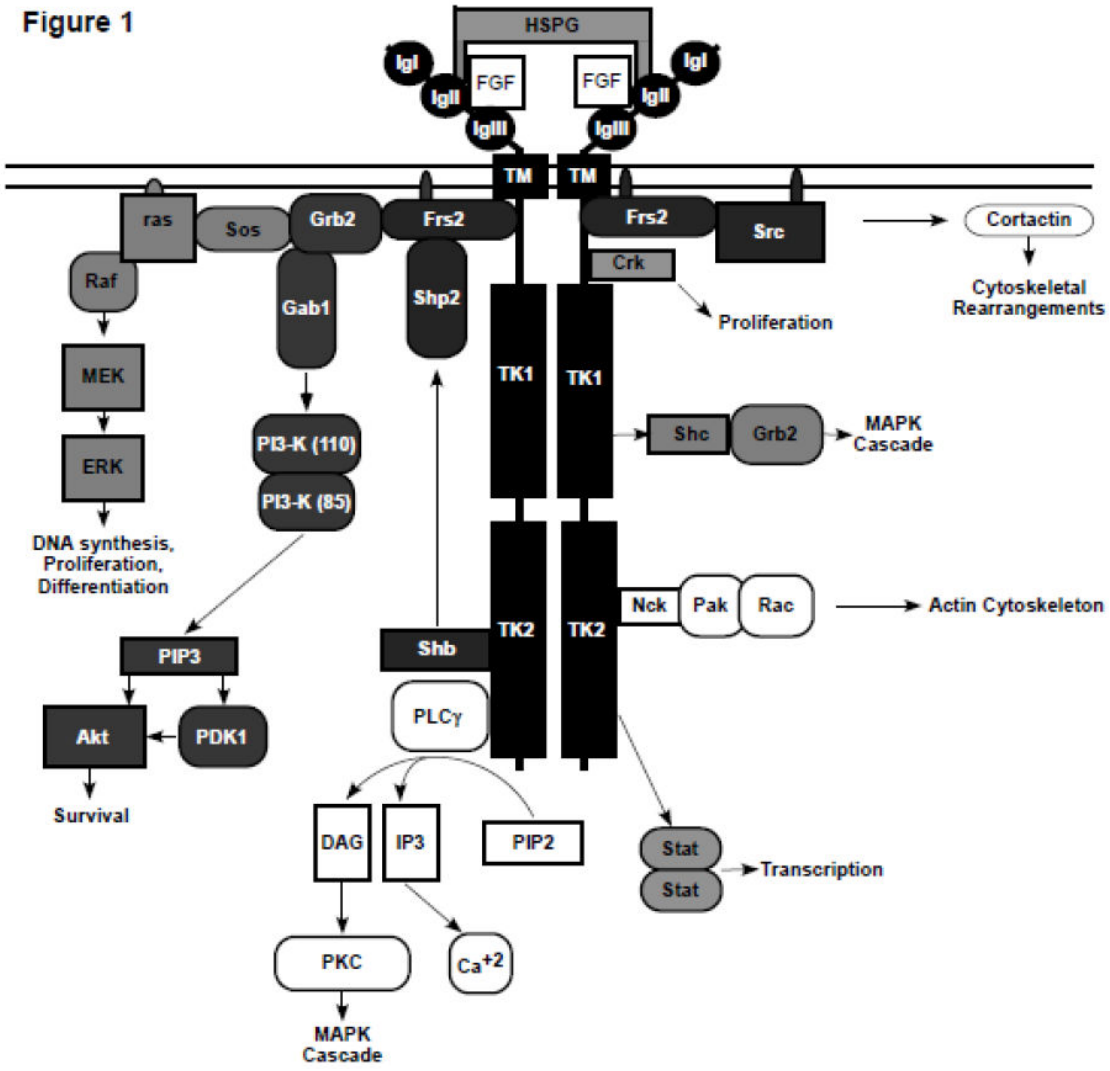

Figure 6-1. Signaling Pathways Activated by FGFRs.
FGFRs dimerize and ungergo autophosphorylation upon ligand stimulation, creating docking sites for various signaling molecules. Additional proteins are recruited to the membrane through modular domain interactions involving SH2, PTB, and other domains. Once at the membrane, these proteins activate multiple cellular signaling pathways, most notably the MAPK, PI3-K, and PLCγ pathways.

FGFRs and Developmental Disorders

Specific mutations in the *Fgfr1-3* genes lead to congenital bone diseases classified as chondrodysplasia and craniosynostosis syndromes, which cause dwarfism, deafness, and abnormalities of the skeleton, skin and eye (59, 60). Almost all of these are activating, gain-of-function mutations, and many occur in the IgII and IgIII domains, which mediate FGF binding (61, 62). Over sixty mutations have been found to be associated with craniosynostosis syndromes, with a majority in FGFR2, including Antley-Bixler-like syndrome (ABS), Apert syndrome (AS), Beare-Stevenson syndrome (BSS), Crouzon syndrome (CS), Jackson-Weiss syndrome (JWS), Muenke-like syndrome (MS), Saethre-Chotzen syndrome (SCS), as well as the FGFR1 associated craniofacial dysplasia with hypophosphatemia (CFDH) and Pfeiffer syndrome (PS) (59, 60, 63-68). All of these mutations are dominant, and craniofacial abnormalities varying in severity result from these syndromes. Missense mutations in FGFR3 result in skeletal dysplasia syndromes and short-limbed dwarfisms, including achondroplasia (ACH), Crouzon syndrome with acanthosis nigricans (CAN), hypochondroplasia (HCH), severe achondroplasia with developmental delay and acanthosis nigricans (SADDAN), and the platyspondylic lethal skeletal dysplasias (PLSDs), including thanatophoric dysplasia (TD) types I and II (69-83). Additionally, two syndromes caused by loss-of-function mutations in FGFRs have been described, including the FGFR1 associated type 2 Kallmann syndrome (KS) (60, 84, 85) and the FGFR3 associated camptodactyly, tall stature, and hearing loss (CATSHL) syndrome (86). To date, no mutations in FGFR4 are associated with any known

chondrodysplasia or craniosynostosis syndromes. A list of the mutations and syndromes associated with their respective FGFR can be seen in Figure 6-2.

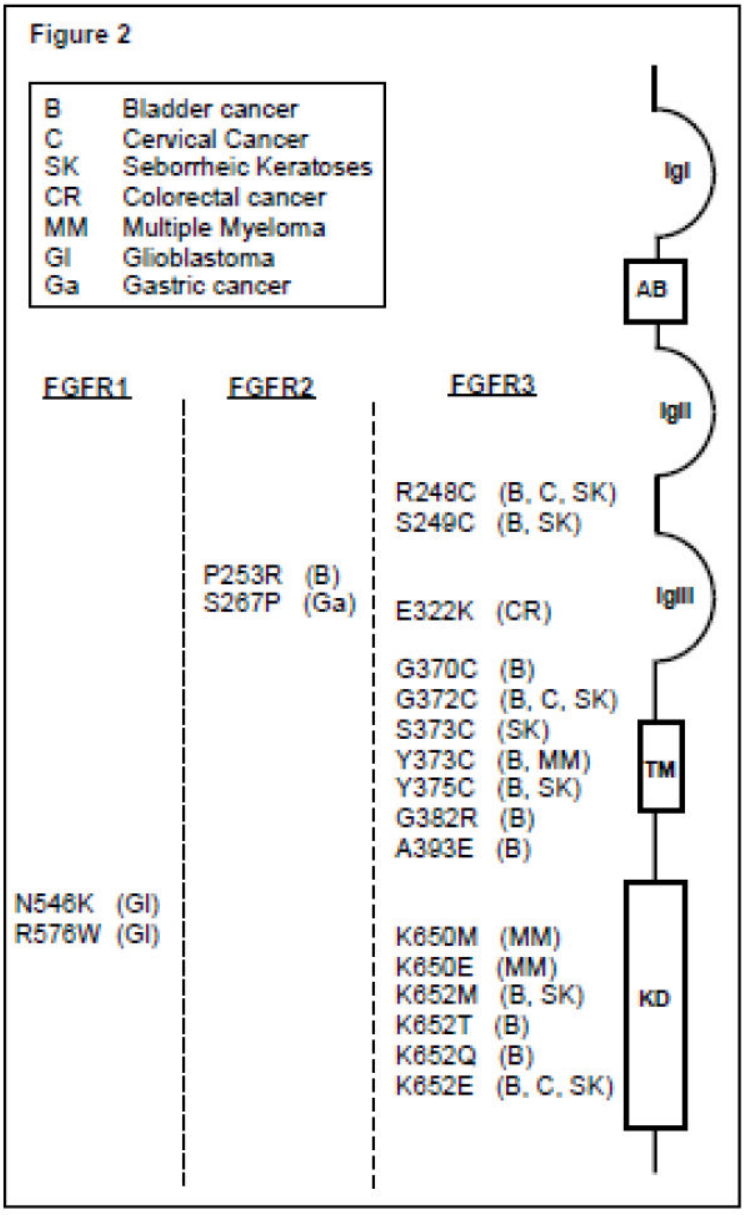

Figure 6-2. FGFR mutations associated with human cancer.
FGFR mutations associated with various human cancers are indicated. The abbreviations are as follows: bladder cancer (B) (135-138), cervical cancer (C) (125), seborrheic keratoses (SK) (139), colorectal cancer (CR) (140), multiple myeloma (MM) (123, 124, 141, 142), glioblastoma (Gl) (143), and gastric cancer (Ga) (140). The mutations are placed at their approximate location in the FGF receptor.

Role of FGFRs in Human Cancer

All four members of the FGFR family and many of their ligands have been implicated in human cancers as well. They play roles in cancer progression by inducing angiogenesis (87), changes in cell morphology, increased motility, and tumor cell proliferation (43). FGFRs are overexpressed or have altered activity in cancers of the colon (88), prostate (89, 90), breast (91), kidneys (92), ovaries (93, 94), central nervous system (95), gastrointestinal system (96), thyroid (97), pituitary (98, 99), brain (100, 101), liver (102, 103), pancreas (104), skin (105), and lung (106) as well as in leukemia (107), multiple myeloma, urological cancers (108), soft tissue sarcomas (109), head and neck squamous cell carcinoma (110), and lymphoma (111). Recent evidence indicates FGFRs may be used to target tumors for growth inhibition (87, 112, 113) and targeted inhibition of FGFRs may provide a therapeutic approach in the fight against cancer.

FGFR1 was recently found to be amplified in a small percentage of breast cancers and contributes to the survival of lobular breast carcinomas (114). In estrogen-receptor positive breast cancer cells, FGFR1 amplification is a prognostic of poor outcome (115). Recent research found that activation of FGFR1 plays a role in the initiation of angiogenesis in prostate cancer (116) and may be a new marker for prostate cancer progression, as it was shown to be upregulated in late stage prostate tumors (117). The role of FGFR1 is most widely described in chronic myeloproliferative disorders (CMPDs). One rare CMPD, known as 8p11 myeloproliferative syndrome (EMS) or stem cell leukemia lymphoma (SCLL), is

caused by an 8p11 translocation of *Fgfr1* (118). This leads to fusion of *Fgfr1* to other genes and constitutive activation of the receptor. The first fusion identified was to a zinc finger gene, *ZNF198*, and subsequently many *Fgfr1* rearrangements involved with a variety of partners have been demonstrated (119).

In two recent genome-wide association studies, FGFR2 was implicated with increased susceptibility to breast cancer (120, 121). It is believed that a splice variant of FGFR2 or possibly an unwarranted estrogen receptor binding site may be the cause for the associated risk of breast cancer (121). Also, certain types of gastric cancers overexpress FGFR2 and recent research has discovered that an inhibitor, AZD2171, exerts potent antitumor activity against gastric cancer xenografts overexpressing FGFR2 (122).

A frequent translocation observed in multiple myeloma, t(4;14)(p16.3;q32.3), involves the *Fgfr3* gene, and results in increased expression of FGFR3 alleles that contain activating mutations (123, 124), including Y373C and K650E, which cause the lethal skeletal syndromes TDI and TDII (72, 79). The splice variant FGFRIIIb is expressed in a wide range of bladder and cervical carcinoma cell lines (125), and these cancers exhibited expression of mutant alleles of FGFRIIIb, including R248C, S249C, G372C and K652E (125). These and other FGFR mutations are shown in Figure 6-2.

Although FGFR4 is not associated with any known syndromes, it is associated with the widest range of cancers. Of recent debate is the significance of the G388R polymorphism. This polymorphism exists in approximately half of the population and appears to have no affect on cancer susceptibility. However, evidence suggests that the

polymorphism leads to reduced disease-free survival in cancer patients and correlates with a poor prognosis compared to the Gly388 allele in head and neck squamous cell carcinoma (110, 126), breast cancer (127-129), melanoma (105), lung adenocarcinoma (106), prostate cancer (130) and high grade soft tissue sarcomas (109). Opposing evidence suggests there is no correlation between the G388R polymorphism and cancer prognosis (101, 131-134). Continued research into the significance of this polymorphism is needed to conclude if it is a valuable marker for cancer prognosis.

Acknowledgements

Chapter 6, in full, is a reprint of the material as it appears in the Handbook of Cell Signaling, second edition. Drafahl, KA; McAndrew, CW; and Donoghue, DJ (2007). The dissertation author was a primary author of this paper.

References

1. Dionne CA, Crumley G, Bellot F, et al. (1990) Cloning and expression of two distinct high-affinity receptors cross-reacting with acidic and basic fibroblast growth factors. *Embo J* 9: 2685-2692.

2. Partanen J, Makela TP, Alitalo R, Lehvaslaiho H, Alitalo K. (1990) Putative tyrosine kinases expressed in K-562 human leukemia cells. *Proc Natl Acad Sci U S A* 87: 8913-8917.

3. Keegan K, Johnson DE, Williams LT, Hayman MJ. (1991) Isolation of an additional member of the fibroblast growth factor receptor family, FGFR-3. *Proc Natl Acad Sci U S A* 88: 1095-1099.

4. Johnson DE, Williams LT. (1993) Structural and functional diversity in the FGF receptor multigene family. *Adv Cancer Res* 60: 1-41.

5. Szebenyi G, Fallon JF. (1999) Fibroblast growth factors as multifunctional signaling factors. *Int Rev Cytol* 185: 45-106.

6. Powers CJ, McLeskey SW, Wellstein A. (2000) Fibroblast growth factors, their receptors and signaling. *Endocr Relat Cancer* 7: 165-197.

7. Ornitz DM, Itoh N. (2001) Fibroblast growth factors. *Genome Biol* 2: REVIEWS3005.

8. Plotnikov AN, Schlessinger J, Hubbard SR, Mohammadi M. (1999) Structural basis for FGF receptor dimerization and activation. *Cell* 98: 641-650.

9. Xu J, Nakahara M, Crabb JW, et al. (1992) Expression and immunochemical analysis of rat and human fibroblast growth factor receptor (flg) isoforms. *J Biol Chem* 267: 17792-17803.

10. Bellot F, Crumley G, Kaplow JM, Schlessinger J, Jaye M, Dionne CA. (1991) Ligand-induced transphosphorylation between different FGF receptors. *Embo J* 10: 2849-2854.

11. Schlessinger J. (2000) Cell signaling by receptor tyrosine kinases. *Cell* 103: 211-225.

12. Hunter T. (2000) Signaling--2000 and beyond. *Cell* 100: 113-127.

13. McKeehan WL, Wang F, Kan M. (1998) The heparan sulfate-fibroblast growth factor family: diversity of structure and function. *Prog Nucleic Acid Res Mol Biol* 59: 135-176.

14. Harmer NJ. (2006) Insights into the role of heparan sulphate in fibroblast growth factor signalling. *Biochem Soc Trans* 34: 442-445.

15. Ibrahimi OA, Zhang F, Hrstka SC, Mohammadi M, Linhardt RJ. (2004) Kinetic model for FGF, FGFR, and proteoglycan signal transduction complex assembly. *Biochemistry* 43: 4724-4730.

16. Pantoliano MW, Horlick RA, Springer BA, et al. (1994) Multivalent ligand-receptor binding interactions in the fibroblast growth factor system produce a cooperative growth factor and heparin mechanism for receptor dimerization. *Biochemistry* 33: 10229-10248.

17. Yayon A, Klagsbrun M, Esko JD, Leder P, Ornitz DM. (1991) Cell surface, heparin-like molecules are required for binding of basic fibroblast growth factor to its high affinity receptor. *Cell* 64: 841-848.

18. Webster MK, Donoghue DJ. (1997) FGFR activation in skeletal disorders: too much of a good thing. *Trends Genet* 13: 178-182.

19. Wilkie AO. (1997) Craniosynostosis: genes and mechanisms. *Hum Mol Genet* 6: 1647-1656.

20. Hughes SE. (1997) Differential expression of the fibroblast growth factor receptor (FGFR) multigene family in normal human adult tissues. *J Histochem Cytochem* 45: 1005-1019.

21. Korhonen J, Partanen J, Eerola E, et al. (1991) Novel human FGF receptors with distinct expression patterns. *Ann N Y Acad Sci* 638: 403-405.

22. Partanen J, Makela TP, Eerola E, et al. (1991) FGFR-4, a novel acidic fibroblast growth factor receptor with a distinct expression pattern. *Embo J* 10: 1347-1354.

23. Katoh M, Hattori Y, Sasaki H, et al. (1992) K-sam gene encodes secreted as well as transmembrane receptor tyrosine kinase. *Proc Natl Acad Sci U S A* 89: 2960-2964.

24. Luqmani YA, Graham M, Coombes RC. (1992) Expression of basic fibroblast growth factor, FGFR1 and FGFR2 in normal and malignant human breast, and comparison with other normal tissues. *Br J Cancer* 66: 273-280.

25. Deng CX, Wynshaw-Boris A, Shen MM, Daugherty C, Ornitz DM, Leder P. (1994) Murine FGFR-1 is required for early postimplantation growth and axial organization. *Genes Dev* 8: 3045-3057.

26. Peters KG, Werner S, Chen G, Williams LT. (1992) Two FGF receptor genes are differentially expressed in epithelial and mesenchymal tissues during limb formation and organogenesis in the mouse. *Development* 114: 233-243.

27. Wilke TA, Gubbels S, Schwartz J, Richman JM. (1997) Expression of fibroblast growth factor receptors (FGFR1, FGFR2, FGFR3) in the developing head and face. *Dev Dyn* 210: 41-52.

28. Heuer JG, von Bartheld CS, Kinoshita Y, Evers PC, Bothwell M. (1990) Alternating phases of FGF receptor and NGF receptor expression in the developing chicken nervous system. *Neuron* 5: 283-296.

29. Yamaguchi TP, Harpal K, Henkemeyer M, Rossant J. (1994) fgfr-1 is required for embryonic growth and mesodermal patterning during mouse gastrulation. *Genes Dev* 8: 3032-3044.

30. Deng C, Bedford M, Li C, et al. (1997) Fibroblast growth factor receptor-1 (FGFR-1) is essential for normal neural tube and limb development. *Dev Biol* 185: 42-54.

31. Arman E, Haffner-Krausz R, Chen Y, Heath JK, Lonai P. (1998) Targeted disruption of fibroblast growth factor (FGF) receptor 2 suggests a role for FGF signaling in pregastrulation mammalian development. *Proc Natl Acad Sci U S A* 95: 5082-5087.

32. Arman E, Haffner-Krausz R, Gorivodsky M, Lonai P. (1999) Fgfr2 is required for limb outgrowth and lung-branching morphogenesis. *Proc Natl Acad Sci U S A* 96: 11895-11899.

33. Werner S, Weinberg W, Liao X, et al. (1993) Targeted expression of a dominant-negative FGF receptor mutant in the epidermis of transgenic mice reveals a role of FGF in keratinocyte organization and differentiation. *Embo J* 12: 2635-2643.

34. Colvin JS, Bohne BA, Harding GW, McEwen DG, Ornitz DM. (1996) Skeletal overgrowth and deafness in mice lacking fibroblast growth factor receptor 3. *Nat Genet* 12: 390-397.

35. Deng C, Wynshaw-Boris A, Zhou F, Kuo A, Leder P. (1996) Fibroblast growth factor receptor 3 is a negative regulator of bone growth. *Cell* 84: 911-921.

36. Marcelle C, Eichmann A, Halevy O, Breant C, Le Douarin NM. (1994) Distinct developmental expression of a new avian fibroblast growth factor receptor. *Development* 120: 683-694.

37. Ozawa K, Uruno T, Miyakawa K, Seo M, Imamura T. (1996) Expression of the fibroblast growth factor family and their receptor family genes during mouse brain development. *Brain Res Mol Brain Res* 41: 279-288.

38. Stark KL, McMahon JA, McMahon AP. (1991) FGFR-4, a new member of the fibroblast growth factor receptor family, expressed in the definitive endoderm and skeletal muscle lineages of the mouse. *Development* 113: 641-651.

39. Yu C, Wang F, Kan M, et al. (2000) Elevated cholesterol metabolism and bile acid synthesis in mice lacking membrane tyrosine kinase receptor FGFR4. *J Biol Chem* 275: 15482-15489.

40. Dailey L, Ambrosetti D, Mansukhani A, Basilico C. (2005) Mechanisms underlying differential responses to FGF signaling. *Cytokine Growth Factor Rev* 16: 233-247.

41. Lemmon MA, Schlessinger J. (1994) Regulation of signal transduction and signal diversity by receptor oligomerization. *Trends Biochem Sci* 19: 459-463.

42. Pawson T. (1995) Protein modules and signalling networks. *Nature* 373: 573-580.

43. Klint P, Claesson-Welsh L. (1999) Signal transduction by fibroblast growth factor receptors. *Front Biosci* 4: D165-177.

44. Xu H, Lee KW, Goldfarb M. (1998) Novel recognition motif on fibroblast growth factor receptor mediates direct association and activation of SNT adapter proteins. *J Biol Chem* 273: 17987-17990.

45. Ong SH, Guy GR, Hadari YR, et al. (2000) FRS2 proteins recruit intracellular signaling pathways by binding to diverse targets on fibroblast growth factor and nerve growth factor receptors. *Mol Cell Biol* 20: 979-989.

46. Browaeys-Poly E, Cailliau K, Vilain JP. (2001) Transduction cascades initiated by fibroblast growth factor 1 on Xenopus oocytes expressing MDA-MB-231 mRNAs. Role of Grb2, phosphatidylinositol 3-kinase, Src tyrosine kinase, and phospholipase Cgamma. *Cell Signal* 13: 363-368.

47. Hadari YR, Gotoh N, Kouhara H, Lax I, Schlessinger J. (2001) Critical role for the docking-protein FRS2 alpha in FGF receptor-mediated signal transduction pathways. *Proc Natl Acad Sci U S A* 98: 8578-8583.

48. Eswarakumar VP, Lax I, Schlessinger J. (2005) Cellular signaling by fibroblast growth factor receptors. *Cytokine Growth Factor Rev* 16: 139-149.

49. Hadari YR, Kouhara H, Lax I, Schlessinger J. (1998) Binding of Shp2 tyrosine phosphatase to FRS2 is essential for fibroblast growth factor-induced PC12 cell differentiation. *Mol Cell Biol* 18: 3966-3973.

50. Cross MJ, Lu L, Magnusson P, et al. (2002) The Shb adaptor protein binds to tyrosine 766 in the FGFR-1 and regulates the Ras/MEK/MAPK pathway via FRS2 phosphorylation in endothelial cells. *Mol Biol Cell* 13: 2881-2893.

51. Sandilands E, Akbarzadeh S, Vecchione A, McEwan DG, Frame MC, Heath JK. (2007) Src kinase modulates the activation, transport and signalling dynamics of fibroblast growth factor receptors. *EMBO Rep*.

52. LaVallee TM, Prudovsky IA, McMahon GA, Hu X, Maciag T. (1998) Activation of the MAP kinase pathway by FGF-1 correlates with cell proliferation induction while activation of the Src pathway correlates with migration. *J Cell Biol* 141: 1647-1658.

53. Carpenter G, Ji Q. (1999) Phospholipase C-gamma as a signal-transducing element. *Exp Cell Res* 253: 15-24.

54. Larsson H, Klint P, Landgren E, Claesson-Welsh L. (1999) Fibroblast growth factor receptor-1-mediated endothelial cell proliferation is dependent on the Src homology (SH) 2/SH3 domain-containing adaptor protein Crk. *J Biol Chem* 274: 25726-25734.

55. Reuss B, von Bohlen und Halbach O. (2003) Fibroblast growth factors and their receptors in the central nervous system. *Cell Tissue Res* 313: 139-157.

56. Li W, Fan J, Woodley DT. (2001) Nck/Dock: an adapter between cell surface receptors and the actin cytoskeleton. *Oncogene* 20: 6403-6417.

57. Hart KC, Robertson SC, Kanemitsu MY, Meyer AN, Tynan JA, Donoghue DJ. (2000) Transformation and Stat activation by derivatives of FGFR1, FGFR3, and FGFR4. *Oncogene* 19: 3309-3320.

58. Kong M, Wang CS, Donoghue DJ. (2002) Interaction of fibroblast growth factor receptor 3 and the adapter protein SH2-B. A role in STAT5 activation. *J Biol Chem* 277: 15962-15970.

59. McIntosh I, Bellus GA, Jab EW. (2000) The pleiotropic effects of fibroblast growth factor receptors in mammalian development. *Cell Struct Funct* 25: 85-96.

60. Passos-Bueno MR, Wilcox WR, Jabs EW, Sertie AL, Alonso LG, Kitoh H. (1999) Clinical spectrum of fibroblast growth factor receptor mutations. *Hum Mutat* 14: 115-125.

61. Plotnikov AN, Hubbard SR, Schlessinger J, Mohammadi M. (2000) Crystal structures of two FGF-FGFR complexes reveal the determinants of ligand-receptor specificity. *Cell* 101: 413-424.

62. Schlessinger J, Plotnikov AN, Ibrahimi OA, et al. (2000) Crystal structure of a ternary FGF-FGFR-heparin complex reveals a dual role for heparin in FGFR binding and dimerization. *Mol Cell* 6: 743-750.

63. Hehr U, Muenke M. (1999) Craniosynostosis syndromes: from genes to premature fusion of skull bones. *Mol Genet Metab* 68: 139-151.

64. Katzen JT, McCarthy JG. (2000) Syndromes involving craniosynostosis and midface hypoplasia. *Otolaryngol Clin North Am* 33: 1257-1284, vi.

65. Park WJ, Meyers GA, Li X, et al. (1995) Novel FGFR2 mutations in Crouzon and Jackson-Weiss syndromes show allelic heterogeneity and phenotypic variability. *Hum Mol Genet* 4: 1229-1233.

66. Freitas EC, Nascimento SR, de Mello MP, Gil-da-Silva-Lopes VL. (2006) Q289P mutation in FGFR2 gene causes Saethre-Chotzen syndrome: some considerations about familial heterogeneity. *Cleft Palate Craniofac J* 43: 142-147.

67. Lajeunie E, Heuertz S, El Ghouzzi V, et al. (2006) Mutation screening in patients with syndromic craniosynostoses indicates that a limited number of recurrent FGFR2 mutations accounts for severe forms of Pfeiffer syndrome. *Eur J Hum Genet* 14: 289-298.

68. Wilkie AO, Bochukova EG, Hansen RM, et al. (2007) Clinical dividends from the molecular genetic diagnosis of craniosynostosis. *Am J Med Genet A* 143: 1941-1949.

69. Oberklaid F, Danks DM, Jensen F, Stace L, Rosshandler S. (1979) Achondroplasia and hypochondroplasia. Comments on frequency, mutation rate, and radiological features in skull and spine. *J Med Genet* 16: 140-146.

70. Rousseau F, Bonaventure J, Legeai-Mallet L, et al. (1994) Mutations in the gene encoding fibroblast growth factor receptor-3 in achondroplasia. *Nature* 371: 252-254.

71. Shiang R, Thompson LM, Zhu YZ, et al. (1994) Mutations in the transmembrane domain of FGFR3 cause the most common genetic form of dwarfism, achondroplasia. *Cell* 78: 335-342.

72. Tavormina PL, Shiang R, Thompson LM, et al. (1995) Thanatophoric dysplasia (types I and II) caused by distinct mutations in fibroblast growth factor receptor 3. *Nat Genet* 9: 321-328.

73. Tavormina PL, Bellus GA, Webster MK, et al. (1999) A novel skeletal dysplasia with developmental delay and acanthosis nigricans is caused by a Lys650Met mutation in the fibroblast growth factor receptor 3 gene. *Am J Hum Genet* 64: 722-731.

74. Brodie SG, Kitoh H, Lachman RS, Nolasco LM, Mekikian PB, Wilcox WR. (1999) Platyspondylic lethal skeletal dysplasia, San Diego type, is caused by FGFR3 mutations. *Am J Med Genet* 84: 476-480.

75. Orioli IM, Castilla EE, Barbosa-Neto JG. (1986) The birth prevalence rates for the skeletal dysplasias. *J Med Genet* 23: 328-332.

76. Rousseau F, Bonaventure J, Le Merrer M, Maroteaux P, Munnich A. (1996) [Mutations of FGFR3 gene cause 3 types of nanisms with variably severity: achondroplasia, thanatophoric nanism and hypochondroplasia]. *Ann Endocrinol (Paris)* 57: 153.

77. Rousseau F, Bonaventure J, Le Merrer M, Munnich A. (1996) [Association of achondroplasia to a mutation in the transmembrane domain of fibroblastic growth factor receptor 3 (FGFR3)]. *Ann Endocrinol (Paris)* 57: 151-152.

78. Rousseau F, Bonaventure J, Legeai-Mallet L, et al. (1996) Clinical and genetic heterogeneity of hypochondroplasia. *J Med Genet* 33: 749-752.

79. Rousseau F, el Ghouzzi V, Delezoide AL, et al. (1996) Missense FGFR3 mutations create cysteine residues in thanatophoric dwarfism type I (TD1). *Hum Mol Genet* 5: 509-512.

80. Rousseau F, Bonaventure J, Legeai-Mallet L, et al. (1996) Mutations of the fibroblast growth factor receptor-3 gene in achondroplasia. *Horm Res* 45: 108-110.

81. Rousseau F, Saugier P, Le Merrer M, et al. (1995) Stop codon FGFR3 mutations in thanatophoric dwarfism type 1. *Nat Genet* 10: 11-12.

82. L'Hote CG, Knowles MA. (2005) Cell responses to FGFR3 signalling: growth, differentiation and apoptosis. *Exp Cell Res* 304: 417-431.

83. Cohen MM, Jr. (2006) The new bone biology: pathologic, molecular, and clinical correlates. *Am J Med Genet A* 140: 2646-2706.

84. Dode C, Levilliers J, Dupont JM, et al. (2003) Loss-of-function mutations in FGFR1 cause autosomal dominant Kallmann syndrome. *Nat Genet*.

85. Cadman SM, Kim SH, Hu Y, Gonzalez-Martinez D, Bouloux PM. (2007) Molecular pathogenesis of Kallmann's syndrome. *Horm Res* 67: 231-242.

86. Toydemir RM, Brassington AE, Bayrak-Toydemir P, et al. (2006) A novel mutation in FGFR3 causes camptodactyly, tall stature, and hearing loss (CATSHL) syndrome. *Am J Hum Genet* 79: 935-941.

87. Rusnati M, Presta M. (2007) Fibroblast growth factors/fibroblast growth factor receptors as targets for the development of anti-angiogenesis strategies. *Curr Pharm Des* 13: 2025-2044.

88. Tassi E, Wellstein A. (2006) The angiogenic switch molecule, secreted FGF-binding protein, an indicator of early stages of pancreatic and colorectal adenocarcinoma. *Semin Oncol* 33: S50-56.

89. Giri D, Ropiquet F, Ittmann M. (1999) Alterations in expression of basic fibroblast growth factor (FGF) 2 and its receptor FGFR-1 in human prostate cancer. *Clin Cancer Res* 5: 1063-1071.

90. Kwabi-Addo B, Ozen M, Ittmann M. (2004) The role of fibroblast growth factors and their receptors in prostate cancer. *Endocr Relat Cancer* 11: 709-724.

91. Penault-Llorca F, Bertucci F, Adelaide J, et al. (1995) Expression of FGF and FGF receptor genes in human breast cancer. *Int J Cancer* 61: 170-176.

92. Zhong H, Deng F, Kong X. (1996) [Expression of basic fibroblast growth factor and its receptor in renal cell carcinoma]. *Zhonghua Wai Ke Za Zhi* 34: 651-654.

93. Jaakkola S, Salmikangas P, Nylund S, et al. (1993) Amplification of fgfr4 gene in human breast and gynecological cancers. *Int J Cancer* 54: 378-382.

94. Valve E, Martikainen P, Seppanen J, et al. (2000) Expression of fibroblast growth factor (FGF)-8 isoforms and FGF receptors in human ovarian tumors. *Int J Cancer* 88: 718-725.

95. Chandler LA, Sosnowski BA, Greenlees L, Aukerman SL, Baird A, Pierce GF. (1999) Prevalent expression of fibroblast growth factor (FGF) receptors and FGF2 in human tumor cell lines. *Int J Cancer* 81: 451-458.

96. Takaishi S, Sawada M, Morita Y, Seno H, Fukuzawa H, Chiba T. (2000) Identification of a novel alternative splicing of human FGF receptor 4: soluble-form splice variant expressed in human gastrointestinal epithelial cells. *Biochem Biophys Res Commun* 267: 658-662.

97. St Bernard R, Zheng L, Liu W, Winer D, Asa SL, Ezzat S. (2005) Fibroblast growth factor receptors as molecular targets in thyroid carcinoma. *Endocrinology* 146: 1145-1153.

98. Abbass SA, Asa SL, Ezzat S. (1997) Altered expression of fibroblast growth factor receptors in human pituitary adenomas. *J Clin Endocrinol Metab* 82: 1160-1166.

99. Ezzat S, Zheng L, Zhu XF, Wu GE, Asa SL. (2002) Targeted expression of a human pituitary tumor-derived isoform of FGF receptor-4 recapitulates pituitary tumorigenesis. *J Clin Invest* 109: 69-78.

100. Yamada SM, Yamada S, Hayashi Y, Takahashi H, Teramoto A, Matsumoto K. (2002) Fibroblast growth factor receptor (FGFR) 4 correlated with the malignancy of human astrocytomas. *Neurol Res* 24: 244-248.

101. Mawrin C, Kirches E, Diete S, et al. (2006) Analysis of a single nucleotide polymorphism in codon 388 of the FGFR4 gene in malignant gliomas. *Cancer Lett* 239: 239-245.

102. Tsou AP, Wu KM, Tsen TY, et al. (1998) Parallel hybridization analysis of multiple protein kinase genes: identification of gene expression patterns characteristic of human hepatocellular carcinoma. *Genomics* 50: 331-340.

103. Qiu WH, Zhou BS, Chu PG, et al. (2005) Over-expression of fibroblast growth factor receptor 3 in human hepatocellular carcinoma. *World J Gastroenterol* 11: 5266-5272.

104. Kornmann M, Beger HG, Korc M. (1998) Role of fibroblast growth factors and their receptors in pancreatic cancer and chronic pancreatitis. *Pancreas* 17: 169-175.

105. Streit S, Mestel DS, Schmidt M, Ullrich A, Berking C. (2006) FGFR4 Arg388 allele correlates with tumour thickness and FGFR4 protein expression with survival of melanoma patients. *Br J Cancer* 94: 1879-1886.

106. Spinola M, Leoni V, Pignatiello C, et al. (2005) Functional FGFR4 Gly388Arg polymorphism predicts prognosis in lung adenocarcinoma patients. *J Clin Oncol* 23: 7307-7311.

107. Armstrong E, Vainikka S, Partanen J, Korhonen J, Alitalo R. (1992) Expression of fibroblast growth factor receptors in human leukemia cells. *Cancer Res* 52: 2004-2007.

108. Cronauer MV, Schulz WA, Seifert HH, Ackermann R, Burchardt M. (2003) Fibroblast growth factors and their receptors in urological cancers: basic research and clinical implications. *Eur Urol* 43: 309-319.

109. Morimoto Y, Ozaki T, Ouchida M, et al. (2003) Single nucleotide polymorphism in fibroblast growth factor receptor 4 at codon 388 is associated with prognosis in high-grade soft tissue sarcoma. *Cancer* 98: 2245-2250.

110. Streit S, Bange J, Fichtner A, Ihrler S, Issing W, Ullrich A. (2004) Involvement of the FGFR4 Arg388 allele in head and neck squamous cell carcinoma. *Int J Cancer* 111: 213-217.

111. Khnykin D, Troen G, Berner JM, Delabie J. (2006) The expression of fibroblast growth factors and their receptors in Hodgkin's lymphoma. *J Pathol* 208: 431-438.

112. Lappi DA. (1995) Tumor targeting through fibroblast growth factor receptors. *Semin Cancer Biol* 6: 279-288.

113. Wang F, McKeehan K, Yu C, McKeehan WL. (2002) Fibroblast growth factor receptor 1 phosphotyrosine 766: molecular target for prevention of progression of prostate tumors to malignancy. *Cancer Res* 62: 1898-1903.

114. Reis-Filho JS, Simpson PT, Turner NC, et al. (2006) FGFR1 emerges as a potential therapeutic target for lobular breast carcinomas. *Clin Cancer Res* 12: 6652-6662.

115. Elbauomy Elsheikh S, Green AR, Lambros MB, et al. (2007) FGFR1 amplification in breast carcinomas: a chromogenic in situ hybridisation analysis. *Breast Cancer Res* 9: R23.

116. Winter SF, Acevedo VD, Gangula RD, Freeman KW, Spencer DM, Greenberg NM. (2007) Conditional activation of FGFR1 in the prostate epithelium induces angiogenesis with concomitant differential regulation of Ang-1 and Ang-2. *Oncogene* 26: 4897-4907.

117. Devilard E, Bladou F, Ramuz O, et al. (2006) FGFR1 and WT1 are markers of human prostate cancer progression. *BMC Cancer* 6: 272.

118. Macdonald D, Cross NC. (2007) Chronic myeloproliferative disorders: the role of tyrosine kinases in pathogenesis, diagnosis and therapy. *Pathobiology* 74: 81-88.

119. Delhommeau F, Pisani DF, James C, Casadevall N, Constantinescu S, Vainchenker W. (2006) Oncogenic mechanisms in myeloproliferative disorders. *Cell Mol Life Sci* 63: 2939-2953.

120. Hunter DJ, Kraft P, Jacobs KB, et al. (2007) A genome-wide association study identifies alleles in FGFR2 associated with risk of sporadic postmenopausal breast cancer. *Nat Genet* 39: 870-874.

121. Easton DF, Pooley KA, Dunning AM, et al. (2007) Genome-wide association study identifies novel breast cancer susceptibility loci. *Nature* 447: 1087-1093.

122. Takeda M, Arao T, Yokote H, et al. (2007) AZD2171 shows potent antitumor activity against gastric cancer over-expressing fibroblast growth factor receptor 2/keratinocyte growth factor receptor. *Clin Cancer Res* 13: 3051-3057.

123. Chesi M, Nardini E, Brents LA, et al. (1997) Frequent translocation t(4;14)(p16.3;q32.3) in multiple myeloma is associated with increased expression and activating mutations of fibroblast growth factor receptor 3. *Nat Genet* 16: 260-264.

124. Richelda R, Ronchetti D, Baldini L, et al. (1997) A novel chromosomal translocation t(4; 14)(p16.3; q32) in multiple myeloma involves the fibroblast growth-factor receptor 3 gene. *Blood* 90: 4062-4070.

125. Cappellen D, De Oliveira C, Ricol D, et al. (1999) Frequent activating mutations of FGFR3 in human bladder and cervix carcinomas. *Nat Genet* 23: 18-20.

126. da Costa Andrade VC, Parise O, Jr., Hors CP, de Melo Martins PC, Silva AP, Garicochea B. (2007) The fibroblast growth factor receptor 4 (FGFR4) Arg388 allele correlates with survival in head and neck squamous cell carcinoma. *Exp Mol Pathol* 82: 53-57.

127. Bange J, Prechtl D, Cheburkin Y, et al. (2002) Cancer progression and tumor cell motility are associated with the FGFR4 Arg(388) allele. *Cancer Res* 62: 840-847.

128. Stadler CR, Knyazev P, Bange J, Ullrich A. (2006) FGFR4 GLY388 isotype suppresses motility of MDA-MB-231 breast cancer cells by EDG-2 gene repression. *Cell Signal* 18: 783-794.

129. Thussbas C, Nahrig J, Streit S, et al. (2006) FGFR4 Arg388 allele is associated with resistance to adjuvant therapy in primary breast cancer. *J Clin Oncol* 24: 3747-3755.

130. Wang J, Stockton DW, Ittmann M. (2004) The fibroblast growth factor receptor-4 Arg388 allele is associated with prostate cancer initiation and progression. *Clin Cancer Res* 10: 6169-6178.

131. Matakidou A, El Galta R, Rudd MF, et al. (2007) Further observations on the relationship between the FGFR4 Gly388Arg polymorphism and lung cancer prognosis. *Br J Cancer* 96: 1904-1907.

132. Mawrin C, Schneider T, Firsching R, et al. (2005) Assessment of tumor cell invasion factors in gliomatosis cerebri. *J Neurooncol* 73: 109-115.

133. Spinola M, Leoni VP, Tanuma J, et al. (2005) FGFR4 Gly388Arg polymorphism and prognosis of breast and colorectal cancer. *Oncol Rep* 14: 415-419.

134. Jezequel P, Campion L, Joalland MP, et al. (2004) G388R mutation of the FGFR4 gene is not relevant to breast cancer prognosis. *Br J Cancer* 90: 189-193.

135. Van Rhijn BW, Van Tilborg AA, Lurkin I, et al. (2002) Novel fibroblast growth factor receptor 3 (FGFR3) mutations in bladder cancer previously identified in non-lethal skeletal disorders. *Eur J Hum Genet* 10: 819-824.

136. Billerey C, Chopin D, Aubriot-Lorton MH, et al. (2001) Frequent FGFR3 mutations in papillary non-invasive bladder (pTa) tumors. *Am J Pathol* 158: 1955-1959.

137. Andreou A, Lamy A, Layet V, et al. (2006) Early-onset low-grade papillary carcinoma of the bladder associated with Apert syndrome and a germline FGFR2 mutation (Pro253Arg). *Am J Med Genet A* 140: 2245-2247.

138. Tomlinson DC, Baldo O, Harnden P, Knowles MA. (2007) FGFR3 protein expression and its relationship to mutation status and prognostic variables in bladder cancer. *J Pathol* 213: 91-98.

139. Hafner C, Hartmann A, van Oers JM, et al. (2007) FGFR3 mutations in seborrheic keratoses are already present in flat lesions and associated with age and localization. *Mod Pathol* 20: 895-903.

140. Jang JH, Shin KH, Park JG. (2001) Mutations in fibroblast growth factor receptor 2 and fibroblast growth factor receptor 3 genes associated with human gastric and colorectal cancers. *Cancer Res* 61: 3541-3543.

141. Chesi M, Nardini E, Lim RS, Smith KD, Kuehl WM, Bergsagel PL. (1998) The t(4;14) translocation in myeloma dysregulates both FGFR3 and a novel gene, MMSET, resulting in IgH/MMSET hybrid transcripts. *Blood* 92: 3025-3034.

142. Fracchiolla NS, Luminari S, Baldini L, Lombardi L, Maiolo AT, Neri A. (1998) FGFR3 gene mutations associated with human skeletal disorders occur rarely in multiple myeloma. *Blood* 92: 2987-2989.

143. Rand V, Huang J, Stockwell T, et al. (2005) Sequence survey of receptor tyrosine kinases reveals mutations in glioblastomas. *Proc Natl Acad Sci U S A* 102: 14344-14349.

Chapter 7:

The Novel Interaction of FGFR4 and IKKβ Negatively Regulates NFκB Activity

Abstract

NFκB signaling is of paramount importance in the regulation of apoptosis, proliferation, and inflammatory responses in many human cancers. However, the relationship between growth factor signaling pathways and NFκB activation is poorly understood. Here, we demonstrate a novel direct interaction between the growth factor receptor FGFR4 and IKKβ, an essential component in the NFκB pathway. This novel interaction was identified utilizing a yeast two-hybrid screen and confirmed by coimmunoprecipitation and immunoblot analysis. Following TNFα stimulation, FGFR4 activation results in significant inhibition of NFκB signaling, as measured by decreased nuclear NFκB localization; reduced NFκB transcriptional activation, as shown by electophoretic mobility shift assays (EMSA); and inhibition of IKKβ kinase activity towards the substrate GST-IκBα. FGF19 stimulation of endogenous FGFR4 in TNFα-treated DU145 prostate cancer cells also leads to a decrease in IKKβ activity and concomitant reduction in NFκB nuclear localization. Additionally, we show that the FGFR4 E681K mutation leads to a decreased ability of FGFR4 to inhibit IKK activity or NFκB nuclear localization in A549 lung adenocarcinoma cells. These results identify a novel link between FGFR4 signaling and the NFκB pathway, providing a unique model of NFκB regulation and implicating FGFR4 as a potential tumor suppressor in some cancers.

Introduction

NFκB is a transcription factor of pivotal importance as a regulator of genes that control cell differentiation, survival, and inflammatory responses in mammalian cells. Thus, NFκB has been the subject of intense research to identify clinically useful inhibitors, and to understand the intersection of NFκB signaling with signaling pathways that are important in cancer cell biology. Upon activation with TNFα, IKKβ phosphorylates IκB, the inhibitor of NFκB, which targets it for proteasomal degradation. Subsequently, NFκB is released from sequestration in the cytoplasm, permitting translocation of NFκB dimers into the nucleus where they activate the transcription of target genes (Dutta *et al.*, 2006; Hacker and Karin, 2006; Karin, 2006; Karin, 2008; Sarkar and Li, 2008; Schmid and Birbach, 2008).

Members of the FGFR family of receptor tyrosine kinases have been strongly implicated in a variety of human cancers, particularly FGFR4, with regards to prostate cancer (Gowardhan *et al.*, 2005; Sahadevan *et al.*, 2007; Wang *et al.*, 2008). Signaling by FGF2 has been shown to be important for inhibition of apoptosis through PI3K/AKT and IKKβ (Huang *et al.*, 2006; Vandermoere *et al.*, 2005), and FGF signaling has also been shown to decrease TNFα-induced apoptosis through activation of the p44/42 MAPK pathway (Gardner and Johnson, 1996). Regulatory interactions between FGFR4 and NFκB signaling pathways have not previously been reported, although both pathways represent major axes of cell signaling. Discovering a two-hybrid interaction between the receptor tyrosine kinase FGFR4 and IKKβ, an important regulatory protein in the NFκB signaling pathway, and confirming this interaction in mammalian cells, we therefore sought to understand the relevance of regulation of NFκB signaling by FGFR4.

Materials and Methods

Cell culture

HeLa, HEK293 and A549 cells were grown in DMEM supplemented with 10% FBS and 1% Pen/strep; DU145 cells were grown in RPMI supplemented with 10% FBS and 1% Pen/strep. HeLa, DU145 and A549 cells were kept in a humid atmosphere of 5% CO_2; HEK293 cells were kept in a humid atmosphere of 10% CO_2.

Plasmid constructs

The full-length FGFR4 wild-type and kinase active (K645E), have been described previously (Hart *et al.*, 2000). The kinase dead (K504M) and E681K forms of full-length FGFR4 were generated by QuikChange site-directed mutagenesis (Stratagene). The HA-IKKβ clone was received from Dr. Mark Hannink (University of Missouri). The HA-tag was removed from this clone by QuikChange site-directed mutagenesis in which a HindIII site was created along with an ATG start site downstream of the HA-tag. The parental clone contained a HindIII site upstream of the HA-tag. The plasmid containing the new HindIII site was digested with HindIII and re-ligated to generate the untagged IKKβ expression clone. Derivatives were confirmed by DNA sequencing at the UCSD Moores Cancer Center Shared Resource facility. The GST-IκB$^{(1-54)}$ plasmid was a gift from the Hoffmann Lab (UCSD).

Antibodies and Reagents

Antibodies were obtained from the following sources: FGFR4 (C-16), IKKβ (H-4), NFκB p65 (F-6), β-tubulin (H-235), IKKγ (FL-419) from Santa Cruz Biotechnology; phospho-p44/42 MAPK (Thr202/Tyr204; E-10) from Cell Signaling;

MAPK (ERK1+ERK2) from Zymed; 4G10 (antiphosphotyrosine) from Upstate Biotechnology; horseradish peroxidase (HRP) anti-mouse, HRP anti-rabbit from GE Healthcare; fluorescein-conjugated anti-mouse from Sigma and rhodamine-conjugated anti-rabbit from Boehringer-Mannheim. FGF19 and TNFα were obtained from R&D. mSin3a antibody was a gift from Dr. Alex Hoffmann. Poly(Glu, Tyr) was obtained from Sigma.

Immunoprecipitation and Immunoblot

HEK293 or A549 cells ($1x10^6$ per 10 cm dish) were plated 1 day prior to transfection with 4-6μg of total DNA by calcium phosphate precipitation at 3% CO_2. After 18 to 20 h, cultures were moved back to 10% CO_2 for 4-6 h before starving overnight in DMEM lacking FBS. Cells were harvested, washed once in PBS, and lysed in 1% NP-40 Lysis Buffer [20mM Tris-HCl, pH 7.5, 137mM NaCl, 1% Nonidet P-40, 5mM EDTA, 50mM NaF, 1mM sodium orthovanadate, 1mM phenylmethylsulfonyl fluoride (PMSF), 10ug/ml aprotinin]. Total protein concentrations were measured by Bradford Assay (Bio-Rad). Immunoprecipitations were performed overnight at 4°C and collected by Protein A-Sepharose (Sigma). Samples were washed three times with Lysis Buffer, boiled for 4 min in sample buffer and separated by SDS-PAGE. Proteins were transferred to Immobilon-P membranes and blocked in 3% or 5% milk/TBS/0.05% Tween 20. Membranes were immunoblotted with antibodies for 2 h at room temperature or overnight at 4°C. After primary incubations, membranes were washed with TBS/0.05% Tween 20 and incubated with HRP-conjugated secondary antibodies. Proteins were detected by enhanced chemiluminescence (ECL) (GE Healthcare) or (Millipore). To reprobe with

subsequent antibodies, membranes were incubated in stripping buffer [100mM β-mercaptoethanol; 2% SDS; 62.5mM Tris-HCl, pH 6.8] at 80°C for 1 h to remove bound antibodies. To detect the endogenous interaction between IKKβ and FGFR4 in the DU145 cells, 400μg of total lysate from starved cells was immunoprecipitated with IKKβ antibody in 1% NP-40 lysis buffer and analyzed by SDS-PAGE and Western Blot.

Yeast two-hybrid assay

The yeast two-hybrid assay was conducted as described (Kong *et al.*, 2000; Vojtek *et al.*, 1993). Briefly, the *Saccharomyces cerevisiae* strain L40 generated by Dr. Stan Hollenberg was transformed with derivatives of pBTM116 (constructed by Dr. Paul Bartel and Dr. Stan Fields). The derivatives constructed for this work encoded a LexA fusion protein containing the juxtamembrane and intracellular region of FGFR4. Briefly, an MluI site and an XhoI site were created in the multiple cloning region of pBTM116. Using these sites, amino acids 373-803 of FGFR4 were moved to the pBTM116 vector in frame with LexA. This bait was screened against a 9.5 d.p.c. mouse embryonic cDNA library encoding fusion proteins with the transactivation domain of pVP16, kindly provided by Dr. Stan Hollenberg. The two-hybrid screen and His± minimal media assays were performed as described previously (Kong *et al.*, 2000). The ability to activate the lacZ reporter was also confirmed by β-galactosidase filter assay as described (Kong *et al.*, 2000).

Indirect Immunofluorescence

HeLa cells were plated on glass coverslips at a density of $7.5x10^4$ cells per 35mm plate. The next day, cells were transfected using Fugene 6 transfection reagent (Roche). The following day, cells were starved in DMEM containing no serum for 24 h. 50ng/ml FGF19 plus 1μg/ml heparin was added for 10 min prior to adding 10ng/ml TNFα for 30 min. A549 cells were plated on glass coverslips at a density of $1x10^6$ per 10cm plate. The next day, cells were transfected using calcium phosphate precipitation. The following day, cells were starved in DMEM containing no serum for 24 h. 10ng/ml TNFα was added for 30 min. Coverslips were washed in PBS, fixed in 3% paraformaldehyde in PBS for 15 min, washed 3 times with PBS, and permeabilized for 10 min with 0.5% Triton-X 100 in PBS. Coverslips were again washed 3 times with PBS before blocking with 3% BSA in PBS for 1 h. Coverslips were incubated with FGFR4 (C-16) at 1:1000 and NFκB p65 (F-6) at 1:250 for 1 h. Coverslips were washed 3 times with PBS and labeled with secondary antibodies for 1 h at room temperature: Rhodamine-Rabbit, 1:1000; FITC-mouse, 1:1000; and Hoechst dye, 1:1000. Coverslips were washed 3 times with PBS before mounting in 90% glycerol, 10% 1M Tris pH 8.5, containing p-phenylenediamine. Cells were photographed using a Nikon Microphot-FXA with a cooled CCD camera (Hamamatsu C5810).

In vitro kinase assays

$1x10^6$ HEK293, DU145 or A549 cells were plated on 10cm dishes. HEK293 and A549 cells were transfected as described above. Cells were then starved in DMEM lacking FBS overnight, prior to being treated with 25ng/ml FGF19 for 10 min. Subsequently, cells were stimulated with 10ng/ml TNFα for 10 min. Cells were then

harvested and washed once in PBS + 1mM EDTA. Cells were then lysed in Cytoplasmic Extract Buffer (CEB) [10mM HEPES-KOH (pH 7.9), 250mM NaCl, 1mM EDTA, 0.5% Nonidet P-40, 0.2% Tween 20, 20mM β-glycerophosphate, 2mM DTT, 10mM NaF, 1mM sodium orthovanadate, 1mM PMSF, 10μg/ml aprotinin]. Protein concentrations were determined by Bradford Assay. 200μg lysates were immunoprecipitated with IKKγ antibody (for IKK kinase assays) or FGFR4 antibody (for the Poly(Glu, Tyr) assay) for 2 h at 4°C. Protein A-Sepharose beads were added and incubated for 1 h at 4°C. The immunoprecipitated samples were washed twice with CEB and twice with Kinase Buffer (KB) [20mM HEPES (pH 7.7), 100mM NaCl, 10mM $MgCl_2$, 20mM β-glycerophosphate, 2mM DTT, 10mM NaF, 0.1mM sodium orthovanadate, 1mM PMSF]. The resulting IKKγ immunoprecipitates were subjected to *in vitro* kinase assays utilizing GST-IκB$^{(1-54)}$ as the substrate (DiDonato *et al.*, 1997). FGFR4 immunoprecipitaates were subjected to *in vitro* kinase assays with Poly(Glu, Tyr) as the substrate. Samples were resuspended in 2X KB with 20μM ATP. 1μCi [γ-^{32}P]-ATP and 0.5μg GST-IκB$^{(1-54)}$ bacterially expressed purified protein or Poly(Glu, Tyr) were added to each reaction and incubated at 30°C for 30 min. Proteins were separated by 10% SDS-PAGE, Coomaisse stained, dried, and exposed to film or a phosphorimager (BioRad) screen directly. Band intensities were quantified using Quantity One Software.

Electrophoretic Mobility Shift Assay (EMSA)

EMSA assays were as described elsewhere (O'Dea *et al.*, 2007). Briefly, cells were collected in PBS, 1mM EDTA, pelleted at 2000 g, resuspended in 200μl CE buffer (10mM HEPES-KOH pH 7.9, 60mM KCl, 1mM EDTA, 0.5% NP-40, 1mM

DTT, 1mM PMSF) and vortexed. Nuclei were pelleted at 4000 g, and the supernatant was removed. Nuclei were resuspended in 50µl NE buffer (250mM Tris pH 7.8, 60mM KCl, 1mM EDTA, 1mM DTT, 1mM PMSF) and lysed by 3 freeze-thaw cycles. Nuclear lysates were cleared by centrifugation and normalized to a concentration of 1µg/µl following Bradford assay. 2µg of total nuclear protein was reacted at room temperature for 15 min with excess ^{32}P-labeled 30 bp double-stranded oligonucleotide containing a consensus κB-site (AGCTTGCTACAA**GGGACTTTCC**GCTGTCTACTTT) in 6µl binding buffer (10mM Tris-HCl pH 7.5, 50mM NaCl, 10% glycerol, 1% NP-40, 1mM EDTA, 0.1µg/µl polydIdC). Complexes were resolved on a non-denaturing 5% acrylamide (30:0.8) gel containing 5% glycerol and 1x TGE (24.8mM Tris-HCl, 190mM glycine, 1mM EDTA) and visualized and quantified using a Phosphorimager (Bio-Rad).

NFκB localization by cell fractionation

DU145 cells were plated on 10cm dishes. Upon reaching 80% confluency, cells were starved overnight and treated the next day with 50ng/ml FGF19 and 1µg/ml heparin for 10 min prior to the addition of 10ng/ml TNFα for 30 min. Cell lysates were fractionated as for EMSA.

Results

Direct interaction of FGFR4 and IKKβ

Using the intracellular domain of FGFR4 as bait, a yeast two-hybrid assay (Vojtek *et al.*, 1993) identified IKKβ. This novel interaction was first demonstrated with a β-galactosidase filter lift assay (Figure 7-1A, left panel), and confirmed by growth on selective media (Figure 7-1A, right panel).

To confirm this interaction by coimmunoprecipitation using full-length proteins, human IKKβ was co-expressed with FGFR4 in HEK293 cells. IKKβ was able to interact with wild-type FGFR4 (FGFR4 WT), a kinase-dead FGFR4 (FGFR4 KD) as well as a constitutively activated mutant of the receptor (FGFR4 K645E) (Figure 7-1B), indicating that kinase activity of the receptor is not essential for interaction with IKKβ. These interactions were further confirmed in the opposite direction by immunoprecipitation of each FGFR4 construct. As before, IKKβ was able to bind to FGFR4 proteins, whether kinase-active or kinase-dead (Figure 7-1C).

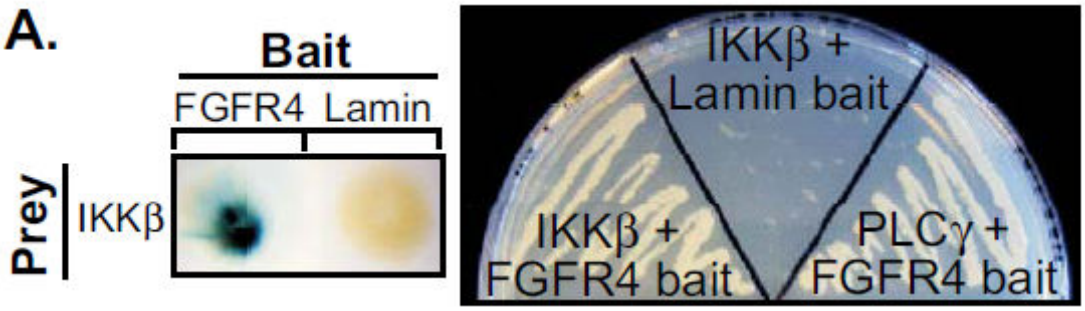

Figure 7-1. Novel interaction of IKKβ with FGFR4.
(A) Confirmation of yeast two-hybrid assay with the intracellular domain of FGFR4 bait protein and IKKβ clone isolated by β-gal filter lift assay (left panel) and growth on selective media (right panel).

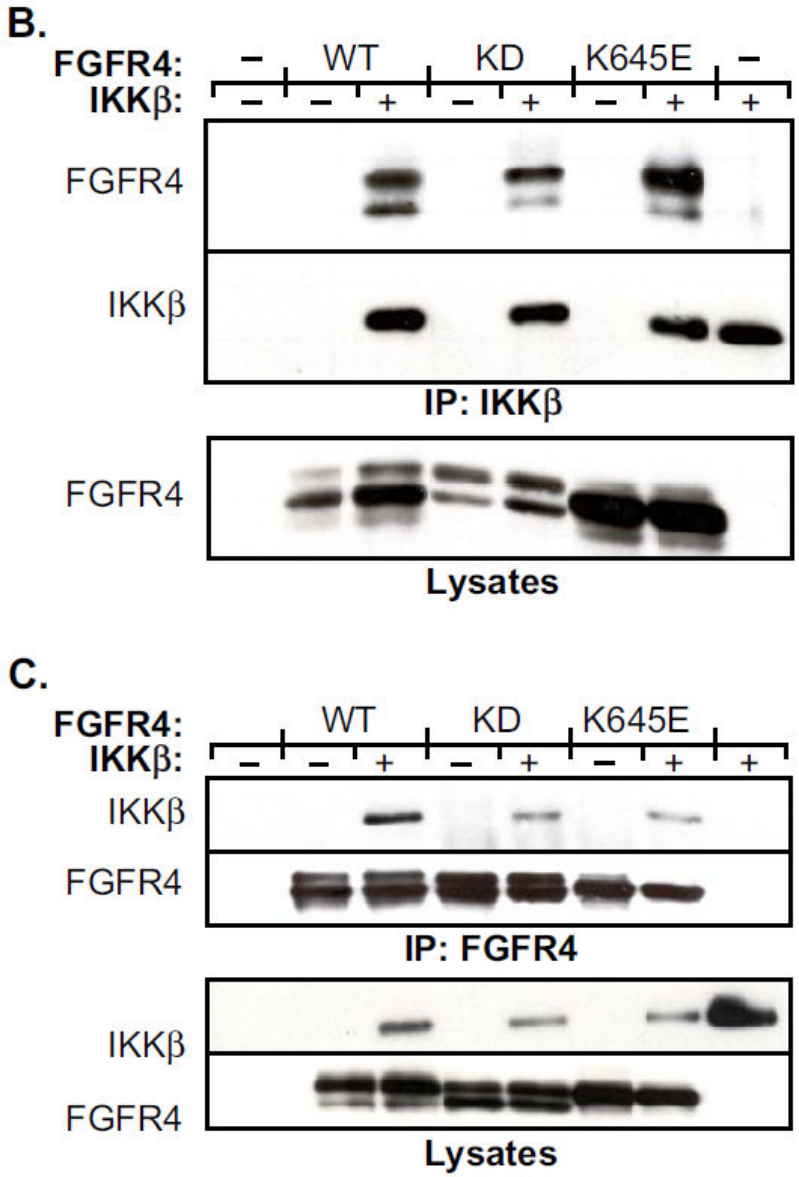

Figure 7-1. Novel interaction of IKKβ with FGFR4, continued.
(B) Full-length IKKβ and full-length FGFR4 derivatives were transfected in HEK293 cells to examine *in vivo* association. Cells were lysed in 1% NP-40 lysis buffer and immunoprecipitated with IKKβ (H-4) antibody. Immunoblot analysis was performed with FGFR4 (C-16) antibody (top panel). The membrane was stripped and reprobed with anti-IKKβ (middle panel). The expression of the FGFR4 derivatives in the whole cell lysate is shown in lower panel. (C) Cells were transfected and lysed as in (B) then immunoprecipitated with FGFR4 (C-16) antibody. Immunoblot analysis was performed with IKKβ (H-4) antibody (top panel). The membrane was stripped and reprobed with anti-FGFR4 (second panel). The expression of IKKβ and FGFR4 in the whole cell lysate are shown in the two lower panels.

FGFR4 decreases IKKβ activity when stimulated with TNFα

IKKβ activated by TNFα stimulation leads to release of NFκB dimers from IκB, allowing movement to the nucleus and increased NFκB transcriptional activity (Ding *et al.*, 1998). Utilizing indirect immunofluoresence, we monitored changes in NFκB translocation to the nucleus in TNFα stimulated cells expressing FGFR4 constructs. In starved unstimulated cells, IκB primarily sequestered NFκB in the cytoplasm (Figure 7-2A). In contrast, TNFα stimulation results in predominantly nuclear localization of NFκB. TNFα-treated cells expressing FGFR4 WT resulted in a 40% decrease in cells with NFκB nuclear localization compared to mock-transfected cells (Figure 7-2B). Expression of the activated mutant of FGFR4 led to a 65% decrease in cells with nuclear localization of NFκB. In contrast, FGFR4 KD led to only a 30% decrease in NFκB nuclear localization. Although single cells are shown in Figure 7-2A, these were representative of a minimum of 100 cells counted (in triplicate) for each condition, as shown in Figure 7-2B. These results indicate that the binding of the FGFR4 KD receptor is able to decrease the nuclear localization of NFκB, however, an activated receptor enhances the effect. This effect will be addressed further in the Discussion.

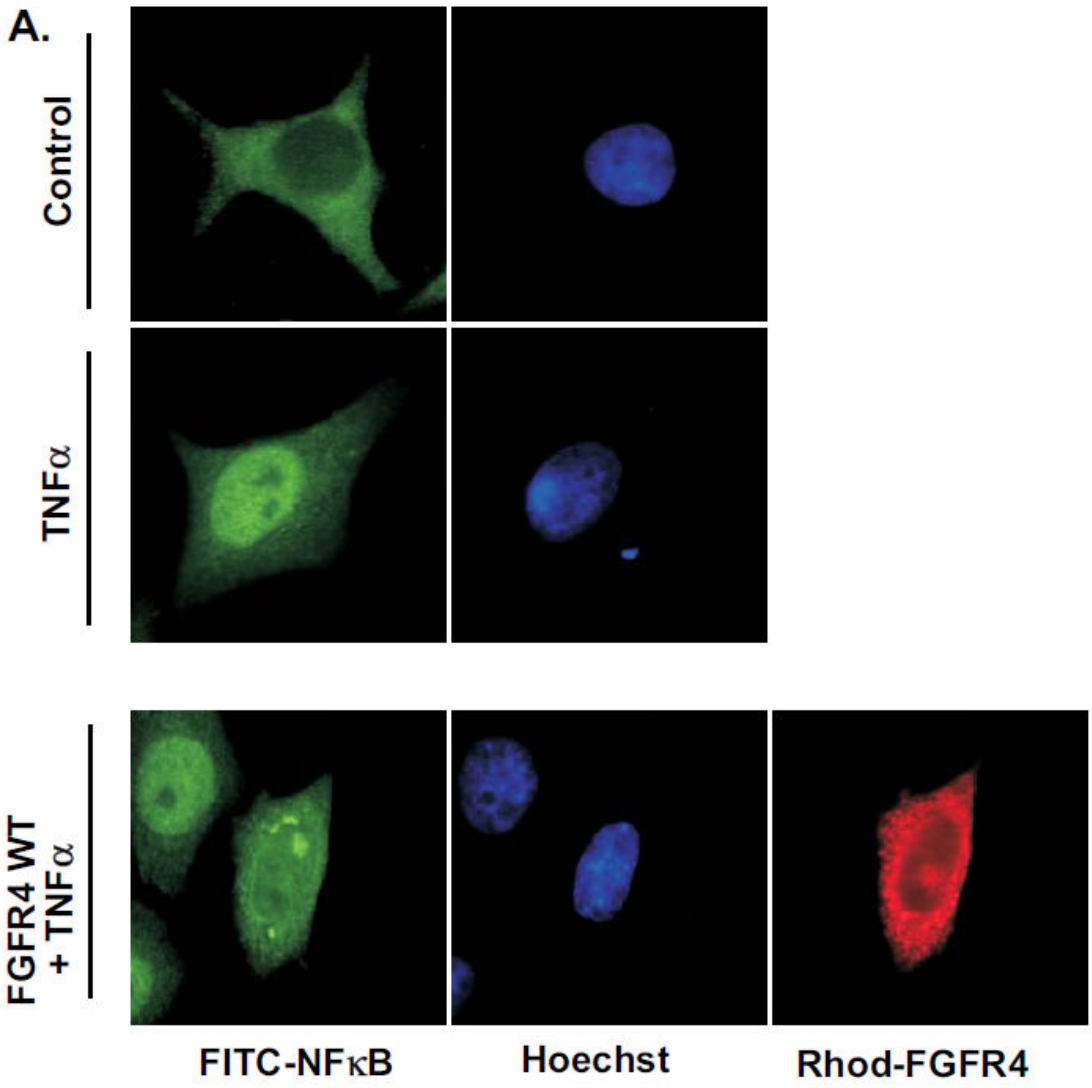

Figure 7-2. Re-localization of NFκB with FGFR4 expression.
(A) HeLa cells were seeded onto glass coverslips and transfected with FGFR4 derivatives. The cells were treated with TNFα for 30 min. Indirect immunofluorscence was performed. The localization of endogenous NFκB was dectected with NFκB p65 (F-6) antibody followed by FITC-conjugated anti-mouse antiserum. Cells expressing the FGFR4 derivatives were stained with anti-FGFR4 (C-16) and Rh-conjugated anti-rabbit secondary antibody. The nuclei were visualized with Hoechst dye. The endogenous localization of NFκB is shown in non-transfected cells -/+ TNFα treatment (top panels). The altered localization of NFκB in a cell expressing FGFR4 WT with TNFα treatment is shown in lower panels.

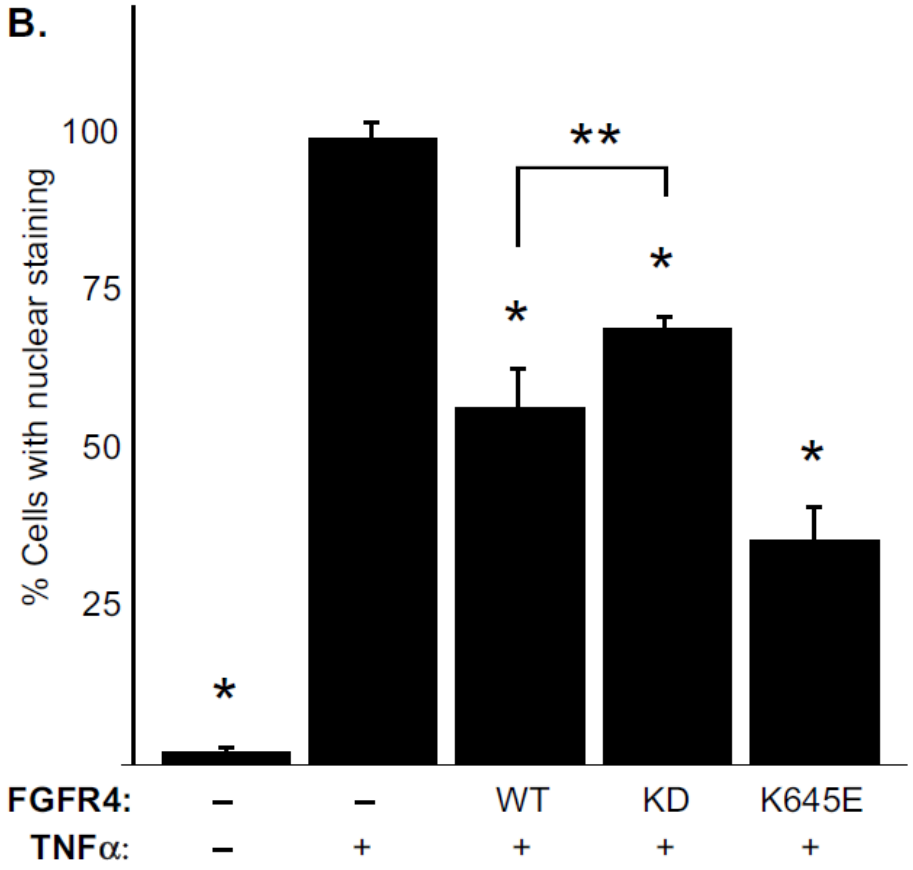

Figure 7-2. Re-localization of NFκB with FGFR4 expression, continued.
(B) Cells expressing FGFR4 derivatives were scored for the localization of NFκB. 100 cells were counted for each sample in three independent experiments. The error bars represent the standard deviation. *, $P \leq 0.0001$; **, $P = 0.0061$.

To further examine the effects of FGFR4 on downstream NFκB signaling, changes in endogenous IKKβ activity were monitored in HEK293 cells expressing FGFR4 and/or treated with the FGFR4-specific ligand FGF19 (Xie *et al.*, 1999). FGFR4 WT, FGFR4 K645E, and FGFR4 KD were transfected into HEK293 cells, followed by stimulation with TNFα. Equal amounts of total protein were subjected to immunoprecipitation with an IKKγ antibody to obtain the active IKK complex. The resulting immunoprecipitates were subjected to *in vitro* kinase assays utilizing GST-IκB$^{(1-54)}$ as the substrate (DiDonato *et al.*, 1997). The reactions were separated by SDS PAGE, and phosphorylation of GST-IκB$^{(1-54)}$ was visualized using a Phosphorimager, and quantitated (Figure 7-3A and B). Treatment with TNFα resulted in an almost ten-fold increase in the IKK complex activity, compared to unstimulated cells. Cells expressing FGFR4 WT exhibited a 30% reduction in IKK complex activity, which was further diminished by treatment of FGFR4 WT expressing cells with the ligand FGF19. Expression of activated FGFR4 K645E resulted in a 45% reduction of IKK activity. The activity of the IKK complex was restored in cells expressing the inactive FGFR4 KD mutant. Most importantly, the reduction in activity was also observed in mock transfected cells treated with FGF19, indicating that activation of the endogenous FGFR4 pathway is sufficient to reduce endogenous IKK activity.

Since previous research has implicated FGFR4 in prostate cancer progression, we sought to examine the effect of FGFR4 activation on NFκB signaling in DU145 prostate cancer cells (Gowardhan *et al.*, 2005; Sahadevan *et al.*, 2007), known to express high levels of endogenous FGFR4 (Chandler *et al.*, 1999). TNFα-treated DU145 cells stimulated with FGF19 exhibited a decrease in IKKβ activity, compared to TNFα-stimulation alone, as measured by IKK kinase assay using GST-IκB$^{(1-54)}$ as a

substrate (Figure 7-3C and D). This indicates that activation of endogenous FGFR4 in DU145 cells can decrease TNFα-stimulated activity of the IKK complex.

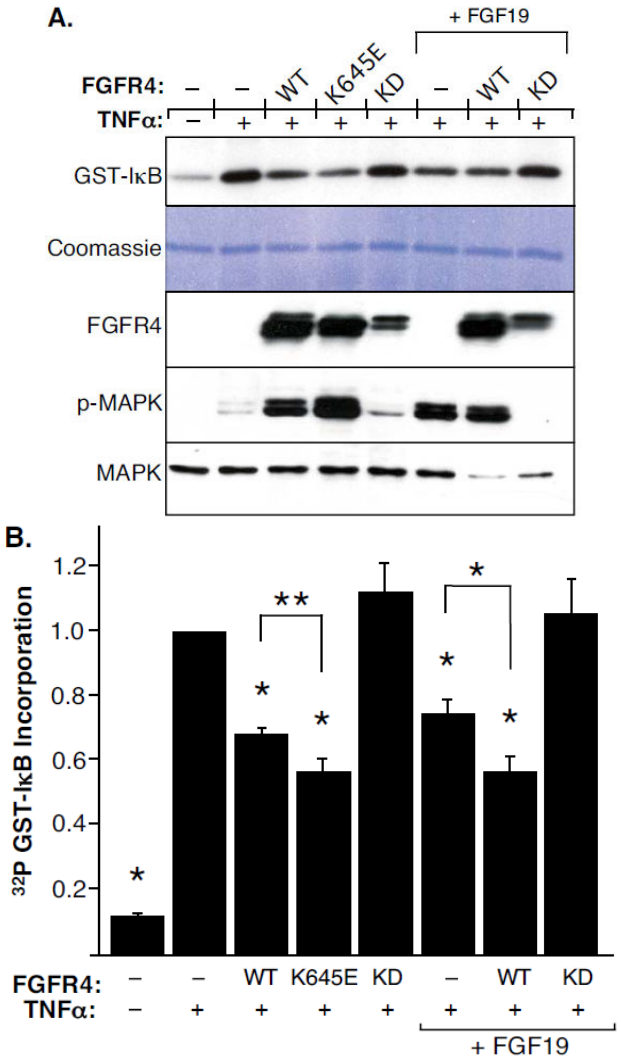

Figure 7-3. FGFR4 expression and/or FGF19 stimulation inhibits endogenous IKKβ activity.

(A) HEK293 cells were transfected with empty vector or the indicated FGFR4 constructs, then starved for 16 h. Cells were then either stimulated with vehicle for 10 min or FGF19 for 10 min prior to the addition of TNFα for an additional 10 min. The IKK complex was then immunoprecipitated from cytoplasmic extracts and subjected to an *in vitro* kinase assay utilizing GST-IκB$^{(1-54)}$ as substrate. The top panel shows ^{32}P incorporation on GST-IκB$^{(1-54)}$ while the second panel shows coomassie-staining as a loading control. Lysates were separated by SDS-PAGE, transferred to Immobilon-P, and probed with the indicated antibodies. (B) Kinase reactions described in (A) were exposed to a Phosphorimager (Bio-Rad). Quantification of ^{32}P incorporation into GST-IκB was performed using the Quantity One software (Bio-Rad). The average ^{32}P incorporation from three independent experiments, normalized to mock transfected cells stimulated with TNFα, is shown +/- std. dev. *, $P \leq 0.0002$; **, $P = 0.004$.

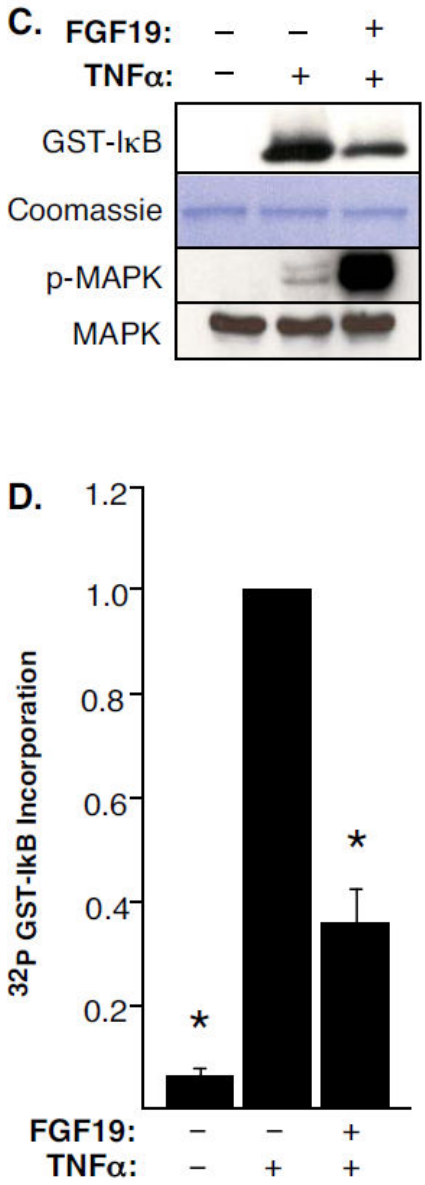

Figure 7-3. FGFR4 expression and/or FGF19 stimulation inhibits endogenous IKKβ activity, continued.
(C) DU145 cells were starved for 24 hr prior to stimulation as described in (A). Kinase assays and Western blots were performed as in (A). (D) Quantification of ^{32}P incorporation into GST-IκB$^{(1-54)}$ was performed as in (B). The average ^{32}P incorporation from three independent experiments, normalized to mock transfected cells stimulated with TNFα, is shown +/- std. dev. *, $P < 0.0001$.

Endogenous FGFR4 and IKKβ functionally interact in DU145 prostate cancer cells

We also examined the interaction of endogenous IKKβ and FGFR4 in DU145 cells by immunoprecipitating IKKβ, and immunoblotting for FGFR4. These experiments revealed that endogenous FGFR4 interacts with endogenous IKKβ in the DU145 cells (Figure 7-4A) further supporting our results utilizing overexpression of these respective proteins. In addition, we examined NFκB localization by cell fractionation and found that activation of endogenous FGFR4 with FGF19 led to a decrease in NFκB translocation to the nucleus when treated with TNFα (Figure 7-4B). FGF19 treatment of DU145 cells also decreased TNFα-induced NFκB DNA binding activity by about 25% as measured by Electrophoretic Mobility Shift Assay (EMSA) (Figure 7-4C, D). The details of the experimental procedure and specificity of NFκB to the DNA-probe have been described (Robbins *et al.*, 2004). These results demonstrate that stimulation of the endogenous FGFR4 receptor has a marked influence on endogenous IKK activity and leads to a significant decrease in the translocation of NFκB to the nucleus, resulting in a decrease in the DNA binding activity of NFκB. These experiments raise the possibility that FGF19, and possibly other FGFs, may be useful in the treatment of chronic inflammation and cancers caused by the misregulation of NFκB.

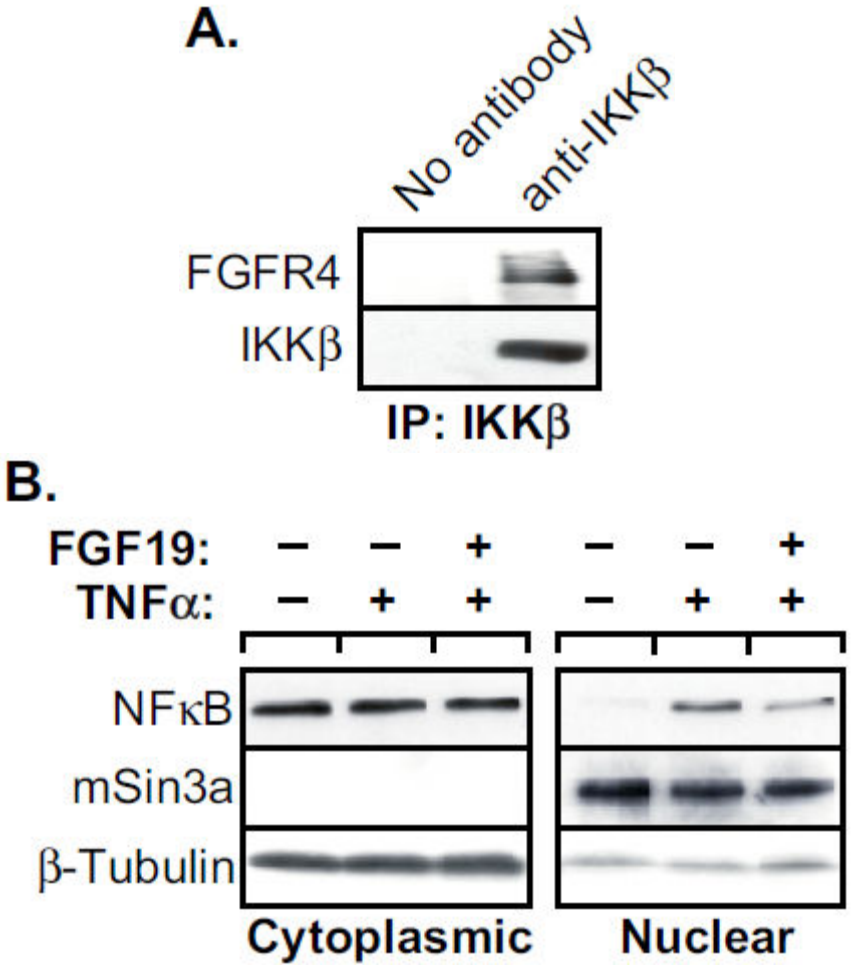

Figure 7-4. Endogenous interaction and effect on downstream signaling in DU145 prostate cancer cells.

(A) Approximately 400μg of total lysate was immunoprecipitated with IKKβ (H-4) antibody in 1% NP-40 lysis buffer. Immunoblot analysis was performed with FGFR4 (C-16) antibody (top panel). The membrane was stripped and reprobed with anti-IKKβ (lower panel). No IKKβ (H-4) antibody was added during the immunoprecipitation for the control lane. (B) DU145 cells were treated with TNFα or TNFα plus FGF19. Cells were fractionated and the cytoplasmic and nuclear fractions were immunoblotted with NFκB p65 (F-6) antibody (top panel). Membranes were stripped and reprobed with β-tubulin and mSin3a antibodies to confirm cytoplasmic and nuclear fractions (lower panels).

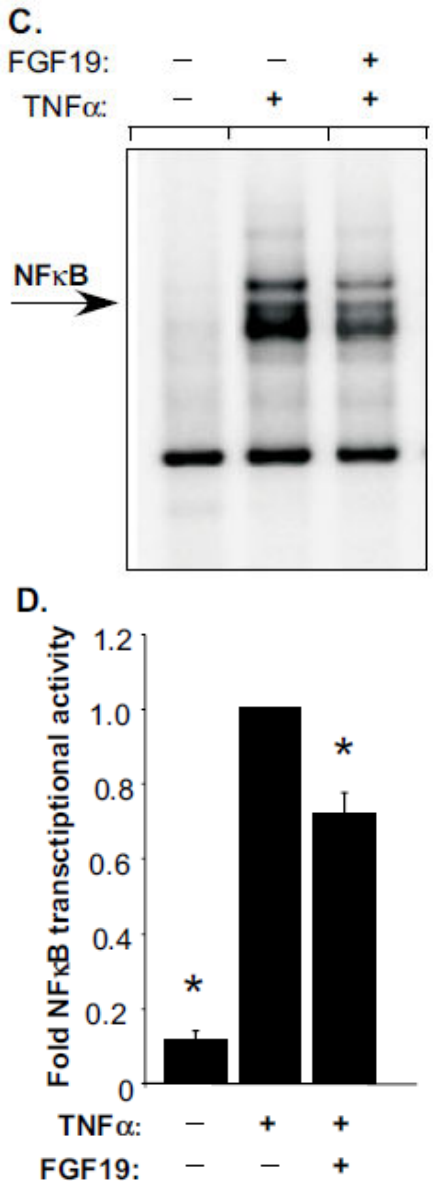

Figure 7-4. Endogenous interaction and effect on downstream signaling in DU145 prostate cancer cells, continued.
(C) DU145 cells were stimulated with vehicle for 30 min, TNFα for 30 min, or FGF19 for 10 min prior to the addition of TNFα for an additional 30 min. Nuclear extracts were prepared and equal amounts of protein (2 μg) were subjected to an electrophoretic mobility shift assay with ^{32}P-labeled 30bp double-stranded oligonucleotide containing a consensus κB-site. (D) Samples from (C) were exposed to a phosphorimager (Bio-Rad). Quantification of NF-κB binding to the probe was performed using the Quantity One software (Bio-Rad). The average NF-κB binding from three independent experiments, normalized to mock transfected cells stimulated with TNFα, is shown +/- std. dev. *, $P < 0.0001$.

FGFR4 E681K mutant is kinase inactive

Recently, during a screen by Varmus and colleagues for mutations in a group of patients with lung adenocarcinomas, a somatic mutation was identified in FGFR4 (Marks *et al.*, 2007). This mutation, E681K, occurs in the kinase domain of FGFR4. Using structural modeling, the authors proposed that this mutation may lead to altered activity of FGFR4 due to the charge of the amino acids, possibly through disruption of an ionic bond with Arg650. We created the E681K mutation in full-length FGFR4 and examined the autophosphorylation of the receptor. Expression of FGFR4 E681K in HEK293 cells showed no tyrosine autophosphorylation, indicating this mutation leads to a kinase-dead receptor (data not shown). To further confirm that the lack of detectable kinase activity associated with FGFR4 E681K, an *in vitro* kinase assay was carried out using Poly(Glu, Tyr) as the substrate. FGFR4 WT was able to phosphorylate this substrate, while the K645E activated mutation showed even greater phosphorylation. The FGFR4 KD and E681K mutation showed no detectable phosphorylation of Poly(Glu, Tyr), indicating that these receptors have no kinase activity and are unable to phosphorylate downstream substrates (Figure 7-5A).

To determine whether the E681K mutant acts as a dominant negative mutation, we co-transfected HEK293 cells with an equal amount of FGFR4 K645E and varied the amount of WT or E681K transfected to obtain a increasing ratio of E681K:WT. As the ratio of E681K to WT increased, the tyrosine phosphorylation of the receptors decreased, indicating that the E681K mutation functions as a dominant negative mutation and can decrease the autophosphorylation of the strongly activated K645E mutant (Figure 7-5B). We examined the ablility of FGFR4 E681K to interact with

IKKβ in HEK 293 cells. The FGFR4 E681K was still able to interact by coimmunoprecipitation with IKKβ (data not shown).

E681K mutation decreases FGFR4 inhibition of NFκB activity in A549 cells

We hypothesized that since the E681K mutation has no kinase activity, it will have a similar effect on NFκB signaling as the kinase-dead mutant of FGFR4. We investigated the effect of the E681K mutation on the FGFR4-mediated decrease in TNFα-induced NFκB activity in the A549 lung adenocarcinoma cell line by performing a GST-IκB kinase assay to measure IKK activity. A549 cells were transfected with the various constructs of FGFR4 and treated with TNFα. Expression of FGFR4 WT and K645E led to a decrease in IKK activity, while the KD and E681K mutations were unable to inhibit TNFα-induced IKK activity (data not shown).

In order to characterize the effect of the E681K mutation on NFκB localization, we examined the nuclear localization by indirect immunofluorescence. A549 cells were transfected with the FGFR4 constructs and treated with TNFα. Representative cells are shown in Figure 7-5C (left panel), and cell counts are shown in Figure 7-5C (right panel). FGFR4 K645E was able to decrease TNF-induced NFκB nuclear localization by 80%, while FGFR4 KD and E681K showed a modest decrease of 40% and 35%, respectively. These results indicate that the E681K mutation decreases the ability of FGFR4 to inhibit NFκB nuclear localization, and thereby may represent one possible mechanism to promote cell survival in lung adenocarcinoma cells.

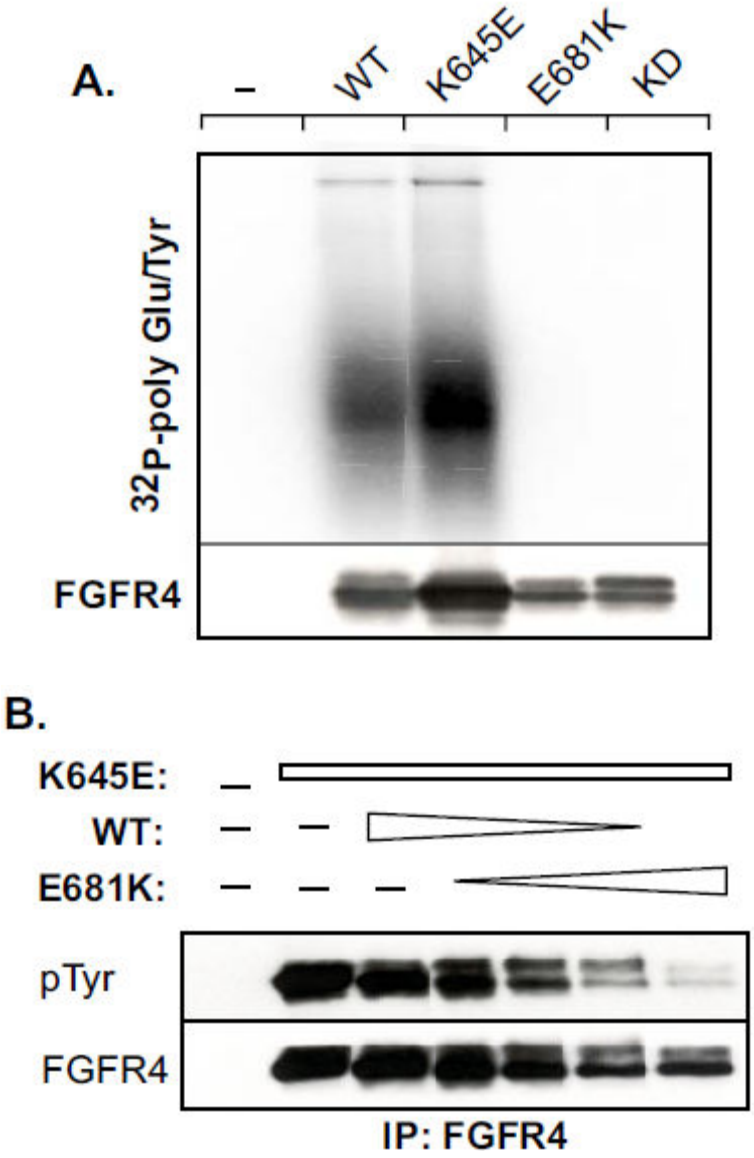

Figure 7-5. Charaterization of the FGFR4 E681K mutant
(A) HEK293 cells were transfected with FGFR4 constructs, immunoprecipitated with anti-FGFR4, and subjected to a Poly(Glu, Tyr) kinase assay. The gel was exposed to phosphoimager to analyze ^{32}P incorporation onto Poly(Glu, Tyr). (B) HEK293 cells were transfected with equal amounts of constitutively active K645E, together with a constant total amount of WT plus E681K FGFR4, at different ratios. Samples were immunoprecipitated for FGFR4 and immunoblotted with anti-phosphotyrosine (top). The membrane was stripped and re-probed with anti-FGFR4 (bottom).

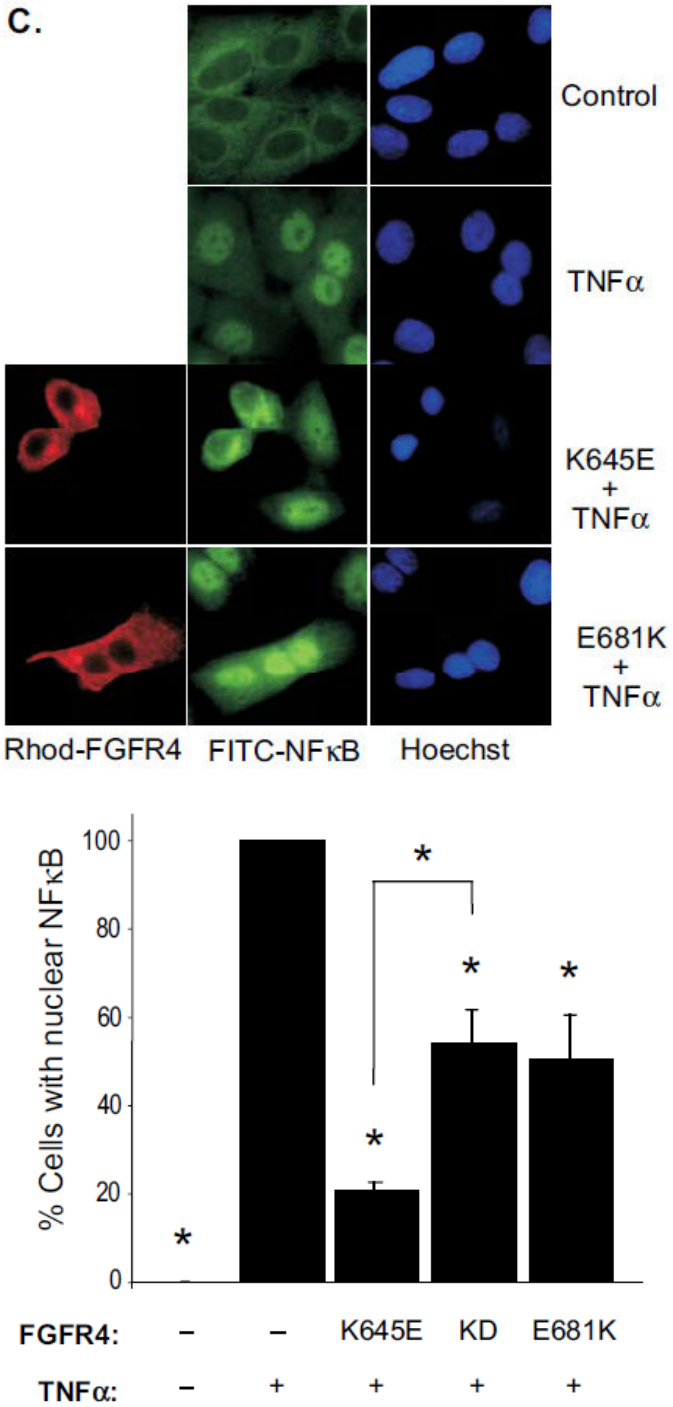

Figure 7-5. Charaterization of the FGFR4 E681K mutant, continued
(C) A549 cells were transfected with various constructs of FGFR4 and treated with TNFα for 30 min. Coverslips were fixed and stained for NFκB p65 (FITC) or FGFR4 (Rhod). 100 cells for each sample were counted in three independent experiments. Error bars represent +/- st. dev. *, $P \leq 0.0001$.

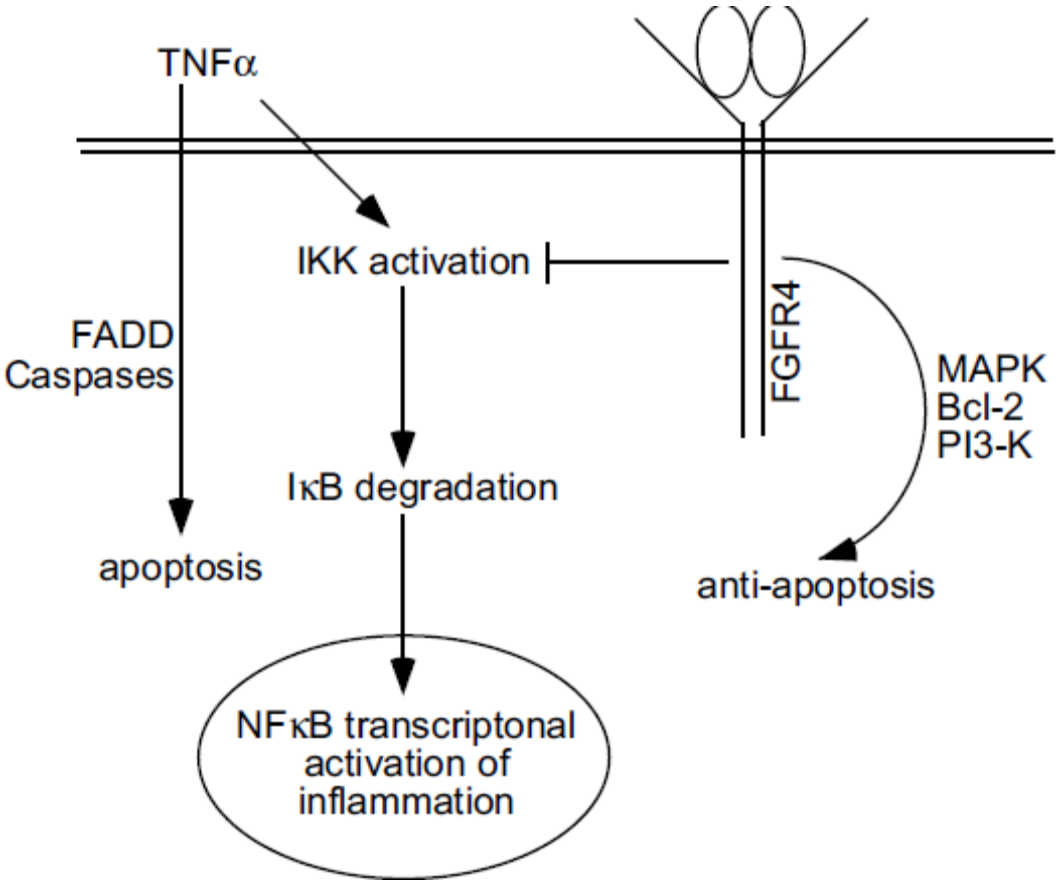

Figure 7-6. FGFR4 and NFκB pathways cross-talk
A schematic of possible FGFR4 involvements in the NFκB pathway.

Discussion

In this report we first demonstrate a novel interaction between FGFR4 and IKKβ using a yeast two-hybrid assay. We confirmed this interaction in HEK293 cells expressing these respective proteins by coimmunoprecipitation in both directions. Furthermore, we demonstrate that endogenous FGFR4 and IKKβ interact in the DU145 prostate cancer cell line. Utilizing kinase assays directed toward the IKKβ substrate GST-IκB$^{(1-54)}$, we show that expression of FGFR4 WT or an activated FGFR4 K645E mutant, but not kinase-dead FGFR4, leads to a decrease in endogenous IKKβ activity, indicating that FGFR4 activity is required for the reduction in IKKβ activity. Moreover, stimulation of endogenous FGFR4 with the ligand FGF19 leads to a decrease in IKKβ activity in both HEK293 and DU145 cell lines. In addition, we show that expression of FGFR4 and/or stimulation of endogenous FGFR4 with FGF19 also leads to a reduction in NFκB nuclear localization utilizing immunofluorescence and cell fractionation techniques, as well as a subsequent decrease in the amount of NFκB available in the nucleus for transcriptional activity, as monitored by EMSA. Four different cell lines were used in these experiments, including HEK293 and HeLa cells, as well as one prostate cancer cell line (DU145) and one lung adenocarcinoma cell line (A549). In these various cell lines, similar effects of FGF19/FGFR4 activation were observed with regards to the downregulation of NFκB signaling.

We have also examined a recently described E681K mutation in FGFR4 (Marks *et al.*, 2007), identified in a primary lung adenocarcinoma, and show that E681K confers a dominant negative phenotype and functions as a kinase dead mutation. Expression of this mutant in the A549 lung adenocarcinoma cell line does not lead to a reduction in IKKβ activity but does decrease NFκB nuclear translocation

modestly, although the effect on NFκB relocalization was less dramatic than that by the activated mutant FGFR4 K645E.

Since NFκB signaling is involved in both the pathogenesis of the inflammatory response and in cellular growth control, this pathway also represents a potential target for inhibition by FGFR4, and possibly by other FGFR family members. TNFα leads to apoptosis through FADD and downstream caspases (Baud and Karin, 2001), while at the same time exerting anti-apoptotic effects through NFκB transcriptional activation. FGF has also been shown to be anti-apoptotic through activation of MAPK, PI3K, and up-regulation of Bcl-2 (Agas *et al.*, 2008). Similar to the dual roles played by TNF, FGF19 activation of FGFR4 may also lead to apoptosis through inhibition of IKKβ activity (Figure 7-5D).

FGFRs are overexpressed or have altered activity in a variety of human diseases, including cancers of the prostate (Giri *et al.*, 1999), breast (Penault-Llorca *et al.*, 1995), and lung (Spinola *et al.*, 2005), and recent evidence indicates FGFRs may be used to target tumors for growth inhibition (Rusnati and Presta, 2007). Our findings indicate a substantially expanded role for FGFR4, not only as a regulator of cellular proliferative pathways, but as an important regulator of NFκB inflammatory pathways previously viewed as distinct. These results implicate FGFR4 as a potential tumor suppressor. The primary mode of IKKβ regulation is through phosphorylation of serine residues, which can be either activating as when Ser177 and Ser181 are phosphorylated, or inhibitory if phosphorylated on C-terminal residues (Delhase *et al.*, 1999; Schomer-Miller *et al.*, 2006; Shambharkar *et al.*, 2007; Zandi *et al.*, 1998). However, IKKβ is also regulated by many stimuli and in numerous other modes

including degradation, microRNAs, phosphorylation by IKKα, binding to IKKγ, and phosphorylation by MEKK1 (Yamamoto *et al.*, 2000).

The results presented here demonstrate a direct interaction between FGFR4, an important receptor tyrosine kinase, and IKKβ, an important regulatory component of the NFκB pathway. We have also demonstrated downregulation of IKKβ activity and decreased NFκB nuclear localization in response to the activation of FGF signaling pathways, either in response to stimulation with the ligand FGF19 or as a result of mutational activation of FGFR4. One conclusion from these experiments is that these two major axes of cellular signaling clearly interact, whereas previously they were not known to do so. Nonetheless, the mechanism mediating these effects clearly requires further study to discriminate between various possible mechanisms. For example, direct tyrosine phosphorylation by FGFR4 of an NFκB regulatory protein is one possibility, although many other proteins are likely to be recruited into a signaling complex that contains, at a mininum, FGFR4 and IKKβ. Other FGFR family members have been shown to recruit a variety of regulatory proteins including Grb2-SOS (Ong *et al.*, 2001), Pyk2/RAFTK (Meyer *et al.*, 2004), RSK2 (Kang *et al.*, 2007), SH2-B (Kong *et al.*, 2002) and others; any of these might mediate effects through interaction with NFκB family members. We expect that mass spectrometric approaches will assist in the identification of other proteins complexed together with FGFR4 and IKKβ, and these experiments are currently underway. These experiments also raise the question whether the interaction with IKKβ and downregulation of NFκB signaling reported here is confined to FGFR4 or whether other FGFR family members interact similarly. This question is also the subject of ongoing research.

Our data actually suggest two different types of effects upon NFκB signaling: one dependent upon functional FGFR4 kinase activity and, second, a more modest effect that is independent of FGFR4 kinase activity. For example, Figure 7-2B shows a significant decrease in TNFα-induced NFκB nuclear localization in response to expression of wild-type FGFR4. In the same experiment, expression of kinase-dead FGFR4 also reduces TNFα-induced NFκB nuclear localization, but to a lesser extent. Thus, we infer that formation of an FGFR4/IKKβ complex, even with a kinase-inactive FGFR4, has the capability of impacting NFκB signaling.

FGF2 stimulation of cells has been previously shown to protect cells from TNFα-induced apoptosis (Gardner and Johnson, 1996), which may lead to uncontrolled cell growth, while we show that in cells with constitutively active NFκB, FGF19 stimulation leads to a decrease in TNFα-induced NFκB nuclear localization. Cells that overexpress FGFR4 may do so in order to circumvent NFκB inflammatory pathways; this predicts that cancers exhibiting overexpressed FGFR4 may actually have acquired a kinase-inactivating mutation that eliminates the tumor-suppressive effect seen with FGFR4 WT. Given the recent evidence to support the importance of NFκB activity in the progression of lung cancer (Dey *et al.*, 2007; Gradilone *et al.*, 2007; Stathopoulos *et al.*, 2008; Tsurutani *et al.*, 2005), it is possible that activation of FGFR4 may provide a tumor-suppressive role by decreasing NFκB signaling. Mutations in FGFR4 such as E681K, which confer a kinase-inactive and dominant negative phenotype, may be important in the progression of cancers that rely on NFκB signaling.

In summary, we have presented a novel interaction by which FGFR4 signaling functions to inhibit IKKβ activity, resulting in decreased NFκB signaling in DU145 prostate cancer cells and in A549 lung adenocarcinoma cells.

Acknowledgements

We thank Prof. Alexander Hoffmann and members of his laboratory, particularly Shannon Werner and Ellen O'Dea, for experimental advice; Prof. Mark Hannink for advice and reagents; Prof. L. Deftos for A549 cells; and Laura Castrejon for editorial assistance. This work was supported by NIH #5 R01 CA090900, the University of California Cancer Research Coordinating Committee, and the University of California Breast Cancer Research Program #14IB-0065 to DJD; a Ruth L. Kirschstein Institutional National Research Service Award #5 T32 CA009523 to KAD; the Achievement Rewards for College Scientists Foundation, and the UCSD Chancellor's Interdisciplinary Collaboratories Fellowship to CWM. Chapter 7, in full, is material submitted for publication, Drafahl, KD; McAndrew, CM; Meyer, AN; Haas, M; and Donoghue, DJ (2009). The dissertation author was a primary investigator and co-author of this paper.

References

1. Agas D, Marchetti L, Menghi G, Materazzi S, Materazzi G, Capacchietti M *et al* (2008). Anti-apoptotic Bcl-2 enhancing requires FGF-2/FGF receptor 1 binding in mouse osteoblasts. *J Cell Physiol* **214:** 145-52.

2. Baud V, Karin M (2001). Signal transduction by tumor necrosis factor and its relatives. *Trends Cell Biol* **11:** 372-7.

3. Chandler LA, Sosnowski BA, Greenlees L, Aukerman SL, Baird A, Pierce GF (1999). Prevalent expression of fibroblast growth factor (FGF) receptors and FGF2 in human tumor cell lines. *Int J Cancer* **81:** 451-8.

4. Delhase M, Hayakawa M, Chen Y, Karin M (1999). Positive and negative regulation of IkappaB kinase activity through IKKbeta subunit phosphorylation. *Science* **284:** 309-13.

5. Dey A, Wong ET, Bist P, Tergaonkar V, Lane DP (2007). Nutlin-3 inhibits the NFkappaB pathway in a p53-dependent manner: implications in lung cancer therapy. *Cell Cycle* **6:** 2178-85.

6. DiDonato JA, Hayakawa M, Rothwarf DM, Zandi E, Karin M (1997). A cytokine-responsive IkappaB kinase that activates the transcription factor NF-kappaB. *Nature* **388:** 548-54.

7. Ding GJ, Fischer PA, Boltz RC, Schmidt JA, Colaianne JJ, Gough A *et al* (1998). Characterization and quantitation of NF-kappaB nuclear translocation induced by interleukin-1 and tumor necrosis factor-alpha. Development and use of a high capacity fluorescence cytometric system. *J Biol Chem* **273:** 28897-905.

8. Dutta J, Fan Y, Gupta N, Fan G, Gelinas C (2006). Current insights into the regulation of programmed cell death by NF-kappaB. *Oncogene* **25:** 6800-16.

9. Gardner AM, Johnson GL (1996). Fibroblast growth factor-2 suppression of tumor necrosis factor alpha-mediated apoptosis requires Ras and the activation of mitogen-activated protein kinase. *J Biol Chem* **271:** 14560-6.

10. Giri D, Ropiquet F, Ittmann M (1999). Alterations in expression of basic fibroblast growth factor (FGF) 2 and its receptor FGFR-1 in human prostate cancer. *Clin Cancer Res* **5:** 1063-71.

11. Gowardhan B, Douglas DA, Mathers ME, McKie AB, McCracken SR, Robson CN *et al* (2005). Evaluation of the fibroblast growth factor system as a potential target for therapy in human prostate cancer. *Br J Cancer*.

12. Gradilone A, Silvestri I, Scarpa S, Morrone S, Gandini O, Pulcinelli FM *et al* (2007). Failure of apoptosis and activation on NFkappaB by celecoxib and aspirin in lung cancer cell lines. *Oncol Rep* **17:** 823-8.

13. Hacker H, Karin M (2006). Regulation and function of IKK and IKK-related kinases. *Sci STKE* **2006:** re13.

14. Hart KC, Robertson SC, Kanemitsu MY, Meyer AN, Tynan JA, Donoghue DJ (2000). Transformation and Stat activation by derivatives of FGFR1, FGFR3, and FGFR4. *Oncogene* **19:** 3309-20.

15. Huang J, Wu L, Tashiro S, Onodera S, Ikejima T (2006). Fibroblast growth factor-2 suppresses oridonin-induced L929 apoptosis through extracellular signal-regulated kinase-dependent and phosphatidylinositol 3-kinase-independent pathway. *J Pharmacol Sci* **102:** 305-13.

16. Kang S, Dong S, Gu TL, Guo A, Cohen MS, Lonial S *et al* (2007). FGFR3 activates RSK2 to mediate hematopoietic transformation through tyrosine phosphorylation of RSK2 and activation of the MEK/ERK pathway. *Cancer Cell* **12:** 201-14.

17. Karin M (2006). Nuclear factor-kappaB in cancer development and progression. *Nature* **441:** 431-6.

18. Karin M (2008). The IkappaB kinase - a bridge between inflammation and cancer. *Cell Res* **18:** 334-42.

19. Kong M, Barnes EA, Ollendorff V, Donoghue DJ (2000). Cyclin F regulates the nuclear localization of cyclin B1 through a cyclin-cyclin interaction. *Embo J* **19:** 1378-88.

20. Kong M, Wang CS, Donoghue DJ (2002). Interaction of fibroblast growth factor receptor 3 and the adapter protein SH2-B. A role in STAT5 activation. *J Biol Chem* **277:** 15962-70.

21. Marks JL, McLellan MD, Zakowski MF, Lash AE, Kasai Y, Broderick S *et al* (2007). Mutational analysis of EGFR and related signaling pathway genes in lung Adenocarcinomas identifies a novel somatic kinase domain mutation in FGFR4. *PLoS ONE* **2:** e426.

22. Meyer AN, Gastwirt RF, Schlaepfer DD, Donoghue DJ (2004). The cytoplasmic tyrosine kinase Pyk2 as a novel effector of fibroblast growth factor receptor 3 activation. *J Biol Chem* **279:** 28450-7.

23. O'Dea EL, Barken D, Peralta RQ, Tran KT, Werner SL, Kearns JD *et al* (2007). A homeostatic model of IkappaB metabolism to control constitutive NF-kappaB activity. *Mol Syst Biol* **3:** 111.

24. Ong SH, Hadari YR, Gotoh N, Guy GR, Schlessinger J, Lax I (2001). Stimulation of phosphatidylinositol 3-kinase by fibroblast growth factor receptors is mediated by coordinated recruitment of multiple docking proteins. *Proc Natl Acad Sci U S A* **98:** 6074-9.

25. Penault-Llorca F, Bertucci F, Adelaide J, Parc P, Coulier F, Jacquemier J *et al* (1995). Expression of FGF and FGF receptor genes in human breast cancer. *Int J Cancer* **61:** 170-6.

26. Robbins JB, Riedel BD, Jones T, Boyd AS (2004). Nasal tumor in a Peruvian man. *Am J Dermatopathol* **26:** 248, 254.

27. Rusnati M, Presta M (2007). Fibroblast growth factors/fibroblast growth factor receptors as targets for the development of anti-angiogenesis strategies. *Curr Pharm Des* **13:** 2025-44.

28. Sahadevan K, Darby S, Leung HY, Mathers ME, Robson CN, Gnanapragasam VJ (2007). Selective over-expression of fibroblast growth factor receptors 1 and 4 in clinical prostate cancer. *J Pathol* **213:** 82-90.

29. Sarkar FH, Li Y (2008). NF-kappaB: a potential target for cancer chemoprevention and therapy. *Front Biosci* **13:** 2950-9.

30. Schmid JA, Birbach A (2008). IkappaB kinase beta (IKKbeta/IKK2/IKBKB)--a key molecule in signaling to the transcription factor NF-kappaB. *Cytokine Growth Factor Rev* **19:** 157-65.

31. Schomer-Miller B, Higashimoto T, Lee YK, Zandi E (2006). Regulation of IkappaB kinase (IKK) complex by IKKgamma-dependent phosphorylation of the T-loop and C terminus of IKKbeta. *J Biol Chem* **281:** 15268-76.

32. Shambharkar PB, Blonska M, Pappu BP, Li H, You Y, Sakurai H *et al* (2007). Phosphorylation and ubiquitination of the IkappaB kinase complex by two distinct signaling pathways. *Embo J* **26:** 1794-805.

33. Spinola M, Leoni V, Pignatiello C, Conti B, Ravagnani F, Pastorino U *et al* (2005). Functional FGFR4 Gly388Arg polymorphism predicts prognosis in lung adenocarcinoma patients. *J Clin Oncol* **23:** 7307-11.

34. Stathopoulos GT, Sherrill TP, Han W, Sadikot RT, Yull FE, Blackwell TS *et al* (2008). Host nuclear factor-kappaB activation potentiates lung cancer metastasis. *Mol Cancer Res* **6:** 364-71.

35. Tsurutani J, Castillo SS, Brognard J, Granville CA, Zhang C, Gills JJ *et al* (2005). Tobacco components stimulate Akt-dependent proliferation and NFkappaB-dependent survival in lung cancer cells. *Carcinogenesis* **26:** 1182-95.

36. Vandermoere F, El Yazidi-Belkoura I, Adriaenssens E, Lemoine J, Hondermarck H (2005). The antiapoptotic effect of fibroblast growth factor-2 is mediated through nuclear factor-kappaB activation induced via interaction between Akt and IkappaB kinase-beta in breast cancer cells. *Oncogene* **24:** 5482-91.

37. Vojtek AB, Hollenberg SM, Cooper JA (1993). Mammalian Ras interacts directly with the serine/threonine kinase Raf. *Cell* **74:** 205-14.

38. Wang J, Yu W, Cai Y, Ren C, Ittmann MM (2008). Altered fibroblast growth factor receptor 4 stability promotes prostate cancer progression. *Neoplasia* **10:** 847-56.

39. Xie MH, Holcomb I, Deuel B, Dowd P, Huang A, Vagts A *et al* (1999). FGF-19, a novel fibroblast growth factor with unique specificity for FGFR4. *Cytokine* **11:** 729-35.

40. Yamamoto Y, Yin MJ, Gaynor RB (2000). IkappaB kinase alpha (IKKalpha) regulation of IKKbeta kinase activity. *Mol Cell Biol* **20:** 3655-66.

41. Zandi E, Chen Y, Karin M (1998). Direct phosphorylation of IkappaB by IKKalpha and IKKbeta: discrimination between free and NF-kappaB-bound substrate. *Science* **281:** 1360-3.

Chapter 8:

FGFR2 Interaction and Tyrosine Phosphorylation of IKKβ Negatively Regulates NFκB in T47D Cells

Abstract

The role of FGFR2 in the pathogenesis of cancer has been widely researched. Evidence exists to implicate FGFR2 signaling in cancer progression as well as protection from inflammatory insults [1-8], indicating FGFR2 may play dual roles as a tumor promoter and a tumor suppressor. We have previously identified the novel interaction of FGFR4 and IKKβ and have shown this interaction leads to a decrease in NFκB activity[9]. In this work, we show a direct interaction between FGFR2 and IKKβ, as well as tyrosine phosphorylation of IKKβ resulting from FGFR2 expression. Additionally, we show that kinase activation of FGFR2 prior to TNFα treatment leads to a decrease in IKK activity as measured by a kinase assay using GST-IκB as a substrate. Furthermore, we demonstrate a decrease in NFκB signaling upon FGFR2 activation, which is dependent upon FGFR2 kinase activity. FGF8b stimulation of endogenous FGFR2b in TNFα-treated T47D breast cancer cells also leads to a decrease in NFκB activity. Our research further implicates FGFR2 as a tumor suppressor and suggests a mechanism through which FGFR2 kinase activity leads to inactivation of IKK and NFκB signaling in breast cancer.

Introduction

FGFR2 is a receptor tyrosine kinase (RTK) belonging to the Fibroblast Growth Factor Receptor (FGFR) family. Like all RTKs, FGFR2 has an extracellular ligand binding domain, a single-pass transmembrane domain, and an intracellular kinase domain that phosphorylates tyrosine residues when activated. FGFR2 mutations are responsible for developmental syndromes, including Antley-Bixler-like syndrome (ABS), Apert syndrome (AS), Beare-Stevenson syndrome (BSS), Crouzon syndrome (CS), Jackson-Weiss syndrome (JWS), Saethre-Chotzen syndrome (SCS), and Pfeiffer syndrome (PS) [10-17]. We were the first to show that mutations in the FGFR2 extracellular domain result in constitutive kinase activation, providing a mechanistic understanding [18, 19]. Also, certain types of gastric cancers overexpress FGFR2 and recent research has discovered that an inhibitor, AZD2171, exerts potent antitumor activity against gastric cancer xenografts overexpressing FGFR2 [20].

There are many isoforms of FGFRs due to splice variants. Two splice forms of FGFR2 in the third IG-like domain result in two separate isoforms, FGFR2b (also known as KGFR) and FGFR2c. FGFR2b is specifically expressed in epithelial cells, while FGFR2c is expressed in mesenchymal cells. FGF7 (or KGF) binds specifically to the FGFR2b isoform and is secreted from mesenchymal cells, which leads to a paracrine mode of receptor activation. The FGFR2b isoform and its ligand, FGF7, have been extensively implicated in the protection of cells from inflammatory insults in the lung, skin, and bowel [1-8], while also implicated in the progression of breast and

ovarian cancers [21-27]. It is possible that FGFR2 may serve as a tumor suppressor as well as tumor promoter under certain conditions and cell types.

We have recently reported the novel interaction of FGFR4 with IKKβ. IKKβ is an important component of the NFκB signaling pathway. Activation of IKKβ through phosphorylation on serine residues leads to phosphorylation and degradation of IκB [28]. IκB inhibits NFκB by sequestering it in the cytoplasm, but upon degradation of IκB, the nuclear localization signal on NFκB is exposed, allowing movement to the nucleus and transcription of a variety of genes which are important in cell survival as well as inflammation [29]. The NFκB inflammatory pathway has been widely studied in its role in cancer progression [29], and targeted inhibition of this pathway is of significant interest. We have shown previously that IKKβ is tyrosine phosphorylated when FGFR4 is co-expressed. We have also shown that interaction with IKKβ as well as FGFR4 kinase activity leads to decreased IKK activity as measured in a kinase assay using GST-IκB as a substrate. Additionally, we have shown decreased NFκB nuclear localization through indirect immunofluorescence and decreased NFκB transcriptional activity by EMSA [9]. This discovery has illuminated an alternate pathway for NFκB inhibition, through FGFR4 signaling, implicating FGFR4 as a tumor suppressor.

We were interested in determining whether FGFR2 may also interact with IKKβ and inhibit NFκB activity. As mentioned above, the FGFR2b isoform has been extensively implicated in the inflammatory pathway. We hypothesized that FGFR2 may also interact with IKKβ to inhibit NFκB activity, and this may be one mechanism

for how it is able to decrease inflammation under certain conditions. We were also interested in determining which specific tyrosines on IKKβ were phosphorylated in response to FGFR activation. One group has suggested that Src-phosphorylation of Tyr188 and Tyr199 is important for activation of the NFκB pathway [30, 31], although this initial observation has not been further studied.

Materials and Methods

Cell culture

T47d and HEK293 cells were grown in DMEM supplemented with 10% FBS and 1% Pen/strep. T47d cells were kept in a humid atmosphere of 5% CO_2; HEK293 cells were kept in a humid atmosphere of 10% CO_2.

Plasmid constructs

Full-length FGFR2 wild-type has been described previously (REF). The HA-IKKβ clone was received from Dr. Mark Hannink (University of Missouri). The HA-tag was removed from this clone by QuikChange site-directed mutagenesis in which a HindIII site was created along with an ATG start site downstream of the HA-tag. The parental clone contained a HindIII site upstream of the HA-tag. The plasmid containing the new HindIII site was digested with HindIII and re-ligated to generate the untagged IKKβ expression clone. It was necessary to delete this tag as it contains numerous tyrosine sites that are phosphorylated by activated FGFR4. Derivatives were confirmed by DNA sequencing at the UCSD Moores Cancer Center Shared Resource facility. The GST-IκB$^{(1-54)}$ plasmid was a gift from the Hoffmann Lab (UCSD).

Antibodies and Reagents

Antibodies were obtained from the following sources: FGFR2 (C-17), IKKβ (H-4), NFκB (F-6), β-tubulin (H-235), IKKγ (FL-419) from Santa Cruz Biotechnology; 4G10 (antiphosphotyrosine) from Upstate Biotechnology; horseradish

peroxidase (HRP) anti-mouse, HRP anti-rabbit from GE Healthcare. FGF19 and TNFα were obtained from R&D.

Immunoprecipitation and Immunoblot

HEK293 cells (1X10 ^{6}) were plated on 10 cm dishes 1 day prior to transfection with 4-6μg of total DNA by calcium phosphate precipitation at 3% CO_2. After 18 to 20 h, cultures were moved back to 10% CO_2 for 4-6 h before starving overnight in DMEM lacking FBS. Cells were harvested, washed once in PBS, and lysed in 1% NP-40 Lysis Buffer [20mM Tris-HCl, pH 7.5, 137mM NaCl, 1% Nonidet P-40, 5mM EDTA, 50mM NaF, 1mM sodium orthovanadate, 1mM phenylmethylsulfonyl fluoride (PMSF), 10ug/ml aprotinin] or radioimmunoprecipitation assay buffer [RIPA; 50mM Tris-HCl, pH 7.5; 150mM NaCl; 0.1% SDS; 1% Triton-X 100; 1% DOC; 50mM NaF; 1mM sodium orthovanadate; 1mM phenylmethylsulfonyl fluoride (PMSF); 10ug/ml aprotinin]. Total protein was measured by Bradford Assay or Lowry Assay (Bio-Rad). Immunoprecipitations were performed overnight at 4°C and collected by Protein A-Sepharose (Sigma). Samples were washed three times with Lysis Buffer, boiled for 4 min in sample buffer and separated by SDS-PAGE. Proteins were transferred to Immobilon-P membranes and blocked in 3% or 5% milk/TBS/0.05% Tween 20 or 3% bovine serum albumin (BSA)/TBS/0.05% Tween 20 (for anti-phosphotyrosine blots). Membranes were immunoblotted with antibodies for 2 h at room temperature or overnight at 4°C. After primary incubations, membranes were washed with TBS/0.05% Tween 20 and incubated with HRP-conjugated secondary antibodies.

Proteins were detected by enhanced chemiluminescence (ECL) (GE Healthcare) or (Millipore). To reprobe with subsequent antibodies, membranes were incubated in stripping buffer [100mM β-mercaptoethanol; 2% SDS; 62.5 mM Tris-HCl, pH 6.8] to remove bound antibodies.

In vitro kinase assays

$1X10^6$ HEK293 or T47d cells were plated on 10cm dishes. HEK293 cells were transfected as described above. Cells were then starved in DMEM lacking FBS overnight, prior to being treated with 25ng/mL FGF8b for 10 min. Subsequently, cells were stimulated with 10ng/mL TNFα for 10min. Cells were then harvested and washed once in PBS + 1mM EDTA. Cells were then lysed in Cytoplasmic Extract Buffer (CEB) [10mM HEPES-KOH (pH 7.9), 250mM NaCl, 1mM EDTA, 0.5% Nonidet P-40, 0.2% Tween 20, 20mM β-glycerophosphate, 2mM DTT, 10mM NaF, 1mM sodium orthovanadate, 1mM PMSF, 10μg/mL aprotinin]. Protein concentrations were determined by Bradford Assay. 200μg lysates were immunoprecipitated with IKKγ antibody for 2 h at 4°C. Protein A-Sepharose beads were added and incubated for 1 h at 4°C. The immunoprecipitated samples were washed twice with CEB and twice with Kinase Buffer (KB) [20mM HEPES (pH 7.7), 100mM NaCl, 10mM $MgCl_2$, 20mM β-glycerophosphate, 2mM DTT, 10mM NaF, 0.1mM sodium orthovanadate, 1mM PMSF]. Samples were then resuspended in 2X KB with 20μM ATP. 1μCi [γ-^{32}P]-ATP and 0.5μg GST-IκB$^{(1-54)}$ bacterially expressed purified protein were added to each reaction and incubated at 30°C for 30 min. Proteins were separated

by 10% SDS-PAGE, Coomaisse stained, dried, and exposed to film or a phosphorimager (BioRad) screen directly. Band intensities were quantified using Quantity One Software.

Electrophoretic Mobility Shift Assay (EMSA)

Cells were collected in PBS, 1mM EDTA, pelleted at 2000 g, resuspended in 200µl CE buffer (10mM Hepes-KOH pH7.9, 60mM KCl, 1mM EDTA, 0.5% NP-40, 1mM DTT, 1mM PMSF) and vortexed. Nuclei were pelleted at 4000 g, and the supernatant was removed. Nuclei were resuspended in 50µl NE buffer (250mM Tris pH7.8, 60mM KCl, 1mM EDTA, 1mM DTT, 1mM PMSF) and lysed by 3 freeze-thaw cycles. Nuclear lysates were cleared by centrifugation and normalized to a concentration of 1µg/µl following Bradford assay. 2µg of total nuclear protein was reacted at room temperature for 15 min. with excess ^{32}P-labeled 30 bp double-stranded oligonucleotide containing a consensus κB-site (AGCTTGCTACAA**GGGACTTTCC**GCTGTCTACTTT) in 6µl binding buffer (10mM Tri.Cl pH7.5, 50mM NaCl, 10% glycerol, 1% NP-40, 1mM EDTA, 0.1µg/µl polydIdC). Complexes were resolved on a non-denaturing 5% acrylamide (30:0.8) gel containing 5% glycerol and 1x TGE (24.8mM Tris, 190mM glycine, 1mM EDTA) and visualized by autoradiography and/or quantified using a Phosphorimager (Bio-Rad).

Results

Although all four members of the FGFR family are similar in structure, FGFR4 and FGFR2 share only 57% amino acid identity [32] and are expressed in distinct patterns in various cell types. Therefore, we sought to determine if FGFR2 was able to interact with IKKβ as we have previously shown for FGFR4. HEK293 cells were transfected with FGFR2 and IKKβ and immunoprecipitated for IKKβ. FGFR2 WT as well as FGFR2 KD were able to interact with IKKβ, indicating as with FGFR4, the kinase activity of the receptor is not important for the interaction (Figure 8-1A). We confirmed this interaction in the opposite direction by immunoprecipitating FGFR2 and immunoblotting for IKKβ (Figure 8-1B). IKKβ forms an active complex with IKKα and IKKγ in order to function in the cell. Of interest was determining whether FGFR2 interacts with free IKKβ or with the IKK complex. HEK293 cells were transfected with IKKβ or FGFR2 and lysed in NP-40 lysis buffer. Lysates were immunoprecipitated for IKKγ and immunoblotted for either FGFR2 or IKKβ. As seen in Figure 8-1C, FGFR2 co-immunoprecipitates with IKKγ, and this interaction increases with overexpression of IKKβ. Similarly, IKKβ co-immunoprecipitates with IKKγ, and this association increases with overexpressed FGFR2. This indicates that FGFR2 does interact with the IKK complex through IKKβ and that overexpression of either protein leads to increased interaction with the IKK complex.

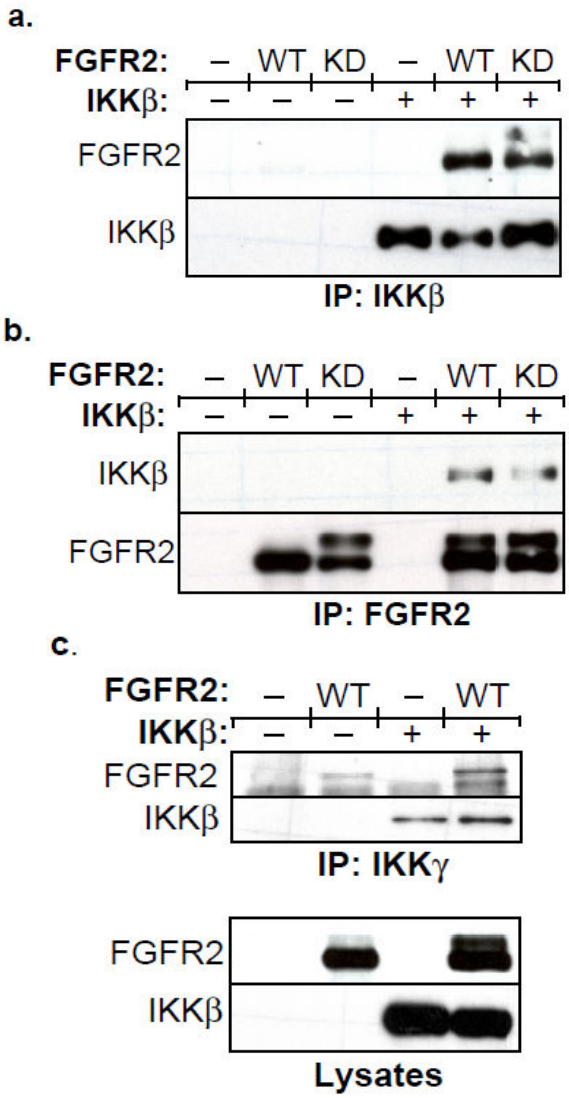

Figure 8-1. Novel interaction of IKKβ with FGFR2
(A) Full-length IKKβ and full-length FGFR2 derivatives were transfected in HEK293 cells to examine *in vivo* association. Cells were lysed in 1% NP-40 lysis buffer and immunoprecipitated with IKKβ (H-4) antibody. Immunoblot analysis was performed with FGFR2 (C-17) antibody (top panel). The membrane was stripped and reprobed with anti-IKKβ (bottom panel). (B) Cells were transfected and lysed as in (A) then immunoprecipitated with FGFR2 (C-17) antibody. Immunoblot analysis was performed with IKKβ (H-4) antibody (top panel). The membrane was stripped and reprobed with anti-FGFR2 (bottom panel). (C) Cells were transfected and lysed as in (A), then immunoprecipitated with IKKγ antibody. Immunoblot analysis was performed with FGFR2 (C-17) antibody (top panel). The membrane was stripped and reprobed with anti- IKKβ (second panel). Expression of FGFR2 and IKKβ was detected by immunoblot of lysates (lower two panels).

IKKβ is activated by serine phosphorylation, which leads to phosphorylation and degradation of IκB. This releases NFκB to translocate to the nucleus and transcribe a variety of genes important for the inflammatory pathway. One group has shown that IKKβ may be tyrosine phosphorylated by Src, and provide evidence that this leads to an increase in IKK activity [30, 31]. We have recently shown that FGFR4 activation leads to tyrosine phosphorylation of IKKβ, but this leads to inactivation of IKK [9]. We sought to determine whether this tyrosine phosphorylation of IKKβ is specific to FGFR4 or if FGFR2 is also able to phosphorylate IKKβ. HEK293 cells were transfected with FGFR2 WT, FGFR2 KD, and IKKβ. Cells were lysed with RIPA lysis buffer, immunoprecipitated using an IKKβ antibody, and immunoblotted with an anti-phosphotyrosine antibody. FGFR2 WT was able to tyrosine phosphorylate IKKβ, while FGFR2 KD was not, indicating that the kinase activity of FGFR2 is essential for the tyrosine phoshorylation of IKKβ and that this activity is not specific to FGFR4 (Figure 8-2, top panel). The membrane was stripped and re-probed for IKKβ to show equal amounts of protein were immunoprecipitated (second panel). Lysates were immunoblotted with FGFR2 and IKKβ antibodies to show equal expression (bottom two panels).

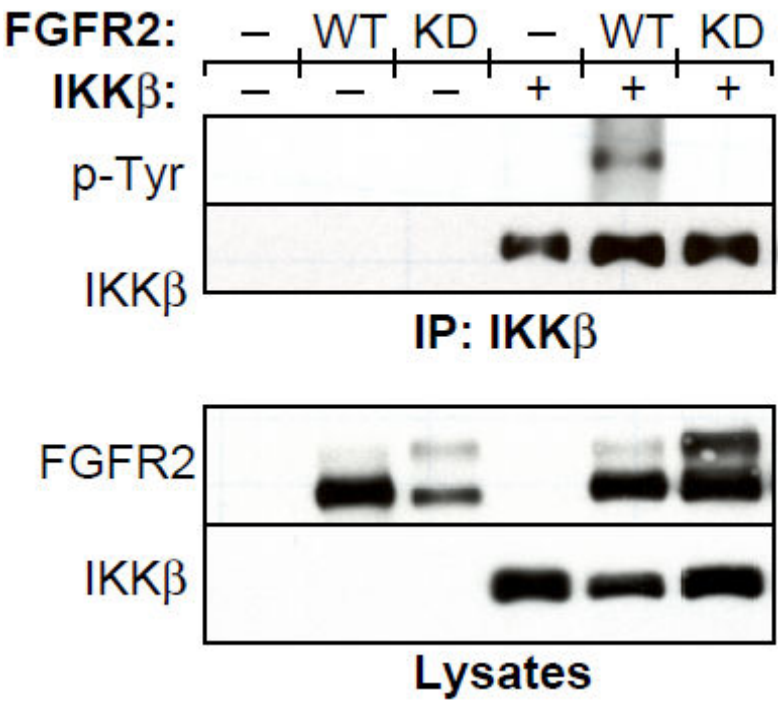

Figure 8-2. Tyrosine phosphorylation of IKKβ by FGFR2.
HEK293 cells were tranfected with IKKβ and FGFR2 derivatives. Cells were lysed in RIPA and immunoprecipitated with IKKβ (H-4) antibody. Immunoblot analysis was performed with the phosphotyrosine-specific antibody 4G10 (top panel). The membrane was stripped and reprobed with IKKβ (H-4) antibody (second panel). The expression of the FGFR2 derivatives and IKKβ in the lysate is shown (lower two panels).

We have previously shown that FGFR4 interaction with IKKβ leads to a decrease in IKK activity and that the kinase activity of the receptor is important for this effect. To determine whether FGFR2 kinase activity has the same effect on IKK activity, we performed a kinase assay using GST-IκB as a substrate. FGFR2 WT, FGFR2 C278F (a kinase active mutation) [33], and FGFR2 KD were transfected into HEK293 cells, followed by stimulation with TNFα. Equal amounts of total protein were subjected to immunoprecipitation with an IKKγ antibody to obtain an active IKK complex. The resulting immunoprecipitates were subjected to *in vitro* kinase assays utilizing GST-IκB$^{(1-54)}$ as the substrate [34]. The reactions were separated by SDS PAGE, and phosphorylation of GST-IκB$^{(1-54)}$ was visualized using a Phosphorimager and quantified (Figure 8-3A and B). Treatment with TNFα led to a dramatic increase in IKK activity. Quantification of TNFα-induced IKK activity was set at a value of 1 and all other samples were relative to this sample. Expression of FGFR2 WT decreased IKK activity by about 35%, while expression of the kinase active FGFR2 C278F led to a 50% decrease in IKK activity. Expression of the kinase-dead FGFR2 led to a minor decrease in IKK activity, indicating the kinase activity of FGFR2 is important for the observed decrease in IKK activity (Figure 8-3B).

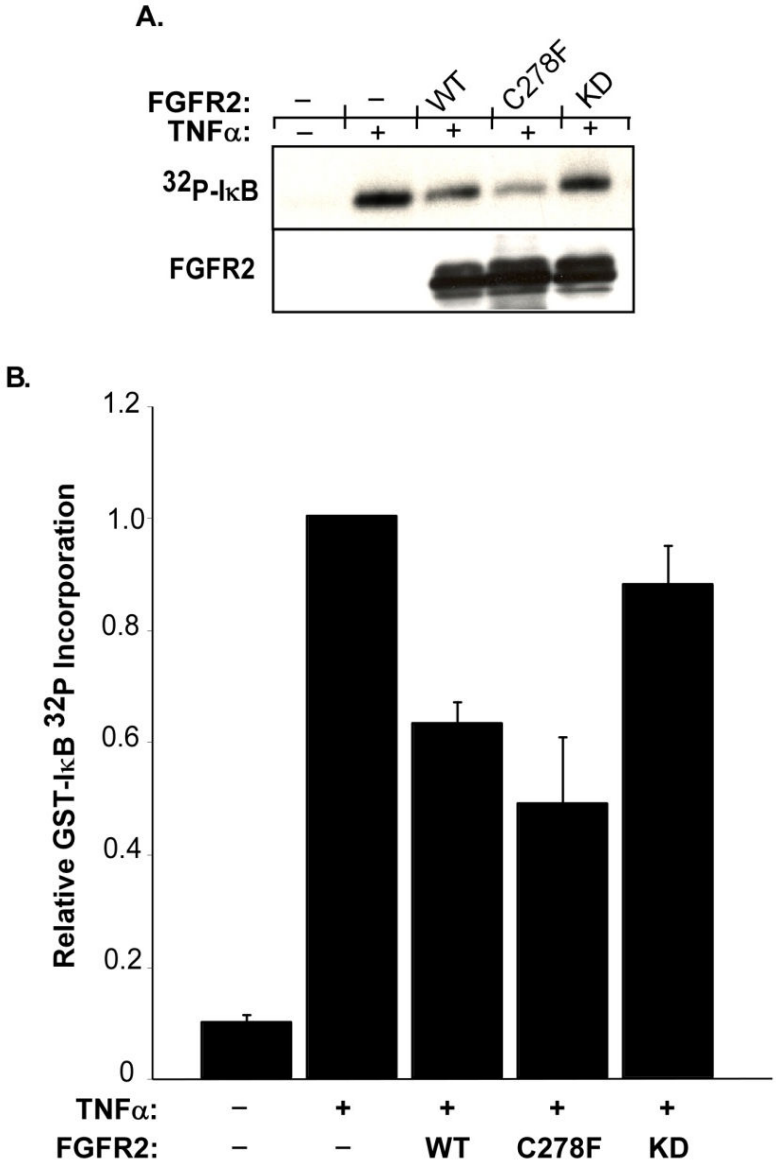

Figure 8-3. FGFR2 expression inhibits TNFα-induced IKKβ activity.
(A) HEK293 cells were transfected with empty vector or the indicated FGFR2 constructs, then starved for 16 h. Cells were then stimulated with TNFα for 10 min. The IKK complex was then immunoprecipitated from cytoplasmic extracts and subjected to an *in vitro* kinase assay utilizing GST-IkB$^{(1-54)}$ as substrate. The top panel shows ^{32}P incorporation on GST-IkB$^{(1-54)}$ while the second panel shows FGFR2 expression in the lysates. (B) Kinase reactions described in (A) were exposed to a Phosphorimager (Bio-Rad). Quantification of ^{32}P incorporation into GST-IkB was performed using the Quantity One software (Bio-Rad). The average ^{32}P incorporation from three independent experiments, normalized to mock transfected cells stimulated with TNFα, is shown +/- std. dev.

After observing that FGFR2 kinase activity leads to a decrease in IKK activity, we sought to examine downstream NFκB activity by EMSA. HEK293 cells overexpressing various constructs of FGFR2 were stimulated with TNFα, lysed, and nuclear extracts were collected. Equal amounts of protein were subjected to an EMSA using a ^{32}P-labeled probe containing a consensus kB-site. TNFα treatment alone led to a dramatic increase in NFκB activity as measured by a shift in the probe. Overexpression of FGFR2 decreased the TNFα-induced NFκB activity by 25%, while overexpression of the kinase active C278F FGFR2 mutant decreased NFκB activity even further. The kinase-dead mutant of FGFR2 was unable to decrease the TNFα-induced NFκB activity, indicating the kinase activity of the receptor is essential for the observed decrease in NFκB activity (Figure 8-4A). Quantification of these results are shown in Figure 8-4B and represent three independent experiments.

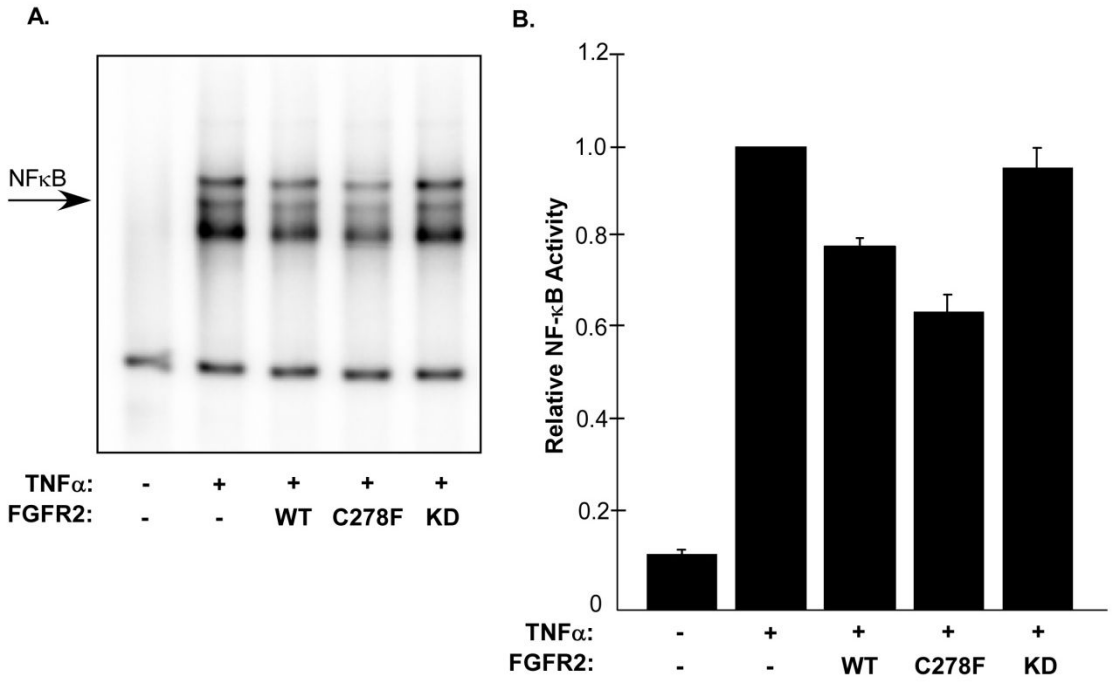

Figure 8-4. Inhibition of NFκB activity by FGFR2.
(A) HEK293 cells were stimulated with vehicle or TNFα for 30 min. Nuclear extracts were prepared and equal amounts of protein (2 μg) were subjected to an electrophoretic mobility shift assay with ^{32}P-labeled 30bp double-stranded oligonucleotide containing a consensus kB-site. (B) Samples from (A) were exposed to a phosphorimager (Bio-Rad). Quantification of NF-kB binding to the probe was performed using the Quantity One software (Bio-Rad). The average NF-kB binding from three independent experiments, normalized to mock transfected cells stimulated with TNFα, is shown +/- std. dev.

As described earlier, FGFR2 expression has been implicated in the progression and pathogenesis of breast cancer and endometrial cancer [21-27]. Research has found that under certain conditions in specific cell types, FGFR2 may protect cells from inflammation and may be considered a tumor suppressor [1-8]. We sought to understand the role of FGFR2 activation in T47D breast cancer cells, which express high levels of the FGFR2b isoform [35]. Of all the FGFR2 isoforms, FGFR2b has been most widely associated with a protective effect against inflammatory insults, and we hypothesized that activation of this receptor would lead to a decrease in NFκB signaling in these breast cancer cells. TNFα treatment alone led to a strong activation of NFκB, while FGF8b pre-treatment decreased this effect (Figure 8-5A). These results are quantified in Figure 8-5B and indicate that FGF8b pre-treatment decreases NFκB activity by 40%.

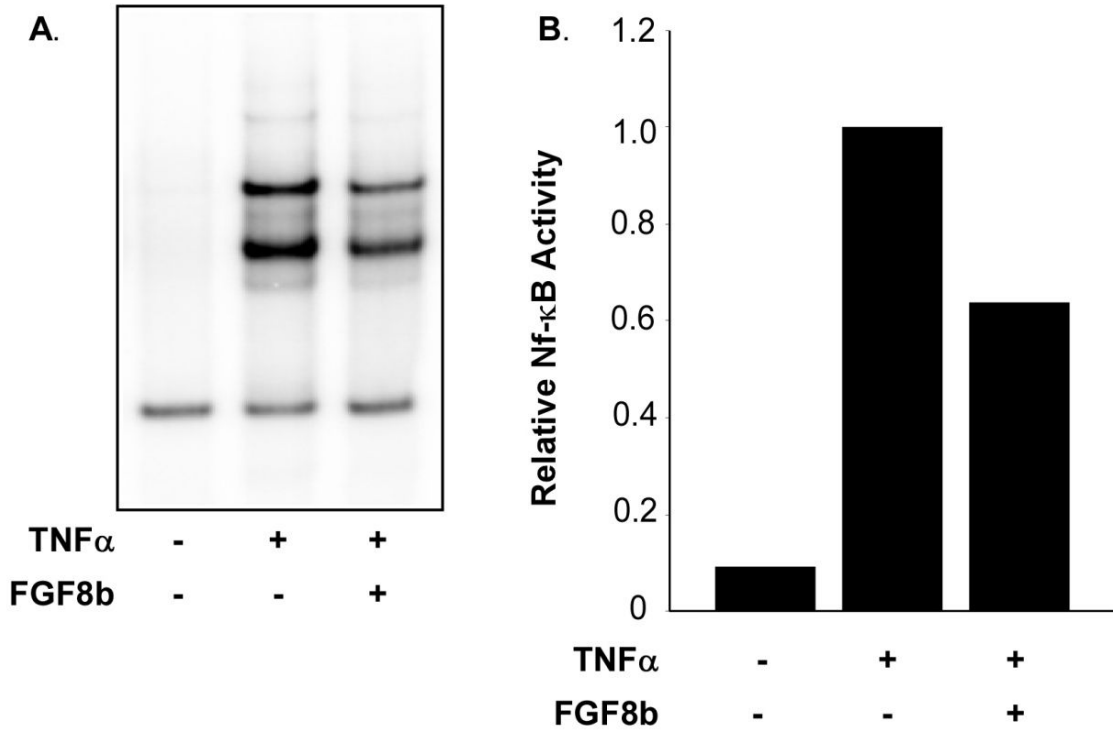

Figure 8-5. Stimulation of T47D cells with FGF8b leads to a decrease in NFκB activity.

(A) T47D cells were stimulated with vehicle for 30 min, TNFα for 30 min, or FGF8b for 10 min prior to the addition of TNFα for an additional 30 min. Nuclear extracts were prepared and equal amounts of protein (2 μg) were subjected to an electrophoretic mobility shift assay with ^{32}P-labeled 30bp double-stranded oligonucleotide containing a consensus kB-site. (B) Samples from (A) were exposed to a phosphorimager (Bio-Rad). Quantification of NF-kB binding to the probe was performed using the Quantity One software (Bio-Rad). The average NF-kB binding from three independent experiments, normalized to mock transfected cells stimulated with TNFα, is shown +/- std. dev.

Discussion

We have previously identified the novel interaction of FGFR4 with IKKβ and shown that this interaction leads to a decrease in IKK and NFκB activity. In this paper, we show that FGFR2 interacts with IKKβ as well. Additionally, FGFR2 kinase activity is essential for tyrosine phosphorylation of IKKβ. The kinase activity of the receptor is also important for a decrease in IKK activity as measured in a kinase assay using IκB as a substrate, as well as NFκB activity as measured in an EMSA. Taken together, these results implicate FGFR2 in the inflammatory pathway and indicate the activation of this receptor may play a protective role against inflammatory insults.

FGFR2 kinase activity is important for tyrosine phosphorylation of IKKβ. However, it is yet to be determined whether the tyrosine phosphorylation of IKKβ is essential for the observed decrease in activity. We are currently working on mutation of the various tyrosine residues in IKKβ as well as determination of phosphotyrosine-peptides by mass-spectrometry analysis. We are also currently working on determining which domain or domains of IKKβ interact with FGFR2 by *in vitro* binding assays using GST-fused constructs.

Evidence exists to suggest that FGFR2 may play a role as a tumor suppressor in some circumstances and a tumor promoter in other circumstances. Previous research has identified FGFR2 in the pathogenesis of breast cancer [21-25]. Additionally, the FGFR2b isoform has been shown to decrease inflammation and play a protective role in the skin [6-8], lung [1-4], and bowel [5]. Our results indicate that in breast cancer cells expressing high levels of the FGFR2b isoform, activation of this receptor leads to a

decrease in the activation of the inflammatory pathway. We have also shown in HEK293 cells, expression of FGFR2 leads to a decrease in NFκB activity, indicating both FGFR2 and the FGFR2b isoform are able to inhibit NFκB activity. It's possible that expression of various FGF ligands in different types of cells or cancers may play a role in dictating how FGFR2 functions. Additionally, dependence on NFκB activity may also determine a specific cell's dependence on FGFR2 as a tumor suppressor. Further research into the various roles of FGFR2 in cancer progression is needed to fully understand how the activity of this signaling pathway might be exploited in the fight against cancer.

Acknowledgements

We are grateful to Dr. Alexander Hoffmann and members of his laboratory, particularly Shannon Werner and Ellen O'Dea, for valuable suggestions and experimental advice; to Mark Hannink for advice and reagents; and to Laura Castrejon for editorial assistance. This investigation was supported by: NIH/NCI #5 R01 CA090900; grants from the UC Cancer Research Coordinating Committee and the UC California Breast Cancer Research Program #14IB-0065; a Ruth L. Kirschstein National Research Service Award NIH/NCI T32 CA009523; the Achievement Rewards for College Scientists Foundation; and the UCSD Chancellor's Interdisciplinary Collaboratories Fellowship. Chapter 8, in full, is material that is material that is currently being prepared for submission. The dissertation author was a primary investigator of this work.

References

1. Baba, Y. *et al.* Keratinocyte growth factor gene transduction ameliorates acute lung injury and mortality in mice. *Hum Gene Ther* 18, 130-141 (2007).

2. Plantier, L. *et al.* Keratinocyte growth factor protects against elastase-induced pulmonary emphysema in mice. *Am J Physiol Lung Cell Mol Physiol* 293, L1230-1239 (2007).

3. Tillie-Leblond, I. *et al.* Keratinocyte growth factor improves alterations of lung permeability and bronchial epithelium in allergic rats. *Eur Respir J* 30, 31-39 (2007).

4. Chapman, K.E., Waters, C.M. & Miller, W.M. Continuous exposure of airway epithelial cells to hydrogen peroxide: protection by KGF. *J Cell Physiol* 192, 71-80 (2002).

5. Han, D.S. *et al.* Keratinocyte growth factor-2 (FGF-10) promotes healing of experimental small intestinal ulceration in rats. *Am J Physiol Gastrointest Liver Physiol* 279, G1011-1022 (2000).

6. Kovacs, D. *et al.* Keratinocyte growth factor down-regulates intracellular ROS production induced by UVB. *J Dermatol Sci* 54, 106-113 (2009).

7. Grose, R. *et al.* The role of fibroblast growth factor receptor 2b in skin homeostasis and cancer development. *Embo J* 26, 1268-1278 (2007).

8. Gartside, M.G. *et al.* Loss-of-function fibroblast growth factor receptor-2 mutations in melanoma. *Mol Cancer Res* 7, 41-54 (2009).

9. Drafahl, K.A., McAndrew, C.W., Meyer, A.N., Haas, M. & Donoghue, D.J. The novel interaction of FGFR4 and IKKβ negatively regulates NFκB activity in DU145 prostate cancer cells. *Manuscript in submission.* (2009).

10. Hehr, U. & Muenke, M. Craniosynostosis syndromes: from genes to premature fusion of skull bones. *Mol Genet Metab* 68, 139-151 (1999).

11. Katzen, J.T. & McCarthy, J.G. Syndromes involving craniosynostosis and midface hypoplasia. *Otolaryngol Clin North Am* 33, 1257-1284, vi (2000).

12. McIntosh, I., Bellus, G.A. & Jab, E.W. The pleiotropic effects of fibroblast growth factor receptors in mammalian development. *Cell Struct Funct* 25, 85-96 (2000).

13. Passos-Bueno, M.R. *et al.* Clinical spectrum of fibroblast growth factor receptor mutations. *Hum Mutat* 14, 115-125 (1999).

14. Park, W.J. *et al.* Novel FGFR2 mutations in Crouzon and Jackson-Weiss syndromes show allelic heterogeneity and phenotypic variability. *Hum Mol Genet* 4, 1229-1233 (1995).

15. Freitas, E.C., Nascimento, S.R., de Mello, M.P. & Gil-da-Silva-Lopes, V.L. Q289P mutation in FGFR2 gene causes Saethre-Chotzen syndrome: some considerations about familial heterogeneity. *Cleft Palate Craniofac J* 43, 142-147 (2006).

16. Lajeunie, E. *et al.* Mutation screening in patients with syndromic craniosynostoses indicates that a limited number of recurrent FGFR2 mutations accounts for severe forms of Pfeiffer syndrome. *Eur J Hum Genet* 14, 289-298 (2006).

17. Wilkie, A.O. *et al.* Clinical dividends from the molecular genetic diagnosis of craniosynostosis. *Am J Med Genet A* 143, 1941-1949 (2007).

18. Robertson, S.C. *et al.* Activating mutations in the extracellular domain of the fibroblast growth factor receptor 2 function by disruption of the disulfide bond in the third immunoglobulin-like domain. *Proc Natl Acad Sci U S A* 95, 4567-4572 (1998).

19. Galvin, B.D., Hart, K.C., Meyer, A.N., Webster, M.K. & Donoghue, D.J. Constitutive receptor activation by Crouzon syndrome mutations in fibroblast growth factor receptor (FGFR)2 and FGFR2/Neu chimeras. *Proc Natl Acad Sci U S A* 93, 7894-7899 (1996).

20. Takeda, M. *et al.* AZD2171 shows potent antitumor activity against gastric cancer over-expressing fibroblast growth factor receptor 2/keratinocyte growth factor receptor. *Clin Cancer Res* 13, 3051-3057 (2007).

21. Tamaru, N. *et al.* Estrogen receptor-associated expression of keratinocyte growth factor and its possible role in the inhibition of apoptosis in human breast cancer. *Lab Invest* 84, 1460-1471 (2004).

22. Hishikawa, Y., Tamaru, N., Ejima, K., Hayashi, T. & Koji, T. Expression of keratinocyte growth factor and its receptor in human breast cancer: its inhibitory role in the induction of apoptosis possibly through the overexpression of Bcl-2. *Arch Histol Cytol* 67, 455-464 (2004).

23. Imagawa, W. & Pedchenko, V.K. In vivo inhibition of keratinocyte growth factor receptor expression by estrogen and antagonism by progesterone in the mouse mammary gland. *J Endocrinol* 171, 319-327 (2001).

24. Rotolo, S. *et al.* Silencing of keratinocyte growth factor receptor restores 5-fluorouracil and tamoxifen efficacy on responsive cancer cells. *PLoS ONE* 3, e2528 (2008).

25. Cha, J.Y., Lambert, Q.T., Reuther, G.W. & Der, C.J. Involvement of fibroblast growth factor receptor 2 isoform switching in mammary oncogenesis. *Mol Cancer Res* 6, 435-445 (2008).

26. Li, Y. & Rinehart, C.A. Regulation of keratinocyte growth factor expression in human endometrium: implications for hormonal carcinogenesis. *Mol Carcinog* 23, 217-225 (1998).

27. Niu, J. *et al.* Keratinocyte growth factor/fibroblast growth factor-7-regulated cell migration and invasion through activation of NF-κB transcription factors. *J Biol Chem* 282, 6001-6011 (2007).

28. Delhase, M., Hayakawa, M., Chen, Y. & Karin, M. Positive and negative regulation of IκB kinase activity through IKKβ subunit phosphorylation. *Science* 284, 309-313 (1999).

29. Karin, M. The IκB kinase - a bridge between inflammation and cancer. *Cell Res* 18, 334-342 (2008).

30. Huang, W.C., Chen, J.J. & Chen, C.C. c-Src-dependent tyrosine phosphorylation of IKKβ is involved in tumor necrosis factor-α-induced intercellular adhesion molecule-1 expression. *J Biol Chem* 278, 9944-9952 (2003).

31. Huang, W.C., Chen, J.J., Inoue, H. & Chen, C.C. Tyrosine phosphorylation of I-κ B kinase α/ β by protein kinase C-dependent c-Src activation is involved in TNF-α-induced cyclooxygenase-2 expression. *J Immunol* 170, 4767-4775 (2003).

32. Jaye, M., Schlessinger, J. & Dionne, C.A. Fibroblast growth factor receptor tyrosine kinases: molecular analysis and signal transduction. *Biochim Biophys Acta* 1135, 185-199 (1992).

33. Meyers, G.A. *et al.* FGFR2 exon IIIa and IIIc mutations in Crouzon, Jackson-Weiss, and Pfeiffer syndromes: evidence for missense changes, insertions, and a deletion due to alternative RNA splicing. *Am J Hum Genet* 58, 491-498 (1996).

34. DiDonato, J.A., Hayakawa, M., Rothwarf, D.M., Zandi, E. & Karin, M. A cytokine-responsive IκB kinase that activates the transcription factor NF-κB. *Nature* 388, 548-554 (1997).

35. Chandler, L.A. *et al.* Prevalent expression of fibroblast growth factor (FGF) receptors and FGF2 in human tumor cell lines. *Int J Cancer* 81, 451-458 (1999).

Appendix A

Nordihydroguaiaretic Acid Inhibits an Activated Fibroblast Growth Factor Receptor 3 Mutant and Blocks Downstream Signaling in Multiple Myeloma Cells

April N. Meyer, Christopher W. McAndrew, and Daniel J. Donoghue

Department of Chemistry and Biochemistry, Moores UCSD Cancer Center, University of California, San Diego, La Jolla, California

Abstract

Activating mutations within fibroblast growth factor receptor 3 (FGFR3), a receptor tyrosine kinase, are responsible for human skeletal dysplasias including achondroplasia and the neonatal lethal syndromes, Thanatophoric Dysplasia (TD) type I and II. Several of these same FGFR3 mutations have also been identified somatically in human cancers, including multiple myeloma, bladder carcinoma, and cervical cancer. Based on reports that strongly activated mutants of FGFR3 such as the TDII (K650E) mutant signal preferentially from within the secretory pathway, the inhibitory properties of nordihydroguaiartic acid (NDGA), which blocks protein transport through the Golgi, were investigated. NDGA was able to inhibit FGFR3 autophosphorylation both *in vitro* and *in vivo*. In addition, signaling molecules downstream of FGFR3 activation such as signal transducers and activators of transcription (STAT)1, STAT3, and mitogen-activated protein kinase (MAPK) were inhibited by NDGA treatment. Using HEK293 cells expressing activated FGFR3-TDII, together with several multiple myeloma cell lines expressing activated forms of FGFR3, NDGA generally resulted in a decrease in MAPK activation by 1 hour, and resulted in increased apoptosis over 24 hours. The effects of NDGA on activated FGFR3 derivatives targeted either to the plasma membrane or the cytoplasm were also examined. These results suggest that inhibitory small molecules such as NDGA that target a specific subcellular compartment may be beneficial in the inhibition of activated receptors such as FGFR3 that signal from the same compartment. [Cancer Res 2008;68(18):7362–70]

Introduction

Receptor tyrosine kinases (RTKs) represent important signal transducers for the transmission of information across the cell membrane, including 58 distinct receptors in 16 different families of homologous proteins in humans (1, 2). The fibroblast growth factor receptor (FGFR) family includes four closely related receptors, designated FGFR1, FGFR2, FGFR3, and FGFR4. All FGFRs exhibit a cleaved NH_2-terminal signal sequence that directs the nascent protein into the endoplasmic reticulum (ER), followed by three extracellular immunoglobulin (Ig)-like domains, a membrane-spanning domain, and a split tyrosine kinase domain (3, 4), and are activated by FGFs, a large family of some 20 related growth factors (5–8). The ligand-binding specificity differs for each FGFR family member, with alternative splicing of FGFR transcripts resulting in further distinctions in ligand specificity accompanied by altered biological properties (4, 9). FGFR activation controls an array of biological processes, including cell growth, differentiation, migration, wound healing, and angiogenesis. Aberrant activation of these receptors, often through gain-of-function mutations, is associated with many developmental and skeletal disorders. Mutational activation of FGFR3 is responsible for the relatively common skeletal dwarfism, achondroplasia, due to the G380R mutation within the transmembrane domain, whereas strong activation by the mutation K650E within the kinase domain results in the neonatal lethal syndrome, thanatophoric dyspasia (TD) type II (10).

Aberrant signal transduction arising from expression of a constitutively activated FGFR3 is also an important event in a variety of human neoplasias, especially multiple myeloma and bladder carcinoma (11–15). Multiple myeloma is typified by the accumulation of secretory plasma cells in the bone marrow, which exhibit low proliferation but an extended life span. A frequent translocation observed in multiple myeloma, t(4;14)(p16.3;q32.3), involves the *FGFR3* gene, and results in increased expression of *FGFR3* alleles (11, 12). This translocation occurs with an incidence of ~20% in multiple myeloma and places the *FGFR3* gene located at 4p16.3 in proximity with the 3′ IgH enhancer at 14q32.3, leading to significant FGFR3 overexpression (11). Furthermore, FGFR3 overexpression is often accompanied by mutational activation, including the mutations Y373C and K650E, corresponding to germline FGFR3 mutations that cause the lethal skeletal syndromes TDI and TDII, respectively (10, 16). The aberrant signaling of overexpressed, mutated FGFR3, acting in concert with other dysregulated genes such as cyclin D1, c-maf, and MMSET, evidently contributes to the increased proliferative potential of B-cell myelomas (17). Mutational activation of FGFR3 has also been reported in human bladder and cervical carcinomas (13–15), including the mutations corresponding to R248C, S249C, G370C, and K650E, previously identified as causing TDI or TDII (10, 16).

Several recent reports show that the high level of kinase activity associated with the strongly activated FGFR3 mutants such as TDII (K650E) leads to accumulation of immature/mannose-rich, phosphorylated receptors in the ER. This can result in direct recruitment of Jak1 and activation of signal transducers and activators of transcription (STAT) 1 from the ER, as well as activation of Erk1/2 from the ER through a FRS2-independent and phospholipase C (PLC) γ-independent pathway (18–20). Given the ability of FGFR3 to signal from intracellular compartments within the secretory pathway, we investigated the possible inhibitory properties of a drug that specifically blocks ER/Golgi transport. Nordihydroguaiaretic acid (NDGA), a naturally occurring polyhydroxyphenolic compound isolated from the creosote bush,

Requests for reprints: Daniel J. Donoghue, University of California, San Diego, UH 6114, 9500 Gilman Drive, La Jolla, CA 92093-0367. Phone: 858-534-2463; Fax: 858-534-7481; E-mail: ddonoghue@ucsd.edu.

doi:10.1158/0008-5472.CAN-08-0575

Larrea divaricatta, has been previously characterized as a lipoxygenase (LOX) inhibitor, as a strong antioxidant, and as an inhibitor of protein transport from the ER to Golgi, leading to a redistribution of Golgi proteins to the ER (21–24). NDGA has also been shown to have effects on cell proliferation, apoptosis, and differentiation. Recently, it was shown to have potentially valuable inhibitory effects against specific RTKs such as insulin-like growth factor receptor (IGF-IR), HER2/neu, and platelet-derived growth factor receptor (25–28).

The experiments presented here explore the ability of NDGA to inhibit signaling by activated FGFR3, including kinase activation and downstream signaling associated with an activated receptor. Given the ability of NDGA to inhibit other RTKs, and the ability of NDGA to collapse the secretory compartment from which activated FGFR3 is known to signal (18–20), we examined the possibility that NDGA would be particularly effective against the strongly activated FGFR3 mutant K650E. Indeed, NDGA was able to inhibit activation of the downstream signaling proteins STAT1, STAT3, and mitogen-activated protein kinase (MAPK). In addition, NDGA increased apoptosis in cells expressing FGFR3-TDII, as measured by poly(ADP)ribose polymerase (PARP) cleavage. NDGA was also able to increase apoptosis in the multiple myeloma cell line KMS-18 that expresses high levels of FGFR3 G384D. To examine possible therapeutic effects of NDGA, multiple myeloma–derived cell lines were treated with FGF2 to activate FGFR3, and the effects of NDGA treatment on downstream signaling pathways were observed. The results are discussed with respect to other therapeutic approaches for treatment of cancers presenting overexpressed and/or mutated FGFR3.

Materials and Methods

FGFR constructs. The full-length wild-type (WT) and kinase active (TDII:K650E) FGFR3 have been described previously (29). The membrane-localized kinase domain derivatives of FGFR3 have also been previously described (30).

Antibodies and reagents. Antibodies were obtained from the following sources: FGFR3 (C-15), STAT1 (E-23), STAT3 (C-20), β-tubulin (H-235) from Santa Cruz Biotechnology; 4G10 (antiphosphotyrosine) from Upstate Biotechnology; Phospho-STAT1 (Tyr701), Phospho-STAT3 (Tyr705; D3A7), Phospho-p44/42 MAPK (Thr202/Tyr204; E-10), cleaved PARP (Asp214) from Cell Signaling; MAPK (ERK1 + ERK2) from Zymed; and horseradish peroxidase (HRP) anti-mouse and HRP anti-rabbit from Amersham. Monoclonal antibody 10E6 was a gift from V. Malhotra Laboratory (University of California, San Diego, La Jolla, CA). Fluorescein-conjugated anti-mouse (Sigma), rhodamine-conjugated anti-rabbit (Boehringer-Mannheim), NDGA, and the poly (4:1 Glu, Tyr) peptide were obtained from Sigma. Zilueton was a gift from Dr. Edward Dennis (University of California, San Diego, La Jolla, CA).

Immunoprecipitation and immunoblot. HEK293 cells were grown in DMEM, supplemented with 10% fetal bovine serum (FBS) and incubated at 37°C in 10% CO_2. Cells (9×10^5) plated on 10-cm dishes were transfected the next day with 2 μg of DNA by calcium phosphate precipitation at 3% CO_2, as previously described (31, 32). After 18 to 20 h, cultures were moved back into 10% CO_2 for 4 to 6 h before starving in 0% DMEM or treating with NDGA in 10% FBS DMEM overnight. Cultures that were starved overnight were treated with NDGA at varying concentrations or time, as indicated in figure legends. Cells were harvested, washed once in PBS, and lysed in 1% NP40 Lysis Buffer [20 mmol/L Tris-HCl (pH 7.5), 137 mmol/L NaCl, 1% Nonidet P-40, 5 mmol/L EDTA, 50 mmol/L NaF, 1 mmol/L sodium orthovanadate, 1 mmol/L phenylmethylsulfonyl fluoride (PMSF), and 10 μg/mL aprotinin] or radioimmunoprecipitation assay buffer [RIPA; 50 mmol/L Tris-HCl (pH 8.0), 150 mmol/L NaCl, 1% Nonidet P-40, 0.5% sodium deoxycholate, 0.1% SDS, 50 mmol/L NaF, 1 mmol/L sodium orthovanadate, 1 mmol/L PMSF, and 10 μg/mL aprotinin]. Total protein was measured by Bradford Assay or Lowry Assay. Lysates were immunoprecipitated with antibody for 2 h at 4°C. Protein A-Sepharose beads were added and incubated for 2 h at 4°C. The immunoprecipitated samples were washed thrice with Lysis Buffer, boiled 5 min in sample buffer, and separated by 10% SDS-PAGE. Proteins were transferred to Immobilon-P membranes (Millipore) and blocked in 3% milk/TBS/0.05% Tween 20 or 3% bovine serum albumin (BSA)/TBS/0.05% Tween 20 (for anti-phosphotyrosine, anti–phospho-STAT1, and anti–phospho-STAT3 blots). Membranes were immunoblotted with antibodies at room temperature for 2 h or overnight at 4°C. After primary incubation, membranes were washed with TBS/0.05% Tween 20 and incubated with HRP-conjugated secondary antibodies. Proteins were detected by enhanced chemiluminescence (ECL; Amersham) or (Millipore). To reprobe with other antibodies, membranes were stripped of bound antibodies in stripping buffer [100 mmol/L 2-mercaptoethanol, 2% SDS, and 62.5 mmol/L Tris-HCl (pH 6.8)] and incubated for 1 h at 55°C.

***In vitro* kinase assays.** FGFR3-TDII was immunoprecipitated from 500 μg of total cell lysate per sample for 1.5 h at 4°C. Protein A-sepharose beads were added for 2 h. After 3 washes with Lysis Buffer, samples were washed once with Kinase Buffer [20 mmol/L Tris (pH 7.5), 10 mmol/L $MnCl_2$, and 5 mmol/L $MgCl_2$]. Immunoprecipitates were preincubated with NDGA in Kinase Buffer for 15 min on ice before the addition of ATP and the poly (4:1 Glu, Tyr) peptide and incubated at 37°C for 15 to 25 min. Reactions were washed thrice with cold Lysis Buffer before adding sample buffer. Proteins were separated by 7.5% or 10% SDS-PAGE and transferred to Immobilon-P membranes for immunoblotting, except for ^{32}P-labeled samples in which the gels were dried and exposed to film or a phosphor screen for use with a Phosphorimager.

Double label indirect immunofluorescence. HEK293 cells were seeded onto Collagen type I–coated glass coverslips (BD Biosciences) and transfected as above. After starving overnight, cells were treated with 30 μmol/L NDGA. At indicated time points, coverslips were fixed with 3% paraformaldehyde/PBS for 15 min, washed with PBS, and placed at −20°C in 50% glycerol/PBS. Before staining, cells were washed with PBS, permeabilized with 0.5% Triton X-100/PBS, and blocked with 3% BSA/PBS. The *cis*-Golgi was detected with monoclonal antibody 10E6 and fluorescein-conjugated anti-mouse secondary antibody. FGFR3 localization was detected with rabbit polyclonal antibody FGFR3 (C-15) and rhodamine-conjugated anti-rabbit secondary antibody. The nuclei were visualized by Hoechst dye added to the Rh secondary antibody mix. All antibodies were diluted in 3% BSA/PBS, and incubations were performed at room temperature. Coverslips were mounted on glass slides with 90% glycerol in 0.1 mol/L Tris (pH 8.5) plus phenylenediamine and photographed using a Nikon Microphot-FXA with a cooled CCD camera (Hamamatsu C5810).

Multiple myeloma cell lines. The human multiple myeloma cell lines, RPMI-8226, LP-1, KMS-18, and KMS-11, were a generous gift from Dr. Leslie Thompson (University of California, Irvine, Irvine, CA). They were grown in RPMI 1640 with L-glutamine medium, supplemented with 10% FBS and pen/strep, and incubated at 37°C in 5% CO_2. For FGF stimulation, 3×10^6 cells per 35-mm well were starved overnight in serum-free RPMI 1640. NDGA was added to the cultures for 1 h at 37°C before simulating with 10 ng/mL FGF2 and 1 μg/mL Heparin for 10 min at 37°C. Plates were put on ice, and cells were collected, transferred to tubes, and spun down for 2 min at 1 krpm. Cell pellets were washed once with PBS before the addition of RIPA Lysis Buffer. Thirty micrograms of total lysate was separated by 10% SDS-PAGE and processed for immunoblotting as described above. For NDGA treatment of the KMS-18 and KMS-11 cell lines, 6×10^6 cells per 5-cm plate were incubated at 37°C with various concentrations of NDGA for 1 h or overnight. Cells were collected by centrifugation as described above. Thirty micrograms of total lysate were separated by 10% SDS-PAGE and transferred to Immobilon-P membranes for immunoblotting.

Results

***In vitro* inhibition of FGFR3-TDII autophosphorylation by NDGA.** An activated FGFR3 clone containing the K650E mutation (FGFR3-TDII) was transfected into HEK293 cells. After an overnight starvation, the receptor was immunoprecipitated from the cell

lysate and subjected to *in vitro* kinase assays. In Fig. 1*A*, γ-^{32}P-ATP was used in the kinase reactions after preincubating with NDGA for 15 minutes. The NDGA concentration of 0.5 μmol/L caused a dramatic reduction in the autophosphorylation of FGFR3-TDII. In Fig. 1*B* and *C*, the kinase reaction was performed in the absence of hot ATP and the phosphotyrosine on the receptor was detected by immunoblotting with a phospho-specific antibody. These results suggest a direct interaction of NDGA with FGFR3. To address if NDGA was inhibiting the ATP binding pocket of FGFR3-TDII, *in vitro* kinase reactions were performed over a range of ATP concentrations in the presence of the peptide substrate poly (4:1 Glu, Tyr). The incorporation of ^{32}P from [γ-^{32}P]-ATP into the peptide was quantified and plotted (Fig. 1*D*). Increasing concentrations of ATP did not affect the K_m at various concentrations of NDGA, indicating the inhibitor NDGA is noncompetitive with ATP. Additionally, the inhibition of FGFR3-TDII autophosphorylation was independent of ATP over the same concentration range (data not shown). This finding further supports the contention that NDGA is noncompetitive with ATP.

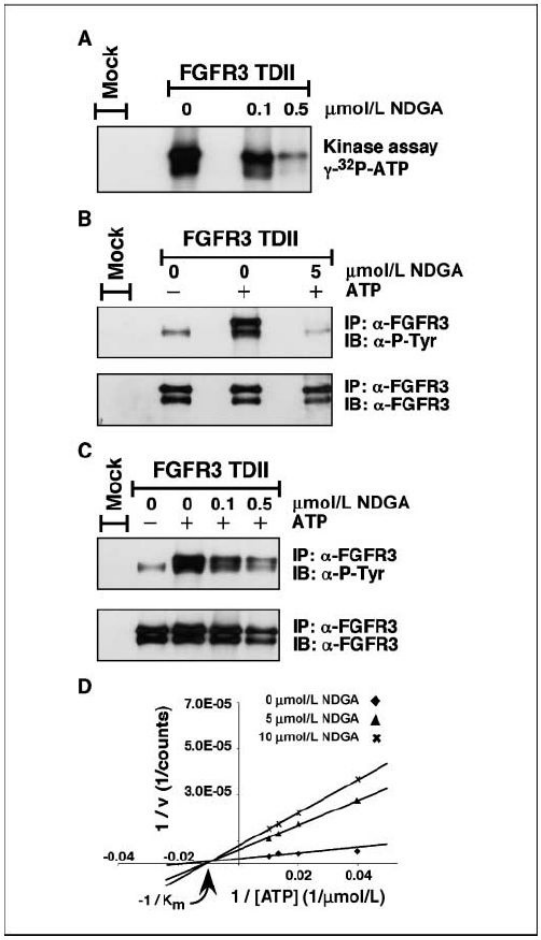

Figure 1. *In vitro* kinase assays. FGFR3-TDII was transfected into HEK293 cells. Twenty-four hours after transfection, cells were starved overnight in medium containing no serum. Cells were collected and lysed in 1% NP40 Lysis Buffer. FGFR3-TDII was immunoprecipitated (*IP*) from lysates as described in Materials and Methods. Immunoprecipitates were preincubated with 0.1, 0.5, or 5 μmol/L NDGA in Kinase Buffer for 15 min on ice before the addition of ATP and incubation at 37°C for 15 min. Proteins were separated by 7.5% SDS-PAGE. The kinase reactions in *A* were performed with 5 μCi [γ-^{32}P]-ATP per sample. The gel was dried and exposed to film directly. The kinase reactions in *B* and *C* were performed with 150 μmol/L ATP. The gels were transferred to Immobilon-P membranes for immunoblotting (*IB*) with antiphosphotyrosine (4G10) antisera (*top*). The membranes were stripped and reprobed with FGFR3 antiserum (*bottom*). Antibodies were detected by ECL. *D*, kinase reactions were performed using FGFR3-TDII immunoprecipitates obtained as in *A*, with 80 μg/mL of the poly (4:1 Glu, Tyr; Sigma) peptide substrate and increasing amounts of ATP (25, 50, 75, and 100 μmol/L) under increasing NDGA concentrations (0, 5, and 10 μmol/L). The reactions were separated by 10% SDS-PAGE. After staining, destaining, and drying, the gel was visualized using a Phosphorimager (Bio-Rad). Quantification of radioactive bands was performed using the Quantity One software (Bio-Rad).

NDGA reduces *in vivo* autophosphorylation of FGFR3. To examine the *in vivo* effect of NDGA on the autophosphorylation of FGFR3-TDII and WT FGFR3, transfected HEK293 cells were treated with 40 μmol/L NDGA for 1 h. As seen in Fig. 2*A*, the NDGA is able to reduce the autophosphorylation of both the WT and activated receptor. In Fig. 2*B*, the time dependence of the NDGA incubations was determined. A concentration of 30 μmol/L was able to begin to inhibit the receptor autophosphorylation in only 5 min, and phosphorylation was almost completely gone by 60 min. Next, we tested a broad range of NDGA concentrations with 40 μmol/L being the highest amount to examine the optimal effect. Figure 2*C* shows ~50% inhibition of FGFR3-TDII autophosphorylation with 10 μmol/L NDGA treatment. Also seen in Fig. 2*C* (*bottom*), there is a decrease in the amount of the immature form of the FGFR3-TDII receptor at 35 μmol/L NDGA. This is most likely due to the ability of NDGA to block ER/Golgi transport. Total cell lysate was examined for STAT1 activation in Fig. 2*D*. The phosphorylation on Y701 of STAT1 caused by FGFR3-TDII is attenuated at the 20 μmol/L concentration of NDGA.

FGFR3 localization and Golgi breakdown with NDGA treatment. Typically, the disassembly of the Golgi begins to occur rapidly after only a few minutes of NDGA treatment and is reversible (23). As seen in Fig. 3*A*, NDGA promoted the disassembly of the Golgi in ~15 min, whereas the subcellular localization of FGFR3-TDII seemed to become more punctate in the cytoplasm with increasing time. This may suggest that inhibition of the autophosphorylation of FGFR3-TDII by NDGA observed in Fig. 2 is due to the change in the receptor localization and/or the altered interaction with downstream molecules. To examine this hypothesis, we expressed targeted kinase domains of activated FGFR3 (30) and treated the cells with NDGA for up to 1 hour. As seen in Fig. 3*B*, the myrR3-TDII derivative, which is targeted to the plasma membrane by a myristylation signal, exhibits membrane localization that is unaltered by NDGA treatment. Similarly, in Fig. 3*C* the localization of the cytoR3-TDII derivative, targeted to the cytoplasm by a nonfunctional myristylation signal, seems unaltered with NDGA treatment.

NDGA reduction of FGFR3 downstream signaling. Next, we examined the change in downstream signaling molecules that are activated in the FGFR3 pathway. Previous work from our laboratory has shown the activation of STAT1, STAT3, and STAT5 in response to FGFR3 activation (31, 32). Given the importance of STAT activation in a variety of human malignancies (33), we surveyed STAT1 and STAT3 for altered activation in response to NDGA treatment. The phosphorylation of MAPK was also determined. In Fig. 4*A*, HEK293-transfected lysates were probed with

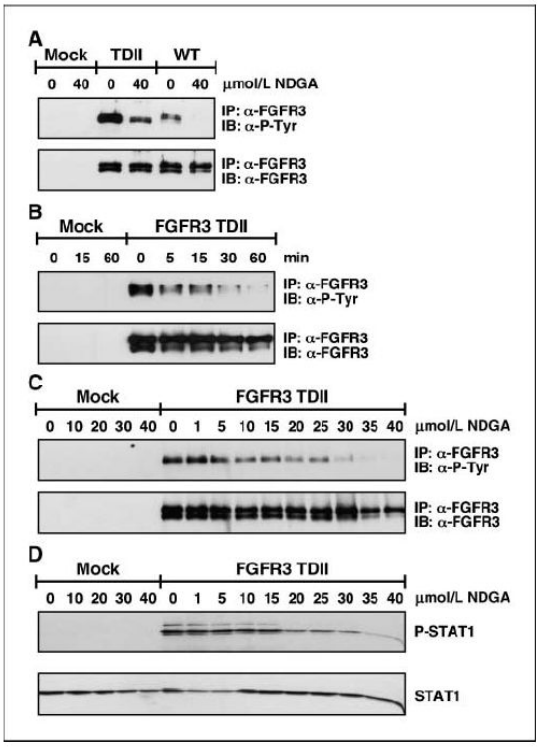

Figure 2. *In vivo* autophosphorylation of FGFR3. HEK293-transfected cells were starved overnight before treatment with NDGA. Cells were collected and lysed in 1% NP40 Lysis Buffer. *A,* FGFR3-TDII and FGFR3-WT–expressing cells were treated with 40 μmol/L NDGA for 1 h. FGFR3 was immunoprecipitated from lysates, separated by 10% SDS-PAGE, and transferred to Immobilon-P membrane for immunoblotting with antiphosphotyrosine (4G10; *top*) and FGFR3 antisera (*bottom*). Antibodies were detected by ECL. *B,* FGFR3-TDII–expressing cells were treated with 30 μmol/L NDGA. Cells were collected and lysed at the indicated times. Immunoprecipitations and immunuoblotting was performed as in *A*. *C,* FGFR3-TDII expressing cells were treated with a range of NDGA (0, 1, 5, 10, 15, 20, 25, 30, 35, and 40 μmol/L) for 1 h before collecting in 1% NP40 Lysis Buffer. FGFR3-TDII was immunoprecipitated and immunoblotted as in *A*. *D,* 35 μg of total cell lysate from *C* were separated by 10% SDS-PAGE and transferred to Immobilon-P membrane. The membrane was first immunoblotted with anti–Phospho-STAT1 and then stripped and reprobed for total STAT1.

phospho-specific antibodies for STAT1, STAT3, and MAPK. The signaling from FGFR3-TDII was greatly attenuated in response to NDGA. The low level of activation caused by the overexpression of FGFR3 WT was also inhibited by 30 μmol/L NDGA in 5 minutes. As seen in Fig. 4, there is an increase in phospho-MAPK at the 60-minute time points. This is consistent with the previous report by Deshpande (34), which showed that the treatment of FL5.12 cells with NDGA led to an increase in activation of MAPKs. In Fig. 4*B*, as a control for the inhibition of autophosphorylation of FGFR3 by NDGA as seen above, FGFR3 was immunoprecipitated from the lysate and examined for phosphotyrosine. Next, in Fig. 4*C*, we examined the STAT1 activation in HEK293 cells transfected with localized activated kinase domains of FGFR3. The phosphorylation on STAT1 caused by the expression of both myrR3-TDII and cytoR3-TDII was inhibited by 5 minutes of NDGA treatment. This would suggest that NDGA is able to block the signaling from an activated receptor independent of its localization. Curiously, for unknown reasons, significantly enhanced STAT1 phosphorylation was observed in response to the cytoR3-TDII, although expression of this FGFR3 derivative was previously shown to lack transforming activity (30).

Zilueton, a LOX inhbitor, does not block FGFR3-TDII autophosphorylation. To determine if the LOX enzyme inhibiting activity of NDGA was important for its effect on FGFR signaling, we examined another LOX inhibitor, Zileuton. Zileuton is a specific 5-LOX inhibitor, whereas NDGA is nonspecific (35, 36). As seen in Fig. 5*A*, when Zilueton was added to HEK293 cells transfected with FGFR3-TDII, there was no decrease in receptor autohosphorylation. Even with 30 μmol/L of Zilueton added for 1 hour, no change was detected. As a control, a duplicated plate was treated with 10 μmol/L NDGA, which again shows a significant decrease in FGFR3-TDII autophosphorylation. This would imply that the ability of NDGA to inhibit LOX is not required to block FGFR signaling.

Overnight treatment with NDGA leads to increased apoptosis in FGFR3-TDII–expressing cells. The above experiments were performed with very short term treatments of NDGA, <1 hour. Next, we examined the effect of a 24-hour exposure of various concentrations of NDGA on HEK293 FGFR3-TDII–transfected cells. PARP is a zinc finger DNA-binding enzyme, which detects DNA strand breaks and is activated at an intermediate stage of apoptosis. During late-stage apoptosis, PARP is cleaved and inactivated by the apoptotic proteases caspase-3 and caspase-7 (37). We examined the PARP cleavage in cell lysates treated with NDGA to determine the extent of apoptosis. As seen in Fig. 5*B*, there is a significant increase in PARP cleavage in FGFR3-TDII–expressing cells as the concentration of NDGA is increased. Thus, in addition to the ability of NDGA to inhibit FGFR3 signaling, it is clearly able to increase cellular apoptosis.

NDGA increases apoptosis in a multiple myeloma cell line with activated FGFR3. To examine the possible therapeutic effects of NDGA for multiple myeloma, a lethal disease that is characterized by the slow proliferation of malignant plasma cells in the bone, we examined two multiple myeloma–derived cell lines that express high levels of mutated FGFR3 for an increase in apoptosis with NDGA treatment. As seen in Fig. 5*C*, there is an increase in PARP cleavage in the KMS-18 cell line (FGFR3 G384D) with overnight treatment of NDGA. In Fig. 5*D*, the same concentrations of NDGA did not seem to have a similar effect on the KMS-11 cell line (FGFR3 Y373C). This may indicate that NDGA is effective only on a subset of activating mutations in FGFR3, for example, kinase domain mutations but not extracellular domain mutations such as Y373C. Resolution of this question will require further detailed analysis.

NDGA blocks downstream signaling in multiple myeloma cells. First, we examined the effect of NDGA on multiple myeloma cell lines treated with FGF2 to activate the FGFR3 receptor. The RPMI-8226 cell line contains "normal" levels of expression of WT FGFR3, whereas the LP-1 cell line has higher levels of FGFR3 expression. The cells were starved overnight and NDGA was added to the medium for 1 hour before stimulating the cells for 10 minutes by the addition of FGF2. As seen in Fig. 6*A*, there is a significant decrease in MAPK activation with 30 μmol/L NDGA treatment before stimulation, which would indicate that NDGA is able to inhibit the activation of endogenous, WT FGFR3. Next, we examined the effect of NDGA on MAPK activation in multiple myeloma cell lines that express high levels of mutationally

activated FGFR3. As the concentration of NDGA increased with the 1-hour treatment of the KMS-18 cell line, the phosphorylation on MAPK decreased in cell lysates (Fig. 6*B*). These data suggest that NDGA is able to block signaling from FGFR3 that is activated by ligand or mutation. However, there was no significant change in MAPK activation with the same concentrations of NDGA in the KMS-11 cell line as seen in Fig. 6*C*, which may be dependent on the particular mutation of FGFR3; in the case of KMS-11, a Y373C mutation that introduces an abnormal disulfide bond in the extracellular domain.

Discussion

NDGA is a natural compound with an interesting history and broad spectrum of biological properties. Initially isolated from the creosote bush *Larrea divaricatta*, it was originally characterized as a potent antioxidant and shown to selectively inhibit arachidonic acid 5-LOX (38, 39), thereby leading to a reduction of inflammatory pathways through decreased leukotriene and prostaglandin synthesis. NDGA also shows profound effects on the secretory pathway, reflected in its ability to block protein transport from the ER to the Golgi apparatus, and to induce the redistribution of Golgi proteins into the ER (22–24, 40). As a nonspecific inhibitor of NADPH oxidase and protein kinase C, NDGA also disrupts the actin cytoskeleton and exerts effects on cell adhesion (41, 42). Although some reports indicate that NDGA treatment can inhibit apoptosis, as in inhibition of CD95L-induced apoptosis of glioma cells (43), other reports show NDGA-induced apoptosis in a variety of cells, including human breast cancer cells, pancreatic carincoma cells, and HL-60 cells (44–46). NDGA has been shown to induce death

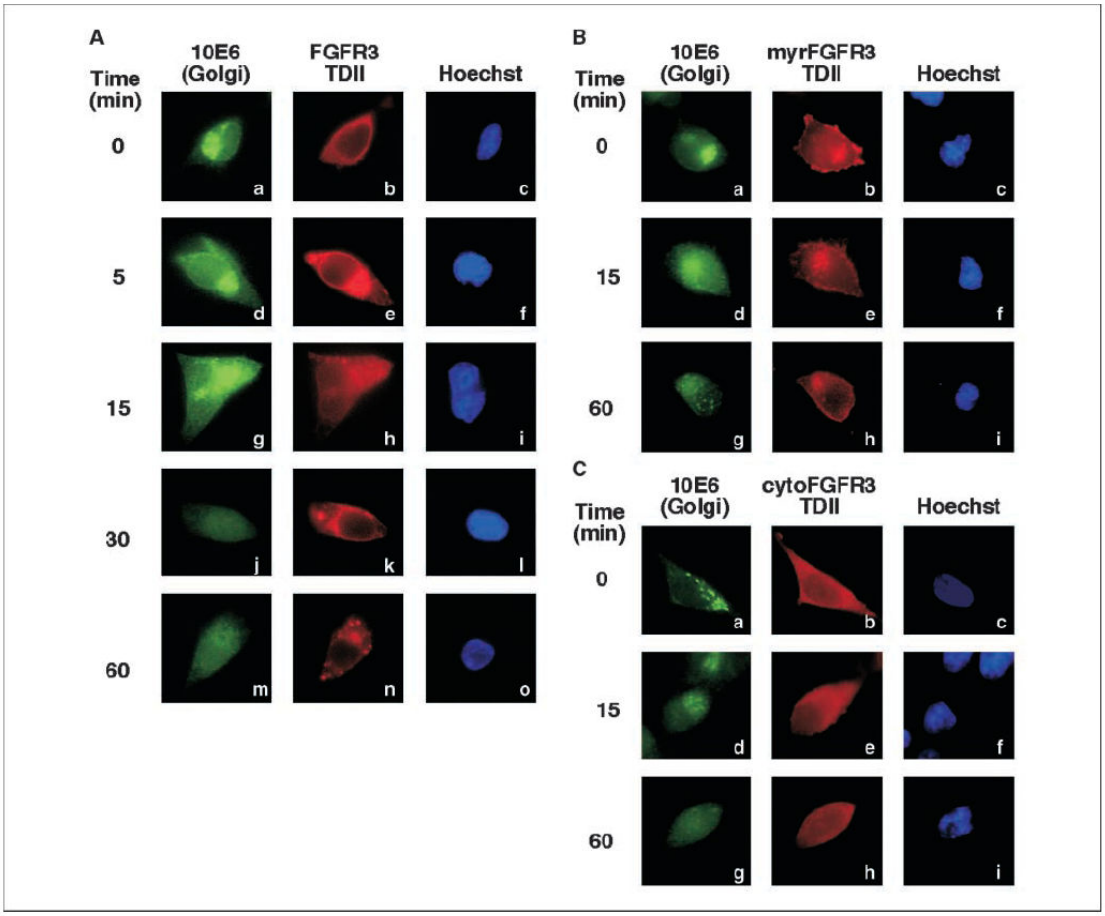

Figure 3. FGFR3-TDII localization with NDGA treatment. HEK293 cells were plated on 10-cm dishes containing Collagen type I–coated glass coverslips 1 d before transfecting with FGFR3-TDII (*A*), myrR3-TDII (*B*), or cytoR3-TDII (*C*). Twenty-four hours after transfection, cells were starved overnight in medium containing no serum. NDGA was diluted in DMSO and added to the plates at a final concentration of 30 μmol/L. Coverslips were fixed with 3% paraformaldehyde/PBS at the indicated times. The 0 time point was treated with DMSO. The *cis*-Golgi was detected with monoclonal antibody 10E6 and fluorescein-conjugated anti-mouse secondary antibody. FGFR3 localization was detected with rabbit polyclonal antibody FGFR3(C-15) and rhodamine-conjugated anti-rabbit secondary antibody. The nuclei were visualized by Hoechst dye added to the Rh secondary antibody mix.

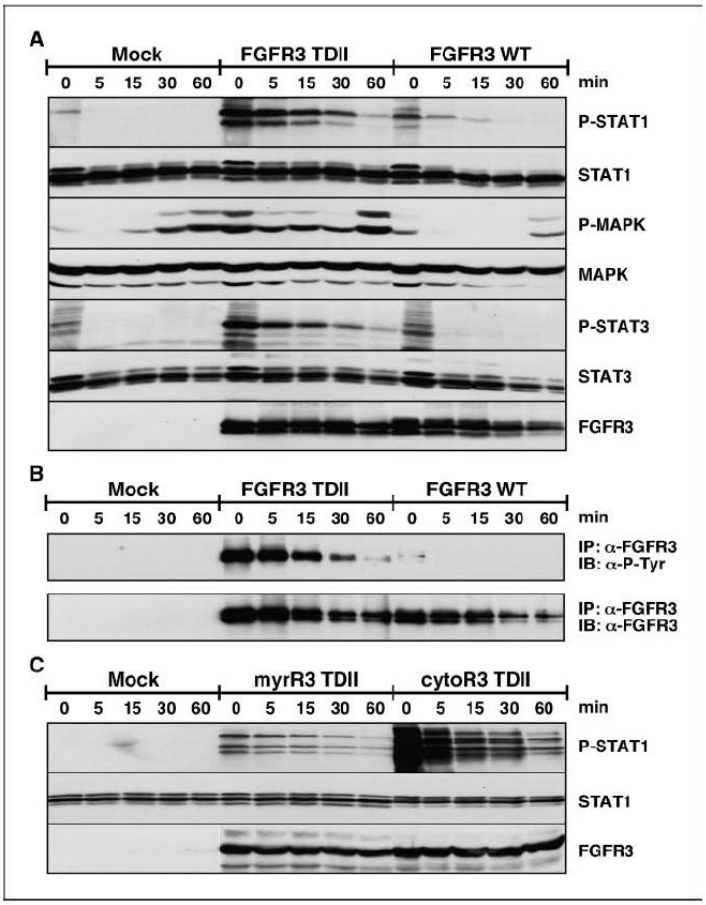

Figure 4. Alteration of FGFR3 signaling. HEK293 cells were transfected with FGFR3-TDII and WT. Twenty-four hours after transfection, cells were starved overnight. Plates were treated with 30 μmol/L NDGA for the indicated times. Cells were collected and lysed in RIPA Lysis Buffer. *A,* duplicate sets of 40 μg of lysate were separated by 10% SDS-PAGE, transferred to Immobilon-P membrane, and immunoblotted. The first membrane was cut in half horizontally and the top was probed with phospho-STAT1, STAT1, and FGFR3 antisera, sequentially. The bottom was immunoblotted with phospho-MAPK and MAPK. The second membrane was immunoblotted with phosph-STAT3 and STAT3 antisera. Membranes were stripped of bound antibodies between primary incubations. *B,* 200 μg of lysate were immunoprecipitaed with FGFR3 antiserum. Proteins were separated by 10% SDS-PAGE, and transferred to Immobilon-P membrane for immmunoblotting with antiphosphotyrosine (4G10; *top*) and FGFR3 antisera (*bottom*). Antibodies were detected by ECL. *C,* HEK293 cells were transfected with myrR3-TDII and cytoR3-TDII. Twenty-four hours after transfection, cells were starved overnight. Plates were treated with 30 μmol/L NDGA for the indicated times. Cells were collected and lysed in RIPA Lysis Buffer. Thirty micrograms of lysate were separated by 10% SDS-PAGE, transferred to Immobilon-P membrane, and immunoblotted. The membrane was cut in half horizontally and the top was probed with phospho-STAT1 and STAT1 antisera, sequentially. The bottom was immunoblotted with FGFR3 antisera.

receptor 5/TRAIL-R2 expression, thereby sensitizing malignant tumor cells to TRAIL-induced apoptosis (47). More recently, NDGA has been shown to directly inhibit activation of two RTKs, the IGF-IR and the c-erbB2/HER2/neu receptor, resulting in decreased cellular proliferation (25, 27, 48, 49).

NDGA is a component of "Chaparral," a natural product proposed several decades ago as a treatment for some cancers but was removed from the Food and Drug Administration (FDA) "generally recognized as safe" list in 1970. Since then, NDGA, also called masoprocol, received FDA approval for inclusion in a topical cream Actinex, under FDA Application No. (NDA) 019940, for treatment of actinic keratoses. Recent studies of its properties have led to rekindled interest in its biochemical and chemotherapeutic properties, as evidenced by an ongoing clinical trial, "Phase I Study of NDGA in Patients With Nonmetastatic, Biochemically Relapsed Prostate Cancer on Androgen Dependent Prostate Cancer (ADPC)" (UCSF-035510; ref. 48). Interestingly, different stereoisomers of NDGA occur, and whether these differ with regard to their biological properties has not been investigated. NDGA is found naturally as a mixture of chiral compounds, including the *meso* forms *R,R*-NDGA and *S,S*-NDGA, and the optically active form *S,R*-NDGA. To fully understand the spectrum of various biological activities exhibited by NDGA with regard to oncogenic RTKs such as IFG-IR and HER2 (25, 27, 49), or FGFR3 examined here, it may be desirable to synthesize chemically pure NDGA isomers for a thorough examination of their biological properties.

Given the importance of FGFR3 activation in several human cancers of clinical importance, it will be significant to determine whether the inhibitory properties of NDGA toward other RTKs, such as IGF-IR or HER2, apply to FGFR3. The activation of cellular signaling pathways by strongly activated mutants of FGFR3 such as the K650E mutant, responsible for TDII (10), or the mutation K650M, responsible for Severe Achondroplasia with Delayed Development and Acanthosis Nigricans (50), has been shown to occur within the secretory compartment, as evidenced by direct recruitment of Jak1 and STAT1 activation, and by Erk1/2 activation from the ER through FRS2α and PLCγ-independent pathways (18–20). Thus, the ability of NDGA to disrupt the secretory compartment, acting together noncompetitively with ATP and its previously shown inhibitory properties toward other

RTKs, suggests that it might be particularly effective against FGFR3.

Indeed, in the experiments described here, we show that NDGA exhibits strong inhibitory effects against FGFR3 kinase activity and the activation of downstream signaling pathways. After expression in HEK293 cells and immunoprecipitation, the activated FGFR3 TDII mutant protein is directly inhibited when assayed for autophosphorylation activity. Furthermore, we show that although NDGA directly inhibits FGFR3-TDII kinase activity, it acts noncompetitively with ATP using this cell-free assay. This mode of inhibition resembles that of a structurally similar compound, AG 538, which was shown to inhibit IGF-IR and act noncompetitively with ATP (51). This indicates that NDGA may be a specific inhibitor toward FGFR3-TDII and other RTKs, rather than nonspecifically inhibiting a wide range of kinases. When cell lysates were examined for Tyr-phosphorylated FGFR3, a concentration of 30 μmol/L NDGA began to show inhibition of receptor phosphorylation in only 5 minutes, and receptor autophosphorylation was almost completely eliminated by 60 minutes. In this assay, the effects of NDGA were almost certainly the result of direct inhibition together with indirect inhibitory effects, such as disruption of protein secretion and collapse of the Golgi. This latter effect was clearly visible by immunofluorescent staining of the Golgi using the *cis*-Golgi marker 10E6. NDGA treatment also resulted in significantly diminished activation of STAT1 and STAT3 by the FGFR3 TDII mutant. Prior work shows that strongly activated mutants of FGFR3 actually recruit Janus-activated kinase 1 directly to the ER, leading to activation of STAT family members, which is not disrupted by brefeldin A (BFA; refs. 18, 19). In our results reported here, we found that NDGA, an agent previously shown to disrupt the Golgi by mechanisms distinct from BFA (52), rapidly blocked activation of STAT1 and STAT3. Although NDGA possesses strong antioxidant activity, the effects of NDGA on FGFR3 activation and

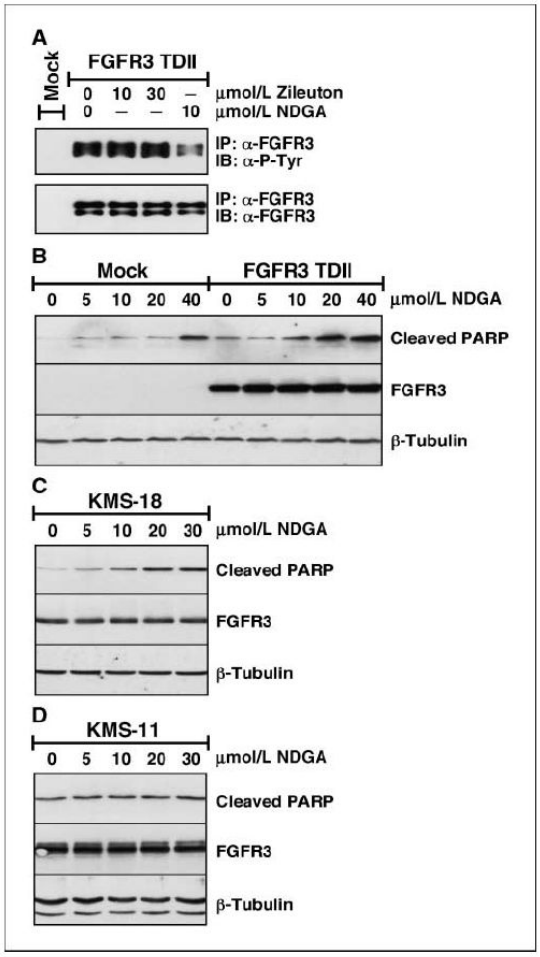

Figure 5. Induction of apoptosis by NDGA, and comparison with Zileuton, another LOX inhibitor. *A*, HEK293-transfected cells were starved overnight before treatment with Zileuton or NDGA. Cells were collected and lysed in 1% NP40 Lysis Buffer. FGFR3-TDII was immunoprecipitated from 250 μg of lysate, separated by 10% SDS-PAGE, and transferred to Immobilon-P membrane for immmunoblotting with antiphosphotyrosine (4G10; *top*) and FGFR3 antisera (*bottom*). Antibodies were detected by ECL. The membrane was stripped between each antibody incubation. *B*, apoptosis was assayed by PARP cleavage in HEK293 cells transfected with FGFR3-TDII or pcDNA3 (*mock*), treated for 24 h with a concentration range of NDGA in 10% FBS medium. Cells were collected and lysed in 1% NP40 Lysis Buffer. Thirty micrograms of lysate were separated by 15% SDS-PAGE, transferred to Immobilon-P membrane, and immunoblotted with cleaved PARP (Asp214; *top*), FGFR3 (*middle*), and β-tubulin antisera (*bottom*), followed by ECL. The membrane was stripped between each antibody incubation. KMS-18 (*C*) or KMS-11 (*D*) cells were treated for 24 h with 0, 5, 10, 20, or 30 μmol/L NDGA. Thirty micrograms of lysate was separated by 10% SDS-PAGE, transferred to Immobilon-P membrane, and immunoblotted as in *B*.

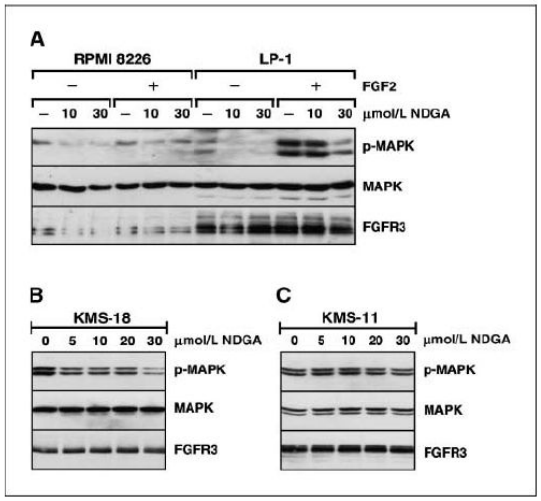

Figure 6. Downstream effect of NDGA on multiple myeloma cells. *A*, the multiple myeloma cell lines RPMI 8226 and LP-1 were starved overnight in RPMI 1640 with 0% serum in 6-well dishes. Duplicate wells for each cell type were preincubated with 0, 10, or 30 μmol/L NDGA for 1 h. Half the cells were then treated with 10 ng/mL FGF2 and 1 μg/mL Heparin for 10 min. Cells were collected and lysed in RIPA Lysis Buffer. Thirty micrograms of lysate were separated by 10% SDS-PAGE, transferred to Immobilon-P membrane, and immunoblotted with (*top*) phospho-p44/42 MAPK, MAPK (ERK1 + ERK2' *middle*), and FGFR3 antisera (*bottom*), followed by ECL. The membrane was stripped between each antibody incubation. KMS-18 cells (*B*) or KMS-11 cells (*C*) cells were treated for 1 h with 0, 5, 10, 20, or 30 μmol/L NDGA. Cells were collected, treated, and immunoblotted as in *A*.

signaling were not attributable solely to antioxidant activity, as shown by the inability of a chemically unrelated antioxidant, Zileuton, to affect FGFR3 activation. Using HEK293 cells expressing FGFR3, we showed that NDGA significantly increases apoptosis for cells expressing the activated TDII mutant and in the multiple myeloma cell line KMS-18, as shown by PARP cleavage. Lastly, using the multiple myeloma cell line LP-1 expressing FGFR3 WT, we show that FGF-dependent signaling, as reflected in the appearance of p-MAPK, is effectively blocked by NDGA treatment. NDGA also reduces p-MAPK in the KMS-18 multiple myeloma cell line expressing FGFR3 G384D.

Collectively, the results presented here indicate that NDGA, acting most likely by multiple mechanisms, including direct inhibition of kinase activity, disruption of the secretory pathway, inhibition of downstream signaling pathways, and increased apoptosis, possesses potentially beneficial attributes that merit further investigation. This is particularly true for those cancers where cellular proliferation depends upon continued stimulation of FGFR3 either by ligand activation or by mutational activation, as in bladder carcinoma and multiple myeloma.

Disclosure of Potential Conflicts of Interest

No potential conflicts of interest were disclosed.

Acknowledgments

Received 2/14/2008; revised 6/24/2008; accepted 7/2/2008.

Grant support: NIH (R01-CA90900) and the Multiple Myeloma Research Foundation.

The costs of publication of this article were defrayed in part by the payment of page charges. This article must therefore be hereby marked *advertisement* in accordance with 18 U.S.C. Section 1734 solely to indicate this fact.

We thank Prof. Leslie Thompson of the University of California, Irvine (Irvine, CA) for providing us with human multiple myeloma cells, Prof. Uli Muller for use of phosphorimaging equipment, Kristy Drafahl and Lisa Salazar for technical assistance, and Laura Castrejon for editorial assistance.

References

1. Manning G, Whyte DB, Martinez R, Hunter T, Sudarsanam S. The protein kinase complement of the human genome. Science 2002;298:1912–34.
2. Robertson SC, Tynan JA, Donoghue DJ. RTK mutations and human syndromeswhen good receptors turn bad. Trends Genet 2000;16:265–71.
3. Jaye M, Schlessinger J, Dionne CA. Fibroblast growth factor receptor tyrosine kinases: molecular analysis and signal transduction. Biochim Biophys Acta 1992;1135:185–99.
4. Johnson DE, Williams LT. Structural and functional diversity in the FGF receptor multigene family. Adv Cancer Res 1993;60:1–41.
5. Bottcher RT, Niehrs C. Fibroblast growth factor signaling during early vertebrate development. Endocr Rev 2005;26:63–77.
6. Ornitz DM. FGF signaling in the developing endochondral skeleton. Cytokine Growth Factor Rev 2005;16:205–13.
7. Chen L, Deng CX. Roles of FGF signaling in skeletal development and human genetic diseases. Front Biosci 2005;10:1961–76.
8. Dailey L, Ambrosetti D, Mansukhani A, Basilico C. Mechanisms underlying differential responses to FGF signaling. Cytokine Growth Factor Rev 2005;16:233–47.
9. Wilkie AO, Morriss-Kay GM, Jones EY, Heath JK. Functions of fibroblast growth factors and their receptors. Curr Biol 1995;5:500–7.
10. Tavormina PL, Shiang R, Thompson LM, et al. Thanatophoric dysplasia (types I and II) caused by distinct mutations in fibroblast growth factor receptor 3. Nat Genet 1995;9:321–8.
11. Chesi M, Nardini E, Brents LA, et al. Frequent translocation t(4;14)(p16.3;q32.3) in multiple myeloma is associated with increased expression and activating mutations of fibroblast growth factor receptor 3. Nat Genet 1997;16:260–4.
12. Richelda R, Ronchetti D, Baldini L, et al. A novel chromosomal translocation t(4; 14)(p16.3; q32) in multiple myeloma involves the fibroblast growth-factor receptor 3 gene. Blood 1997;90:4062–70.
13. Sibley K, Stern P, Knowles MA. Frequency of fibroblast growth factor receptor 3 mutations in sporadic tumours. Oncogene 2001;20:4416–8.
14. van Rhijn BW, Lurkin I, Radvanyi F, Kirkels WJ, van der Kwast TH, Zwarthoff EC. The fibroblast growth factor receptor 3 (FGFR3) mutation is a strong indicator of superficial bladder cancer with low recurrence rate. Cancer Res 2001;61:1265–8.
15. Cappellen D, De Oliveira C, Ricol D, et al. Frequent activating mutations of FGFR3 in human bladder and cervix carcinomas. Nat Genet 1999;23:18–20.
16. Rousseau F, el Ghouzzi V, Delezoide AL, et al. Missense FGFR3 mutations create cysteine residues in thanatophoric dwarfism type I (TD1). Hum Mol Genet 1996;5:509–12.
17. Chesi M, Kuehl WM, Bergsagel PL. Recurrent immunoglobulin gene translocations identify distinct molecular subtypes of myeloma. Ann Oncol 2000;11 Suppl 1:131–5.
18. Lievens PM, Liboi E. The thanatophoric dysplasia type II mutation hampers complete maturation of FGF receptor 3, which activates STAT1 from the endoplasmic reticulum. J Biol Chem 2003;279:43254–60. Epub 2004 Aug 2.
19. Lievens PM, Mutinelli C, Baynes D, Liboi E. The kinase activity of fibroblast growth factor receptor 3 with activation loop mutations affects receptor trafficking and signaling. J Biol Chem 2004;279:43254–60.
20. Lievens PM, Roncador A, Liboi E. K644E/M FGFR3 mutants activate Erk1/2 from the endoplasmic reticulum through FRS2 α and PLC γ-independent pathways. J Mol Biol 2006;357:783–92.
21. Fujiwara T, Misumi Y, Ikehara Y. Dynamic recycling of ERGIC53 between the endoplasmic reticulum and the Golgi complex is disrupted by nordihydroguaiaretic acid. Biochem Biophys Res Commun 1998;253:869–76.
22. Fujiwara T, Misumi Y, Ikehara Y. Direct interaction of the Golgi membrane with the endoplasmic reticulum membrane caused by nordihydroguaiaretic acid. Biochem Biophys Res Commun 2003;301:927–33.
23. Fujiwara T, Takami N, Misumi Y, Ikehara Y. Nordihydroguaiaretic acid blocks protein transport in the secretory pathway causing redistribution of Golgi proteins into the endoplasmic reticulum. J Biol Chem 1998;273:3068–75.
24. Drecktrah D, de Figueiredo P, Mason RM, Brown WJ. Retrograde trafficking of both Golgi complex and TGN markers to the ER induced by nordihydroguaiaretic acid and cyclofenil diphenol. J Cell Sci 1998;111:951–65.
25. Blecha JE, Anderson MO, Chow JM, et al. Inhibition of IGF-1R and lipoxygenase by nordihydroguaiaretic acid (NDGA) analogs. Bioorg Med Chem Lett 2007;17:4026–9.
26. Meyer GE, Chesler L, Liu D, et al. Nordihydroguaiaretic acid inhibits insulin-like growth factor signaling, growth, and survival in human neuroblastoma cells. J Cell Biochem 2007;102:1529–41.
27. Youngren JF, Gable K, Penaranda C, et al. Nordihydroguaiaretic acid (NDGA) inhibits the IGF-1 and c-erbB2/HER2/neu receptors and suppresses growth in breast cancer cells. Breast Cancer Res Treat 2005;94:37–46.
28. Domin J, Higgins T, Rozengurt E. Preferential inhibition of platelet-derived growth factor-stimulated DNA synthesis and protein tyrosine phosphorylation by nordihydroguaiaretic acid. J Biol Chem 1994;269:8260–7.
29. Webster MK, D'Avis PY, Robertson SC, Donoghue DJ. Profound ligand-independent kinase activation of fibroblast growth factor receptor 3 by the activation loop mutation responsible for a lethal skeletal dysplasia, thanatophoric dysplasia type II. Mol Cell Biol 1996;16:4081–7.
30. Webster MK, Donoghue DJ. Enhanced signaling and morphological transformation by a membrane-localized derivative of the fibroblast growth factor receptor 3 kinase domain. Mol Cell Biol 1997;17:5739–47.
31. Hart KC, Robertson SC, Donoghue DJ. Identification of tyrosine residues in constitutively activated fibroblast growth factor receptor 3 involved in mitogenesis, Stat activation, and phosphatidylinositol 3-kinase activation. Mol Biol Cell 2001;12:931–42.
32. Hart KC, Robertson SC, Kanemitsu MY, Meyer AN, Tynan JA, Donoghue DJ. Transformation and Stat activation by derivatives of FGFR1, FGFR3, and FGFR4. Oncogene 2000;19:3309–20.
33. Buettner R, Mora LB, Jove R. Activated STAT signaling in human tumors provides novel molecular targets for therapeutic intervention. Clin Cancer Res 2002;8:945–54.
34. Deshpande VS, Kehrer JP. Oxidative stress-driven mechanisms of nordihydroguaiaretic acid-induced apoptosis in FL5.12 cells. Toxicol Appl Pharmacol 2006;214:230–6.
35. Carter GW, Young PR, Albert DH, et al. 5-lipoxygenase inhibitory activity of zileuton. J Pharmacol Exp Ther 1991;256:929–37.
36. Tang DG, Chen YQ, Honn KV. Arachidonate lipoxygenases as essential regulators of cell survival and apoptosis. Proc Natl Acad Sci U S A 1996;93:5241–6.
37. Decker P, Muller S. Modulating poly (ADP-ribose) polymerase activity: potential for the prevention and therapy of pathogenic situations involving DNA damage and oxidative stress. Curr Pharm Biotechnol 2002;3:275–83.
38. Salari H, Braquet P, Borgeat P. Comparative effects of indomethacin, acetylenic acids, 15-HETE, nordihydroguaiaretic acid and BW755C on the metabolism of arachidonic acid in human leukocytes and platelets. Prostaglandins Leukot Med 1984;13:53–60.
39. Chang J, Skowronek MD, Cherney ML, Lewis AJ. Differential effects of putative lipoxygenase inhibitors on arachidonic acid metabolism in cell-free and intact cell preparations. Inflammation 1984;8:143–55.
40. Tagaya M, Henomatsu N, Yoshimori T, Yamamoto A, Tashiro Y, Mizushima S. Inhibition of vesicle-mediated protein transport by nordihydroguaiaretic acid. J Biochem 1996;119:863–9.
41. Holland JA, Goss RA, O'Donnell RW, Chang MM, Johnson DK, Ziegler LM. Low-density lipoprotein induced actin cytoskeleton reorganization in endothelial cells: mechanisms of action. Endothelium 2001;8:117–35.

42. Papadogiannakis N, Barbieri B. Lipoxygenase inhibitors counteract protein kinase C mediated events in human T lymphocyte proliferation. Int J Immunopharmacol 1997;19:263–75.
43. Wagenknecht B, Schulz JB, Gulbins E, Weller M. CrmA, bcl-2 and NDGA inhibit CD95L-induced apoptosis of malignant glioma cells at the level of caspase 8 processing. Cell Death Differ 1998;5:894–900.
44. Park S, Hahm ER, Lee DK, Yang CH. Inhibition of AP-1 transcription activator induces myc-dependent apoptosis in HL60 cells. J Cell Biochem 2004;91:973–86.
45. Nishimura K, Tsumagari H, Morioka A, et al. Regulation of apoptosis through arachidonate cascade in mammalian cells. Appl Biochem Biotechnol 2002; 102–103:239–50.
46. Tong WG, Ding XZ, Adrian TE. The mechanisms of lipoxygenase inhibitor-induced apoptosis in human breast cancer cells. Biochem Biophys Res Commun 2002;296:942–8.
47. Yoshida T, Shiraishi T, Horinaka M, et al. Lipoxygenase inhibitors induce death receptor 5/TRAIL-R2 expression and sensitize malignant tumor cells to TRAIL-induced apoptosis. Cancer Sci 2007;98: 1417–23.
48. Ryan CJ, Harzstark AH, Rosenberg J, et al. A pilot dose-escalation study of the effects of nordihydroguaretic acid on hormone and prostate specific antigen levels in patients with relapsed prostate cancer. BJU Int 2008;101:436–9.
49. Zavodovskaya M, Campbell MJ, Maddux BA, et al. Nordihydroguaiaretic acid (NDGA), an inhibitor of the HER2 and IGF-1 receptor tyrosine kinases, blocks the growth of HER2-overexpressing human breast cancer cells. J Cell Biochem 2007;103:624–35.
50. Tavormina PL, Bellus GA, Webster MK, et al. A novel skeletal dysplasia with developmental delay and acanthosis nigricans is caused by a Lys650Met mutation in the fibroblast growth factor receptor 3 gene. Am J Hum Genet 1999;64:722–31.
51. Blum G, Gazit A, Levitzki A. Substrate competitive inhibitors of IGF-1 receptor kinase. Biochemistry 2000; 39:15705–12.
52. Kim SM, Park TW, Park JW. Effect of nordihydroguaiaretic acid on the secretion of lipoprotein lipase. J Biochem Mol Biol 2002;35:518–23.